# Characterization of Met receptor tyrosine kinase-mediated endocytosis and its role in signal transduction and cellular migration

by

Christine Anna Parachoniak

A thesis submitted to McGill University in partial fulfillment of the requirements of the degree of Doctor of Philosophy



Department of Biochemistry
McGill University
Montréal, QC, Canada
August 2011

# ABSTRACT

The Met receptor tyrosine kinase (RTK) and its ligand, hepatocyte growth factor (HGF) are potent regulators of epithelial remodeling, dispersal, and invasion and their deregulation is frequently observed in human cancers. These processes are coordinated through signal transduction pathways activated downstream of Met. In turn, it is now understood that an important aspect of signalling outcome is modulated through RTK downregulation via receptor internalization, degradation and also RTK recycling to spatially restricted subcellular domains. Although a strong relationship between RTK endocytosis and signalling had been established prior to this thesis, the precise mechanism(s) of how this is achieved is still poorly understood and little was known for the Met RTK.

To address this specifically for the Met RTK, I have characterized the function of two endocytic proteins in Met RTK trafficking and the consequence for biological response. Work in this thesis shows that following HGF-mediated Met activation, the endocytic adaptor protein, Eps15, is recruited to the Met receptor, and becomes both tyrosine-phosphorylated and ubiquitinated. Recruitment of Eps15 requires Met receptor kinase activity and involves two distinct Eps15 domains. Unlike previous reports for other receptors, recruitment of Eps15 to Met involves a distinct mode of recruitment involving the coiled-coil domain of Eps15 and the signaling adaptor molecule, Grb2. This identified a new mechanism of recruitment for Eps15 downstream of the Met receptor.

In the third part of my thesis, I establish that the endocytic adaptor molecule, Golgi-localized gamma-ear containing Arf-binding protein 3 (GGA3), interacts selectively with Met when stimulated by HGF, to sort Met for recycling through a Rab4 positive compartment rather than degradation. I provide evidence supporting a molecular mechanism through which GGA3 regulates Met recycling and demonstrate that this is essential for both prolonged signaling and HGF-mediated biological response. This data defines an active recycling pathway involving GGA3, and supports a broader role for GGA3-mediated cargo selection in targeting receptors destined for recycling.

Finally, in the fourth chapter of this thesis, evidence for microtubule interactions in Met-mediated Rab4 vesicle recycling is presented. We characterize a mechanism reliant on the microtubule +TIP, CLIP-170, linking Met/Rab4-positive recycling vesicles to microtubules for transport to the lamellipodia. We propose that the specific targeting of the Met receptor to the leading edge functions as a specialized signalling microenvironment, required for maintaining normal migration dynamics. These studies identify Met RTK endocytosis as a crucial regulatory process for RTK signalling and biology and stress the need for further studies examining the interplay of RTK endocytosis and signalling in the context of normal development and cancer settings.

# ABRÉGÉ

Le récepteur tyrosine kinase (RTK) Met, ainsi que son ligand, le facteur de croissance des hepathocytes (HGF), sont de puissants régulateurs du remodelage, de la dispersion et de l'invasion des cellules épithéliales, et leur dérèglement est fréquemment observé dans divers types de cancers chez l'humain. Ces processus sont coordonnés par l'activation de voies de signalisation induites par Met. Il est maintenant connu que l'internalisation, la dégradation ainsi que le recyclage des RTKs vers des domaines spécifiques de la cellule constituent des facteurs importants influençant les conséquences de l'activation de ces voies de signalisation. Bien que le lien entre l'endocytose et la signalisation des RTKs ait été démontré avant ce mémoire, les mécanismes spécifiques de cette association restent encore mal compris.

Pour aborder ce problème spécifiquement concernant le récepteur Met, j'ai caractérisé les rôles de deux protéines endocytiques impliquées dans le trafic de Met, et leur implication dans les réponses biologiques induites par Met. Les travaux présentés dans ce mémoire montrent qu'en réponse à l'activation de Met par HGF, l'adaptateur endocytique Eps15 est recruté par le récepteur et devient tyrosine phosphorylé et ubiquiné. Le recrutement d'Eps15 requiert l'activation du récepteur tyrosine kinase Met, et implique deux domaines distincts d'Eps15. Contrairement à ce qui a été rapporté pour d'autres récepteurs, le recrutement d'Eps15 par Met met en jeu un mode de recrutement distinct impliquant le faisceau d'hélices (coiled-coil domain) d'Eps15 et l'adapteur signalétique Grb2. Ceci a permis d'identifié un nouveau mécanisme de recrutement d'Eps15 par le récepteur Met.

Dans la troisième partie de ce mémoire, j'ai établi que l'adaptateur endocytique Golgi-localized gamma-ear containing Arf-binding protein 3 (GGA3) interagit spécifiquement avec Met lorsque celui-ci est stimulé par HGF. En conséquence, GGA3 trie Met pour le recyclage via un compartiment contenant Rab4, plutôt que de le trier pour être dégradé. J'y démontre un nouveau mécanisme moléculaire par lequel GGA3 contrôle le recyclage de Met, ce qui est essentiel pour la signalisation prolongée de Met et des réponses biologiques

induites par HGF. Ces données définissent un nouveau mécanisme de recyclage actif impliquant GGA3 et supportent un rôle plus large joué par GGA3 dans la sélection des récepteurs destinés au recyclage.

Finalement, le rôle des microtubules dans le recyclage des vésicules contenant Rab4 induit par Met est présenté dans le quatrième chapitre de ce mémoire. Nous avons caractérisé un mécanisme dépendant d'une protéine de l'extrémité (+TIP), CLIP-170, qui lie les vésicules de recyclage contenant Met et Rab4 aux microtubules, contrôlant ainsi leur transport vers les lamellipodes. Nous proposons que le ciblage spécifique du récepteur Met vers le front de migration fonctionne comme un microenvironnement signalétique spécifique requis pour le maintient de la dynamique migratoire. Ces travaux ont permis d'identifié l'endocytose du récepteur tyrosine kinase Met comme étant un processus de régulation cruciale pour la signalisation des RTK et pour les réponses biologiques associées à cette signalisation. Ces travaux démontrent qu'il y a un besoin important d'examiner la relation entre l'endocytose des RTKs et leur signalisation aussi bien dans le contexte du développement normal que dans le cadre du développement cancéreux.

# ACKNOWLEDGMENTS

There are many people who I would like to thank for their support.

Firstly, I would like to thank my supervisor Dr. Morag Park for giving me the opportunity to work in her 'fabulous' lab and in particular, on a project that has been both exciting and intellectually challenging. I am grateful for her mentorship, teachings and enthusiasm for science, at all hours of the day.

- I would like to thank members of my Research Advisory Committee, Dr. Jason Young and Dr. Stephane Laporte for their critical feedback and suggestions.
- I wish to acknowledge Dr. Claire Brown of the McGill Imaging Facility for her expertise and assistance with Metamorph and Ken McDonald from the Flow Cytometry Core Facility for FACS sorting assistance.
- I would like to thank collaborators, Dr. Jim Keen and Dr. Yi Lui at the Kimmel Cancer Centre, of the Thomas Jefferson University in Philadelphia for their contribution to the GGA3 project. I would also like to thank Dr. Kossay Zaoui for his collaboration on the CLIP-170 project.

I would like to acknowledge both past and present member of the Park lab and Molecular Oncology Group/Goodman Cancer Centre for their friendship and support. In particular, I would like to thank the following individuals:

- Jasmine Abella, who introduced me to the wonderful world of endocytosis, and embraced me into the lab. I am appreciative for her willingness to discuss and share her knowledge and ideas with me. You are an amazing scientist and I wish you all the best in your postdoctoral studies and beyond.
- Colin Ratcliffe, with whom I have enjoyed working with during his time as an undergraduate student in the lab, and now, as a (rookie) graduate student in the lab. I wish you the best of luck continuing the sorting signal

project and all the rest of the endocytosis projects to come. Make sure to always keep your student room cabinet full. Additional thanks to Nicole Darricarrere for helping me initiate the sorting signal project.

- Hayley Mak, Kelly Fathers, Ryan Dowling, Greg Paliouras, Marisa Ponzo, Annina Spilker, Laurent Sansregret, Mary Truscott, Jon Rayment and Jason Turpin- for their fruitful science discussions and friendship.
- Andrea Lai, Richard Vaillancourt, Charles Rajadurai, Emily Bell and Sadiq Saleh –for their support and friendship both in and out of the lab. I wish all of you the best of luck pursuing your projects during the remainder of your graduate studies and hopefully bringing home a championship mug for team Boyakasha. Also, an additional thanks to Richard for helping translate my abstract into French. Merci!
- Monica Naujokas- for her infinite knowledge of all things tissue culture and Park lab related and ensuring I had all the necessary resources for my research. I am also grateful for her contagious positivity and friendship.
- Dongmei Zuo- for her technical assistance with microscopy and teaching me how to take beautiful confocal images. Tina Lin- for DNA and protein technical assistance.

Last but certainly not least; I would like to thank members of my family: Mom, Dad, Tete, aunts, uncles and cousins as well as close friends: Vanessa Lundgren, Linsie Kolshuk, and Kari-Jean McKenzie, for their love and support. Thanks to Tete for sending banana bread care packages from Vancouver. I am especially grateful to my parents, Ron and Hala, for their daily encouragement, unconditional love and unwavering confidence in me; I am lucky to have such amazing parents. I love you both. Thank you for sharing all the ups and downs with me; I could not have gotten to this point without you.

Funding: This work was supported by a CIHR Canada Graduate Scholarship (CGS) Masters award, McGill University Health Centre (MUHC), Dept of Medicine studentship and CIHR CGS Doctoral Award.

# PREFACE

This thesis is written in manuscript-based format. It contains two published articles and one manuscript in preparation, incorporated into Chapters 2-4.

**First author publications arising from this work:**

1. "Distinct recruitment of Eps15 via Its coiled-coil domain is required for efficient down-regulation of the Met receptor tyrosine kinase."
   **Parachoniak CA**, Park M. J. Biol. Chem. (2009) 284(13):8382-94

2. "GGA3 Functions as a Switch to Promote Met Receptor Recycling, Essential for Sustained ERK and Cell Migration"
   **Parachoniak CA**, Lui Y, Abella JV, Keen, JH and Park M.
   Developmental Cell (2011), Jun 14;20(6):751-63.

3. "CLIP-170 Links HGF-dependent Vesicle Motility to Microtubules During Cell Migration"
   Zaoui K*, **Parachoniak CA*** and Park M. Manuscript in preparation.

* authors contributed equally to this work.

**Contributions of Authors**

1. I designed, performed and analyzed all the experiments in the paper. I wrote the manuscript together with my supervisor, M Park.

2. Y. Lui performed the live-cell imaging of Alexa-555 HGF with GFP-GGA3 (Fig. 3D and Movie S1) and its quantification (Fig. 3E) plus supplemental movie S2, of mCherry-Clathrin and GFP-GGA3. JH Keen helped in the analysis of data collected by Y. Lui and edited the text corresponding to Fig.

3D and 3E. JV Abella made the initial observation that GGA3 associates with the Met receptor. I designed and performed all other experiments (Fig. 1A-F, 2A-D, 3A-C, 4A-F, 5A-G, 6A-G, 7A-C plus supplemental Fig. S1A-C, S2A-C, S3A, S4A-C, S5A-D, S6A-C). I wrote the paper along with M Park.

3. K. Zaoui performed all the live-cell imaging experiments including: Rab4 vesicle mobility, Arp3, Actin, VASP and Paxillin localization and cell velocity movies which are presented in Fig. 3**b-e**, 4**a-f**, 5**a-f,** S3**a** and shown in supplemental movies 1-7 as well their analysis. He also wrote the material and methods for these experiments. I performed all other experiments including: immunofluorescence with line scan analysis and 3D rendering, recycling assays, western blots, immunoprecipitations and generation of GFP-CLIP-170 domain and mCherry-Rab4 constructs, which are presented in Fig. 1**a-e**, 2**a-i**, 3**a**, S1**a-d**, S2**a**, S3**b** as well as the analysis of these experiments. K. Zaoui, M. Park and I all contributed to the overall analysis of the design of this project. I assembled all the figures and wrote the text presented in this thesis with editing help from M. Park.

**Additional Publications:**

"Dynamics of Receptor Trafficking in Tumorigenicity"
**Parachoniak CA**, Park M. Review in preparation for Trends in Cell Biology.

"Dorsal ruffle microdomains potentiate Met RTK signalling and downregulation." Abella JV, **Parachoniak CA**, Sangwan V, Park M (2010) J. Biol. Chem. 285(32):24956-67

# TABLE OF CONTENTS

# LIST OF FIGURES

## CHAPTER 1



## CHAPTER 2



## CHAPTER 3

**CHAPTER 4**



**CHAPTER 5**

# LIST OF TABLES

## CHAPTER 1



## CHAPTER 5

# Chapter 1

## 1. LITERATURE REVIEW

### 1.1. RECEPTOR TYROSINE KINASES

The family of receptor tyrosine kinases (RTKs) constitutes one of the most prominent classes of cell surface receptors, with 58 members in humans assigned into 20 subfamilies[1]. The general structure, mode of activation and signalling pathways triggered by RTKs are evolutionarily conserved among organisms, highlighting the fundamental role these proteins play in biology[2]. Since the discovery of the first RTK approximately 30 years ago[3-6], much research has gone into elucidating the key functions of RTKs. Importantly, RTKs are now known to play pivotal roles in most cellular responses, including cell migration, proliferation, differentiation, survival and metabolism[7]. RTKs are therefore under strict regulation and when abnormally altered, RTKs act as oncoproteins. To date, over half of the known RTKs have been causally linked to the development and progression of human cancer[1]. Accordingly, RTKs have become prime candidates for therapeutic intervention, with several RTK-based cancer therapies currently in use and/or in clinical trials[3].

Prior to the start of this PhD thesis, a variety of mechanisms leading to RTK deregulation had been characterized. Receptor amplification, chromosomal translocation, and point mutations represented quintessential mechanisms leading to the enhanced and inappropriate activity of RTKs[1,8]. However a growing number of studies (from this lab and others) had begun to establish an additional, alternative mechanism leading to RTK deregulation. This mechanism involves the concept of loss of negative regulation[8,9]. The ability of RTKs to escape downregulation opened up a hitherto under-appreciated arm of RTK biology and prompted us to investigate mechanisms through which this occurs for the Met

RTK with the hope of gaining a better understanding of its normal function and its deregulation in disease.

## 1.2. THE HGF/MET RECEPTOR AXIS

The Met receptor belongs to a family of RTKs which also includes RON (recepteur d'origine nantais), the receptor for hepatocyte growth factor-like (HGFL)/Macrophage-stimulating protein (MSP)[10] and a cellular orthologue of an avian erythroblastosis S13 virus, c-Sea[11-13]. Like other RTKs, the HGF/Met receptor signalling axis plays a pivotal role in controlling essential biological responses such as cell migration and proliferation and has been shown to be deregulated in human diseases such as cancer. Importantly, the HGF/Met receptor axis is a primary controller of epithelial-mesenchymal transitions (EMT) *in vitro*[14,15] and *in vivo*[16].

### 1.2.1. Met Receptor Structure

The Met receptor is synthesized as a single chain precursor that becomes cleaved at a furin site located between residues 307 and 308. This creates an alpha and beta chain that forms a heterodimer through disulphide linkage. The alpha chain and the first 212 amino acids of the beta chain fold into a sema domain, homologous to the sema domain of the semaphorin axon-guidance proteins and is structurally similar to the beta propeller of integrin alpha chains[11]. This region is followed by a small cysteine rich region and four immunoglobulin-like domains, which compose the remainder of the extracellular region of Met. The rest of the beta-chain is made up of a membrane-spanning helix, an usually long 110 amino acid juxtamembrane domain, a 256 amino acid kinase domain and a 45 amino acid cytoplasmic c-terminus tail (Figure 1.1).

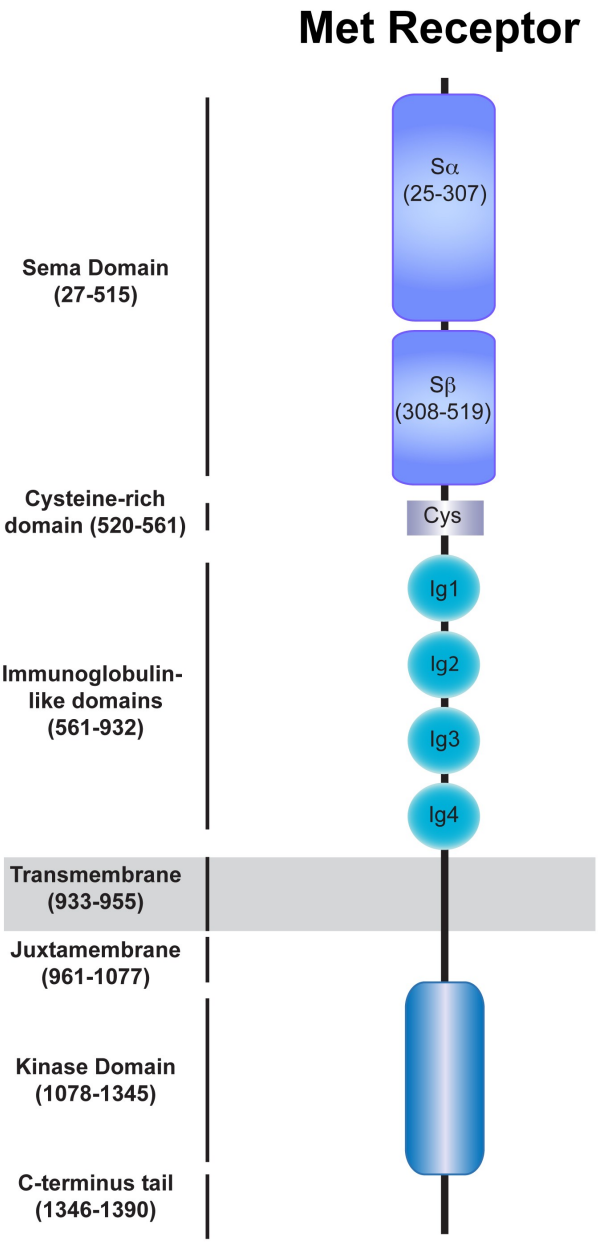


**Figure 1.1. Structural domains of the Met receptor tyrosine kinase.** Shown are the major structural domains of the Met receptor, as described in the text. Amino acids of each domain are indicated in brackets.

### 1.2.2. Hepatocyte Growth Factor

Hepatocyte growth factor (HGF) was independently identified as both a fibroblast-derived 'scatter factor'[17] and serum-born factor, purified and cloned as a mitogenic factor for hepatocytes[18-20], later shown to be the same molecule[21,22] and ligand for the Met receptor[23]. HGF is the only ligand for the Met receptor, although decorin, has been recently identified as an antagonistic ligand[24] and the bacterial pathogen *Listeria monocytogenes* surface protein InlB[25] can also bind to Met (Figure 1.2). HGF binds to Met with high affinity ($K_d$~0.2nM)[14]. HGF is secreted as an inactive precursor (pro-HGF) by mesoderm-derived cells, and then subsequently processed into its active alpha-beta heterodimeric form through the action of plasminogen activators including uPA (urokinase-type plasminogen activator)[26], tPA (tissue-type plasminogen activator)[26], coagulation factors X, XI and XII; and a close homologue of factor XII[11]. Small-angle x-ray scattering and cryo-electron microscopy studies indicate that processing of HGF results in major conformational changes going from a closed, compact conformation to an elongated open form[27]. Interestingly, plasminogenic activators have been found to be elevated in highly metastatic tumors[28] and during injury repair. As both Met and HGF can also be transcriptionally elevated during these events[29,30], the combination of both mechanisms (increased protein production of Met and HGF and increased biological processing of pro-HGF) would provide a powerful mechanism to promote HGF/Met paracrine signaling. Structurally, the alpha subunit of HGF contains an amino-terminal domain, followed by four kringle domains (Figure 1.2) while the beta domain folds into a serine proteinase homology domain (SPH) which lacks enzymatic activity[31]. The two chains associate through a disulphide bridge.

HGF is found at concentrations ranging from 0.26-0.39ng/ml in human serum. Importantly, levels of HGF are elevated in various diseases, including tumor cells, with reports reaching as high as 2.1ng/ml. Additionally, higher concentrations (9.6ng/ml and 19.3ng/ml) are found in the cerebral cortex and urine, respectively[32].

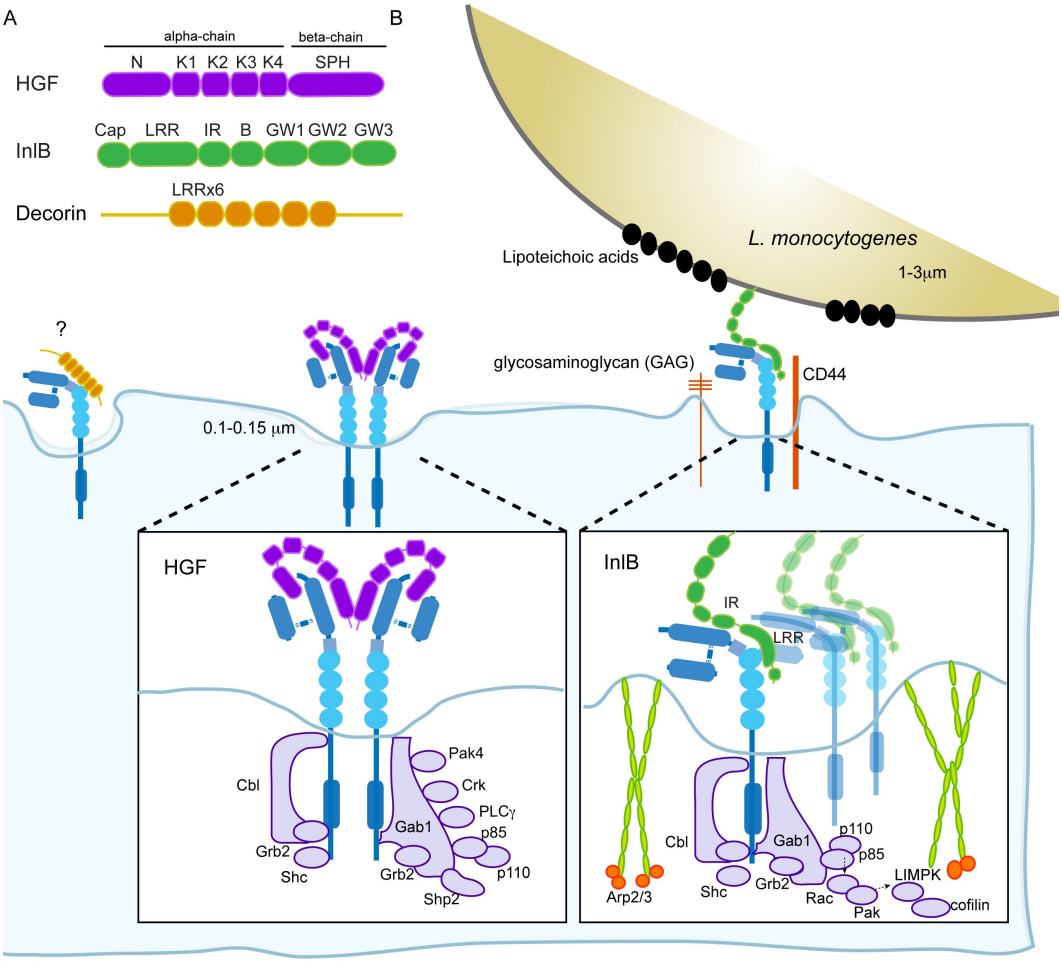


**Figure 1.2. Known Met receptor ligands and signalling complexes.** Three ligands have been reported to date for the Met receptor, hepatocyte growth factor receptor (HGF), Interlin B (InlB) and Decorin. A. Structural domains of the 3 Met ligands, (N=amino-terminal domain, K= kringle domain, SPH=serine proteinase homology domain, LRR=Leucine Rich Repeats, IR= interrepeat Immunoglobulin-like region, B= B-repeat, GW=GW domain). B. HGF binds to the Sema domain of Met to activate its phosphorylation. Met activation results in the recruitment of adaptor molecules (Cbl, Shc, Grb2 and Gab1). Gab1 acts as a scaffold for additional proteins such as Pak4, Crk, PLC gamma, p85-p110 (PI3K) and Shp2 to activate downstream pathways. InLB binds predominantly through the Ig-like 1 domain of Met. Activation of Met results in the recruitment of Cbl, Grb2, Shc and Gab2. Activation of PI3K leads to actin rearrangments, likely through a Rac1, Pak, LIMK-1, cofilin and Arp2/3 pathway. Please refer to text for further details.

### 1.2.3. Ligand Binding

Active HGF requires the N and Kringle (NK) domains in the alpha chain in order to activate the Met receptor[33]. Binding occurs in a 2:2 ratio with the Sema domain of the Met receptor[33] and also the IgG3 and IgG4 domains[34]. How ligand binding induces Met receptor dimerization and activation is currently unclear. Due to the pivotal role of Met activation in tumor initiation and progression, alternatively spliced NK1 fragments engineered with mutations that inhibit dimerization are now being developed as possible antagonists for cancer treatment[35]. Additionally, HGF has also been shown to interact with glycosaminoglycans, which may compete out Met-HGF interactions. Glycosaminoglycan (GAG) mimics are thus another target for therapeutic intervention[36].

The bacterial surface protein Internalin B (InlB) found on the surface of *Listeria monocytogenes*, binds to Met and mimics the function of HGF to cause activation of the Met receptor during infection[25]. Engagement of InlB with the Met receptor triggers intracellular signals within the host cell leading to cytoskeletal actin rearrangements, which are required for bacterial engulfment[37,38]. In this way, the bacteria can gain entry and infect the host cell.

Despite both eliciting Met activation, InlB and HGF do not share structural homology and activate the receptor through distinct binding surfaces[39]. This is in agreement with the observation that HGF and InlB do not compete with each other[25]. InlB binds to the IgG1 domain of the Met receptor whereas HGF contacts the Sema domain of Met[40] (Figure 1.2). Binding of InlB occurs mainly through the first Ig-like domain (Ig1) of the Met receptor as no significant increase in binding affinity was detected by appending additional Ig-like domains as assayed using solid-phase binding[41]. The structure of InlB in complex with the binding region of the extracellular region on Met has now provided further details into the distinguishing features of this interaction. The leucine-rich repeats (LRR) domain of InlB contains eight ß sheets that form a concave surface with the Ig1 domain of Met. This interaction then allows the interrepeat Ig-like region (IR) of InlB to make a secondary contact with the Sema domain, in what the authors refer to as a

"molecular clamp"[41]. While the unbound receptor exists in a flexible state, ligand binding restricts movement of the Sema domain to lock the receptor into an active conformation. This is in agreement with experimental data showing that while the LRR domains are sufficient for mediating an InlB-Met interaction, it is unable to activate the Met receptor without the addition of the IR domain[25,42].

Other molecules such as lipoteichoic acid, heparan sulphate proteoglycans (HSPG) and CD44 may also enhance activation of ligands for Met by promoting receptor clustering[43]. Indeed, certain cancer cells may require CD44 isoforms for HGF-Met activation[44].

### 1.2.4. HGF/Met in Development

Mice with genetic ablation of *HGF* or *Met* die *in utero* owing to placental defects in the survival and growth of trophoblasts[45,46]. These mice also have reduced liver size due to decreased proliferation and increased apoptosis of hepatocytes. Another important characteristic of *HGF-/-* and *Met-/-* mice is the inability of skeletal muscle precursor cells to delaminate from the dermomyotome to the limb bud[47]. This defect is not due to incorrect cell formation but an inability to undergo long range migration[48]. The finding that HGF is expressed along the path and final destination of these cells demonstrates a requirement for Met signalling in both the initiation and maintenance of migratory signals[11]. Additionally, neuronal development defects have been reported in *Met* null mice[49], however whether these are indirect or direct consequences of Met signalling has not yet been determined.

### 1.2.5. HGF/Met in the Adult

HGF and Met are widely expressed in tissues of the adult[50]. HGF/Met coordinates wound healing in various organs such as the liver[51,52], heart[53] and kidney[54]. Specifically, HGF is upregulated in response to cytokines such as interleukin-1 and interleukin-6[29] and can attenuate the renal inflammatory response following acute renal injury[55]. Met expression has also been observed to be highest within the most severe regions of kidney damage[56]. In agreement with the role of HGF/Met as a protective factor *in vivo*, treatment with HGF prior to or shortly after injury has been shown to increase proliferation[57] and regeneration of hepatocytes[29] and suppresses apoptosis in cardiomyocytes[53] following injury to the liver and heart respectively.

### 1.2.6. HGF/Met in Disease

Met derives it's name after the "Methyl" group of the chemical *N*-methyl-*N*'-nitro-*N*-nitroso-guanidine (MNNG) which was used to treat human osteosarcoma (HOS) cells during a transformation assay screen for oncogenes in the early 1980s[58]. As Met was one of the first oncogenes identified that was not formally discovered as a viral-oncogene, it should not be referred to as c-Met.

Follow-up studies showed that the transforming gene was a chromosomal translocation of *tpr* (translocated promoter region) on chromosome 1q25 and *met* on chromosome 7q31[59,60]. Tpr contains a dimerization leucine-zipper motif, and *met* was found to encode a protein homologous to src and the tyrosine kinase domains of the insulin receptor and v-abl[60,61] thus the fusion protein results in the constitutively active kinase domain of Met[62].

Since it's identification, the Met receptor has been linked to many human pathologies, ranging from tissue degeneration to cancer. Several experimental studies have demonstrated a role for HGF/Met in cancer. Over-expression of Met and HGF in cell lines are tumorigenic and metastatic when injected into nude mice[63] and conversely, downregulating Met or HGF in tumor cells decreases their tumorigenicity[64]. Interestingly, other oncogene-driven tumors (such as Ras-transformed cells) have been shown to transcriptionally upregulate *Met* to

promote tumorigenesis[65,66]. Transgenic expression of Met and HGF[67] results in mice with diverse histological tumors. When specifically targeted to the mammary epithelium of mice, expression of an oncogenic Met induces tumors with multiple phenotypes and importantly, is reflective of luminal and basal subtypes of human breast cancer[68,69]. Additionally, Met has been shown to be expressed in carcinomas and its over or mis-expression correlates with poor prognosis[11,70-72]. A complete table of Met and cancer can be found at: http://www.vai.org/met/. A short summary of some of the most common types of dysregulation of Met in cancers follows.

#### 1.2.6.1. Somatic Mutations

Mutations within the juxtamembrane and kinase domain of Met have been found in several carcinomas including hereditary and sporatic papillary renal cell carcinomas[73-75], gastric[76], head and neck[77], hepatocellular carcinomas[74] and non-small cell lung cancer[78]. Some of these mutations have been shown to increase Met activation[79,80], however the precise mechanism leading to cell transformation for many other mutations has yet to be elucidated.

#### 1.2.6.2. Amplification/Over-expression

Met has been found to be over-expressed in several cancers including osteosarcomas[81-84], gastric[85-88], gliomas[89-93], lung[94] and breast[95-101]. Activation of Met in these cases has been shown to occur through both autocrine and/or paracrine mechanisms[102] as serum levels of HGF are also elevated in some patients[103,104]. In breast cancer, Met expression has been reported to be raised by 15-20%[105] and importantly, as stated above, Met expression is an independent prognostic marker of poor outcome[11,70-72]. Of the different subsets of breast cancer, Met expression correlates with the most highly aggressive, poor outcome class known as the triple negative or basal group[70] and thus these types of basal cancers may benefit from anti-Met treatments.

#### 1.2.6.3. Genetic Re-arrangements

Many cancers exhibit genetic re-arrangements resulting in chromosomal translocations, DNA insertions or deletions. An alternatively spliced isoform of Met has been identified in lung[106] and gastric[107] cancer. This deletion removes exon 14 comprising the juxtamembrane domain of Met, and importantly, results in a receptor lacking the Cbl-binding site (see later section on the Cbl adaptor). In agreement with earlier studies showing that loss of direct Cbl binding retards Met degradation and leads to sustained MAPK signaling[8,9,108], primary tumors harbouring this deletion show similar alterations in delayed Met downregulation and subsequent *in vivo* tumor growth[106].

## 1.3. MAJOR MET SIGNALLING PATHWAYS

Met is a potent regulator of epithelial mesenchymal transitions (EMT), cell scatter and invasion[109]. Several ligand-dependent signal transduction pathways lie downstream of Met including the mitogen-activated protein kinase (MAPK), phosphoinositide 3-kinase (PI3K)-Akt, signal transducer and activator of transcription protein (STAT) and nuclear factor-κb (NF-κB) cascades, which will be discussed in further detail later in this section. The HGF/Met axis induces prolonged signaling compared to most other RTKs corresponding to its ability to promote an invasive program. In contrast, RTKs that activate only a transient signal induce a proliferative rather than an invasive response[110]. How Met mediates a distinct signaling program using common signaling pathways, is still incompletely understood.

### 1.3.1. Met RTK Activation

In general, RTKs use a conserved mode of activation dependent on ligand-mediated dimerization[111]. The kinase domain of Met most structurally resembles the kinase domain of the insulin and fibroblast growth factor receptor kinases, folding into separate N-terminal and C-terminal lobes connected through an activation loop[112]. HGF-binding to the Met receptor induces dimerization[27,113] and

*trans*-autophosphorylation of twin tyrosine residues (Y1234 and Y1235) located within the activation loop of the kinase domain to activate it[7,114,115]. Once activated, the juxtamembrane and cytoplasmic tail of Met becomes phosphorylated and collectively, these create binding sites for Cbl tyrosine kinase binding TKB domain[116], src homology 2 (SH2) domain[117] and phosphotyrosine binding (PTB) domain[118] containing molecules. Characteristic of Met signalling, is the creation of a multifunctional docking site centered around phospho-tyrosines 1349 and 1356 and adjacent residues. These amino acids have been shown to be necessary and sufficient for all Met-mediated biological responses in the context of an activated receptor[119]. In particular, studies using intracellular Met chimeras with extracellular CSF-1R[15], NGFR[14] and EGFR[120] elicit biological responses attributed to HGF. Furthermore, in cells, mutation of Y1349/Y1356 is sufficient to abrogate the ability of Tpr-Met (an oncogenic variant form of Met) to cause transformation[119], epithelial cell dispersal and experimental metastasis[121], while knock-in mice with phenylalanine substitutions results in an embryonic lethal phenotype similar to what is observed in the Met and HGF knockout mice[122].

### 1.3.2. Scaffold and Adaptor Recruitment

First discovered over 15 years ago[123-128], scaffold proteins facilitate the physical association of molecular complexes in many signaling pathways[129]. The Met signaling axis is no exception; the multifunctional docking site of Met has been demonstrated to activate and/or directly associate with Grb2[119,130,131], the p85 subunit of PI3K[119,131], PLCγ[119], c-src[119], Shc[132,133], Shp2[133], (SH2-domain-containing insositol 5-phosphatase) SHIP-1[134,135] and Gab1[136,137] (Figure 1.3). Moreover, Grb2 binds specifically to the pYXNX motif in Y1356 to indirectly recruit Shc, Gab1[138], Cbl[139], plus others and Gab1 in turn can recruit additional adaptor and signaling molecules (see below). Importantly, plasma membrane recruitment of adaptor proteins and scaffolds serves to increase the average lifetime of protein-protein signal transduction complexes[140]. The result of this is an enhancement of 1000-fold in downstream signaling[140]. Thus Grb2 and Gab1 recruitment serve to

amplify Met signaling. Due to steric restraints, two proteins cannot physically occupy both pY1349 and pY1356 of the same Met protein simultaneously[11,135], however many of these association have been shown to occur with rapid rates of association and dissociation[119] and could be associated in complexes formed by dimeric or higher order complexes of Met. Thus Met activation orchestrates composite and dynamic signaling complexes. Hence, one of the prevailing questions for Met signaling, is how are these complexes spatially and temporally regulated.

Additional documented associations with Met include Grb10[141], STAT3[142] and FAK[143]. As well, Y2H screening has identified SNAPIN, DCOHM, VAV-1, SNX-2, DAPK-3, SMC-1, CENPC, and hTID-1[144] as Met interacting partners. The relevance of most of these interactions *in vivo* however, has yet to be fully tested.

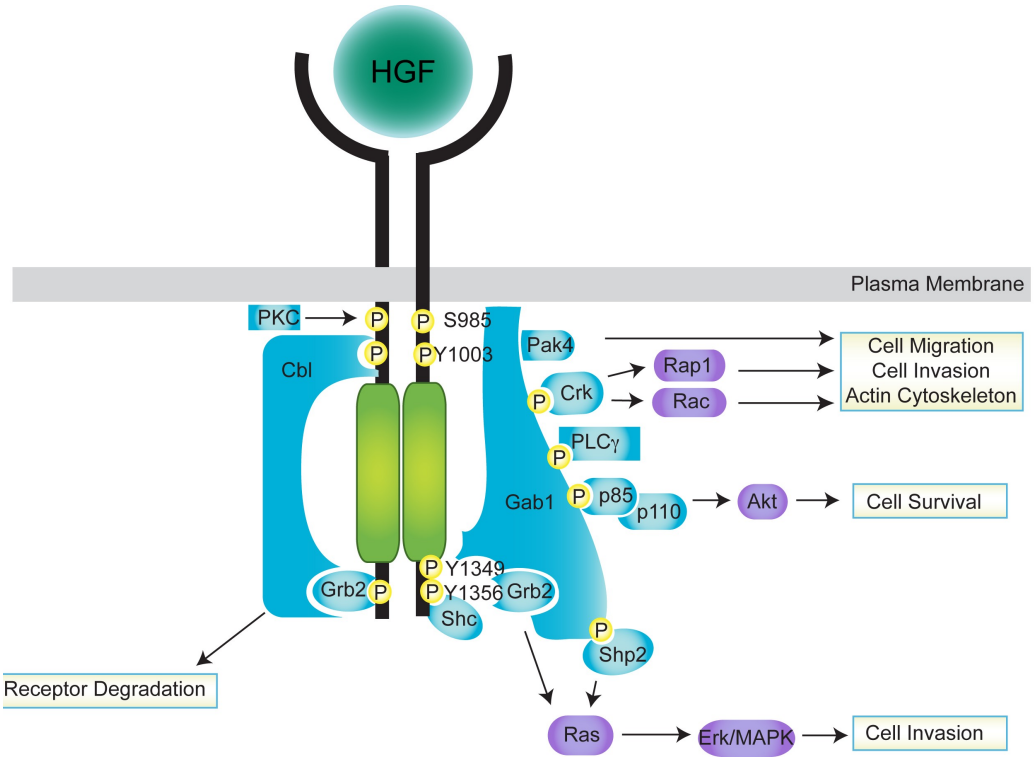


**Figure 1.3. Met RTK and major adaptor and scaffold proteins**. Listed are the major scaffold and adaptors recruited to the Met receptor and the downstream pathways activated upon ligand stimulation. Please refer to text for further details. Modified from ref.[145].

#### 1.3.2.1. The Gab1 Scaffold

Gab1 warrants a brief section in its own right owing to the fundamental and unique role it has in Met signal transduction. Several lines of evidence stemming from genetic and cell biology-based experiments support a requirement for Gab1 in Met signaling, however only a brief summary will be given here.

As stated previously, Gab1 can be recruited to Met via Grb2 through two proline rich motifs, one of which is atypical (PXXXR)[138]. In addition, Gab1 can be directly recruited to Met through a unique 13 amino acid sequence encompassing Y1349 known as the Met binding domain (MBD)[146]. This direct recruitment of Gab1 allows for prolonged phosphorylation and signaling of Gab1[109,110] downstream of Met and does not occur downstream of EGF. Gab1 is able to recruit several key adaptors to Met including Shc[147], Shp2[147], Crk, Crk L [147], PI3K[147], PLCγ, Pak4 [148], p12-Ras-GAP, Nck1/2[149] and N-Wasp[149,150].

Genetic deletion of *Gab1* results in a strikingly similar (yet slightly attenuated) phenotype to *Met* null animals, including impaired migration of muscle precursor cells, reduced liver size and placental defects[151]. In cell models, Gab1 recruitment to Met is required for branching tubulogenesis[136]. Met mutants impaired in Gab1 recruitment fail to form tubes and this can be rescued by Gab1 over-expression[137,147]. Thus, although Gab1 is recruited downstream of several receptors, the evolutionary selection of a direct Met-Gab1 interaction seems to be a unique attribute in the contribution of Gab1 as a pivotal scaffold protein in the transmission of Met signals.

#### 1.3.2.2. The Cbl Adaptor

In addition to positive regulatory signals generated by adaptor recruitment to Met, Met also recruits the E3 ligase Cbl which serves to negatively regulate Met signaling. Cbl is able to directly bind to protein tyrosine kinases through its tyrosine kinase binding (TKB) domain or indirectly through the adaptor proteins Grb2 or APS[152]. Ubiquitination of several RTKs including the colony-stimulating factor-1 receptor (CSF-1R)[153], the epidermal growth factor receptor (EGFR)[154,155], the Met receptor[9], Ron[156] and the platelet-derived growth factor receptor

(PDGFR)[157] occurs upon c-Cbl recruitment[8]. In the case of the Met receptor, Cbl is recruited to the juxtamembrane domain of Met via a DpYR motif located around Y1003[9,116].

As ubiquitination was originally demonstrated to target proteins to the proteasome for degradation, Cbl-mediated ubiquitination of RTKs for proteasomal degradation seemed a plausible mechanism for inducing receptor downregulation. Later work however, demonstrated that ubiquitin serves as an important tag for entering the lysosomal-degradative pathway. Prior to the commencement of this thesis, several significant contributions surrounding Cbl and the ubiquitination field were made, in our lab and others (see Figure 1.4 for a timeline summary). Pivotal was the discovery that loss of RTK ubiquitination constitutes a mechanism that can lead to tumorigenesis[9]. This served as a foundation for the working hypothesis of this thesis, that additional endocytic regulatory mechanisms exist and are required to maintain appropriate Met RTK function.

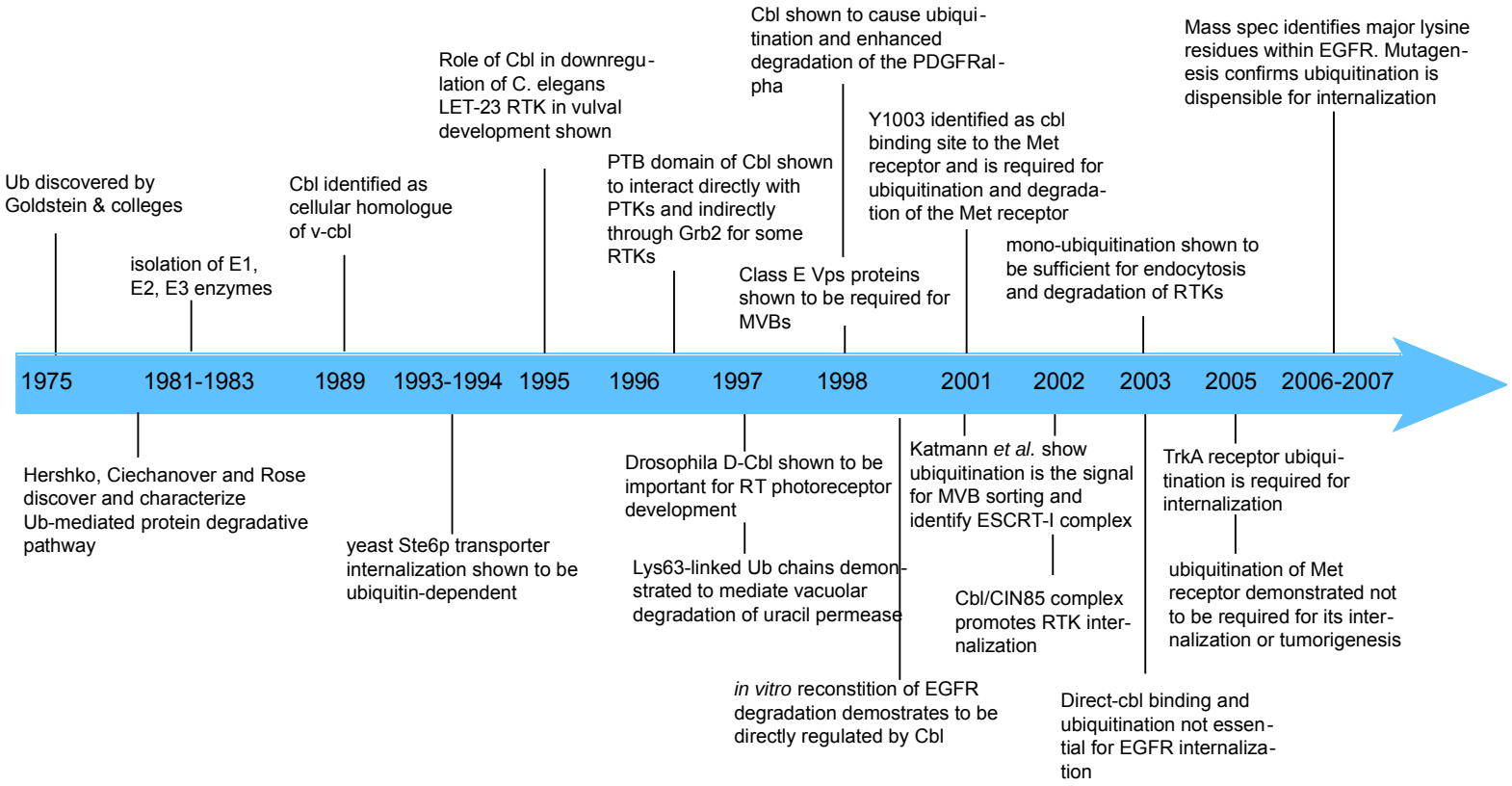


**Figure 1.4. Timeline of major events in RTK ubiquitination**. Key discoveries are placed according to their reported publication date. Due to space limitations, not all finding are shown. Refs from left to right: 1975[158], 1978[159] and 1980[160], 1981-1983[161,162], 1989[163], 1993-1994[164], 1995[165], 1996-1997[166-168], 1997 (Drosophilia[169], K63[170]), 1998 (PDGFR⋄[157], Class E[171] ),1999[155], 2001 (Y1003[9], Katmann[172]), 2002[173,174], 2003; top[175,176] bottom; [177], 2005 (TrkA[178], Met[108]), 2006-2007[179,180]

### 1.3.3. MAPK Signalling

The MAPK cascade is divided into three branches (extracellular signal-regulated kinases (ERKs), Jun amino terminal kinases (JNKs) and p38s), each composed of a hierarchy of serine/threonine kinases, which phosphorylate and activate a downstream kinase, namely (from top down) a MAPKK kinase (MAPKKK), a MAPK kinase (MAPKK) and finally a MAP kinase (MAPK).

#### 1.3.3.1. The ERK Pathway

Downstream of HGF, the SH3 domain of Grb2 binds proline rich motifs in the guanine nucleotide exchange factor, son-of-sevenless (SOS) to recruit it to the membrane and localizing it with Ras to promote Ras GDP exchange[181]. Ras activation recruits the first MAPKKK, Raf which phosphorylates MEK1 (MAPKK1) and MEK2 (MAPKK2) which then proceed to phosphorylate ERK1 and ERK2 (final MAPK). Once phosphorylated, the ERKs can translocate to the nucleus where they can phosphorylate a subset of transcription factors leading to regulation of gene expression.

The Raf-MEK-ERK pathway is also positively modulated through recruitment of Shp2 to Gab1. Shp2 recruitment results in the dephosphorylation of the p120-Ras-GAP binding site on Gab1, inhibiting p120-Ras-GAP from turning off Ras signaling and allowing sustained ERK signaling[182,183]. This has been shown to be required for the initial cell depolarization and migration during HGF-dependent epithelial morphogenesis[182,184]. Additionally, mice with liver specific deletion of either Gab1 or Shp2 have a reduced ability to regenerate after hepatic injury and show blunted ERK signaling[185]. Collectively this data supports cooperation between Gab1 and Shp2 in promoting ERK signaling.

Additionally, Gab1 and ERK1/2 both localize to lamellipodia[186] and dorsal ruffles[187] and are required for formation of these structures downstream of HGF stimulation. Thus, localized, spatial organization of ERK1/2 signaling complexes is likely to be an additional component of Met-mediated signaling.

#### 1.3.3.2. The JNK and p38 Pathways

The JNKs and p38 MAPKs are both activated through the small GTPase Rac. Rac activation through a Ras-PI3K pathway can stimulate MAPKKK1-MAPKKK4 (also called MEKK1-MEKK4) which in turn phosphorylate either MEK4 and MEK7 leading to JNK1, JNK2 and JNK3 activation or MEK3 and MEK6 leading to p38α, p38β, p38γ and p38δ activation[188]. Activation of the JNK pathway is required for anchorage-independent growth induced by Tpr-Met[189,190]. Moreover, transcriptional upreguation of cyclin D1 though activation of the transcription factor activating transcription factor-2 (ATF-2) occurs via p38 and JNK pathways downstream of HGF to induce mouse melanoma proliferation[191]. The p38 MAPK pathway has also specifically been shown to be important for HGF sensitization of ovarian cancer cells to chemotherapeutic cisplatin and paclitaxel[192,193].

### 1.3.4. PI3K-Akt Signalling

PI3K is composed of a regulatory p85 subunit and a p110 subunit. As mentioned above, PI3K can be recruited directly to Met or indirectly through Gab1. Additionally, PI3K can be activated through Ras. Activation of PI3K leads to the conversion of phosphatidylinositol-4,5-diphosphate (PIP2) to phosphatidylinositol-3,4,5-triphosphate (PIP3) in the plasma membrane resulting in the recruitment of pleckstrin homology (PH) domain containing proteins, including Gab1 and Akt. Importantly, PH-dependent recruitment of Gab1 is required for its localization to sites of cell-cell contacts, and the ability of Gab1 to promote HGF-dependent tubulogenesis[110]. Akt has many intracellular targets including regulators of apoptosis such as Bcl2 antagonist of cell death (BAD) and MDM2[188], cell cycle regulators such as glycogen synthase kinase 3β (GSK3β) and mammalian target of rapamycin (mTOR).

### 1.3.5. STAT and NF-kB Signalling

Downstream of Met, STAT3 is tyrosine phosphorylated at residue 705[142] and required for HGF-induced invasion[194] and tumorigenesis[195]. Interestingly, Met localizes with STAT3 on endosomes and trafficking of Met to a perinuclear localization has been shown to be required for the nuclear accumulation of STAT3[196]. In the nucleus, STAT3 controls transcription through binding to the specific promoter element Sis-inducible element (SIE)[142] to control cell proliferation and differentiation. HGF can also activate NF- kB through an Akt and Src-dependent pathway[197]. Translocation of NF- kB leads to the transcription of multiple genes to impinge on cell proliferation[198], epithelial tubulogenesis[198] and cell survival[197,199] pathways.

### 1.3.6. Membrane Localized Signalling

Classic views of RTK activation show plasma membrane localization and subsequent recruitment of signaling complexes to the plasma membrane. Originally plasma membrane localization was thought to increase the rate of encounter of signaling molecules, however, more recent views suggest that functionally, membranes serve to increase the number of functional signaling complexes by extending their life-time of encounter[140]. The same principles of membrane recruitment of signaling complexes can also be extended to subcellular organelles, such as endosomes. Endosomes have been shown to localize signaling molecules[200] and thus may act as intracellular signaling 'platforms'[201]. In agreement with this hypothesis, computational modeling of EGFR signaling, taking into account receptor trafficking, reveals that intracellular compartments are crucial for the generation of specific signals[202]. Thus the emerging understanding is that localized membrane-mediated signaling microenvironments are important aspects in the generation and maintenance of RTK signaling.

## 1.4. ENDOCYTOSIS

Discoveries on endocytosis can be traced back as early as the 1800s, when Maetchnikoff reported that litmus particles changed from blue (alkaline) to red (acidic) after being internalized into cells, indicating that these particles had became localized to an acidic compartment[203]. In 1964, electron micrographs of oocytes taken by Roth and Porter captured snapshots of the formation and pinching off of "bristle-coated" pits and vesicles[204], now commonly recognized as clathrin-coated pit and vesicles. This was later followed by Kanaseki and Kadota's images of hexagon and pentagon structures[205], a key finding in helping understand the molecular nature of how these structures are able to bend[203]. Further studies by Heuser[206] and Pearse, resulted in the purification of clathrin-coated vesicles and the main constituent, clathrin[207,208]. These were some of the first discoveries on what is now the best-studied pathway of internalization, the clathrin-mediated pathway. By the 1970's seminal work on the low-density lipoprotein (LDL)[209] and other nutrients demonstrated that extracellular molecules are aided in internalizing by binding to specific receptors. This helped formulate the basis of our current understanding of receptor-mediated endocytosis[203,210].

### 1.4.1. Receptor-Mediated Endocytosis

Cellular homeostasis requires that growth-factor mediated signalling be tightly modulated through the process of downregulation. For some time now, it has been well established that in response to ligand binding, RTKs are rapidly internalizated into the cell resulting in one of two fates; to be recycled back up to the plasma membrane or to be degraded in the lysosome.

Endocytosis is achieved through the assembly of protein-protein and protein-lipid complexes. Recruitment of a network of specific endocytic adaptor proteins couples cargo molecules to additional factors required for transport. These adaptor proteins harbour conserved protein and lipid interaction domains, which become stabilized upon growth factor stimulation. Formation of these complexes drives membrane curvature and helps package receptors into vesicles

(Figure 1.5).

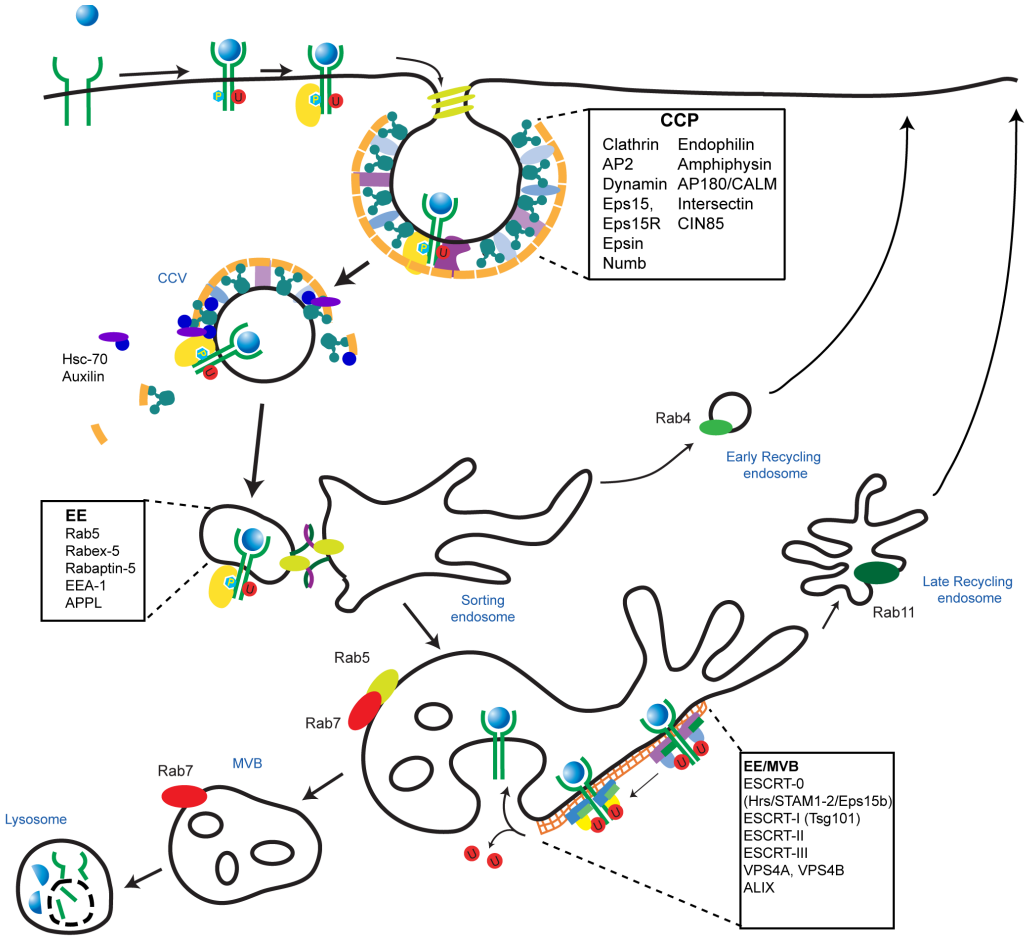


**Figure 1.5. The canonical clathrin-mediated pathway for RTKs.** Upon ligand stimulation, RTKs enter into clathrin-coated pits (CCPs), a process that is dependent on the recruitment of multiple endocytic adaptor molecules. Examples of these are shown. Upon release from the plasma membrane, nascent clathrin-coated vesicles loose their coat through the action of Hsc-70 and auxilin and undergo fusion with the early or sorting endosome. Also shown are typical proteins found at the early endosome (rab5, rabex-5, rabaptin-5, EEA-1 and APPL) which may aid targeting, tethering or fusion. At the sorting endosome, cargo proteins may be recycled through an early rab4 positive, recycling pathway, a late, rab11 positive recycling pathway or targeted into multivesicular bodies (MVBs) through the ESCRT complexes for degradative targeting to the lysosome in a ubiquitin-dependent manner.

#### 1.4.1.1. RTK Internalization

Receptor activation accelerates endocytosis and in general, is thought to concentrate receptors into clathrin-coated pits[211] although various other mechanisms of non-clathrin mediated internalization exist, including macropinocytosis, phagocytosis, caveolin-dependent endocytosis or a less well characterised clathrin- and caveolin-independent pathway (see ref.[212]). Proteomic studies have identified over 60 different proteins associated with clathrin-coated vesicles[213]. However, the basic proteins include the trimer clathrin, the heterotetrameric adaptor protein (AP) complex (AP-2) and accessory proteins. Changes in conformation in the juxtamembrane and intracellular region of the receptor expose hidden linear sorting motifs, which engage with these specialized adaptor proteins.

#### 1.4.1.2. Sorting Motifs

Sorting motifs generally fall into the following categories, tyrosine base motifs: NPXY or YXXΦ , dileucine motifs: [DE]XXXL[LI] or DXXLL, or others including: acidic clusters and ubiquitin[214]. Importantly, these signals are often saturable and of low affinity[214], consistent with their recognition by a limited number of endocytic adaptor proteins (Table 1.1). Thus the existence of multiple different types of motifs enables discrimination and flexibility amongst the entry of different cargo proteins.

In addition to plasma membrane derived clathrin-coats, clathrin-coated regions of the trans-Golgi network (TGN) and endosomes also contain adaptors for mediating protein sorting. Such additional adaptors include Epsin, Epidermal growth factor receptor pathway substrate 15 (Eps15), the monomeric Golgi-localized, γ-ear-containing, ARF-binding proteins (GGAs: GGA1, GGA2 and GGA3), the remaining members of the AP family (AP-1, AP-3 and AP-4), STAM1 and Hrs (Table 1.1).

#### 1.4.1.2.1. NPXY-Type Signals

NPXY tyrosine based motifs have been found to participate in the internalization of a subset of transmembrane proteins including the insulin and EGF receptors[214]. These motifs have been shown to bind directly to clathrin[215], adaptor protein 2 (AP-2)[216] and phosphotyrosine binding (PTB) domain proteins, such as disabled 2 (Dab2)[217]. Elucidation of which of these particular adaptors is most important in any one system has proven difficult as each of these proteins can form interactions with several other endocytic adaptor molecules. Additionally, there is likely to be redundancy among the adaptors, highlighting the plasticity of the system. Thus although individually each protein interaction is of low affinity, collectively these multivalent interactions serve to selectively recognize cargo.

#### 1.4.1.2.2. YXXΦ-Type Signals

The second type of tyrosine-based signal, the YXXΦ motif, is more prevalent than the NPXY motif and in addition to mediating internalization has also been found to direct sorting to lysosomes[218,219] and basolateral targeting in polarized epithelial cells[220,221]. Thus, several receptors contain these motifs including the transferrin receptor, cation-dependent and independent mannose-6-phosphate receptors (M6PR), LAMP-1, LAMP2, TGN38 and furin[214]. These motifs are recognized by the entire family of adaptor proteins (AP-1, AP-2, AP-3 and AP-4) through the μ subunit[222] with varying preferences and affinities ranging from 0.5-100 μM[222-224]. Additional surrounding residues and the exact nature of the "XXΦ" residues as well as the position of the motif within the cytoplasmic tail all aid in determining the specificity and strength of the signal. For example, YXXΦ motifs that serve in lysosomal targeting often contain a glycine residue prior to the tyrosine[219] and acidic residues in the 'X' positions[225]. Available structural data on AP-2 binding indicates that the μ subunit undergoes large conformational changes upon binding which may occur through threonine phosphorylation [226], possibly through AAK1 kinase[227]. Additional regulatory control of AP-2 recruitment occurs through phosphoinositide-binding [224] and interactions with associated binding partners.

#### 1.4.1.2.3. Dileucine Motifs

Dileucine motifs conforming to [DE]XXXL[LI], like YXXΦ motifs, mediate internalization, lysosomal and basolateral targeting[214]. Although both of these motifs are recognized by AP complexes, they do not compete with each other indicating that different site(s) are used to recognize dileucine motifs from tyrosine motifs. Originally, differing reports of the entire[228] μ subunit, a 119-123 segment[229] of the μ subunit and the beta-subunit[230] were all identified to interact with these dileucine motifs. However, more recent analyses suggest that the sigma subunit is primarily responsible for mediating binding[231].

Distinct from the above dileucine motif, DXXLL motifs form a separate class of sorting signal, which are not recognized by AP complexes but by the GGA family of proteins[232,233]. Typically found in receptors that cycle between the *trans*-Golgi network (TGN) and endosomes[214], these signals are highly dependent on the Asp residue and are often found in regions containing acidic clusters and/or adjacent serine residues. Biochemical analysis has revealed that the VHS domain of the GGA proteins binds to dileucine motifs within a broad range of affinities, between 5-100μM[234,235]. Interestingly, other VHS-domain containing proteins, including Hrs, STAM1, TOM1 and TOM1L1 proteins do not bind to DXXLL motifs[232]. Crystollography of the VHS domain with the DXXLL from M6PR peptides has confirmed the specificity of this interaction[234,236] and confirmed the increased affinity with an upstream phosphorylated serine residue[235].

#### 1.4.1.2.4. Acidic Clusters

Acidic cluster motifs as its name implies, contain acidic residues that often contain sites for phosphorylation by casein kinase II (CKII). These have been show to mediate retrieval of proteins from endosomes to the TGN. Recognition of these phosphorylated sites occurs through the adaptor protein, phosphofurin acidic cluster sorting protein 1 (PACS-1)[237,238] which may help link cargo to additional sorting factors including AP-1 or AP-3[214]. Interestingly, serine phosphorylation has also been observed to modulate endocytosis of CD4 upstream of an atypical dileucine motif[231] possibly through disruption of interaction with p56-LCK, a src-family non-RTK[239]. It has also been suggested that the alpha subunit of AP-1 and

AP-3 may engage with acidic cluster motifs[240]. Thus, many aspects of the regulation and function of these motifs are still unknown.

#### 1.4.1.2.5. Ubiquitin as a Sorting Signal

In some instances, ubiquitin can also serve as a critical internalization sorting signal, as has been most notably defined with genetic studies in *S. cerevisiae*. Yeast essentially lack all traditional tyrosine and dileucine-based sorting motifs and do not require AP2-like adaptors for endocytosis[241,242]. For example, in yeast cells harbouring either endocytic or ubiquitin-conjugating enzyme deficiencies, the transporter protein, Ste6p accumulates as a ubiquitinated protein at the plasma membrane[164]. Additionally, mutation of a single lysine residue to arginine of Ste2p (a GPCR yeast protein), has been shown to prevent both ubiquitination and endocytosis of this receptor[243,244]. Interestingly, Lys63-linked ubiquitin chains, were demonstrated to mediate the vacuolar degradation of the uracil permease in yeast through a proteasome-independent pathway[170] and were later shown to also be important in mammalian systems[245]. Structural studies on Lys63-linked chains show that Lys63-chains adopt a more extended conformation than Lys48-linked chains, providing molecular evidence of how these different chain types may be differentially recognized[246].

In mammalian cells, the ubiquitination of the TrkA receptor has also been demonstrated to serve a similar function. Expression of ubiquitin harbouring a lysine mutation to inhibit K63-linkages (K63R) or using brain extracts from E3 TRAF6 null mouse resulted in decreased TrkA ubiquitination, and subsequent loss of internalization, differentiation and survival signals[178]. Although these findings were quickly extended to other receptors including RTKs[173,174], more recent studies on both the Met[108] and EGF[179,180] receptors have convincingly demonstrated that the chief function of RTK ubiquitination is not to mediate internalization. Indeed, identification and mutation of the major lysine residues involved in EGFR ubiquitination does not inhibit receptor internalization[179,180]. Instead, these ubiquitination-defective RTKs show post-internalization trafficking deficiencies: the Met receptor is unable to efficiently engage and phosphorylate the endocytic MVB sorting protein Hrs[108]. This results in impaired protein degradation leading to receptor protein stabilization and sustained Ras-MAPK

signaling[108]. The EGFR equivalent also shows defects in receptor downregulation[155], but not internalization[177]. This indicates that while ubiquitin is critical in certain systems, such as yeast, to mediate clathrin coat assembly, multiple adaptors proteins have since evolved to mediate this function in mammalian cells and provide redundancy to ensure proper RTK down-regulation.

| Protein Adaptor | Sorting Motif |
|---|---|
| AP-1/AP-3 | YXXΦ<br>[DE]XXXL[LI] |
| AP-2 | YXXΦ<br>[DE]XXXL[LI] |
| AP-4 | [DE]XXXL[LI] |
| Clathrin | NPXY |
| Dab2 | NPXY |
| Epsin | Ubiquitin |
| Eps15 | Ubiquitin |
| GGA1/GGA2/GGA3 | DXXLL<br>Ubiquitin |
| HRS | Ubiquitin |
| STAM1/2 | Ubiquitin |
| PACS-1 | Acidic Cluster |

**Table 1.1. Adaptors and sorting motifs found in endocytosis.** Identified protein adaptors and their recognition motifs. Single letter amino abbreviations have been used. Φ designates any bulky amino acid with a hydrophobic side chain.

#### 1.4.1.3. The Eps15 Adaptor

Epidermal growth factor receptor pathway substrate 15 (Eps15), was first identified in a screen for tyrosine-phosphorylated substrates of the EGFR[247]. It has been observed to colocalize in clathrin-coated pits and vesicles with the EGF receptor upon EGF stimulation[248,249]. It acts as a molecular scaffold by forming several associations with other adaptors including AP-2, Epsin and Hrs[250-253]. It contains three Eps15 homology (EH) domains in the amino-terminus which target it to the plasma membrane through interactions with proteins containing the tripeptide motif asparagine-proline-phenylalanine[254] and direct binding to phospholipids[255,256]. It also contains a coiled-coil domain, which mediates homo- and heterodimerization[257] and which we show is necessary and sufficient for association with the Met receptor (see Chapter 2). This is in contrast to the EGFR, which primarily associates with Eps15 through the Eps15 c-terminal UIM domain[258-260]. Downstream of other RTKs including insulin, platelet-derived growth factor or keratinocyte growth factor[248,261] receptors, Eps15 is not tyrosine phosphorylated and no role for Eps15 has been identified.

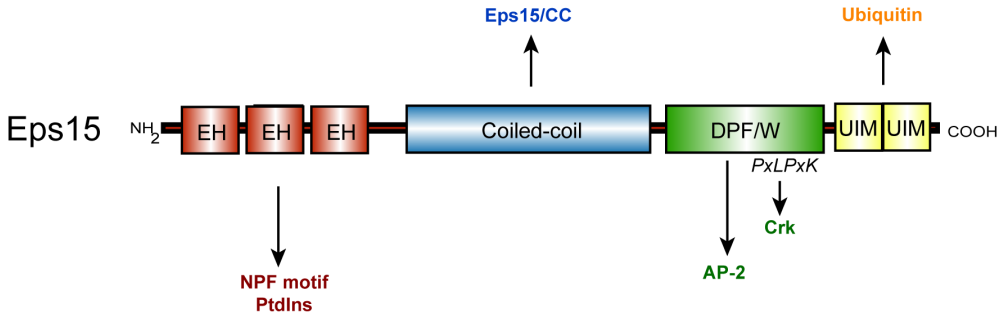


**Figure 1.6. Schematic of Eps15 and its major interactors.** Individual domains of Eps15 have been given different colours. Arrows in each domain point to specific proteins or motifs shown to be recognized by Eps15 for that domain. Please refer to text for further details.

#### 1.4.1.4. Clathrin-Coat Assembly and Budding

In general, clathrin-coat assembly is composed of sequential steps of nucleation, growth, stabilization, invagination, scission and uncoating (Figure 1.7). Cargo capture (driven by sorting motif and adaptor protein recruitment) likely occurs simultaneously, with the initial nucleation and growth of clathrin-coated structures and biases the system towards forming productive budding events[262]. The "recruitment signature" of 34 different proteins, belonging to seven different subgroups has recently been identified in mammalian cells[263] and is consistent with similar results obtained previously in yeast[264] (Figure 1.7). Clathrin and adaptors are the first proteins recruited to the plasma membrane and are observed to build up slowly within a forming bud, maximally peak at scission then drop off during the uncoating process[263]. Several endocytic proteins including AP-2, Epsin N-terminal homology (ENTH) and AP180 N-terminal homology (ANTH) domain containing proteins, such as epsin, and (clathrin assembly myeloid lymphoid leukemia) CALM, preferentially bind to phosphatidylinositol-4,5-bisphosphate PI(4,5)P2 which becomes highly enriched at sites destined to become clathrin-coated pits[265] and are likely assembled during cargo loading. Within this group of proteins, a subset of adaptors have been observed to drop off prior to the departure of clathrin, suggesting that these proteins segregate within the nascent bud and/or are removed prior to clathrin disassembly[263].

It is now generally accepted that actin polymerization is involved in most types of clathrin-mediated endocytosis[266-269]. Interestingly, neuronal Wiskott-Aldrich Syndrome protein (N-WASP), an Arp2/3 complex activator, has been observed to be the first actin machinery protein complex recruited to forming clathrin-coated pits, and is recruited significantly earlier than other actin regulatory factors[263]. Subsequent recruitment of positive regulators of actin polymerization, including Arp3, Abp1 and cortactin occur prior to pit severing, while negative regulators including cofilin and coronin are maximally recruited post-scission[263].

A third group of proteins involved in clathrin-coated vesicle (CCV) formation includes the (BIN-amphiphysin-RVS) BAR family of proteins. N-Bar-containing proteins, such as amphiphysin, and endophilin partially intercalate into

the inner plasma membrane leaflet to aid in membrane curvature[270]. These proteins are rapidly recruited to aid in constriction and disassembled during the scission process. Interestingly, the F-BAR proteins CIP4 and FBP17 show complex biphasic kinetics of recruitment during CCV formation, distinct from the other BAR containing proteins[263]. After membrane curvature, the final step in vesicle formation involves abscission of the neck region. This is accomplished through the mechanochemical energy provided by the large GTPase dynamin.

Following dynamin-mediated scission, the newly-formed vesicle quickly sheds its clathrin-coat through dephosphorylation of PI(4,5)P2 into PI(4)P by synaptojanin[265] and recruitment of Hsc70 by its co-chaperones auxilin or cyclin-G–associated kinase (GAK)[271]. The final module observed to be recruited during CCV formation includes the GTPase Rab5 and its effector, APPL1.

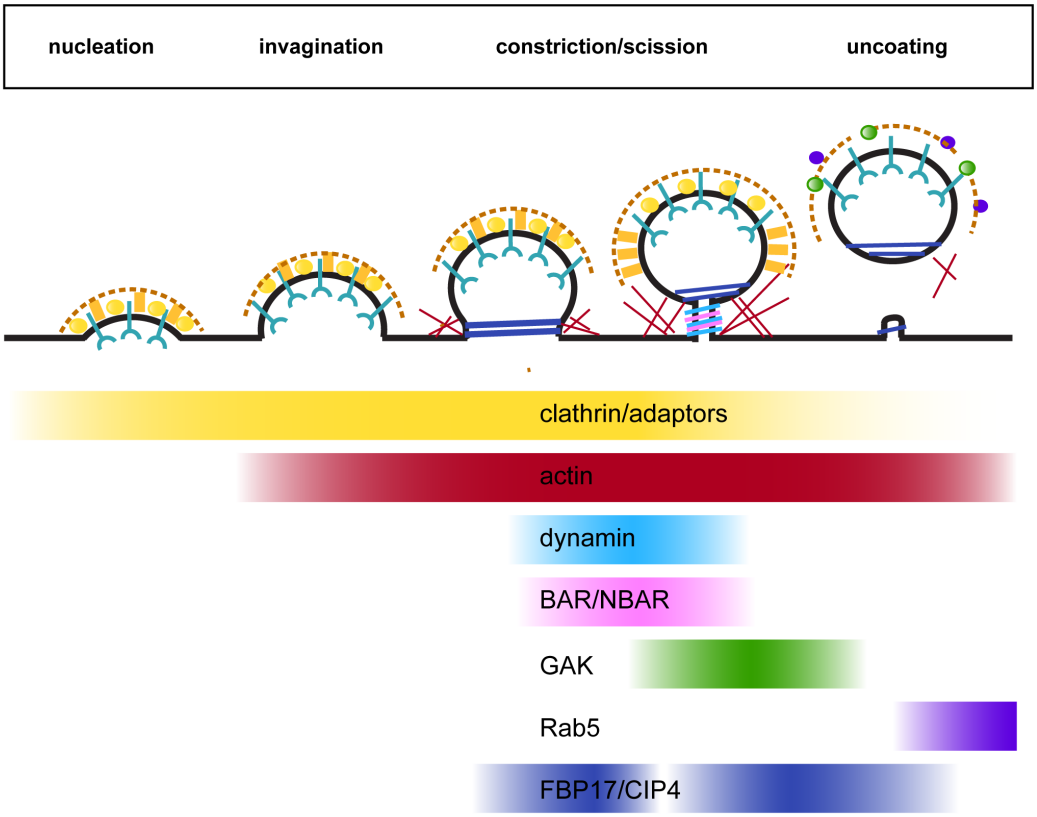


**clathrin module**: (Clathrin light chain, epsin2, CALM, NECAP, AP-2, Eps15, FCHo1, FCHo2)

**actin module**: (Arp3, Abp1, cortactin, LifeAct (F-actin), cofilin, coronin, SNX9)

**dynamin module**: ( dynamin1, Hip1R, Dynamin2, myosin6, N-WASP, Eps8, myosin1E,synaptojanin2beta1, syndaptin2)

**BAR/NBAR module**: ( Amphiphysin1, BIN1, Endophilin2)

**GAK module**: (GAK, OCRL1, ACK1)

**Rab5 module**:( Rab5, APPL)

**FBP17/CIP4 module:** (FBP17/CIP4)

**Figure 1.7. Steps of clathrin-mediated internalization**. Shown are the temporal dynamics of recruitment of 7 major groups of adaptor proteins. Clathrin-mediated internalization is shown as sequential steps of nucleation, growth, stabilization, invagination, scission and vesicle uncoating.

#### 1.4.1.5. Transport Through Endosomes

From the plasma membrane, small endosomes undergo homotypic or heterotypic fusion with sorting endosomes, often simply referred to as early endosomes. These endosomes are characterized by being peripherially located, small (~50nm) and slightly acidic (~pH 6.0). Importantly, they are highly enriched in PI(3,4,5)$P_3$ and Phosphatidylinositol 3-phosphate (PI(3)P), due to the presence of Class I and II PI3Ks[272]. PI(3)P recruits proteins containing zinc finger motif FYVE domain containing proteins such as early endosomal antigen 1 (EEA1)[273] a key component of the endosomal membrane docking and fusion machinery and mediates its specific localization to early endosomes.

In general, endosome tethering and fusion are regulated by Rab GTPase and SNAREs (soluble N-ethylmaleimide-sensitive factor attachment protein receptors)[274]. Like other small GTPases, the Rabs cycle between their cytosolic GDP-bound and membrane-bound GTP-bound (guanosine triphosphate) states. The activity of Rab GTPases is governed by the amount of protein in its GTP-bound (active) versus GDP-bound (inactive) form. GDP/GTP exchange promotes conformational changes, which are required for their interaction with regulatory, and effector proteins[275,276]. The localized action of Rabs contributes to the functional identity of endocytic compartments and makes them ideal markers to follow receptor trafficking. To date, more that 60 Rabs have been identified in the human genome, highlighting the complexity and high degree of regulation of the vesicular transport system[277].

The plasma membrane and early endosomes contain Rab5[278], which functions in the fusion of early endosomes in a GTP-dependent manner. Several Rab5 effectors, which specifically bind to GTP-bound Rab5, have been identified, including class I and II PI3Ks, EEA-1 and Rabaptin-5. Rabaptin-5, for example, has been shown to aid in membrane fusion and docking events[279]. It does so in part by recruiting the Rab5 GEF, Rabex-5[280] and together, Rapabtin-5/Rabex-5 synergize to promote homotypic fusion[281] . In addition to Rabaptin-5 mediated recruitment, a pool of membrane-bound Rabex-5 is directly recruited to Rab5 through an early endosomal targeting (EET) domain[280]. Thus the dual recruitment of Rabex-5 (directly through the EET and indirectly through Rabaptin-5) contributes to maintaining Rab5 activity on early endosomes.

The early endosome accepts incoming endosomes for a brief period of time before being transported along microtubules and maturing into a late endosome[282]. During this time, cargo at the early endosome may be quickly recycled back up to the plasma membrane through tubular-extensions of the early endosome, transported to the endocytic recycling compartment (ERC), or progress to the late endosomal compartment.

#### 1.4.1.6. Degradative Targeting

Endosomes transitioning from early to late endosomal compartments are accompanied by the gradual loss of Rab5 and the acquisition of Rab7. In yeast, conversion has been shown to be controlled by the protein SAND-1/Mon1. SAND-1/Mon1 simultaneously coordinates inhibition of Rab5 activation, through de-localization of the Rab5 GEF, Rabex-5, and activation of Rab7 through the recruitment of the Rab7 GEF, HOPS complex[283].

Concomitant with endosome maturation, receptors progressing to late endosomes are captured into flat clathrin-bilayer regions of the endosome[284]. From here, the limiting membrane of the late endosome can invaginate, bud into the lumen, and result in the formation of a multivesicular body (MVB)[172]. This is a critical step in receptor downregulation, as once sequestered in an intraluminal vesicle (ILV), the signalling competent c-terminus of the receptor is occluded from cytosolic signal transduction proteins[285].

First discovered in yeast[286], specialized proteins containing ubiquitin-recognition motifs recognize ubiquitinated transmembrane proteins for sorting. Through screens, genes required for vacuolar protein sorting (Vps) of which a subset of these- the class E, have been identified to be required for sorting of MVB cargo. These proteins assemble into large complexes known as the endosomal sorting complex required for transport (ESCRT)s[287]. As homologues for most of the class E Vps proteins exist in mammalian cells, ubiquitin-mediated sorting through ESCRT complexes represents a highly conserved mechanism for targeting proteins for degradation. In support of ubiquitination as a sorting signal, the transferrin receptor, which normally recycles and is not generally degraded, can be made to enter the degradative pathway through fusion of ubiquitin to its c-terminus[288]. Recognition of ubiquitinated cargo is performed sequentially by four

ESCRT complexes, namely, ESCRT-0, -I, -II and -III[287,289-291]. ESCRT-0 is composed of the subunits hepatocyte growth factor–regulated tyrosine kinase substrate (Hrs), Eps15b and signal-transducing adaptor molecules STAM1 or STAM2 (often just referred to as STAM)[253,292]. Altogether, ESCRT-0 contains five ubiquitin binding domains[293] for clustering ubiquitinated cargo. Initially, ESCRT-0 is recruited to early endosomes through the FYVE and coiled-coil domains of Hrs via phosphatidylinositol-3-phosphate (PtdIns3P) interactions[294]. Hrs is responsible for recruiting clathrin, STAM and ESCRT-I to early endosomes[292] and initiating intraluminal vesicle formation[295]. Hrs contains a Ub Interaction Motif (UIM) which recognizes and recruits ubiquinated proteins to the flat clathrin microdomain[288,296,297]. Importantly, depletion of Hrs impairs EGFR[295] and Met receptor degradation[298]. From ESCRT-0, cargo is handed off to ESCRT-I[299] through interaction between the Hrs and Tsg101 subunits respectively[300-302]. ESCRT-II can then be recruited via ESCRT-I and PI3P[303,304]. Finally ESCRT-III is recruited via ESCRT-II[305,306]. Together ESCRT-II and –III drive membrane budding[307]. ESCRT-III, through the recruitment of deubiquitinating enzymes (DUBs) may also aid in recycling ubiquitin prior to inclusion of cargo in an ILV[308]. Finally, lysosomes fuse with the limiting membrane of MVBs resulting in the degradation of their contents through the action of acid hydrolases[309].

#### 1.4.1.7. Recycling Pathways

As opposed to degradation, receptors may also enter a recycling pathway. Recycling of RTKs to the cell surface can occur either directly from the early endosome via a “fast route”[310,311], or indirectly through a “slow route”[312,313], traversing the endocytic recycling compartment (ERC)[314]. These pathways are labeled by Rab4 and Rab11 GTPases, respectively[277]. Early endosomes positive for Rab5, have been shown to contain subdomains containing only Rab5, Rab5 and Rab4 or Rab4 and Rab11[315]. The presence of different subdomains is consistent with distinct morphological features of the early endosome, including vesicular and tubular-cisternal structures[316,317]. Thus it is thought that recycling receptors entering the early endosome first enter the Rab5 domain, rapidly translocate to tubular Rab4 domains which can pinch off (for fast recycling)

and/or finally progress to Rab11 over extended periods of time (for slow recycling) [317].

While the nature of the Rab compartments involved in recycling has been extensively studied, less is known on the molecular mechanisms involved in recycling. Early studies demonstrated that recycling from early endosomes mainly occurs through bulk flow[311]-- i.e. the surface-area-to-volume ratio of the early endosome in tubules is greater than the vesicular region causing membrane proteins to be preferentially sorted to tubules and pinched off for recycling[282]. However these studies have mainly focused on constitutively recycling receptors, such as the transferrin receptor and therefore do not necessarily reflect receptors that are under more stringent control, such as RTKs. Indeed, more recent work on G-protein coupled receptors has shown that the existence of a sequence-dependent sorting pathway distinct from bulk membrane recycling[318].

From early endosomes, the Met receptor has been documented to translocate to a nondegradative perinuclear compartment via a microtubule and PKCα –dependent mechanism[319,320]. However prior to this thesis, whether the Met receptor recycles and through which mechanism this may occur by was not known.

#### 1.4.1.8. The GGA3 Adaptor

The GGAs are a family of three proteins in mammalian cells (GGA1, GGA2 and GGA3) with GGA1 and GGA3 sharing more homology to each other than GGA2[321]. GGAs associate with a variety of proteins involved in protein sorting through their conserved modular domains (Figure 1.8). The N-terminal Vps27, Hrs and STAM (VHS) homology domain interacts with acidic cluster dileucine sorting motifs, the GGA and TOM (target of myb) (GAT) domain recruits GGA proteins to membrane through interaction with GTP-Arfs as well as binding to ubiquitin and Tsg101, the hinge domain binds clathrin and lastly, the C-terminal gamma adaptin ear (GAE) domain binds several proteins involved in trafficking including Rabaptin-5, epsinR and gamma-synergin [232,321-325]. GGAs have been shown to aid in the transport of the mannose-6-phosphate receptor (M6PR) and sortilin between the *trans*-Golgi network and endosomes[232,321]. GGA proteins also facilitate trafficking to the plasma membrane of Gag proteins

required for HIV release [232,326]. GGA3 has also been observed on early endosomes positive for the EGFR and siRNA of GGA3 delays EGF degradation[324]. Due to its ability to bind ubiquitin[324,325], it was proposed that GGA proteins may act as additional proteins required for ubiquitin-dependent sorting for MVB-mediated degradative targeting. The exact nature and function for GGA3 on the EGFR was not followed up. In contrast, we now demonstrate an alternative role for GGA3 in cargo-mediated fast recycling (see Chapter 3) for the Met receptor.

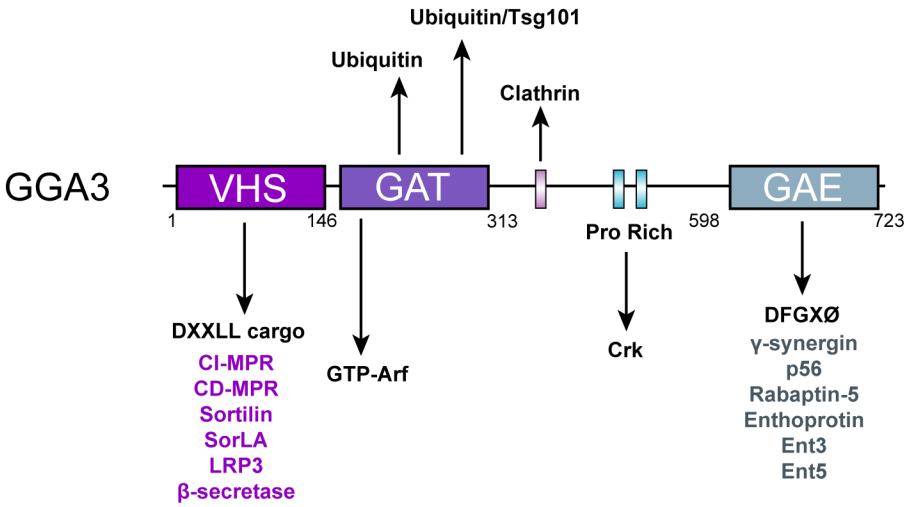


**Figure 1.8. GGA3 domain structure**. Shown are some of the major interactors of GGA3 and the motifs within GGA3 that they have been shown to bind.

### 1.4.2. RTK Trafficking In Tumorigenicity

During the past several years, a greater knowledge of the underlying molecular mechanisms governing RTK endocytosis has been gained. With this, has been the realization that defective trafficking or imbalanced recycling/degradation of RTKs can cause tumorigenesis[8,327].

#### 1.4.2.1. Endocytic Proteins in Cancer

Several proteins involved in endocytosis have been shown to be differentially expressed in different types of cancer. One of the first endocytic adaptors identified to be altered in cancer is the clathrin adaptor, Huntingtin Interacting Protein 1 (Hip1)[328,329]. In prostate cancer, HIP1 over-expression correlates with cancer progression and metastasis[329]. HIP1 functions in clathrin pit formation and maturation and requires clathrin for its localization to clathrin-coated pits[330]. Over-expression of HIP1 in NIH 3T3 cells leads to decreased EGFR endocytosis, hyperphosphorylation of MAPK proteins, cell transformation and tumor growth in nude mice[328]. Thus, through its role in clathrin-mediated trafficking it appears that HIP1 can control transformation.

Tumor suppressor 101 (Tsg101), a component of the ESCRT-1 complex, which functions in sorting ubiquitated cargo into multivesicular bodies, was first identified in a screen looking for tumor suppressor proteins in NIH 3T3 cells[331]. Knockdown of Tsg101 in these cells promotes neoplastic transformation and *in vivo* tumor growth when injected into nude mice[331]. Although it is currently unclear exactly how Tsg101 functions in promoting tumorigenesis, one study suggests that Tsg101, in conjunction with MDM2, controls the protein levels of the tumor suppressor, p53[332]. Additionally, as Tsg101 is required for the ubiquitin-mediated targeting of RTKs for degradation[333], Tsg101 may control tumorigenesis by impacting RTK downregulation.

Numb is another interesting example of an endocytic adaptor, which is lost in ~30% of non-small cell lung carcinomas[334], and 50% of primary breast carcinomas through its ubiquitination and proteosomal degradation[335]. Numb was initially characterized to control cell fate during *Drosophilia* development[336]. During sensory organ development, Numb is asymmetrically segregated during

cell division where it exerts its effect by downregulating the Notch receptor and repressing Notch signaling[337]. In addition to Notch, Numb has also been implicated in numerous other signaling pathways including Hedgehog[338], TP53[339], integrin[340], polarity proteins[340] and adhesion and tight junctions[341]. In breast cancer, loss of Numb causes both increased Notch signaling and downregulation of TP53[335,339]. This results in tumors that exhibit a less-differentiated phenotype that express cancer stem cell markers[342] and through loss of p53, may skew cell division towards symmetric rather than asymmetric cell division. Numb may therefore function as a tumor-suppressor by targeting transformation of the stem cell compartment and increasing the plasticity of the stem cell compartment[343].

Altered Rab25 expression has also been observed in ovarian, breast, prostate and intestinal cancers[344]. Approximately half of ovarian and breast cancers contain amplification of chromosome 1q22, which contains the region encoding *Rab25,* as determined by comparative genomic hybridization (CGH) studies[345-349]. Importantly, increased *Rab25* expression correlates with poor clinical outcome of ovarian cancer[344,345]. Functional studies have demonstrated that over-expression of Rab25 increases tumor development while RNAi-mediated downregulation of Rab25 inhibits tumor growth *in vitro* and *in vivo* in ovarian and breast cancer cells[345,350]. Furthermore, amplification and over-expression of the Rab25 interacting proteins Rab11FIP1/RCP also occurs in breast cancer [349,351]. Rab25 has been shown to promote ovarian cancer cell migration and invasion by altering the trafficking of integrin $\alpha5\beta1$[352]. Additionally, RCP has been shown to coordinate the recycling of $\alpha5\beta1$ with EGFR during cell migration [353]. Finally, a link between the tumor suppressor, p53 and RCP-mediated integrin and EGFR recycling has also been documented[354]. Taken together, these studies highlight a role for Rab25 and its associated proteins in cancer cell migration and invasion.

In addition to Rab25, altered expression of other Rab family members, including Rab1B, Rab4B, Rab10, Rab22A and Rab24 have been reported in hepatocellular carcinomas[355]. Several Rab interactors have also been shown to be dysregulated in tumorigenesis. For example, the Rab4A effector, the N-myc down regulated gene1 (NDRG1) has been reported to be a metastasis suppressor in breast and prostate cancer[356,357]. NDRG1 controls recycling of the adhesion molecule, E-cadherin[358], and thus may exert its ability to function in metastasis by

controlling epithelial cell adhesion turnover. HIF-dependent transcriptional downregulation of Rabaptin-5, a Rab5/Rab4 effector, has been reported in primary kidney and breast tumors with strong hypoxic signatures[359]. Importantly, this leads to inefficient early endosomal fusion resulting in retention of the EGFR in the endocytic pathway and prolonged activation of downstream signaling pathways[359]. Rabaptin-5 has also be reported to be a fusion partner with PDGFβR in chronic myelomonocytic leukemia[360] suggesting Rabaptin-5 may be a key protein in the progression of several tumor types.

Interestingly, besides Rabaptin-5, several other endocytic proteins, including Eps15[361], HIP1[362], clathrin assembly myeloid lymphid leukemia (CALM)[363,364], endophilin II[365] and clathrin heavy chain[366] have been found to be fused to other regulatory proteins in chromosomal translocation events of hematological malignancies[367]. In some cases, these endocytic proteins contain oligomerizing domains which can promote activation of its chimeric partner, and thereby lead to its oncogenicity[367]. In other cases, endocytic fusions may act as dominant negatives on their wild-type counterparts, leading to impaired endocytosis of cargo proteins[367]. More studies will likely uncover further oncogenic mechanisms involving endocytic adaptor fusion proteins.

In addition to endocytic proteins, chromosomal translocations observed in hematological malignancies and solid tumors often harbour constitutively active cytosolic regions of RTKs[368,369]. These oncogenic chimeric proteins act two-fold; they are often cytosolic and are thus excluded from the endocytic pathway[370] and additionally, often no longer contain their Cbl-TKB binding site, preventing them from being efficiently ubiquitinated and downregulated[8]. Mutations in RTKs[94,106,371-374] and Cbl itself[375-378] have also been reported in cancer cells. Finally, other mechanisms, which act by sequestering Cbl proteins away from RTKs, have been documented[379]. Taken together, this suggests that loss of Cbl-mediated downregulation of RTKs is an important pathway selected for in tumorigenesis.

## 1.5. CELL MIGRATION

Cell migration is a complex process that involves coordinated regulation of the cytoskeleton and signalling pathways. It is often described as a cyclical process[380], composed of cell polarization, protrusion, adhesion formation and rear retraction (Figure 1.9).

### 1.5.1. Protrusion

In response to growth factors, chemokines or other stimuli, cells extend protrusions in the direction of migration and thus become front-back polarized[381]. Cells can form several types of protrusions, the most common being flat, broad-shaped lamellipodia and spike-like filipodia. Polymerization of branched actin drives lamellipodia formation while polymerization of actin into parallel bundles forms spike-like filopodia[382]. The branched actin in lamellipodia is nucleated by a complex of seven proteins known as the Arp2/3 complex[382]. Arp2/3 is in turn regulated by Wiskott–Aldrich syndrome protein (WASP) and WASP-family verprolin homologue (WAVE) proteins (WAVE 1, 2 and 3) which become locally activated at the membrane[383]. Additional proteins that regulate capping and severing of actin filaments also contribute to actin formation by limiting the availability of actin monomers for polymerization[383]. The small GTPases Rac, Cdc42 and Rho control protrusion formation by either directly[384,385] or indirectly[386] influencing the activation of WAVE/WASP complexes. In addition, proteins containing SH3 domains have also been shown to regulate WASP[387] and WAVE [385]. Altogether, the polymerization of lamellipodium actin results in pushing the membrane at the front of the cell forward.

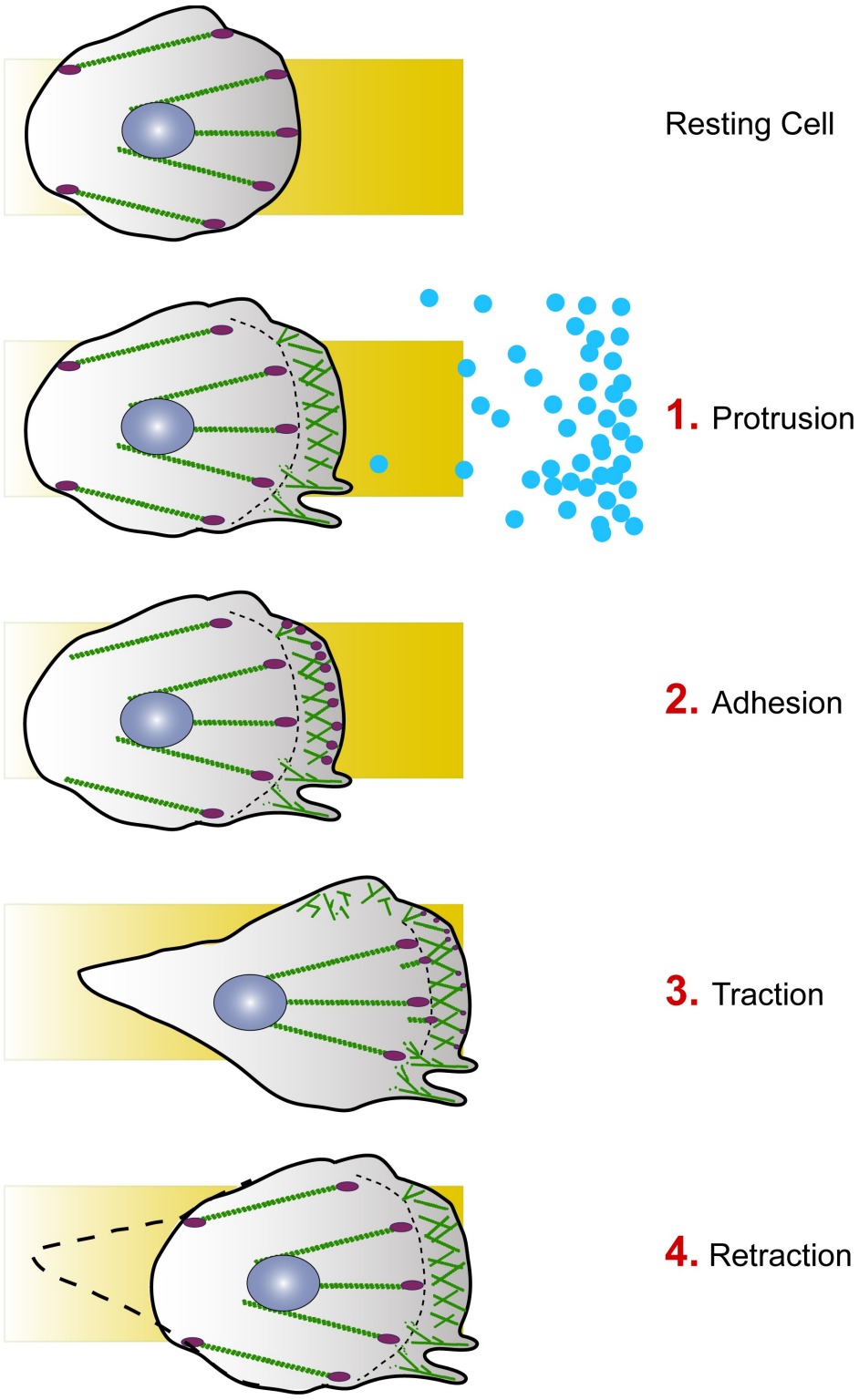


**Figure 1.9. Steps leading to cell migration**. A. The cyclical process of cell migration. In response to stimuli (blue dots) a cell responds by forming a protrusion and making adhesions. These adhesions serve as traction points over which the cell moves. Finally the cell must retract its rear tail from the ECM. See text for details.

### 1.5.2. Adhesion Formation

In order for a cell to productively migrate, it must stabilize the lamellipodium by forming attachments to the extracellular matrix (ECM). The integrin family of transmembrane receptors provides a bidirectional structural link to both ECM components, and the actin cytoskeleton. The extracellular domains of integrins recognize specific sequence motifs in ECM components such as collagen, fibronectin or laminin[388]. Binding to the ECM leads to integrin clustering and transmission of intracellular signals that can ultimately regulate the strength and formation of adhesion sites[383]. Activation of integrins also promotes recruitment of new adhesions to the leading edge. These nascent adhesions can either disassemble or mature into larger (~1μm) focal complexes located slightly further down from the leading edge, in the boundary between the lamellipodium and lamellum (region just below the lamellipodium)[388] (Figure 1.10). As cells continue to migrate, these can continue to mature into larger, elongated focal adhesions which attach to stress fibers[389]. Adhesions are multiprotein complexes; proteomic analysis has identified over 905 different proteins localized to focal adhesions[390]. Arguably, the two most widely studied of these include paxillin and focal adhesion kinase (FAK), which are regulated by phosphorylation events and couple the ECM through integrins to actin[391]. Adhesions serve as important traction points over which cells can migrate.

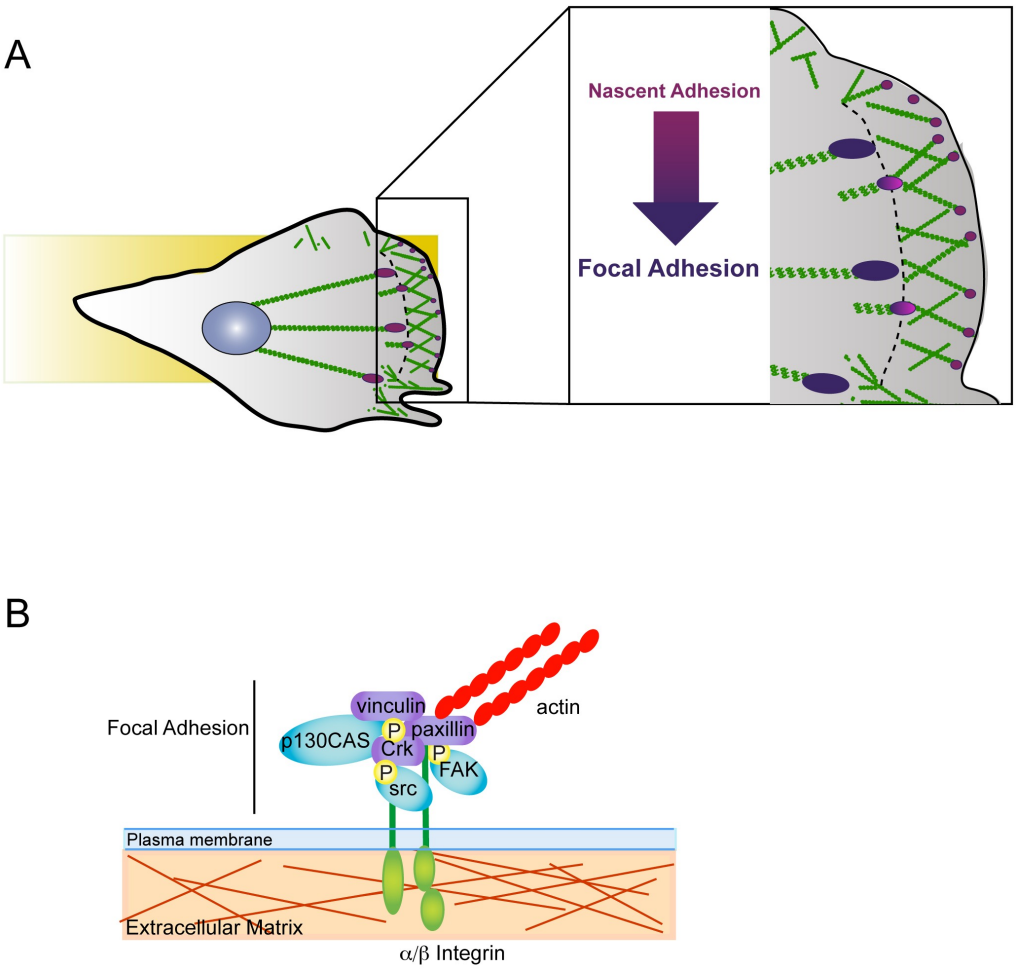


**Figure 1.10. Adhesions.** A. Nascent adhesions form at the leading edge of a cell and rapidly turn-over or mature into focal complexes which in turn can mature into larger focal adhesions (see text for details). Actin shown in green. B. Focal adhesions attach to the extracellular matrix through integrin heterodimers. These are linked through various focal adhesion proteins (a few are shown here), which may become tyrosine phosphorylated upon integrin engagement, and connect to actin stress fibers.

### 1.5.3. Rear Retraction

The final step in cell migration involves disassembling the adhesions at the rear of the cell and contraction of the rear. Adhesion disassembly is controlled through several pathways including those involving FAK, ERK, Src, Rho, calpain and microtubules[388]. High tension on the rear adhesions induces the cell to detach from the ECM[380]. This process is dependent on Rho and myosin II for generating contraction[391].

## 1.6. MICROTUBULES AND MICROTUBULE DYNAMICS

Microtubules have been shown to function in mitosis, cytokinesis and vesicular transport. In particular, they are highly regulated during cell migration and are required for the migration of several cell types[392]. The basic subunit of microtubules is an α- and β- tubulin heterodimer which polymerizes into protofilaments such that the α tubulin of one dimer contacts the β tubulin of another subunit[393]. Incorporation of a tubulin subunit requires that the β-tubulin subunit to be bound to GTP[393] (Figure 1.11). Thirteen of these protofilaments bundle together in parallel, to make up a hollow, cylindrical fibre (microtubule) of 25nm in diameter[394]. The head-to-tail incorporation of tubulin subunits into profilaments creates polarity; one end exposes α-tubulin subunits (referred to as the minus end) while the other end exposes β-tubulin (referred to as the plus end). In most cells, the minus end of the microtubule is anchored to the microtubule organizing centre (MTOC) which is attached to the centrosome and prevents the microtubule from depolymerizing[392].

In contrast, the plus-end of microtubules is dynamic. GTP-bound β-tubulin hydrolyses to GDP within the microtubule structure. GDP-bound tubulin depolymerizes and causes the tubulin subunits to disassemble. Thus if a GTP-bound cap of tubulin exists at the end of a microtubule, additional GTP-bound tubulin can be incorporated and the microtubule will grow. Additional post-translational modifications such as α-tubulin acetylation or detyrosination (proteolytic removal of c-terminus tyrosine) may also aid in stabilizing microtuble ends[395]. If however the region of GDP-bound tubulin within a microtubule catches up to the tip such that there is no more GTP-bound tubulin, the tubulin will

rapidly dissociate from the microtubule leading to shrinkage of the microtubule. The switch from a growing to a shrinking microtubule is known as a 'catastrophe'. Shrinking microtubule ends often appear as bending or "peeling" protofilaments as viewed by cryo-electron microscopy[396]. Conversely, if GTP-bound tubulin gets incorporated into the shrinking microtubule, a new cap can be formed and the microtubule can begin to grow again. This event is called a 'rescue'. These phases of growth, pausing and shrinking create the inherent dynamic instability of microtubules and allows for the rapid remodeling of microtubule contacts.

During cell migration, the MTOC reorients to face the leading edge and the plus end of microtubules are captured and stabilized at the cell cortex near the leading edge[392]. This is thought to contribute to directed vesicular transport. Importantly, microtubule capture mechanisms have been shown to be conserved among species[397], thus pointing to the fundamental role microtubules serve across organisms.

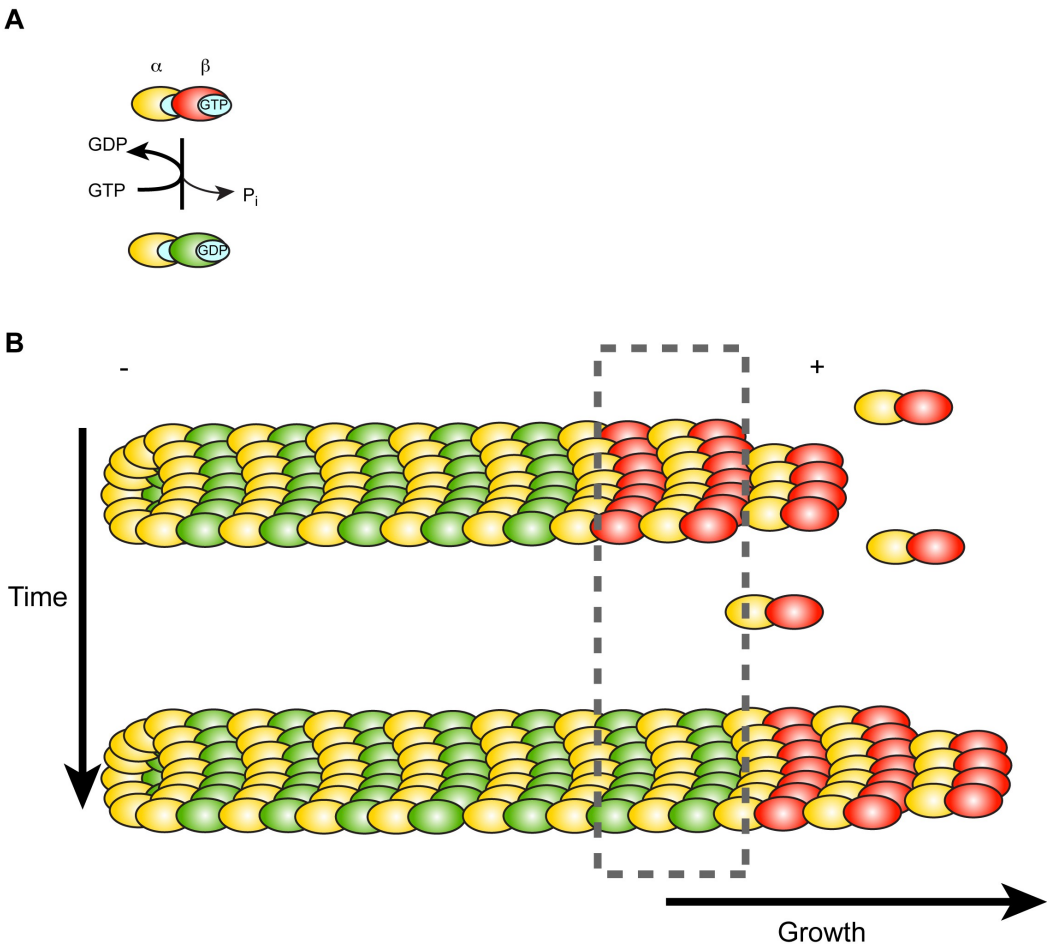


**Figure 1.11. Microtubule and Microtubule Dynamics.** A. An alpha and a beta tubulin heterodimer make up the core subunit of a microtubule. GTP-bound beta-tubulin can be incorporated into a growing protofilament. B. Within the protofilament, GTP is hydrolysed to GDP. Adapted from ref.[393].

### 1.6.1. Microtubule Associating Proteins

A variety of microtubule associating proteins (MAPs) have been shown to specifically localize to the plus ends of microtubules[392]. These so-called plus end tracking proteins (+TIPs) associate and regulate the plus ends of microtubules. Currently, over 20 different families of +TIP proteins[398] have been described including the end binding (EB) proteins, cytoskeleton-associated protein glycine rich (CAP-Gly) domain proteins, SxIP containing proteins, TOG and TOG-like proteins, motor proteins and others[398].

#### 1.6.1.1. Motor proteins

The transmission of signals over distances greater than a few microns requires facilitated transport. Transport along microtubules is assisted by motor proteins and associated proteins. Motor proteins use ATP hydrolysis to generate the force required to "step" along the microtubule track[399]. They fall into three classes, myosins, kinesins and dyneins. Recruitment to cargo can occur via three mechanisms, association with membrane lipids, binding to integral membrane proteins or association with scaffold complexes[399]. The motor protein KIF16B belonging to the kinesin-3 family of plus-end directed motors for example, has been implicated in early endosome motility and contains a PX domain at its C terminus domain which allows for its interactions with PI(3)P[400]. Consistent with this, at steady-state, this motor protein is highly localized to early endosomes in HeLa cells[400]. The small GTPase Rab5 has also been implicated in regulating vesicle docking on microtubules and movement towards the minus end *in vitro* [401]. The kinesin-3 motor KIF16B has also been shown to play an essential role in Golgi-to-endosome trafficking of the FGFR during embryonic development[402]. The molecular details of which motor protein functions for a particular cargo and how they are regulated are still under active investigation and are likely to involve the cooperation of several complexes. Additionally, motor proteins have also been shown to function in membrane tubulation and fission for cargo sorting, endosomal inheritance and positioning[403]. Thus, motor proteins may coordinate several aspects of endosome motility.

#### 1.6.1.2. CLIP-170

Endocytic vesicles can associate with microtubules in the absence of motor proteins *in vitro*[404]. Thus it was speculated that additional microtubule associating proteins could be involved in capturing endosomes for transport along microtubules. A 170 kDa protein that fits these requirements was later identified[405] and shown to be required for endocytic vesicle binding to microtubules[406]. Because of this function, this protein was named cytoplasmic linker protein, CLIP-170[406]. CLIP-170 belongs to the family of CAP-Gly proteins. It contains two CAP-Gly domains which have been show to be required for binding to microtubules[406], a coiled-coil domain and two amino-terminus zinc knuckles[393] (Figure 1.12). Additionally, the amino CAP-Gly region has also been shown to associate with the Rac and Cdc42 effector, IQGAP1[407], while the CLIP-associating proteins, CLASP-1 and CLASP-2, through a yeast-2-hybrid screen and structure-function analysis, have been defined to interact with CLIP-170 through a region overlapping the amino terminus and extending into the coiled-coli domain of CLIP-170[408]. CLIP-170 exists in cells, as a parallel dimer[409] and through its N-terminal CAP-Gly domains, can fold-up on itself through interactions with the zinc-fingers[410]. Finally, the dynactin subunit p150$^{Glued}$ and the dynein regulator, Lissencephaly 1 (Lis1) compete for binding to the second zinc-knuckle of CLIP-170[410,411]. p150$^{Glued}$ is the largest subunit of the dynactin complex, identified *in vitro* to activate dynein for minus-end directed vesicle transport[412,413]. This complex is required for all known functions of dynein by targeting dynein to intracellular localizations, linking dynein to cargo, and increasing processivity[414]. Lis1 functions in cell division and is recruited to the cell cortex and kinetochores during mitosis[415]. It is also able to recruit CLIP-170 to kinetochores[411]. Thus, several CLIP-170 binding partners may dictate the specific function of CLIP-170 at different subcellular localizations.

In addition to intra- and inter-molecular interactions, CLIP-170 is also regulated through phosphorylation. CLIP-170 is serine phosphorylated and is sensitive to okadaic acid treatment[416]. This phosphorylation inhibits its *in vitro* binding to MTs [416]. Clip-170 is also serine phosphorylated at 311 by AMPK[417]. This phosphorylation is required for the removal of Clip-170 from MTs and its

function on MT dynamics. Clip-170 treadmills along the distal ends of MTs at a rate of 0.15–0.4 μm/s[418].

The more well characterized functions of CLIP-170 as a +TIP include regulation of chromosome segregation[419], promoting rescue of MTs[420], localizing dynactin/dynein complex to microtubule + ends[393] and generating cell polarity through "search and capture" of MTs[393]. Curiously, besides capturing melanosomes (pigment organelles) for transport to the cell centre[421], little evidence exists showing a direct role for CLIP1-70 in vesicle transport. Where investigated, no change in ER-to-Golgi transport, intracellular distribution of early endosomes and lysosomes or uptake of transferrin was observed in CLIP-170 depleted cells[422], suggesting that CLIP-170 is not required for the steady-state transport or localization of these organelles**.** Given its initial characterization in vesicle-capture for microtubule transport, this suggests that CLIP-170 may serve a function in selective cargo capture. Thus, as described in the fourth chapter of this thesis, we tested the hypothesis that CLIP-170 aids in microtubule-directed recycling of the Met receptor.

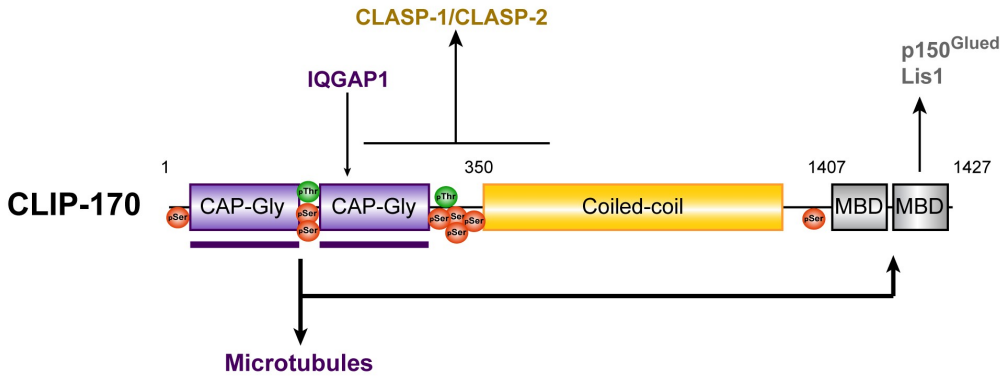


**Figure 1.12. CLIP-170 domain structure and interactors**. Schematic of CLIP-170 and the proteins that have been shown to be associated with each region. Major sites of serine/threonine phosphorylation are also indicated on the diagram.

# Chapter 2

## 2. Distinct Recruitment of Eps15 via Its Coiled-coil Domain Is Required For Efficient Down-regulation of the Met Receptor Tyrosine Kinase

Christine A. Parachoniak and Morag Park

## 2.1. PREFACE

At the time of this work, the role of the endocytic adaptor protein, Eps15 had been mainly characterized downstream of the EGFR, thus it was generally accepted that the recruitment and function of Eps15 downstream of other RTKs occurred via a similar mechanism. This work describes the first demonstration for an alternative mechanism of Eps15 recruitment to RTKs independent of its UIM (ubiquitin interaction motif) downstream of the Met receptor, involving the coiled-coil domain of Eps15 as well as interaction of Eps15 with Grb2.

## 2.2. ABSTRACT

Down-regulation of receptor tyrosine kinases (RTK) through receptor internalization and degradation is critical for appropriate biological responses. The hepatocyte growth factor RTK (also known as Met) regulates epithelial remodeling, dispersal, and invasion and is deregulated in human cancers. Impaired down-regulation of the Met RTK leads to sustained signaling, cell transformation, and tumorigenesis, hence understanding mechanisms that regulate this process is crucial. Here we report that, following Met activation, the endocytic adaptor protein, Eps15, is recruited to the plasma membrane and becomes both tyrosine-phosphorylated and ubiquitinated. Recruitment of Eps15 requires Met receptor kinase activity and involves two distinct Eps15 domains. Unlike previous reports for the EGF RTK, which requires the Eps15 ubiquitin interacting motif, recruitment of Eps15 to Met involves the coiled-coil domain of Eps15 and the signaling adaptor molecule, Grb2, which binds through a proline-rich motif in the third domain of Eps15. Expression of the coiled-coil domain is sufficient to displace the wild-type Eps15 protein complex from Met, resulting in loss of tyrosine phosphorylation of Eps15. Knockdown of Eps15 results in delayed Met degradation, which can be rescued by expression of Eps15 WT but not an Eps15 mutant lacking the coiled-coil domain, identifying a role for this domain in Eps15-mediated Met down-modulation. This study demonstrates a new mechanism of recruitment for Eps15 downstream of the Met receptor, involving the coiled-coil domain of Eps15 as well as interaction of Eps15 with Grb2. This highlights distinct regulation of Eps15 recruitment and the diversity and adaptability of endocytic molecules in promoting RTK trafficking.

## 2.3. INTRODUCTION

Growth factor receptor tyrosine kinases (RTKs) regulate multiple key cellular processes, including proliferation, differentiation migration, and survival. RTK activation must be tightly controlled through multiple levels of regulation to

maintain cellular homeostasis. Failure to due so is associated with the development and progression of human disease such as cancer [45,76,371]. Ligand-induced activation of RTKs promotes their rapid removal from the plasma membrane, a key event in their down-regulation, because it is a prerequisite to their lysosomal degradation. The process of RTK internalization modulates levels of RTK at the cell surface and the duration of signals activated in response to growth factors. Ligand-activated RTKs are mainly internalized through clathrin-dependent pathways to be eventually delivered to sorting endosomes[423], although other mechanisms of receptor internalization exist[212]. From the sorting endosome, RTKs can recycle back to the plasma membrane or become internalized and accumulate on the limiting and internal membranes of multivesicular bodies. This latter event terminates RTK signaling by sequestering the signaling-competent intracellular domain of RTKs and preventing recycling back to the plasma membrane. Multivesicular bodies subsequently fuse with lysosomes, leading to the degradation of proteins located within intralumenal membranes[424,425]. These internalization and trafficking events are controlled via a complex network of protein-protein and protein-lipid interactions that are evolutionary conserved. Ligand-dependent internalization and trafficking of RTKs is regulated in part through ubiquitination and tyrosine phosphorylation of the receptor[426]. In addition, endocytic proteins themselves are modified by RTK-dependent ubiquitin and tyrosine phosphorylation, which serve as signal switches to promote or disassemble protein-protein interactions[426,427]. Many of these interactions have been studied extensively for the epidermal growth factor (EGF) RTK[428], yet the mechanisms regulating internalization and trafficking of other RTKs remain poorly understood.

The hepatocyte growth factor (HGF) RTK (also known as Met) is primarily expressed in epithelial and endothelial cells in the adult. The HGF/Met signaling axis regulates key cellular processes such as scattering of epithelia sheets, as well as epithelial cell proliferation, migration, invasion, and survival[109]. HGF/Met signaling is essential for embryonic development, namely the growth and survival of epithelial cells as well as the migration of myogenic precursor cells and the

outgrowth of motor neurons[11]. Chronic activation of the Met receptor is associated with several human and murine tumors[11,429] and in the adult, the HGF/Met signaling axis is involved in wound healing and liver regeneration[51,52].

Activation of the Met receptor by binding to HGF promotes tyrosine phosphorylation of the intracellular domain and recruitment of signaling complexes, including the Cbl E3 ubiquitin ligase[109]. Cbl promotes ubiquitination of the Met receptor, an event that is critical for ligand-dependent Met degradation[9,116,430,431]. Importantly, although deregulation of the Met receptor in human cancers can occur through receptor amplification, point mutations, and chromosomal translocations leading to ligand-independent RTK activation, we and others have recently shown that escape from down-regulation constitutes another mechanism leading to Met RTK deregulation in human cancers[8,106,108].

Internalization of the Met RTK following HGF stimulation uses canonical pathways and is clathrin-dependent[298,432], however, little is known of the protein complexes that regulate these events. Multiple proteins have been shown to regulate EGFR internalization. One of these, epidermal growth factor receptor pathway substrate 15 (Eps15), was first identified as a tyrosine-phosphorylated substrate of the EGFR kinase [247]. Eps15 has been characterized as a general endocytic adaptor protein, because it is constitutively associated with the adaptor protein complex AP-2, and forms complexes with other endocytic proteins, including Epsin and Hrs[250-253]. Studies with the EGFR have shown that Eps15 translocates to the rim of budding clathrin-coated pits upon EGF stimulation and colocalizes with the receptor[248,249]. Eps15 acts as a molecular scaffold by promoting interactions through its many domains. The N terminus contains three Eps15 homology (EH) domains that are required for plasma membrane targeting of Eps15 through engagement with proteins containing the tripeptide motif asparagine-proline-phenylalanine and direct binding to phospholipids[255,256]. Eps15 also contains a central coiled-coil domain, which mediates homo- and heterodimerization[257] and a stretch of aspartate-proline-phenylalanine repeats, which can bind the alpha-subunit of AP-2. The c-terminus harbors two ubiquitin interacting motifs (UIM) of which the second has been shown to participate in

ubiquitin binding[258] and is required for recruitment to a ubiquitinated EGFR[259]. Mutations within the Eps15 UIM domain that abrogate ubiquitin binding disrupt the localization of Eps15 to the plasma membrane upon EGF stimulation[260]. In addition, deletion of the UIM or use of a poorly ubiquitinated EGFR mutant (Y1045F) also abrogates co-immunoprecipitation of the two proteins[259]. Hence, Eps15 acts to recognize ubiquitinated EGFR cargo, which is thought to contribute to selection of the EGFR for internalization[259,260,433].

Although Eps15 has been shown to play a role in the internalization of the EGFR, the extent to which it functions downstream of other RTKs is currently unknown. Where investigated, tyrosine phosphorylation of Eps15 has not been observed downstream of other stimuli such as insulin, platelet-derived growth factor or keratinocyte growth factor[248,261]. Given the biological importance of the more than 50 RTKs encoded in the human genome, elucidation and validation of the molecular mechanisms governing the down-regulation of different RTKs will be important to determine which commonalities and differences exist between these family members. Because deregulation of trafficking of the Met RTK contributes to its oncogenic potential, we have investigated the role of Eps15 downstream of the Met receptor. Here, we report that HGF-induced activation of the Met receptor results in recruitment of Eps15 to the plasma membrane and causes its rapid tyrosine phosphorylation and ubiquitination. In contrast to previous studies with the EGFR, we have mapped the coiled-coiled domain of Eps15 as being sufficient and essential for the interaction of Eps15 with the Met receptor and propose a new mechanism for recruitment and regulation of RTKs by Eps15.

## 2.4. RESULTS

### 2.4.1. Eps15 Is Recruited to the Met Receptor upon HGF Treatment

To examine the role of Eps15 downstream from the Met RTK, we first determined if Eps15 is recruited to the Met receptor following stimulation with

HGF. HeLa cells were stimulated with physiological concentrations of HGF (0.60 nM) for 1 h at 4°C, fixed, and immunostained for endogenous Eps15 and Met proteins and visualized using confocal microscopy. Under these conditions RTKs do not internalize but bind ligand and accumulate into clathrin-coated pits at 4°C. Receptors are then synchronously internalized upon temperature release from 4°C to 37°C[434-436]. This experimental procedure is depicted in Fig. 2.1*A* and shall subsequently be referred to as a cold load stimulation. Prior to ligand stimulation, Eps15 was localized in punctate structures resembling endosomes as well as being concentrated at the *trans*-Golgi network, as assessed by co-staining with mannose-6-phosphate receptor (supplemental Fig. S2.1*A*), whereas the Met RTK was predominantly localized at the plasma membrane (Fig. 2.1*B*, *panel a*). Following temperature switch to 37°C post HGF treatment, Met is rapidly internalized and enters the endocytic pathway[108]. Eps15 co-localizes with Met following 1 h at 4°C (Fig. 2.1*B*, *panels d–f*) and as Met internalizes for up to 60 min post temperature switch (Fig. 2.1*B*, *panels g–o*). These structures were confirmed to be endosomes through co-staining for the endosomal marker, EEA-1 (supplemental Fig. S2.1*B*).

To further validate the association between Eps15 and the Met receptor, endogenous Eps15 was immunoprecipitated from HeLa cells and immunoblotted for the Met receptor (Fig. 2.1*C*). Interestingly, a biphasic, HGF-dependent association was observed (*lanes 2* and *4*), similar to what has been reported for the EGFR[259]. Co-immunoprecipitation was also detected in HEK293 cells transiently transfected with constructs expressing these proteins (supplemental Fig. S2.1*C*). Thus, taken together, Eps15 can be recruited to a Met receptor complex upon HGF stimulation.

Because ligand concentration has been shown to influence which internalization machinery is utilized by the EGFR[259], we also determined the role of Eps15 in Met trafficking under low concentrations of HGF (0.12nM) in comparison to the moderate levels (0.60nM) described above[32]. After a cold load stimulation and a 15-min release to 37°C, Met internalized into early endosomes in response to low HGF concentrations, and no significant differences for the

recruitment and co-trafficking of Eps15 and Met were observed (Fig. 2.1*D*). This demonstrates that Eps15 is recruited to the Met receptor at multiple and/or various stages of internalization and trafficking irrespective of ligand concentration.

### 2.4.2. Eps15 becomes Tyrosine-phosphorylated at Site Tyr-850 and Is Ubiquitinated in Response to Met Activation

Tyrosine phosphorylation of Eps15 has been shown downstream of the EGF receptor but not other growth factor receptors, such as the platelet-derived growth factor [248], insulin[248], or keratinocyte growth factor receptors[261]. We therefore investigated whether HGF could induce tyrosine phosphorylation of Eps15. To test for phosphorylation of Eps15, we utilized T47D breast epithelial cells, which have undetectable protein levels of the Met receptor, and where we have stably expressed either a wild-type Met or kinase-dead (K1110A) Met receptor mutant (see "Experimental Procedures")[108]. These T47D cells express levels of Met similar to or lower than HeLa cells, which contain moderate levels of endogenous Met protein (Fig. 2.2*A*) and have previously been used successfully to study the biology of the Met receptor[108]. Cells were stimulated under cold load conditions with HGF, and the phosphorylation status of Eps15 was assessed for the indicated times (Fig. 2.2*B*). Phosphorylation of Eps15 was induced by 2- to 5-min post temperature release but was attenuated by 15 min (Fig. 2.2*B*). A second wave of Eps15 phosphorylation occurred ~30–60 min after temperature release, consistent with our observation that Eps15 and Met are localized in the same vicinity in a perinuclear compartment at this time point (Fig. 2.1*B*). No tyrosine phosphorylation of Eps15 was observed in response to HGF stimulation in the K1110A-expressing T47D cells, showing that phosphorylation of Eps15 is strictly dependent on the kinase activity of the Met receptor. Additionally, no change in Eps15 binding to AP-2 μ-subunit was observed before and after release of HGF treatment, indicating that this complex is still functional under these conditions. To confirm these results using endogenous proteins, Eps15 tyrosine phosphorylation was examined in HeLa cells under both cold load (Fig. 2.2*C*) and HGF treatment at 37°C (Fig. 2.2*D*). In both cases, tyrosine

phosphorylation of Eps15 was detected, in agreement with our previous results, albeit with distinct but consistent kinetics depending on the condition and cell line used. Additionally, increasing amounts of WT Met receptor, when transiently transfected in HEK293 cells, led to enhanced tyrosine phosphorylation of Eps15 (Fig. 2*E*), further demonstrating a role for the Met RTK in Eps15 tyrosine phosphorylation. Tyrosine residue 850 of Eps15 has been implicated in the internalization of the EGF receptor and has been shown to be phosphorylated downstream of the EGFR [437]. To assess whether residue Tyr-850 also plays a role in the tyrosine phosphorylation in Eps15 downstream of Met, the extent of tyrosine phosphorylation of a Y850F Eps15 mutant was compared with the wild-type protein upon Met activation. Although the wild-type Eps15 protein becomes tyrosine-phosphorylated when co-expressed with the activated but not kinase-dead Met receptor (Fig. 2.2*F*, *lanes 2* and *3*), the Y850F mutant was not detectably phosphorylated (Fig. 2.2*F*, *lanes 5* and *6*). These results demonstrate that tyrosine 850 is required for tyrosine phosphorylation of Eps15 downstream of the Met receptor. Recently, monoubiquitination of Eps15 has been reported to play a regulatory role in the ability of Eps15 to bind to ubiquitinated cargo[438]. Monoubiquitination of Eps15 prevents UIM-ubiquitin interactions with other proteins[438]. To establish whether Eps15 is ubiquitinated downstream of HGF and hence determine the ability of Eps15 to recognize cargo, HeLa cells were transiently transfected with HA-tagged ubiquitin and subjected to a cold load stimulation (Fig. 2.2*G*). Ubiquitination of endogenous Eps15 was detected upon HGF stimulation (*lane 3*), but not in the absence of HGF (*lanes 2*) or in non-transfected control cells (*lane 1*). Ubiquitination of Eps15 was detected with biphasic kinetics at 0–2 min (*lanes 3* and *4*) and 30 min (*lane 6*) post-temperature shift.

### 2.4.3. Eps15 Associates with the Met Receptor Primarily through Its Coiled-coil Domain

To determine the structural requirements involved in the Eps15-Met interaction, a panel of Eps15 deletion mutants[439,440] was tested for their ability to

co-immunoprecipitate with the Met receptor (Fig. 2.3, *A* and *B*). Eps15 contains four distinct domains, namely the N terminus domain (domain I), which contains three EH domains, a central coiled-coil (CC) (domain II), a DPF repeats domain (domain III), and domain IV at the C terminus, which contains two UIM domains (Fig. 2.3*C*). Recruitment of Eps15 to the membrane and its ability to be tyrosine phosphorylated upon HGF stimulation occurs with similar kinetics to that reported for EGF (Figs. 2.1*B* and 2.2*C*)[441]. Because the Met RTK is rapidly ubiquitinated in response to HGF[9,431], we hypothesized that the Met-Eps15 interaction would also follow the proposed model for the EGFR and be dependent on the UIM domains of Eps15 [258,433,442,443]. Surprisingly, the ΔUIM Eps15 mutant protein (Eps15ΔIV) co-immunoprecipitated with the Met receptor to the same extent as the WT protein (Fig. 2.3*A*, *lane 6*). The UIM domain of Eps15 has been shown to bind to Lys-48 and Lys-63-liked ubiquitin chains *in vitro*, with preference for chains over monoubiquitin [444]. We verified that Met was ubiquitinated under our experimental conditions (supplemental Fig. S2.2*A*). Additionally, removal of the UIMs (Eps15ΔIV mutant) disrupted ubiquitin binding as expected (supplemental Fig. S2.2*B*). Furthermore, because Eps15 recruitment to the EGFR is dependent on the integrity of the Eps15 UIM, and the ubiquitination status of the EGFR, we tested the capacity of a poorly ubiquitinated Met receptor (Y1003F) to co-immunoprecipitate with Eps15. We observed no decrease in co-immunoprecipitation with a Met Y1003F mutant, which is poorly ubiquitinated due to impaired Cbl recruitment [9] (Fig. 2.3*D*). In contrast, the Eps15ΔII (delta CC domain) mutant failed to co-immunoprecipitate with a WT Met receptor (Fig. 2.3*A*, lane 4 and Fig. 2.3*B*, lane 3) while the Eps15ΔIII mutant was impaired in its association with Met (Fig. 2.3*A*, *lane 5*, Fig. 2.3*B*, *lane 4*). Consistent with this, expression of the Eps15 CC domain alone was sufficient to interact with the Met receptor, whereas expression of domain III was consistently seen to interact weakly with the receptor (Fig. 2.3*B*, *lanes 5* and *6*, respectively). To test whether the coiled-coil domain also plays a role in the interaction with the EGFR we tested our Eps15-truncated mutants for co-immunoprecipitation with the EGFR. Interestingly, following transient co-transfection the EGFR-Eps15

interaction was disrupted when the coiled-coil domain was removed, whereas, removal of the C-terminal UIMs did not abrogate this association when proteins were overexpressed (Fig. 2.3*E*). Hence, unlike previous reports and implications based on the EGFR, Eps15 domain II, namely the coiled-coil domain, is necessary and sufficient for the association of Eps15 with the Met receptor, whereas Eps15 domain III can compensate to a lesser extent to its association.

### 2.4.4. Grb2 Interacts with Eps15 through a Proline-rich Motif

To gain insight into the possible role of Eps15 domain III in complex formation with Met, we used Scansite[445] to identify potential binding protein motifs within domain III of Eps15. Scansite identified a putative Grb2 SH3 binding motif in Eps15, centered on proline residue 770 with a score of 0.564 (Fig. 2.4A). The known Grb2 binding partner, SOS, by comparison resulted in Scansite scores for three prolines ranging from 0.540 to 0.6345, whereas Gab1, another known Grb2 binding partner, contains a proline-rich domain with three consensus proline motifs with scores ranging from 0.525 to 0.611. Grb2 is an adaptor protein that contains one SH2 domain and two SH3 domains. Upon HGF stimulation, Grb2 is rapidly recruited to the Met receptor through its SH2 domain[446]. Grb2 is required for the internalization of the EGFR[447] and recently has been shown to play a role in the clathrin-mediated endocytosis of the Met receptor[448]. We therefore investigated whether Grb2 could associate with Eps15. In cells that co-express both FLAG-tagged Eps15 and Myc-tagged Grb2, these proteins co-immunoprecipitate in the presence and absence of an activated Met receptor (Fig. 2.4B). Parallel co-immunoprecipitations were also carried out between GFP-tagged Eps15 and Gab1 with Myc-tagged Grb2 (supplemental Fig. S2.3A) for a qualitative comparison between these two Grb2-associating proteins. Additionally, in HeLa cells, endogenous Grb2 was detected in Eps15 immunoprecipitates from both unstimulated and stimulated cells (Fig. 2.4C) demonstrating a constitutive association indicative of an SH3 domain proline-rich interaction[449]. Furthermore, structure function studies demonstrate that neither an Eps15 mutant lacking the putative proline motif (Eps15ΔIII, Fig. 2.4D, lane 6) nor

an Eps15 point mutant (P770A, Fig. 2.4D, lane 9) fully associates with Grb2, demonstrating the requirement for this proline residue for this interaction (Fig. 2.4, D and E). We confirmed this interaction using a GST-Grb2 fusion protein and pulldown assays, where we observe a decreased capacity of Grb2 to interact with the P770A mutant as compared with WT Eps15 (Fig. 2.4F). To assess the functional significance of the Grb2-Eps15 interaction, we tested the ability of the P770A mutant to be tyrosine-phosphorylated and ubiquitinated upon HGF stimulation. The Eps15 P770A mutant showed less ubiquitination and tyrosine phosphorylation when compared with the WT protein upon HGF stimulation (Fig. 2.4G, compare lanes 1–5 with lanes 6–10). This reduction was not due to reduced recruitment to the Met receptor, because the P770A mutant was able to co-immunoprecipitate with Met to a similar extent as the WT protein (supplemental Fig. S2.3B). Altogether, these results indicate that Grb2 can bind to Eps15 through an interaction that is dependent of proline 770. This association is maintained upon Met receptor activation and is required for full recruitment and post-translational modification of Eps15.

### 2.4.5. The Coiled-coil Domain Is Sufficient to Displace Eps15-Met Interactions

To further elucidate the role of the coiled-coil domain of Eps15 upon Met activation, we used increasing levels of Eps15 CC domain to determine whether this region of Eps15 could directly compete for binding to Met (Fig. 2.5A). Titrating increasing amounts of the Eps15 coiled-coil domain resulted in a displacement of the WT Eps15 from its association with the Met receptor and coincident loss of tyrosine phosphorylation of Eps15 (Fig. 2.5A, first and third panels, respectively). Binding of both FLAG-Eps15 and FLAG-CC was specific, because no binding was observed in parallel immunoprecipitations where no antibody was used (data not shown). Thus, the coiled-coil domain of Eps15 is sufficient to displace the wild-type Eps15 protein from a Met complex, and results in a loss of tyrosine phosphorylation of Eps15 following its uncoupling from the Met RTK. Because the mechanisms for tyrosine phosphorylation of Eps15

downstream of HGF are the same as downstream of EGF (Fig. 2.2F), we next determined the ability of the coiled-coil domain to compete in the presence of EGF stimulation. The coiled-coil domain of Eps15 was able to co-immunoprecipitate with EGFR, however, in contrast to the Met receptor, the coiled-coil domain of Eps15 associated poorly with the EGFR and was less efficient at displacing the association of the full-length Eps15 protein with the EGFR (Fig. 2.5, B–D). This demonstrates that, unlike the Met RTK, the coiled-coil domain of Eps15 does not play a significant role in the recruitment of Eps15 to the EGFR.

### 2.4.6. Eps15 Knockdown Delays Met Degradation

Knockdown of Eps15 has been reported to cause a modest reduction in the internalization of the EGFR[450]; however, infection of the bacterium *Listeria monocytogenes*, which can occur via a Met-dependent mechanism, was drastically reduced upon Eps15 silencing[451]. To directly assess the role of Eps15 in Met down-regulation, siRNA was used to reduce Eps15 protein expression levels in HeLa cells. A dose-dependent knockdown of Eps15 was observed with increasing concentrations of siRNA (Fig. 2.6A), with optimal knockdown consistently observed to be 70% at a concentration of 10 nM (Fig. 2.6A). Knockdown was specific, as a control scramble siRNA did not affect levels of endogenous Eps15. Cells with knockdown of Eps15 showed a delay in Met trafficking to a perinuclear compartment in comparison to scramble negative control cells (Fig. 2.6B). By 60 min, control cells were observed to be in a perinuclear compartment, whereas Eps15 siRNA-treated cells showed a less defined cellular localization in the cell (Fig. 2.6*B*). By 2 h of HGF treatment, Met is normally degraded and poorly detected by immunofluorescence, however in Eps15 siRNA-treated cells, Met was still detected in a perinuclear compartment (Fig. 2.6*B*). This delay in trafficking was found to correlate with enhanced stability of protein levels as observed by Western blot analysis (Fig. 2.6*C*). Densitometric analysis of Met protein levels was also used to demonstrate a delay in Met degradation (Fig. 2.6*C*). We verified the specificity of the siRNA knockdown by re-expressing

siRNA resistant full-length Eps15. Low levels of Eps15 restored Met degradation dynamics to that of scramble siRNA-treated cells, confirming that the delayed degradation is due to a loss of Eps15 protein levels and not due to off-target effects (Fig. 2.6*D*).

### 2.4.7. Eps15 Knockdown Is Rescued by Full-length and P770A Mutant but Not Eps15ΔCC Protein or Eps15ΔUIM Mutant

We have shown that the coiled-coil domain of Eps15 is responsible for mediating Eps15-Met interactions. To assess the importance of the coiled-coil domain-mediated Met interaction for Met degradation, we sought to re-introduce siRNA-resistant Eps15ΔCC protein and compare this with the full-length Eps15 protein for its ability to restore Met degradation. After HGF stimulation for 2 h, HeLa cells were fixed and assessed through indirect immunofluorescence for Met staining in the perinuclear compartment. Cells transfected with siRNA to Eps15 and transfected with Eps15ΔCC displayed persistent Met perinuclear localization 2h post-HGF treatment in a similar manner to control knockdown cells transfected with vector (Fig. 2.7, *A* and *B*). In contrast, knockdown cells transfected with WT-Eps15 exhibited less Met protein as observed through immunofluorescence (Fig. 2.7*A*) and Western blot (Fig. 2.7*C*). We next determined whether the Eps15 P770A and Eps15ΔIV (Eps15ΔUIM) proteins could also rescue the delay in Met degradation. Expression of Eps15 P770A rescued Met levels similar to Eps15 WT-expressing cells (Fig. 2.7). Interestingly, the Eps15ΔUIM was unable to fully rescue Met degradation as detected by immunofluorescence but was not as effective as the Eps15ΔCC in preventing Met degradation (Fig. 2.7*B*). Hence these results support that the coiled-coil domain is critical for Eps15-mediated Met trafficking and degradation and that ubiquitin-Eps15 UIM domain interactions are also critical for promoting Met trafficking and degradation.

## 2.5. DISCUSSION

Here we report induced recruitment and post-translational modification of Eps15 downstream from the Met receptor tyrosine kinase. Few studies have directly addressed the role of Eps15 for ligand-dependent endocytosis of RTKs other than for the EGFR. In fact, where investigated, tyrosine phosphorylation of Eps15 has not been reported for other stimuli[248,261]. Although Eps15 is commonly used as a marker for clathrin-dependent endocytosis, many details beyond its interaction with other endocytic proteins are lacking. In this study we have performed the first systematic analysis of Eps15 downstream from the Met RTK. Similar to reports carried out with the EGFR[247], Eps15 is a downstream target for the Met receptor. In this study, we show that Eps15 is recruited to the plasma membrane and undergoes rapid but biphasic tyrosine phosphorylation and ubiquitination in response to HGF (Figs. 2.1*B*, 2.2*B*, 2.2*C*, and 2.2*G*).

Using structure-function analysis, we have mapped the region of Eps15 responsible for the interaction with Met to the coiled-coil domain and a proline-rich domain. This is in contrast to published data based on the EGFR supporting a model whereby Eps15 is recruited to the EGF receptor through the UIM domain of Eps15[452]. Our data demonstrate that an Eps15 construct that lacks its UIM domains associates with the Met receptor to a similar level as the wild-type Eps15 protein (Fig. 2.3*A*) and argue that the mechanism for Eps15 recruitment to the Met receptor does not follow this model. In further support of this, Eps15 co-immunoprecipitated equally well with a mutant Met receptor (Y1003F) that is poorly ubiquitinated due to impaired Cbl recruitment (Fig. 2.3*D*). Instead, we demonstrate a novel mode of recruitment of Eps15 to the Met receptor, and we show that removal of the coiled-coil domain is sufficient to disrupt the recruitment of Eps15 to an activated Met complex (Fig. 2.3, *A* and *B*). Moreover an siRNA-resistant Eps15 mutant lacking the coiled-coil domain was unable to promote Met receptor degradation as observed upon expression of an siRNA-resistant WT Eps15, further confirming a role for the coiled-coil domain in the recruitment of Eps15 to Met (Fig. 2.7). Interestingly, removal of the coiled-coil domain also disrupts the recruitment of Eps15 to the EGFR (Fig. 2.3*E*). Whereas previous data have mapped the UIM domain of Eps15 for recruitment to the

EGFR, a role for the coiled-coil domain was not addressed[259]. Although the UIM domain of Eps15 is not essential for recruitment to the Met receptor, an Eps15 mutant lacking this domain failed to promote degradation of the Met receptor (Fig. 2.7). While this mutant was not as ineffective as the Eps15ΔCC mutant (Fig. 2.7*B*), it nonetheless highlights the importance of ubiquitin-UIM interaction in the overall function of Eps15 downstream of the Met receptor, which is in agreement with previous studies carried out with the EGFR[259,260].

The coiled-coil domain of Eps15 has been shown to be involved in forming homo- and hetero-dimers and tetramers[257]. The formation of these higher order molecular complexes may be required to stabilize low affinity associations of Eps15 with the Met receptor. Yet, because the coiled-coil domain alone is sufficient for binding to the Met receptor, and can compete with the wild-type protein for binding, an alternative (but not exclusive) hypothesis is that this domain is directly involved in binding to the receptor. As endogenous Eps15 protein is present, we also cannot exclude the possibility that endogenous Eps15 may dimerize with the coiled-coil domain to contribute to its recruitment to a Met complex. This interaction, however, appears to be minimal as an Eps15 mutant (ΔIII) with an intact coiled-coil domain was also impaired in its ability to associate with the Met receptor (Fig. 2.3*A*). Additionally, the coiled-coil domain of Eps15 has been reported to mediate interactions with another coiled-coil-containing protein, Hrs[253,295]. We therefore cannot rule out indirect protein interactions, although recently, for the case of Hrs, it has been shown that Hrs preferentially interacts with Eps15b rather than Eps15 *in vivo*[292] .

Recruitment of Eps15 to Met depends on the kinase activity of the Met receptor (Fig. 2.2*A*). Here we have shown that a pool of Grb2 is constitutively bound to Eps15 though a proline-rich motif and that this interaction is maintained upon Met activation (Fig. 2.4, *B* and *C*). An Eps15 mutant uncoupled from Grb2 (P770A) shows decreased ubiquitination and tyrosine phosphorylation when compared with the WT-Eps15 protein, in particular at the later (30 min) time point (Fig. 2.4*G*), supporting a role for Grb2 in the recruitment of Eps15 *in vivo*.

Interestingly, this proline motif within Eps15 has been shown to interact with

the SH3 domain of the adaptor protein Crk[453]. Crk and Grb2 would therefore be predicted to compete for binding to Eps15. Although, whether this competition occurs *in vivo* and the significance of this competition remain to be tested.

Several studies have demonstrated a requirement for Grb2 in mediating RTK internalization[447]. Knockdown of both Eps15 and Grb2 has been shown to inhibit Met-dependent bacterial entry of *L. monocytogenes*[451]. Studies depleting or, conversely, overexpressing Grb2 have also been used to show a requirement for Grb2 in the clathrin dependent internalization of the Met receptor[448]. Grb2 is rapidly recruited to the Met receptor following phosphorylation of Tyr-1356, a consensus Grb2 SH2 domain binding site in the C terminus of Met[119]. Grb2 recruitment to Met is essential for the full morphogenic response elicited by HGF[446] and required for the tyrosine phosphorylation of Cbl and Gab1 signaling adaptor proteins[139]. By analogy, Grb2 is likely involved as an adaptor bridging endocytic proteins such as Eps15 to the activated Met receptor, serving as an additional factor in the recruitment of Eps15 to the vicinity of the Met receptor.

Recently, a second isoform of Eps15, Eps15b, has been reported to localize to endosomes[292]. This isoform lacks the EH domains and differs in the first 32 N-terminus residues from Eps15. Knockdown of both Eps15 and Eps15b resulted in delayed EGFR degradation, whereas siRNA to Eps15 alone had no effect[292]. Disparity between these results and ours may be due to receptor-specific differences between the Met receptor and EGFR, because the coiled-coil domain, as opposed to the UIM domain of Eps15, is required for Met receptor-Eps15 interactions (Fig. 2.3, *A* and *B*). Additionally, we observed that high levels of Eps15 were not as effective as low levels in rescuing our Eps15 knockdown. As a biphasic tyrosine phosphorylation and ubiquitination of Eps15 was observed (Fig. 2.2, *B* and *G*), it is possible that a pool of Eps15 may dimerize with Eps15b to cause this secondary wave.

In conclusion, we demonstrate a novel mode of recruitment of Eps15 to the Met RTK. As Eps15 is a key scaffold protein involved in the internalization of RTKs, this study reinforces the need to gain a better understanding of the molecular mechanisms of the interactions of Eps15 and its interacting partners

downstream of growth factors.

## 2.6. EXPERIMENTAL PROCEDURES

### Antibodies and Reagents

Antibody 145 was raised in rabbit against a C-terminal peptide of human Met[454]. Phosphotyrosine (4G10) and Met DL-21 antibodies were purchased from Upstate Biotechnology (Lake Placid, NY). Anti-Eps15 (C-20), anti-ubiquitin (P4D1) and anti-GST were obtained from Santa Cruz Biotechnology (Santa Cruz, CA). Met antibody AF276 were from R&D Systems (Minneapolis, MN), FLAG and actin antibodies were from Sigma-Aldrich, anti-GFP, Alexa-Fluor 488-, 555-, and 647-conjugated secondary antibodies were obtained from Molecular Probes (Eugene, OR), and phosphor-specific Met tyrosine 1234/35 and EGFR were from Cell Signaling Technology (Mississauga, Ontario, Canada). Monoclonal EEA1 antibody and AP-2 (μ2) were obtained from BD Biosciences (Mississauga, Ontario, Canada), HA.11 and Myc 9E10 monoclonal antibodies were from Covance (Berkeley CA) and BabCO (Richmond, CA), respectively. Mannose 6-phosphate receptor, cation-dependent antibody (22d4) was obtained from the developmental studies hybridoma bank (Iowa City, IA). HGF was a kind gift from Genentech (San Francisco, CA). EGF was purchased from Roche Diagnostics (Laval, Quebec, Canada). Cycloheximide purchased from Sigma was reconstituted in water to 10 mg/ml (100X).

### Cell Culture and Transient Transfections

T47D breast epithelial cells, HeLa cells, and HEK293 cells were cultured in Dulbecco's modified Eagle's medium containing 10% fetal bovine serum. T47D stable cell lines expressing wild-type Met was established and described previously[108]. K1110A Met stable cells were made through electroporation with pLXSN-Met K1110A cDNA in a similar manor. Transient transfections in HEK293 and HeLa cells were performed using Lipofectamine Plus reagent according to the manufacturer's instructions (Invitrogen).

**Immunoprecipitation and Western Blotting**

Following stimulation with HGF (0.60nM unless otherwise indicated), T47D cells, HeLa cells, and HEK293 cells were harvested in TGH lysis buffer (50mM HEPES, pH 7.5, 150mM NaCl, 1.5mM MgCl2, 1 mM EGTA, 1% Triton X-100, 10% glycerol, 1 mM phenylmethylsulfonyl fluoride, 1 mM sodium vanadate, 10μg/ml aprotinin, and 10 μg/ml leupeptin). HEK293 transfections were harvested 48 h post-transfection. Lysates were incubated with antibody for 1 h at 4°C with gentle rotation followed by 1-h incubation with protein A- or G-Sepharose beads. For FLAG-immunoprecipitations, lysates were directly incubated with Anti-FLAG M2 beads (Sigma) and incubated for 4 h. Captured proteins were collected by washing three times in their respective lysis buffers, eluted by boiling in SDS sample buffer, resolved by SDS-PAGE, and transferred to a nitrocellulose membrane. Membranes were blocked in 3% bovine serum albumin in TBST (10mM Tris, pH 8.0, 150mM NaCl, 2.5mM EDTA, 0.1% Tween 20) for 1 h and incubated with primary then secondary antibodies in TBST for 1 h. After three washes with TBST, bound proteins were visualized with an ECL detection kit (Amersham Biosciences). To detect Eps15 ubiquitination, cells from a 10-cm dish were lysed in radioimmunoprecipitation assay buffer (0.05% SDS, 50mM Tris, pH 8.0, 150 nM NaCl, 1% Nonidet P-40, 0.05% sodium deoxycholate) and processed as above. Densitometric analysis of Western blots was performed using NIH ImageJ software.

**Confocal Immunofluorescence Microscopy**

Cells were seeded at $1x10^4$ to $5x10^4$ on glass coverslips (Bellco Glass Inc., Vineland, NJ) in 24-well plates (Nalgene Nunc, Rochester, NY) and transfected 24 h later or left untransfected. 24 h posttransfection cells were serum-starved for 2 h prior to HGF treatment in the presence of cycloheximide. Coverslips were washed once with PBS and then fixed with 3% paraformaldehyde (Fisher Scientific) in PBS for 20 min followed by washing four times in PBS. Residual

paraformaldehyde was removed with three 5-min washes with 100 mM glycine in PBS. Cells were permeabilized with 0.3% Triton X-100/PBS and blocked for 30 min with blocking buffer (5% bovine serum albumin, 0.2% Triton X-100, 0.05% Tween 20, PBS). Coverslips were incubated with primary and secondary antibodies diluted in blocking buffer for 1 h and 40 min, respectively, at room temperature, and nuclei were counterstained with 4',6-diamidino-2-phenylindole. Coverslips were mounted with immu-mount (Thermo-Shandon, Pittsburgh, PA). Confocal images were taken using a Zeiss 510 Meta laser scanning confocal microscope (Carl Zeiss, Canada Ltd., Toronto, Ontario, Canada) with 100x objective and 1.5x zoom. Image analysis was carried out using the LSM 5 image browser (Empix Imaging, Mississauga, Ontario, Canada).

**Generation of Eps15 Constructs**

GFP-Eps15, FLAG-Eps15 WT, delta-I, -II, -III, and -IV, and Y850F constructs were kind gifts from Dr. Edward A. Fon (Montreal, CA) and have been described previously[439]. FLAG Eps15-II, -III, and -II/III constructs were made by subcloning fragments amplified by PCR using primers designed with BamHI and XbaI restriction digest sites using the FLAG-Eps15-WT pcDNA3.1zeo as a template. The FLAG-Eps15 P770A point mutation was created using the QuikChange site-directed mutagenesis kit (Stratagene), using FLAG-Eps15-WT pcDNA3.1zeo as a template. Primers were designed to include a BstUI restriction enzyme site (underlined). Forward primer, 5'-GTGAAGATGTGCCCGCGGCACTGCCGCCC-3'; reverse primer, 5'-GGGCGGCAGTGCCGCGGGCACATCTTCAC-3'. GFP-CC construct was made by subcloning a PCR fragment amplified using primers designed with HindIII/BamHI restriction digest site using the FLAG-Eps15-WT cDNA as a template into pEGFP-C2 (Clontech). GFP-Eps15ΔCC was made by subcloning a PCR fragment using primers designed with SalI/BamHI restriction digest sites using FLAG-Eps15ΔII cDNA as a template into pEGFP-C2 (Clontech). All DNA sequences were verified by sequencing.

**GST Pulldown Assays**

Fusion proteins were produced in DH5, or BL 21 gold *Escherichia coli* strain, by induction with isopropyl-1-thio-β-D-galactopyranoside. GST and GST-Grb2 constructs have been described previously (42, 43). For pulldown assays, lysates were pre-cleared with glutathione-Sepharose beads for 1 h, whereas 5–10 μg of GST fusion proteins were immobilized to glutathione-Sepharose beads at room temperature for 30 min. Beads were washed three times with lysis buffer containing inhibitors, then pre-cleared lysates were added to the beads. Samples were gently rocked at 4 °C for 1 h, washed three times in TGH with inhibitors, eluted by boiling in SDS sample buffer, and analyzed by Western blotting with the appropriate antibodies.

**siRNA**

HeLa cells were seeded at $3x10^5$ cells/well in a 6-well dish and 24 h later transfected with 10 nM scramble control siRNA or Eps15 siRNA (target sequence: ATG CTG TAG GTT GAA CCA TTA) with HiPerFect as per the manufacturer's instructions (Qiagen). Cells were replated 24 h later at $3x10^5$ cells/60-mm dish and re-transfected with siRNA (10 nM) or transfected with siRNA-resistant Eps15 cDNA. The following day cells were stimulated with HGF in the presence of cycloheximide and lysed.

## 2.7. ACKNOWLEDGMENTS

We thank members of the Park laboratory for helpful comments on the manuscript. We thank Genetech Inc. for HGF as well as Dr. E. Fon and Dr. P. M. P. van Bergen en Henegouwen for Eps15 reagents.

## 2.8. FIGURES AND FIGURE LEGENDS

FIGURE 2.1. **Eps15 is recruited to the Met receptor upon Met activation.** *A*, schematic diagram depicting the experimental protocol for a cold load stimulation, used to assess synchronized internalization and trafficking of RTKs. *B*, confocal images of endogenous Eps15 and Met upon cold load stimulation. HeLa cells were serum-starved in the presence of cycloheximide to reduce newly synthesized Met staining, then fixed and imaged (*a– c*) or treated with HGF (0.60 nM) for 1 h at 4 °C (*d–f*), followed by warming to 37 °C for the indicated times (*g–o*). Met (*red*), Eps15 (*green*), and 4',6-diamidino-2-phenylindole. Magnification, 100x; zoom, 1.5x; *bar* = 10μm. *C*, HeLa cells were subjected to a cold load stimulation, and endogenous Eps15 was immunoprecipitated (1 mg) and blotted for Met and total Eps15 levels. Whole cell lysates (*WCL*) were blotted (*WB*) for phospho-Met (p1234/1235) and actin levels. *D*, HeLa cells were plated on coverslips. 24 h later, cells were serum-starved in the presence of cycloheximide for 2 h, followed by cold load stimulating with 0.12 nM HGF followed by warming to 37 °C for 15 min. Cells were stained for Met (*red*), Eps15 (*green*), and 4',6-diamidino-2-phenylindole. *Bar* =10μm.

## Figure 2.1

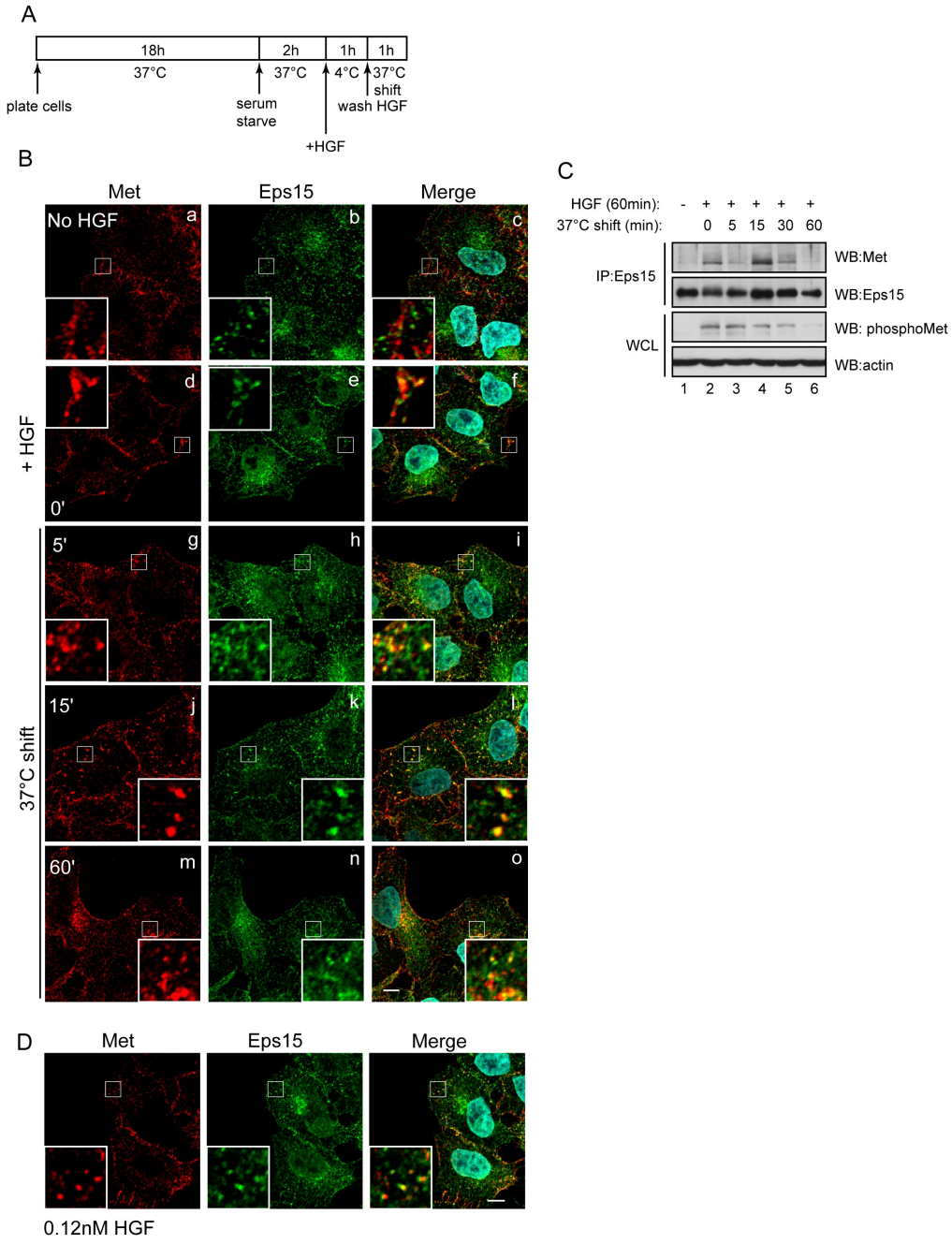
A
18h
37°C
2h
37°C
1h
4°C
1h
37°C
shift
wash HGF
plate cells
serum
starve
+HGF
B
Met
Eps15
Merge
No HGF
+ HGF
37°C shift
0'
5'
15'
60'
C
HGF (60min): - + + + + +
37°C shift (min): 0 5 15 30 60
IP:Eps15
WB:Met
WB:Eps15
WCL
WB: phosphoMet
WB:actin
1 2 3 4 5 6
D
Met
Eps15
Merge
0.12nM HGF

FIGURE 2.2. **Eps15 is subject to post-translational modifications in response to HGF stimulation.** *A*, HeLa and T47D stable cells expressing Met were blotted for protein levels. *B*, T47D cells stably expressing either Met WT or Met K1110A (kinase-dead) were cold load stimulated with HGF for 1 h at 4 °C then released to 37 °C for the time indicated. Endogenous Eps15 or Met was immunoprecipitated (*IP*) and blotted for 4G10 anti-phosphotyrosine (*pTyr*) and total protein levels. *AP2*, mu2 subunit was also blotted. *C*, HeLa cells were cold load-stimulated, immunoprecipitated for endogenous Eps15, and blotted for tyrosine phosphorylation. *D*, HeLa cells were stimulated with HGF at 37 °C for the indicated times, and lysed. Endogenous Eps15 was immunoprecipitated and phosphotyrosine levels were assessed. *E*, HEK293 cells were co-transfected with GFP-Eps15 and increasing amounts of Met WT cDNA expression vector. Eps15 was immunoprecipitated using anti-GFP antibodies, and phosphotyrosine levels were examined. *F*, HEK293 cells were transfected with either FLAG-Eps15 WT or Y850F and co-transfected with Met WT or K1110A. Immunoprecipitations were performed using anti-Met or anti-FLAG M2 beads and analyzed through Western blotting as indicated. *G*, HeLa cells transfected with HA-Ubiquitin (*HA-Ub*) were cold load-stimulated with HGF and immunoprecipitated for Eps15 then blotted for HA-Ubiquitin, and reprobed for Eps15. *UT* = untransfected.

**Figure 2.2**

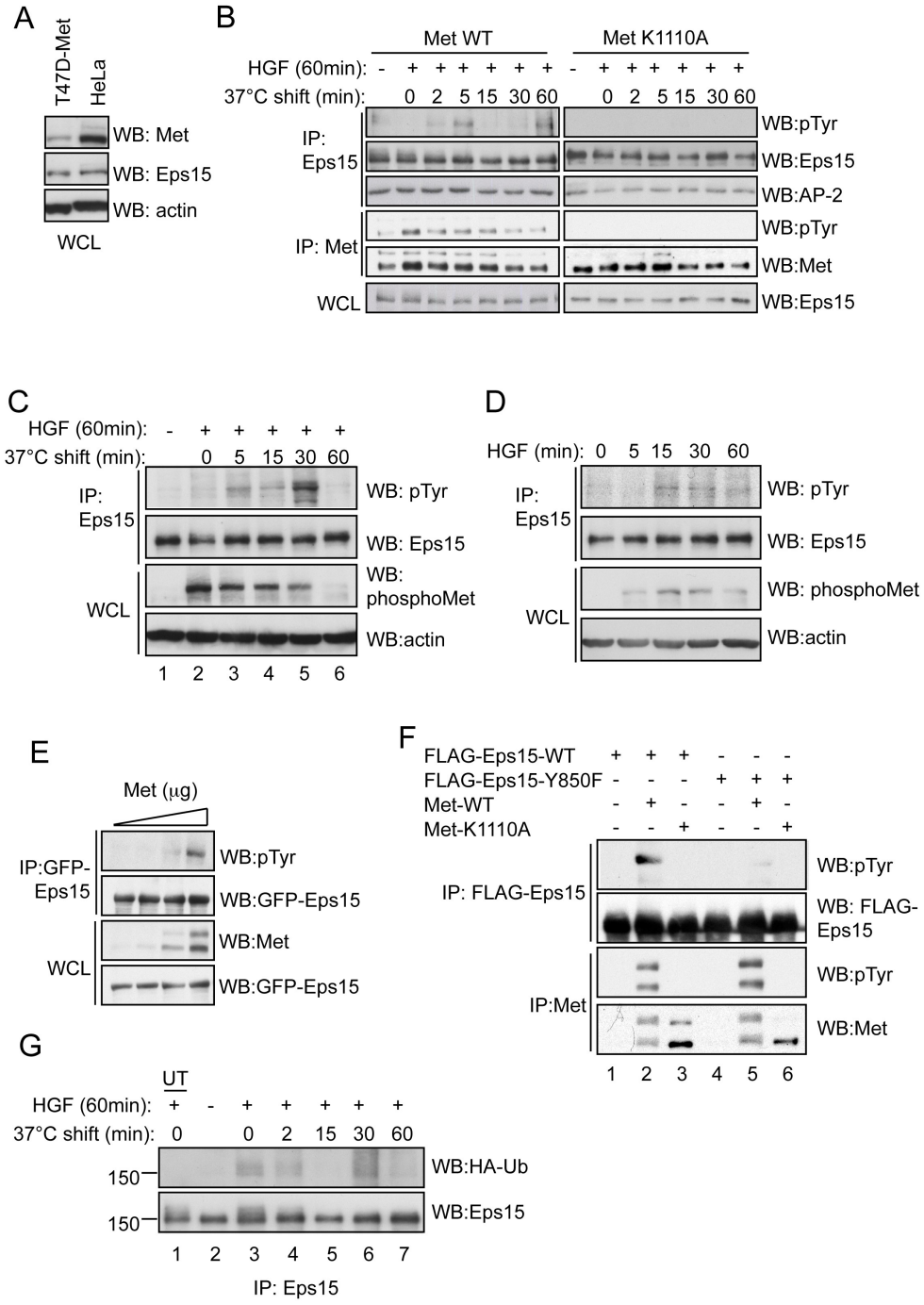
A
T47D-Met
HeLa
WB: Met
WB: Eps15
WB: actin
WCL
B
Met WT
Met K1110A
HGF (60min): - + + + + + + - + + + + + +
37°C shift (min): 0 2 5 15 30 60 0 2 5 15 30 60
IP: Eps15
WB:pTyr
WB:Eps15
WB:AP-2
IP: Met
WB:pTyr
WB:Met
WCL
WB:Eps15
C
HGF (60min): - + + + + +
37°C shift (min): 0 5 15 30 60
IP: Eps15
WB: pTyr
WB: Eps15
WCL
WB: phosphoMet
WB:actin
1 2 3 4 5 6
D
HGF (min): 0 5 15 30 60
IP: Eps15
WB: pTyr
WB: Eps15
WCL
WB: phosphoMet
WB:actin
E
Met (μg)
IP:GFP-Eps15
WB:pTyr
WB:GFP-Eps15
WCL
WB:Met
WB:GFP-Eps15
F
FLAG-Eps15-WT + + + - - -
FLAG-Eps15-Y850F - - - + + +
Met-WT - + - - + -
Met-K1110A - - + - - +
IP: FLAG-Eps15
WB:pTyr
WB: FLAG-Eps15
IP:Met
WB:pTyr
WB:Met
1 2 3 4 5 6
G
UT
HGF (60min): + - + + + + +
37°C shift (min): 0 0 2 15 30 60
150
WB:HA-Ub
150
WB:Eps15
1 2 3 4 5 6 7
IP: Eps15

FIGURE 2.3. **Eps15 is recruited to a Met complex through its coiled-coil domain.** *A*, HEK293 cells were transiently transfected with Met and truncation mutants of Eps15, followed by immunoprecipitation of Met and FLAG-Eps15 48h post-transfection and Western blotted (*WB*) as shown. *B*, individual domains of Eps15 II, III, or II and III were co-transfected with Met and immunoprecipitated as in *A*. Eps15 WT, Eps15ΔII and Eps15ΔIII were separated out on the same gel for level comparison. *C*, schematic diagram of Eps15 mutants and a summary of the immunoprecipitation (*IP*) analysis. Binding to Met was characterized as strong (+++), good (++), weak (-/+) or poorly/not at all (-). *D*, FLAG-Eps15 and Met WT or Met Y1003F were transiently transfected in HEK293 cells. Lysates were immunoprecipitated for Met and FLAG then Western blotted as indicated. *E*, HEK293 cells were transiently co-transfected with EGFR and truncation mutants of Eps15. 24 h later cells were serum-starved overnight, then stimulated with 100 ng/ml EGF for 8 min, followed by immunoprecipitation of EGFR, and Western blotted as shown.

**Figure 2.3**

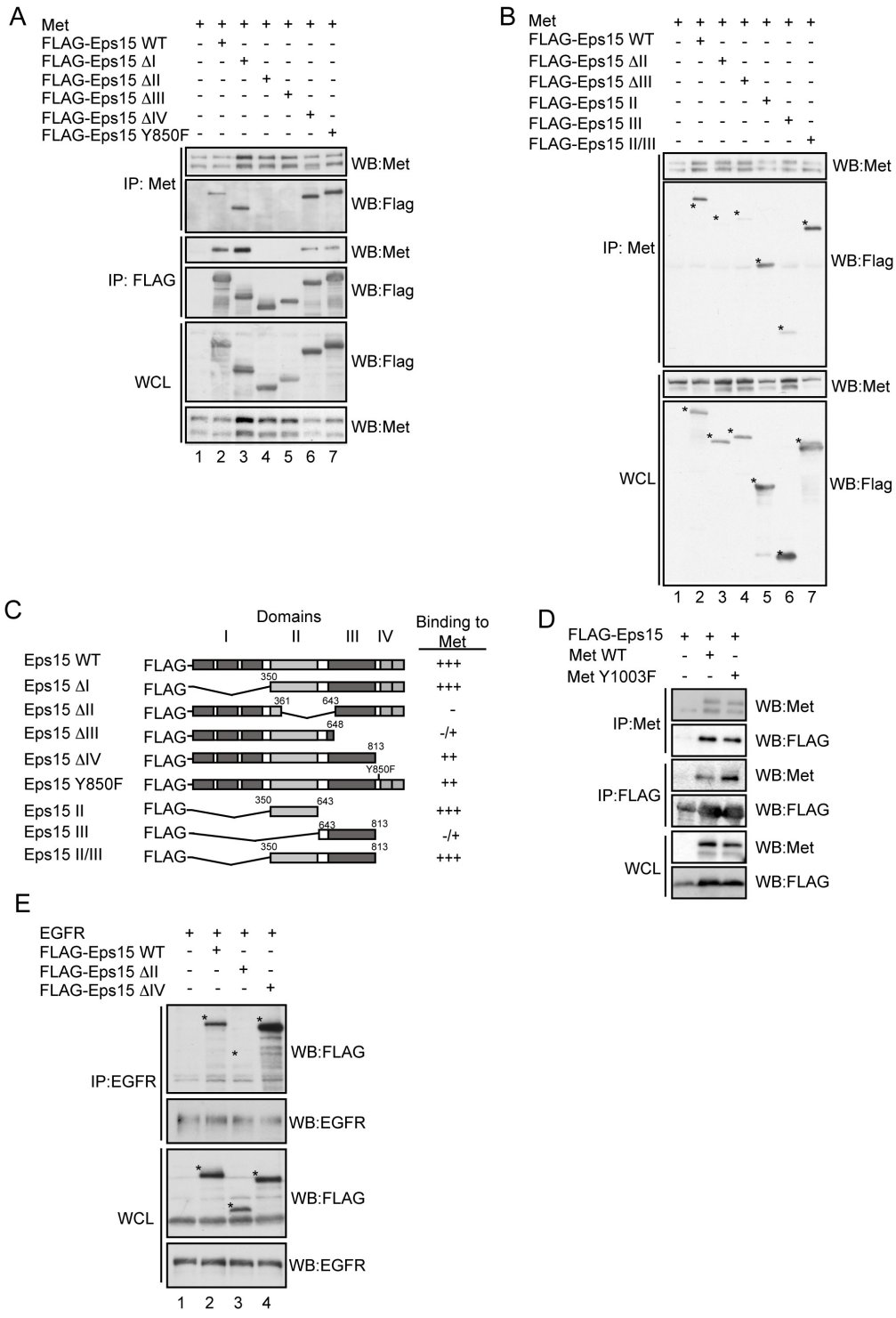
A
Met
FLAG-Eps15 WT
FLAG-Eps15 ΔI
FLAG-Eps15 ΔII
FLAG-Eps15 ΔIII
FLAG-Eps15 ΔIV
FLAG-Eps15 Y850F
IP: Met
IP: FLAG
WCL
WB:Met
WB:Flag
1 2 3 4 5 6 7
B
Met
FLAG-Eps15 WT
FLAG-Eps15 ΔII
FLAG-Eps15 ΔIII
FLAG-Eps15 II
FLAG-Eps15 III
FLAG-Eps15 II/III
IP: Met
WCL
WB:Met
WB:Flag
1 2 3 4 5 6 7
C
Domains
I II III IV
Binding to Met
Eps15 WT
Eps15 ΔI
Eps15 ΔII
Eps15 ΔIII
Eps15 ΔIV
Eps15 Y850F
Eps15 II
Eps15 III
Eps15 II/III
FLAG
350
361
643
648
813
Y850F
+++
+++
-
-/+
++
++
+++
-/+
+++
D
FLAG-Eps15
Met WT
Met Y1003F
IP:Met
IP:FLAG
WCL
WB:Met
WB:FLAG
E
EGFR
FLAG-Eps15 WT
FLAG-Eps15 ΔII
FLAG-Eps15 ΔIV
IP:EGFR
WCL
WB:FLAG
WB:EGFR
1 2 3 4

FIGURE 2.4. **Grb2 associates with Eps15 through a proline-rich motif.** *A*, schematic of Eps15 and Grb2 domains. Proline 770 of Eps15 within the P*XX*P motif with surrounding amino acids identified using Scansite are indicated along with the score. The scores for one of the proline residues of SOS and Gab1 as identified by Scansite are also given for comparison. *B*, FLAG-Eps15 and Myc-Grb2 expression constructs were transfected with or without Met and immunoprecipitated (*IP*) as indicated followed by blotting for Eps15 (FLAG), Grb2 (*myc*), or Met levels. *C*, HeLa cells left unstimulated or stimulated with HGF for 15 min were lysed and immunoprecipitated using Eps15 antibodies (+*Ab*) and blotted for Grb2. Parallel control immunoprecipitates were carried out without antibody addition (-*Ab*). *D*, a panel of FLAG-Eps15 truncation mutants were co-transfected with myc-Grb2 in HEK293 cells and immunoprecipitated and blotted as indicated. *E*, summary of co-immunoprecipitations of Eps15 and Grb2, (+) = co-immunoprecipitation observed, (-) = no co-immunoprecipitation observed. *F*, GST pulldown assays using GST-Grb2 using lysates transfected with Eps15 WT or Eps15 P770A expression constructs. GST-alone was used as a control. *G*, HeLa cells transfected with Eps15 WT or P770A and HA-Ub were cold load-stimulated with 0.60nM HGF and immunoprecipitated for Eps15 then blotted for HA and phosphotyrosine. Met activation was assessed through Western blotting using phosphospecific Met tyrosine 1234/35 antibodies.

**Figure 2.4**

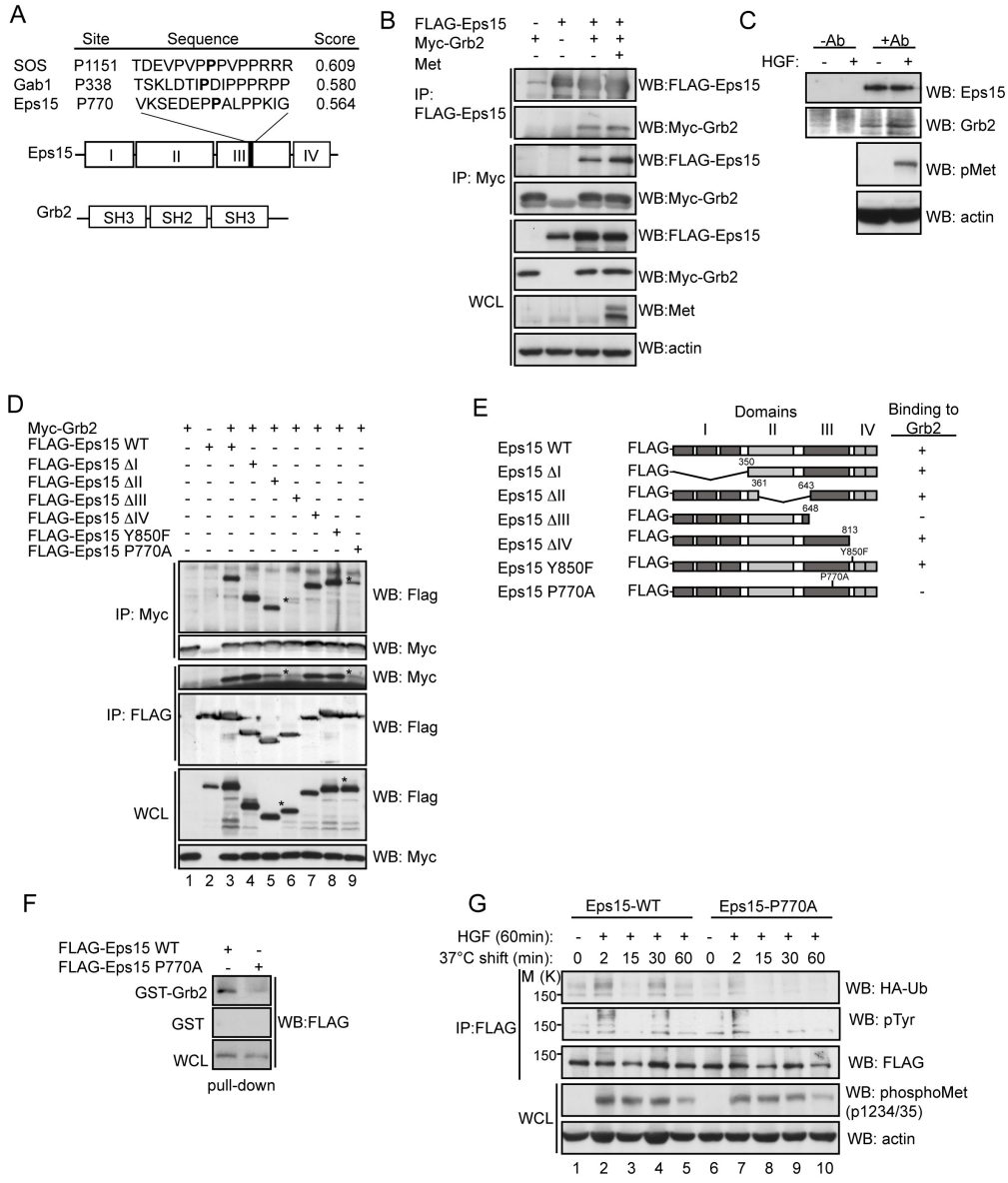
A
Site
Sequence
Score
SOS P1151 TDEVPVPPPVPPRRR 0.609
Gab1 P338 TSKLDTIPDIPPPRPP 0.580
Eps15 P770 VKSEDEPPALPPKIG 0.564
Eps15
I
II
III
IV
Grb2
SH3
SH2
SH3
B
FLAG-Eps15
Myc-Grb2
Met
IP: FLAG-Eps15
WB:FLAG-Eps15
WB:Myc-Grb2
IP: Myc
WB:FLAG-Eps15
WB:Myc-Grb2
WCL
WB:FLAG-Eps15
WB:Myc-Grb2
WB:Met
WB:actin
C
-Ab
+Ab
HGF:
WB: Eps15
WB: Grb2
WB: pMet
WB: actin
D
Myc-Grb2
FLAG-Eps15 WT
FLAG-Eps15 ΔI
FLAG-Eps15 ΔII
FLAG-Eps15 ΔIII
FLAG-Eps15 ΔIV
FLAG-Eps15 Y850F
FLAG-Eps15 P770A
IP: Myc
WB: Flag
WB: Myc
IP: FLAG
WB: Myc
WB: Flag
WCL
WB: Flag
WB: Myc
1 2 3 4 5 6 7 8 9
E
Domains
I
II
III
IV
Binding to Grb2
Eps15 WT
Eps15 ΔI
Eps15 ΔII
Eps15 ΔIII
Eps15 ΔIV
Eps15 Y850F
Eps15 P770A
FLAG
350
361
643
648
813
Y850F
P770A
F
FLAG-Eps15 WT
FLAG-Eps15 P770A
GST-Grb2
GST
WCL
WB:FLAG
pull-down
G
Eps15-WT
Eps15-P770A
HGF (60min):
37°C shift (min): 0 2 15 30 60 0 2 15 30 60
M (K)
150
IP:FLAG
WB: HA-Ub
WB: pTyr
WB: FLAG
WCL
WB: phosphoMet (p1234/35)
WB: actin
1 2 3 4 5 6 7 8 9 10

FIGURE 2.5. **Coiled-coil domain is sufficient for displacing a WT-Eps15-Met complex but not an EGFR-Eps15 complex.** *A*, HEK293 cells were transfected with Met and Eps15 WT expression constructs in the presence of increasing amounts of the coiled-coil domain (*Eps15 CC*). Immunoprecipitations (*IP*) were performed on the lysates as indicated. *Arrows* show migration of wild-type (*Eps15 WT*) and Eps15 CC proteins. Molecular weight protein marker migration is indicated to the *left* of the blots. *B*, HEK293 cells transfected with either Met or EGFR and FLAG-Eps15 expression constructs with increasing amounts of FLAG-CC. EGFR cells were stimulated with 100 ng/ml EGF for 8 min prior to lysing. Lysates were immunoprecipitated with anti-Met and anti-EGFR antibodies and blotted for FLAG. *Arrows* show migration of wild-type (*Eps15 WT*) and Eps15 CC proteins and heavy chain. Molecular weight protein marker migration is indicated to the *left* of the blots. *C*, quantification of coiled-coil protein levels co-immunoprecipitated with anti-Met or anti-EGFR antibodies with increasing CC domain protein levels. Results were quantified using densitometric analysis from at least three independent experiments. For Met immunoprecipitations; $p < 0.03$, Student's *t* test, mean S.E. *D*, quantification of FLAG-Eps15 WT protein levels co-immunoprecipitated in the presence of increasing amounts of coiled-coil domain using anti-Met and anti-EGFR antibodies. Results are quantified using densitometric analysis from at least three independent experiments. Shown is the mean S.E. For Met co-immunoprecipitation; $p < 0.003$, Student's *t* test.

**Figure 2.5**

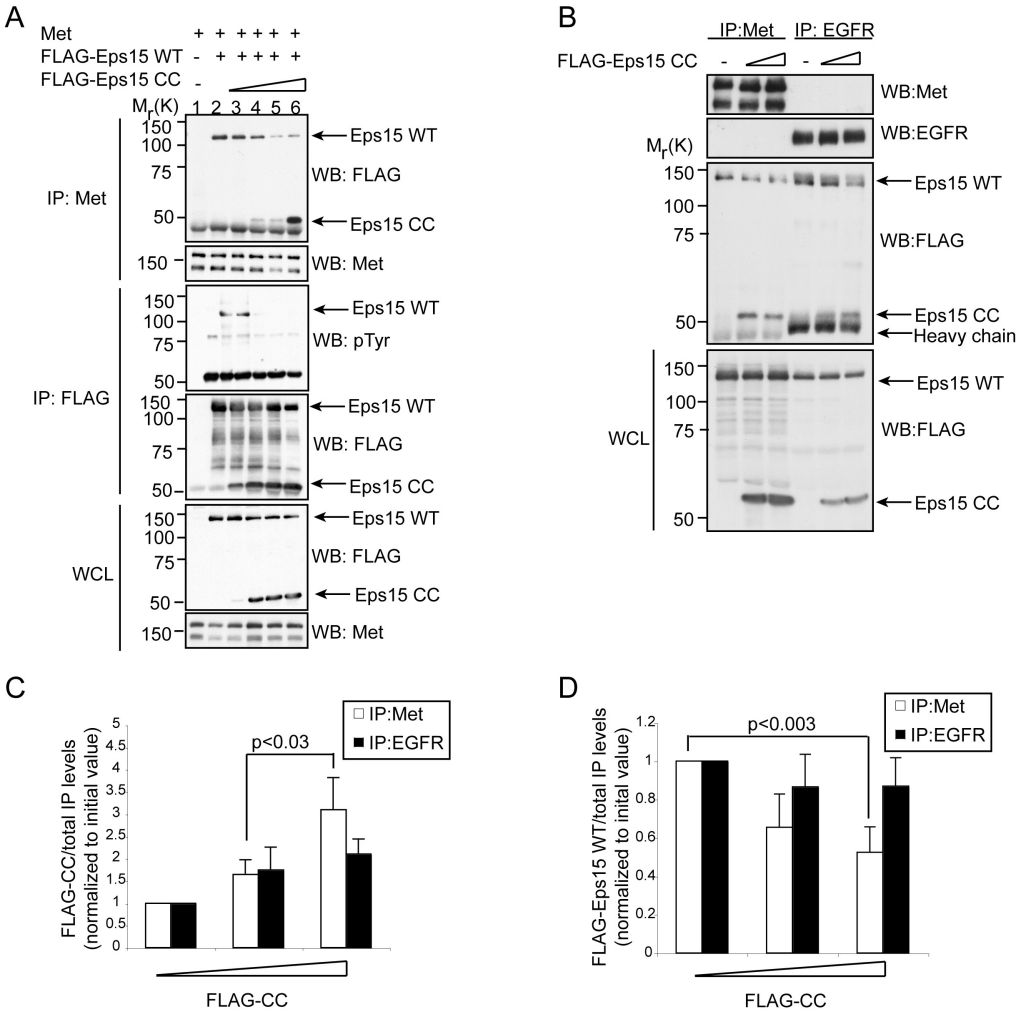
A
Met + + + + + +
FLAG-Eps15 WT - + + + + +
FLAG-Eps15 CC -
Mr(K) 1 2 3 4 5 6
IP: Met
IP: FLAG
WCL
150
100
75
50
Eps15 WT
Eps15 CC
WB: FLAG
WB: Met
WB: pTyr
B
IP:Met
IP: EGFR
FLAG-Eps15 CC - -
WB:Met
WB:EGFR
Mr(K)
WB:FLAG
Heavy chain
WCL
C
FLAG-CC/total IP levels (normalized to initial value)
p<0.03
IP:Met
IP:EGFR
FLAG-CC
D
FLAG-Eps15 WT/total IP levels (normalized to inital value)
p<0.003
IP:Met
IP:EGFR
FLAG-CC

FIGURE 2.6. **Eps15 knockdown delays Met degradation and is rescued by WT Eps15.** *A*, HeLa cells transfected with control scramble siRNA (10nM) or Eps15 siRNA at 5 nM or 10 nM concentrations were harvested 72 h post-transfection and assessed for protein levels. *B*, HeLa cells transfected with scramble or Eps15 siRNA were stimulated with HGF in the presence of cycloheximide then stained for Met and 4',6-diamidino-2-phenylindole and imaged using confocal microscopy for the indicated times. *Arrows* point to Met-positive staining. *Bar* = 20 μm. *C*, Western blots of HeLa cells transfected with scramble and Eps15 siRNA. Cells were stimulated with HGF in the presence of cycloheximide for the indicated amount of time. Lysates were blotted for Met, Eps15, and actin (*top panel*). Mean Met protein levels were quantified through densitometric analysis and graphed as percentage of initial protein levels. *Error bars* represent S.E. Results shown are from four independent experiments (*bottom panel*). *D* (*left panel*): HeLa cells transfected with Eps15 siRNA were transiently transfected with siRNA-resistant Eps15 cDNA and compared with scramble control or Eps15 siRNA-treated cells. Met protein levels were quantified as in *C*, after HGF stimulation in the presence of cycloheximide. Shown is the mean value of Met levels at the 4-h time point. Results are from four independent experiments. The difference between Eps15-depleted cells *versus* rescued cells is statistically significant; $p < 0.01$, Student's *t* test. *Right panel*: Western blots of siRNA-treated cells; *, GFP-Eps15 protein levels.

**Figure 2.6**

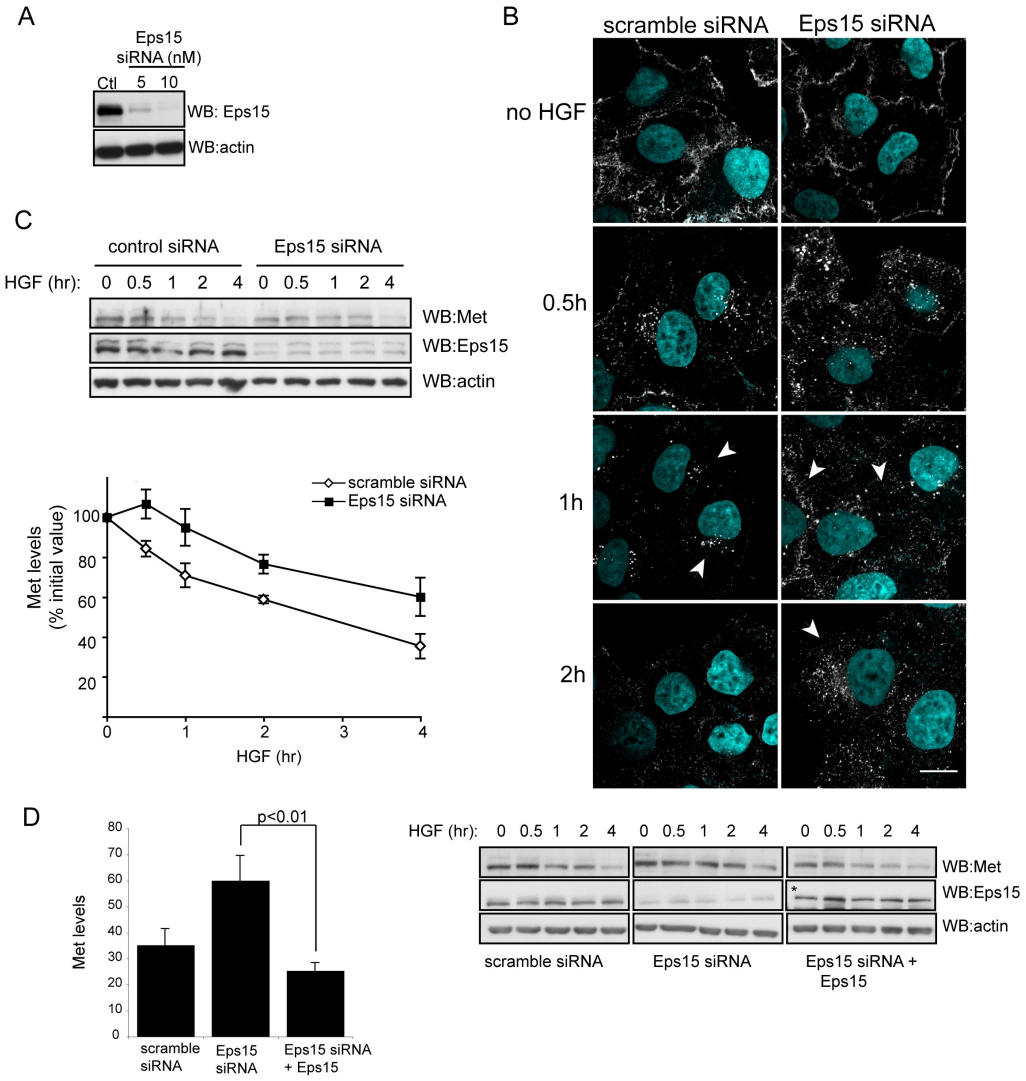
A
Eps15 siRNA (nM)
Ctl 5 10
WB: Eps15
WB:actin
B
scramble siRNA
Eps15 siRNA
no HGF
0.5h
1h
2h
C
control siRNA
Eps15 siRNA
HGF (hr): 0 0.5 1 2 4 0 0.5 1 2 4
WB:Met
WB:Eps15
WB:actin
scramble siRNA
Eps15 siRNA
Met levels (% initial value)
HGF (hr)
D
p<0.01
Met levels
scramble siRNA
Eps15 siRNA
Eps15 siRNA + Eps15
HGF (hr): 0 0.5 1 2 4 0 0.5 1 2 4 0 0.5 1 2 4
WB:Met
WB:Eps15
WB:actin
scramble siRNA
Eps15 siRNA
Eps15 siRNA + Eps15

FIGURE 2.7. **Eps15 knockdown is rescued by WT and P770A mutant but not rescued by Eps15ΔCC or Eps15ΔUIM mutants.** *A*, HeLa cells treated with siRNA as described under "Experimental Procedures," were transfected with either vector, siRNA-resistant Eps15 WT, Eps15ΔCC, Eps15 P770A, or Eps15ΔUIM. 24 h later, cells were treated with HGF in the presence of cycloheximide for 2 h, fixed, stained for Met and Eps15 (or vector), and viewed using confocal microscopy. Magnification, 100x; zoom, 1.5; *bar* = 10μm. *B*, Eps15 knockdown cells expressing Eps15 constructs from *A* were counted for anti-Met staining. Results shown are from three independent experiments with at least 30 cells counted per condition. *C*, Western blot of knockdown cells expressing Eps15 constructs. Cells were stimulated with HGF for 2 h in the presence of cycloheximide, and protein levels were blotted as indicated.

**Figure 2.7**

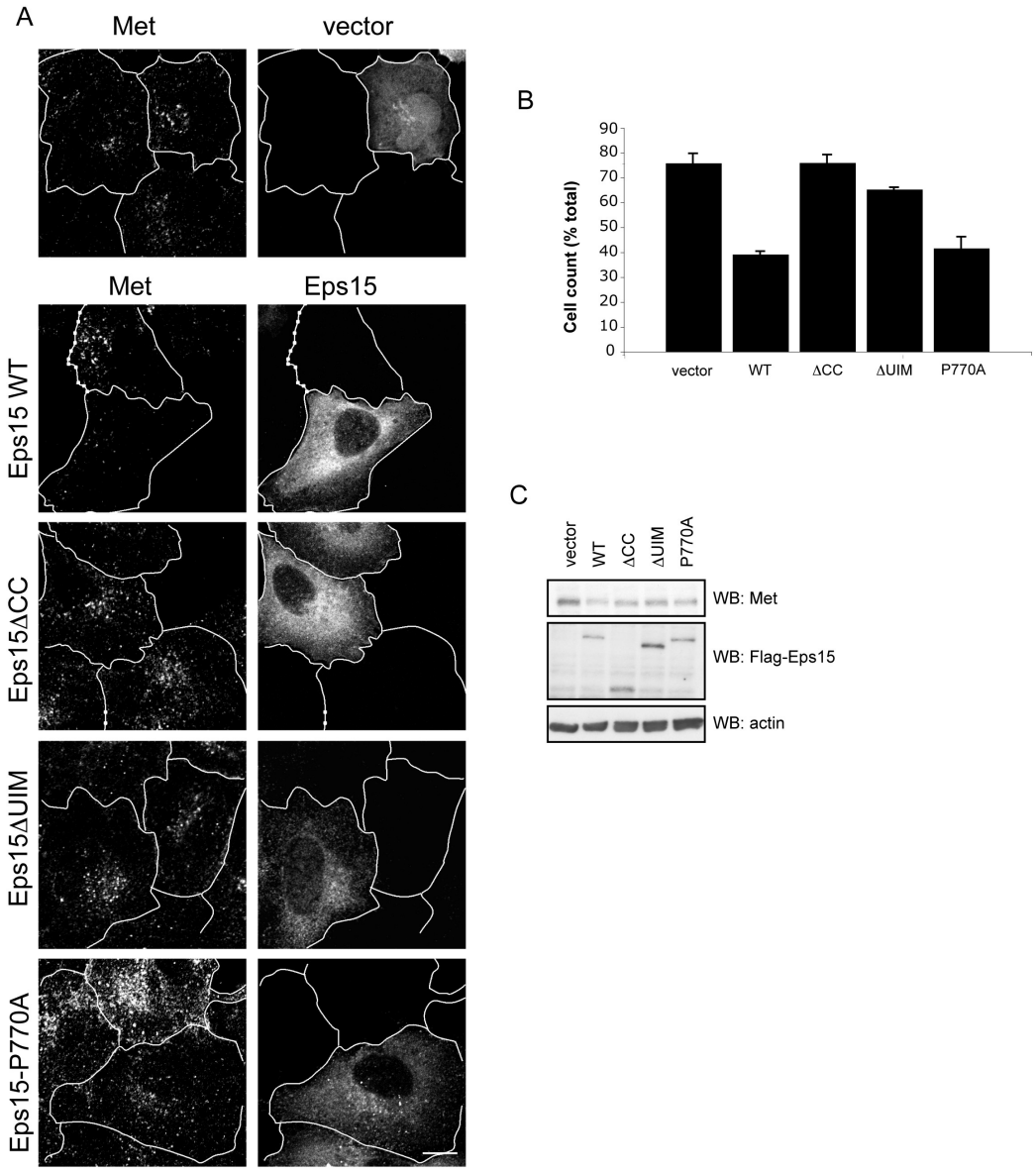
A
Met
vector
Met
Eps15
Eps15 WT
Eps15ΔCC
Eps15ΔUIM
Eps15-P770A
B
Cell count (% total)
90
80
70
60
50
40
30
20
10
0
vector
WT
ΔCC
ΔUIM
P770A
C
vector
WT
ΔCC
ΔUIM
P770A
WB: Met
WB: Flag-Eps15
WB: actin

**Supplemental Figures**

FIG. S2.1. **Eps15 is recruited to a Met complex that is EEA-1 positive upon Met activation**. *A*, Confocal images of HeLa cells stained for endogenous Eps15 and Mannose-6-phosphate receptor (M6PR). M6PR (red), Eps15 (green) and DAPI. 100x mag, 1.5x zoom. *B*, Confocal images of HeLa cells cold load stimulated with HGF and released for 15 min then stained for Eps15 (green) and early endsome marker EEA-1 (red) and DAPI. 100x mag, 1.5x zoom. *C*, HEK293 cells were transiently transfected with Met, GFP-Eps15 or both. Lysates were immunoprecipitated (IP) for Met and blotted with the indicated antibodies (pTyr = phosphotyrosine).

FIG. S2.2. **Ubiquitination occurs upon Met over-expression and Eps15 WT but not ΔUIM binds to Ub**. *A*, HEK293 cells transiently transfected with vector or Met and HA-Ub were immunoprecipitated with anti-Met antibodies and blotted for ubiquitin (Ub) stripped then reprobed for total Met levels. *B*, HEK293 cells were transiently transfected with Eps15 WT or Eps15ΔUIM (also referred to as Eps15ΔIV) immunoprecipitated with anti-FLAG M2 beads and blotted as indicated. Molecular weight is indicated on the left-hand side. Heavy chain is denoted with and asterisk.

FIG. S2.3. **Comparison of Gab1 and Eps15 co-immunoprecipitation with Grb2 and Eps15 P770A and WT co-immunoprecipitation with Met**. *A*, HEK293 cells transfected with GFP-tagged Eps15 or GFP-Gab1 were co-transfected with Myc-Grb2 and immunoprecipated as indicated. *B*, Met and either Eps15 WT or P770A expression constructs were immunoprecipitated as indicated and blotted.

## Supplemental Figure S2.1

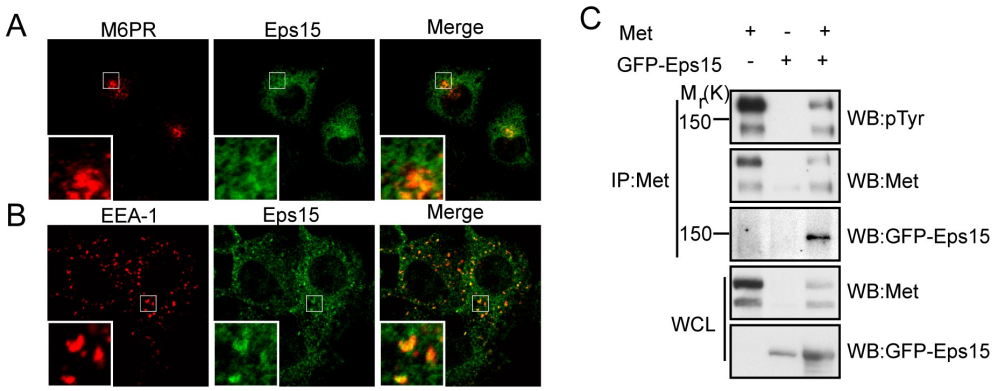


## Supplemental Figure S2.2

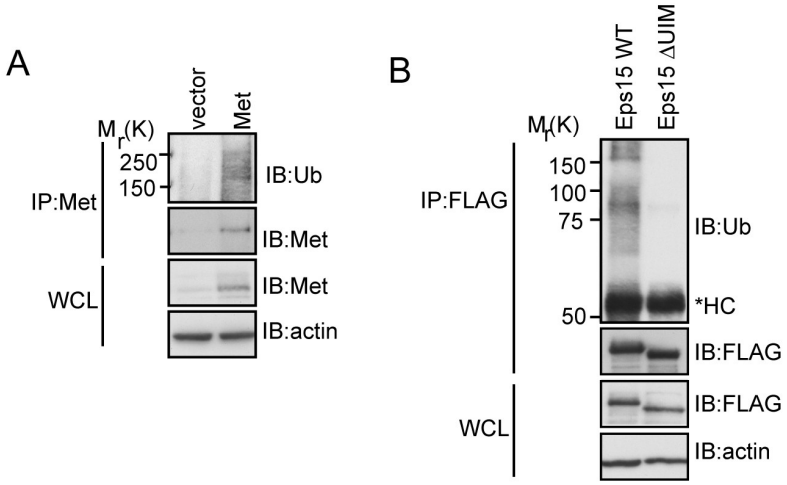


## Supplemental Figure S2.3

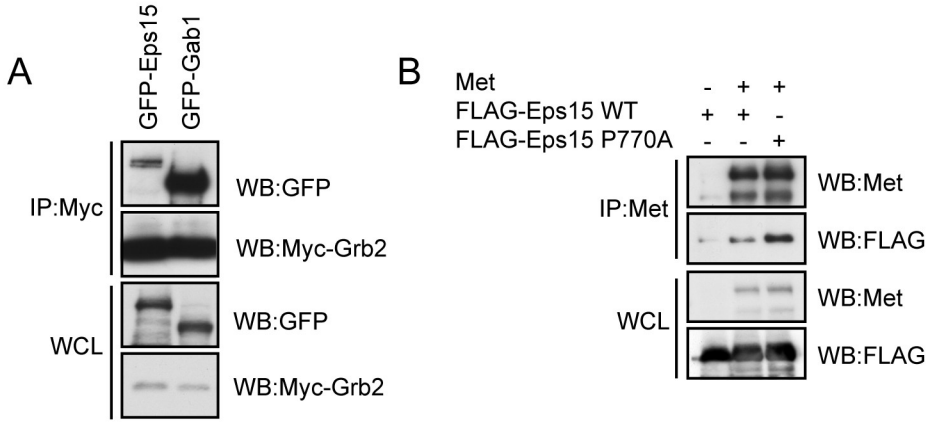

# Chapter 3

## 3. GGA3 Functions as a Switch to Promote Met Receptor Recycling, Essential for Sustained ERK and Cell Migration

Christine A. Parachoniak, Yi Luo, Jasmine V. Abella, James H. Keen and Morag Park

## 3.1. PREFACE

In Chapter 2, we characterized the interaction of Eps15, an endocytic adaptor protein previously characterized to play a role downstream of the EGFR, downstream from the Met receptor. Similarly, in this chapter, we have characterized the role of another endocytic adaptor, namely GGA3. Although an extensive body of work has characterized the molecular mechanisms leading to RTK ubiquitination and degradation, virtually nothing in the way of RTK recycling, in particular for the Met RTK was known prior to this thesis. Here we demonstrate that HGF-induces fast, GGA3-dependent recycling of the Met receptor and have characterized the molecular complex required for recycling. By identifying the key players in this pathway, we argue that recycling provides an alternative and equally important contribution to sustaining ERK activation and cell migration as the ubiquitin-dependent degradative pathway.

## 3.2. ABSTRACT

Cells are dependent on correct sorting of activated receptor tyrosine kinases (RTKs) for the outcome of growth factor signaling. Upon activation, RTKs are coupled through the endocytic machinery for degradation, or recycled to the cell surface. However, the molecular mechanisms governing RTK recycling are poorly understood. Here, we show that Golgi-localized gamma-ear containing Arf-binding protein 3 (GGA3) interacts selectively with the Met/Hepatocyte Growth Factor RTK when stimulated, to sort it for recycling in association with "gyrating"-clathrin. GGA3 loss abrogates Met recycling from a Rab4 endosomal subdomain, resulting in pronounced trafficking of Met towards degradation. Decreased Met recycling attenuates ERK activation and cell migration. Met recycling, sustained ERK activation and migration require interaction of GGA3 with Arf6 and an unexpected association with the Crk adaptor. The data show that GGA3 defines an active recycling pathway and support a broader role for GGA3-mediated cargo selection in targeting receptors destined for recycling.

## 3.3. INTRODUCTION

Receptor Tyrosine Kinases (RTKs) control many aspects of cell behavior including proliferation, survival, differentiation and migration in response to their environment. Upon ligand binding, RTKs become catalytically active and tyrosine phosphorylated enabling the recruitment of signaling proteins to initiate downstream signaling cascades. This process is balanced by the simultaneous recruitment of endocytic proteins, which enhance RTK internalization, allowing for their removal from the cell surface and subsequent signal termination[455]. However, it is now recognized that internalization, in addition to regulating signal termination, is an integral part of signaling, controlling strength, spatial and temporal restrictions to RTK signals[201,455]. Thus a molecular understanding of the processes that regulate entry of RTKs into endocytic compartments is key to our understanding of a biological response.

The Hepatocyte growth factor (HGF) and its receptor, Met, are potent regulators of epithelial-mesenchymal transitions, cell scatter and invasion[109]. During development, their action is essential for the growth and survival of placental trophoblasts, outgrowth of motor neurons and migration of muscle precursor cells[46,49,456,457]. In the adult they coordinate wound healing in various organs such as the liver, heart and kidney[458-461]. The chronic activation of Met is associated with several human tumors[462]. One mechanism involves mutations that impair trafficking of Met by limiting its access to the degradative compartment and resulting in sustained signaling[9,106,108,463]. Since defects in cargo trafficking have now emerged as a common feature associated with several human diseases, a full understanding of the pathways that regulate RTK trafficking is essential.

Following ligand activation, RTKs, including Met, are internalized through clathrin-dependent or -independent mechanisms[464-466], eventually converging to deliver cargo to early endosomes[455]. From here, RTK cargo is diverted towards one of two fates to be routed to late endosomes/lysosomes for degradation, or to be recycled back to the plasma membrane. Many studies have provided molecular insights into the details of how RTKs such as the EGFR[175,179,288], and Met receptor[9,108,298] are targeted towards the degradative pathway, however, mechanisms that regulate and coordinate recycling pathways remain unclear.

Recycling of RTKs to the cell surface can occur either directly from the early endosome via a “fast route”, or indirectly through a “slow route”, traversing the endocytic recycling compartment[314]. In general, control of vesicle trafficking depends on the Rab and ADP-ribosylation factor (Arf) small GTPases and their binding proteins[467]. Although activation of RTKs leads to activation of Arf and Rab GTPases[468,469], the mechanisms by which these proteins are coupled to, and regulate, RTK trafficking are incompletely understood.

The Golgi-localized, gamma-ear-containing, Arf-binding proteins (GGAs) are adaptor proteins, evolutionarily conserved from yeast to humans. The GGA family is comprised of three proteins in humans, GGA1, 2, 3[321]. GGA proteins promote clathrin assembly and mediate intracellular transport of cargo, such as

mannose-6-phosphate receptor (M6PR) and sortilin, as well as plasma membrane trafficking of Gag proteins required for HIV release[232,326]. Despite detailed structural data on the modular domains of the GGA proteins, less is known about the dynamics of GGA complexes that mediate transport events. GGA proteins have been observed on early endosomes[324] and dynamic clathrin-coated structures positive for the transferrin receptor (TfR)[470], yet the functional significance of this localization is poorly understood. These observations raise the question of whether GGA proteins regulate vesicle transport for a broader range of cargo than initially proposed.

Here, we report that GGA3 defines a recycling compartment for the Met RTK. GGA3 is essential for functional recycling of the Met RTK, sustained Met-dependent ERK activation and cell migration. Selective recruitment of GGA3 with an activated Met RTK occurs through the Crk adaptor protein following Met internalization and trafficking to a Rab4/Rab5-positive compartment. These results identify a new function for GGA3 and provide mechanistic insight into selective Met RTK recycling.

## 3.4. RESULTS

### 3.4.1. GGA3 Is Recruited to an Activated Met RTK during Endocytosis

To investigate the relevance of GGAs to Met RTK trafficking, we first examined the ability of GGAs to associate with the Met RTK. Endogenous GGA3 was found to coimmunoprecipitate with endogenous Met RTK upon HGF stimulation of HeLa cells as early as 5 min; maximal association occurred by 15 min (Figure 3.1A). No association of Met was observed with endogenous GGA1 or GGA2, although lower levels of endogenous GGA1 were detected (Figure 3.1A). Consistent with recruitment of GGA3 to a Met RTK once internalized, GGA3 failed to localize with the Met RTK in the absence of HGF (Figure 3.1B). In response to HGF a 1.4-fold increase in localization of GGA3 to endosomes was observed, and at this time, GGA3 localized with Met-positive punctae, typical of early endosomes (Figures 3.1B and 3.1C).

### 3.4.2. GGA3 Localizes with Met to a Rab4 Compartment

To better understand the GGA3-Met association, we sought to determine more precisely the intracellular localization of GGA3 within the endocytic network. A subset of GFP-tagged Rab proteins was expressed and used as markers to distinguish subdomains of endocytic compartments[471]. Quantitative colocalization analysis revealed that GGA3 localizes predominantly with early Rab5- and Rab4-positive vesicles (~43.6% and ~67.7%) (see Figure S3.1A), whereas less colocalization was observed with the late markers Rab7 or Rab11 (~36.5%, and ~35.1%) (Figure S3.1A). At 15 min post-HGF stimulation, Met localizes to both Rab4- and Rab5-positive vesicles (~55.3% and ~54.6%, respectively) (Figures 3.1C, 3.1D, and S3.1B), consistent with overlap of these Rab microdomains on early endosomes[471]. Moreover, in response to HGF, GGA3 shows a preferential increase to Rab4 over Rab5-positive vesicles (1354 versus 913/ per cell, Figures 3.1E, 3.1F, and S3.1C), giving an overall 1.48-fold increase of Met and GGA3 to Rab4 over Rab5-positive vesicles. Together, this supports a possible role for GGA3 as an endocytic adaptor for Met.

### 3.4.3. GGA3 Knockdown Promotes Rapid Degradation of the Met Receptor

To understand the role of GGA3 on Met receptor function, the effect of RNAi-mediated knockdown (KD) of GGA3 on the trafficking and degradation of Met was analyzed. In HeLa cells depleted for GGA3, the half-life of the Met receptor was 50% that of control cells (T/2 ~54.5 min compared to 106.7 min) (Figures 3.2A and 3.2B). Comparable results were obtained using three independent siRNA duplexes, confirming specificity of the KD (Figure S3.2A). Following 15 min of HGF, Met internalizes into endosomes, as visualized by immunofluorescence (IF) (Figures 3.1B and S3.2B). At this time point, no detectable differences were observed in Met localization in GGA3 KD cells versus control cells (Figure S3.2B). However, consistent with the observed increased rate of Met degradation, by 60 min post-HGF stimulation, a decrease in

Met protein signal is apparent in GGA3 KD cells compared to control cells (Figure S3.2B). The increase in Met degradation following GGA3 KD is not due to increased Met protein turnover under basal conditions because treatment with the protein translation inhibitor cycloheximide had no effect (data not shown). Additionally, synthetic transport of Met to the plasma membrane was similarly not affected by GGA3 KD, using a 20ºC temperature block and release to follow TGN export (Figure S3.3A). Moreover, no significant differences in Met receptor ubiquitination (ratio Ub-Met of 2.1 and 1.0 in control versus 2.6 and 0.9 in GGA3 KD cells at 5 min and 30 min post- HGF stimulation, respectively) were observed in GGA3-depleted cells following HGF stimulation, arguing against an increase in ubiquitination as a cause for enhanced Met RTK degradation (Figure 3.2C).

In contrast to GGA3 KD, depletion of the ESCRT component, Tsg101, resulted in enhanced stabilization of Met protein levels in response to HGF (Figure S3.2C). This is in agreement with previous studies for a role of ESCRT complexes promoting Met degradation[298], dependent on Met ubiquitination[108]. Hence, under these conditions, GGA3 KD has an opposite effect to Tsg101 KD on Met stability, supporting a role for GGA3 to abrogate Met trafficking to the degradative compartment. In support of this, by 15 min of HGF treatment, the colocalization between the Met RTK and the late endosomal marker, Rab7, increased by 26% in GGA3 KD cells versus control cells (Figure 3.2D). Taken together, these data support enhanced entry of the Met RTK into the canonical degradative pathway in the absence of GGA3.

### 3.4.4. GGA3 KD Decreases Met Recycling

The HGF-dependent coimmunoprecipitation of endogenous Met and GGA3 proteins at 5 min, and their colocalization to Rab4/Rab5-positive vesicles, suggests that GGA3 could serve as an adaptor to recruit Met into the Rab4-positive tubular domains of the early endosome to promote recycling. Hence, we addressed whether GGA3 KD decreases entry of Met into recycling vesicles. To establish that Met recycles, we employed a thiol-cleavable amine-reactive biotinylation reagent to label and follow the recycling pool of Met. Cells were

surface labeled with Sulfo-NHS-SS biotin at 4ºC, and internalization was initiated by incubating cells for 7 min with HGF at 37ºC to allow Met to accumulate in early endosomes. During cell surface biotinylation and chase, no significant differences in the amount of labeled internalized Met receptors were observed following HGF treatment (7 min), indicating that Met internalization occurs at a similar efficiency in GGA3 KD and control cells (data not shown). In contrast, GGA3 KD cells displayed reduced levels of Met returning to the cell surface (~9% compared to ~32% in control cells) (Figure 3.3A), supporting a role for GGA3 in Met recycling.

To further address a role for GGA3 in Met recycling, an IF-based assay, adapted from those previously established for the TfR[472], was performed. Following a brief 5 min pulse with HGF, washout, and 20 min chase, the majority of the Met receptor was localized at the plasma membrane or in small endosomes in control cells (Figure 3.3B). By contrast, GGA3 KD cells showed accumulation of the Met receptor in large endosomes, some of which had already reached a perinuclear compartment, consistent with decreased entry into a recycling compartment (Figures 3.3B and 3.3C). Cell surface levels of Met were also reduced following HGF pulse/chase (~46%) in GGA3 KD cells, compared to control cells (~64%), when measured using flow cytometry (Figure S3.4A). Under similar pulse/chase conditions, KD of Rab4A also altered the distribution of the Met receptor toward larger endosomes, albeit to a lesser extent than GGA3 KD (Figure S3.4B). This supports a role for Rab4 in Met recycling and is in keeping with Met accumulation to Rab4, but not Rab11, positive recycling compartments when Rab proteins were overexpressed (Figure S3.4C).

To probe the relationship between structures containing Met and GGA3, we used live-cell microscopy. COS1 cells transiently expressing GFP-GGA3 were incubated with Alexa 555-HGF for 20 min to track Met receptor-positive vesicles. Numerous examples of vesicular Alexa 555-HGF with coincident or nearby GFP GGA3-coated membranes were observed (Figure 3.3D). Examination of these regions using simultaneous two-color streaming (continuous) imaging reveals fast-moving GFP-GGA3 structures around most of the Alexa 555-HGF spots

(Movie S3.1). Notably, the Alexa 555-HGF content in endosomes with overlapping dynamic GFP-GGA3 structures declined over time, whereas in isolated endosomal structures devoid of these GGA3-positive structures, the Al555-HGF intensity remained steady or increased over time (Figure 3.3E). Moreover, the majority of fast-moving GFP-GGA3 structures (92%, total of 257 GFP-GGA3 spots counted) contain detectable mCherry-tagged clathrin (Movie S3.2), though not all clathrin spots (e.g., coated pits) contain GGA3. Thus, the GFP GGA3 structures appear analogous to the ‘‘gyrating’’ clathrin and GGA1-containing structures implicated in TfR recycling observed previously[470], and support the concept that the dynamic GGA3 structures function as recycling tubules in association with endocytic HGF-Met complexes. Together, these multiple approaches provide evidence for GGA3 functioning as an adaptor involved in Met recycling.

### 3.4.5. GGA3 KD Attenuates Met-Dependent ERK Signaling and Cell Migration

Activation of Met leads to the formation of intracellular signaling complexes and induces cell motility, invasion, and branching tubulogenesis[182]. Thus, altered Met recycling due to GGA3 KD may impact on downstream signaling. To test this, we examined the phosphorylation status of Akt and ERK1/2 in response to HGF as a readout for activation of the PI3K and MAPK pathways, respectively. Although no significant differences were observed in p-Akt levels, the duration of p-ERK1/2 was markedly attenuated in GGA3 KD cells during 4 hr of HGF treatment (Figures 3.4A and 3.4B). This supports the observed rapid degradation of Met under these conditions (Figures 3.2A and 3.2B) and our previous data that Met can activate ERK1/2, but not PI3K, from an endosomal compartment[108]. Consistent with only transient activation of ERK1/2, reduced nuclear localization of p-ERK1/2 was observed after 60 min of HGF stimulation in GGA3 KD cells (Figure 3.4C). Sustained ERK1/2 signaling is a prerequisite for HGF-induced cell migration[182]. Significantly, GGA3 KD reduced cell migration to 26% of control cells in response to HGF (Figures 3.4D and 3.4E) and correlated

with reduced localization of Met toward actin-rich membrane ruffles (Figure 3.4F). This is in accordance with defects in Met recycling (Figure 3.3A) and our observations that ERK1/2 activation is required for lamellipodia formation and cell migration downstream of HGF[182].

### 3.4.6. Arf6 Is Required for GGA3-Mediated Met Recycling

To establish the mechanism through which GGA3 regulates Met recycling, we utilized a structure function approach to uncouple GGA3 from specific binding proteins. GTP-bound Arf proteins interact with GGAs [322,323]. To test a requirement for GGA3-Arf interactions in Met recycling, stable HeLa cell lines expressing either siRNA-resistant GFP-GGA3, or GFP-GGA3 N194A, a mutant that specifically uncouples GGA from interaction with Arf-GTP proteins[473], were generated. Upon siRNA transfection and KD of endogenous GGA3, expression of GFP-GGA3, but not GGA3-N194A, restored Met recycling back to the plasma membrane (Figures 3.5A and 3.5B). Moreover, restoration of Met trafficking to a recycling compartment resulted in enhanced Met stability, prolonged ERK1/2 phosphorylation, and cell migration in response to HGF (Figures 3.5C, 3.5D, and S3.5A). Hence, an interaction between GGA3 and Arf-GTP is required for the regulation of Met RTK recycling by GGA3.

In order to identify which Arf family member is responsible for GGA3-mediated recycling of the Met RTK, specific siRNA depletion of Arf1, Arf3, and Arf6 was performed, and cells were assessed for their ability to support Met recycling (Figures S3.5B and S3.5C). KD of Arf1 resulted in accumulation of the Met receptor in a cycloheximide-sensitive intracellular compartment, suggestive of a secretory defect from the Golgi (Figure S3.5B). This is in agreement with previous data that Arf1 can affect secretory traffic[474]. No observable change in Met transport in response to HGF was observed following Arf3 KD (Figure S3.5B). In contrast, upon HGF treatment following Arf6 KD, Met localized predominantly to endocytic vesicles rather than recycling to the plasma membrane as observed in control cells (Figure S3.5B), whereas KD of Arf1 and Arf3 did not result in endosomal accumulation of the Met RTK under similar conditions

(Figure S3.5B). In support of a role for Arf6 in Met trafficking, Met localized with both WT-Arf6 and constitutively active Arf6Q67L in tubulo-vesicular structures (Figure S3.5D). Moreover, activation of endogenous Arf6 was observed by 5–15 min post-HGF stimulation (Figure 3.5E), coincident with the ability of WT, but not the GGA3-N194A mutant, to interact with GTP-Arf6 (Figure 3.5F). Furthermore, endosomal structures triple labeled for Met, Arf6, and Rab4 were observed in response to HGF (Figure 3.5G). Taken together, these data support that GGA3 and Arf6 function together to enhance recycling of Met from a Rab4-positive compartment.

### 3.4.7. GGA3 Binds the Crk Adaptor

Previously identified GGA cargo, such as the M6PR, contains acidic cluster dileucine motifs (DXXLL), which directly interact with the VHS domain of GGAs[321]. However, the intracellular domain of Met lacks putative, consensus dileucine motifs. To understand mechanisms through which GGA3 could be recruited to the Met RTK, we analyzed the protein sequence of GGA3 for predicted binding sites of known proteins recruited to Met. Using Scansite[445], two putative Crk SH3 domain proline-rich binding sites (prolines 404 and 463) were identified within the hinge segment of GGA3 (Figure 6A). Consistent with this prediction, endogenous GGA3 coimmunoprecipitates with Crk in the absence of HGF stimulation (Figure 3.6B). Hence, at steady state these proteins can exist in a complex. Furthermore, glutathione S-transferase (GST) fused Crk, Crk-SH3 domain, but not GST protein alone, was able to pull down GGA3 protein (Figure S3.6A; data not shown). Although mutagenesis and substitution of either predicted Crk proline-binding site for alanine residues failed to significantly abrogate this association (Figure 3.6C), substitution of both prolines significantly decreased the association between GGA3 and Crk (Figures 3.6C and S3.6B). This identifies prolines 404 and 463 as components of Crk-binding sites on GGA3.

### 3.4.8. A GGA3-Crk Interaction Is Required for Met Recycling, ERK Activation, and Cell Migration

In support of a requirement for Crk in the recruitment of GGA3 to a Met complex, reduced association between Met and GGA3 was observed in Crk KD cells following HGF treatment (Figure 3.6D). To test the specific requirement of GGA3-Crk interactions, stable cell lines expressing siRNA-resistant GGA3 containing the double proline mutant (referred to as ΔCrk) were generated (Figure 3.6E). Importantly, expression of GGA3ΔCrk was unable to compensate for the depletion of GGA3 in promoting sustained ERK activation, Met stability, and cell migration in response to HGF (Figures 3.6F, 3.6G, and S3.6C). Hence, these data demonstrate a requirement for a specific GGA3-Crk complex, in acting as a conduit to the Met receptor, thereby promoting Met recycling, sustained ERK activation, and cell migration.

### 3.4.9. Arf6 and Crk Cooperate to Recruit GGA3 to Met-Positive Endosomal Membranes

As published previously, GGA3-N194A, which fails to bind GTP Arfs, is diffusely cytosolic and does not detectably localize to endosomal membranes[473]. However, in response to HGF, a proportion of GGA3-N194A could associate with endosomes (Figure 3.5A), suggesting that additional factors besides Arf-GTP binding can promote endosome recruitment of GGA3. Because GGA membrane recruitment has been proposed to occur via multiple low-affinity interactions between Arfs and cargo[475], we tested the requirement for GGA3-Crk binding to act as such a factor during GGA3 recruitment in response to HGF. To this end, the subcellular localization of GGA3-N194A, GGA3ΔCrk, and a GGA3-N194A/ΔCrk double mutant to Met-positive endocytic vesicles was scored in response to HGF (Figures 3.7A and 3.7B). Although HGF-dependent recruitment to Met-positive vesicles of the GGA3-N194A mutant was decreased by ~44%, recruitment of GGA3-N194A/ΔCrk was reduced by ~88%. Thus, in response to HGF the Crk-binding sites of GGA3 can compensate for Arf binding, and both Arf-GTP and Crk binding are required for full recruitment of GGA3 to

endosomes. These data support a model whereby dual recruitment of Arf-GTP and Crk promote HGF-dependent targeting of GGA3 to Met-positive endosomes and Met recycling (Figure 3.7C).

## 3.5. DISCUSSION

Although it is generally considered that a portion of internalized RTKs recycle following ligand-dependent internalization, the mechanisms that regulate entry of RTKs and other cargo into the recycling compartment, rather than the degradative compartment, are poorly understood. Here, we identify an active RTK-recycling pathway by which GGA3 functions as a specific cargo adaptor to target the Met RTK into recycling tubules. This was established by analyzing Met internalization, recycling, and degradation under conditions in which GGA3 levels were depleted and rescued with various GGA3 mutants, and coupling the outcomes with Met-dependent signaling and migration. These multiple approaches yielded quantitative, complementary results that support a model whereby GGA3 is recruited to an activated Met RTK cargo complex present within the early tubular endosomal network via Crk and Arf6. The formation of a GGA3-Met complex localized to a Rab4-enriched endosomal compartment would promote access of Met into a recycling pathway while decreasing entry of Met into the degradative pathway. GGA3-dependent entry of Met into the recycling pathway promotes sustained ERK1/2 activation and relocalization of Met toward the leading edge to initiate localized signaling required for cell migration.

At steady-state, GGA3 is predominantly localized to the *trans*-Golgi network, [322,323], however a subpopulation of GGA3 localizes to vesicles [476], previously defined as early endosomal in nature [324]. This is consistent with our observations that GGA3 is enriched in Rab4 and, to a lesser extent, Rab5-positive early endosomes and colocalizes with endocytosed Met cargo in these endosomes. Rab4 is a regulator of recycling vesicle formation at the early endosome[477,478], consistent with our functional assignment of GGA3 as an early recycling adaptor for Met. Furthermore, GGA3 may spatially restrict Met accessibility within the

early endosome by modulating the Rab-based protein machinery. In this regard, GGA3 binds Rabaptin-5 [479], which can complex with Rab4 and Rab5 [480] as well as the GDP/GTP exchange factor, Rabex-5 [481]. Interestingly, GGA1 has been observed in association with clathrin on dynamic and rapid recycling structures[470]. Similarly, in live cells we observe GGA3 and clathrin in dynamic structures surrounding endocytosed HGF-Met complexes. Although we failed to observe GGA1 recruitment to Met, given the high degree of structural homology of GGA family proteins, these results support a role for other GGA family proteins in rapid recycling pathways.

The Met RTK lacks traditional DXXLL GGA-binding motifs. We identified an alternative mechanism through which GGA3 is recruited to Met, involving the constitutive interaction of GGA3 with the Crk adaptor. Although Crk does not have direct binding sites on Met, the major substrate for Met, the scaffold protein Gab1, contains six Crk SH2 domain phosphotyrosine-binding sites and robustly recruits Crk to Met in response to HGF[482]. GGA3 recruitment via Crk provides a mechanism for ligand-dependent specificity of engagement with the Met RTK complex. Because neither GGA1 nor GGA2 contains these Crk-binding proline-rich motifs and fails to associate with Crk (data not shown), this provides an explanation why neither of these proteins was observed to be recruited to a Met complex.

Key to the mechanism by which GGA3 regulates Met recycling is the finding that coupling of GGA3 to both Crk and Arf6 is necessary for efficient Met recycling. Arf6 is activated downstream from the Met receptor[468], which we show corresponds to the time kinetics of GGA3 recruitment and Met recycling. Additionally, Arf6 KD attenuates recycling of Rac-positive endosomes to the plasma membrane in response to HGF[483]. The finding that the uncoupling of GGA3 from Arf (N194A mutant) results in partial recruitment of GGA3 (~50%) to endosomes indicates that initial membrane recruitment of GGA3 to Met can also occur in an Arf-independent manner. Therefore, these data support a model whereby activation of Arf6 by Met could aid in retaining a GGA3-Crk-Met complex in endosomal recycling membranes or serve to recruit other factors

required for mediating Met recycling.

Internalized RTKs can continue to signal from endosomal compartments and it is now recognized that the ability of endosomes to serve as an intracellular signaling platform is an important component of the RTK signaling cascade[201]. Sustained ERK1/2 signaling is required for Met induced cell migration[182]. Our results point to a mechanism through which Met promotes prolonged ERK1/2 activation and cell migration. GGA3-dependent entry of Met into a recycling network, rather than the degradative pathway, allows for prolonged activation of ERK1/2 from endosomes. GGA3-dependent recycling also localizes Met to regions of the plasma membrane that are required for actin dynamics and cell motility. Somewhat similar to HGF, the bacterial protein, InlB, can activate Met to trigger actin remodeling and *Listeria monocytogenes* internalization[484], which requires several endocytic proteins[451] including GGA3 (E. Veiga and P. Cossart, personal communication). Thus, in the context of Listeria entry, GGA3 may be required to recycle Met-signaling complexes to sites of bacterial entry for phagocytic uptake.

Unlike Met, GGA3 KD was associated with a delay in degradation of internalised EGF[324]. In a similar manner to the EGFR, ligand-dependent degradation of Met is dependent on ubiquitination of the Met receptor[9,108]. In contrast, GGA3 KD promotes ligand-dependent degradation of the Met RTK, supporting a distinct role for GGA3 in Met trafficking and recycling. Thus, the difference observed between the roles for GGA3 in trafficking of these two RTKs may reflect their differential ability to recruit Crk and undergo recycling. In addition to the indirect recruitment via Grb2[485] of the major Crk binder, Gab1, Met contains a direct binding motif for Gab1 that may enhance the ability of Met to engage with a GGA3-Crk complex. In a similar manner to Met, a role for GGA3 in the exocytosis of retroviral Gag proteins is independent of the ability of GGA3 to bind ubiquitin but requires the ability of GGA3 to bind Arf proteins[486].

The unexpected observation that GGA3-N194A can still be recruited to Met-positive endosomes led us to test whether GGA3-Crk binding was involved in the endosomal association of GGA3. Precedence for coincident detection

between clathrin adaptors and their interactors in mediating membrane recruitment has previously been established[475]. Because mutation of both the Arf-GTP and Crk-binding sites was necessary to abolish recruitment of GGA3 to endosomes, this identifies Crk as a key player in GGA3 endosomal recruitment.

Our results clearly establish that GGA3 coordinates the recycling, signaling, and degradative fates of the Met RTK. Recycling in recent years has emerged as a mechanism to spatiotemporally coordinate localized signaling complexes, actin dynamics, and directed cell movement downstream of motogenic stimuli and their receptors, such as Met[483,487,488]. Given the importance of Met and RTKs in cancer progression, it will be important to assess the role of GGA3 in these processes.

## 3.6. EXPERIMENTAL PROCEDURES

### Chemicals, DNA Constructs, Antibodies, and Cells

A detailed list of chemicals, antibodies, and DNA constructs is described in the Appendix: Supplemental Experimental Procedures. HeLa, HEK293, and COS1 cells were cultured in DMEM containing 10% FBS. Transient transfections in HEK293 and HeLa cells were performed using Lipofectamine Plus according to manufacturer's instructions (Invitrogen).

### Biochemical Assays

Lysis and immunoblotting (IB) were as described in ref.[489]. For Met degradation assays, cells were stimulated with 0.5 nM HGF containing cycloheximide at 37ºC for the indicated time points. For blots requiring quantification, membranes were blocked with LI-COR blocking buffer (LI-COR Biosciences), incubated with primary antibodies as above, followed by incubation with infrared (IR)-conjugated secondary antibodies prior to detection and analysis on the Odyssey IR Imaging System (LI-COR Biosciences).

**Colocalization Studies**

IF assays were performed as described in ref.[489]. For colocalization quantification, MetaMorph software was used for object-based colocalization measurements. Images were smoothed with a 3x3 low-pass filter, and endosomes were identified and counted using size estimates and intensity thresholds in each image set using the ‘‘Count Nuclei’’ application. Binary images were created for each set of endosomal spots and combined pairwise using logical AND operation to give only the ‘‘colocalized’’ spots. These spots were then counting using the ‘‘Count Nuclei’’ module. The minimum spot size was set so as to remove any small spots due to partial, and likely random, overlap of spots. Results were logged into Excel for analysis. Values for all analyses including colocalization and vesicle counting represent mean value ± standard error of the mean (SEM).

**Recycling Assays**

For biotinylation assay, cells were serum starved and pretreated with low
levels of 10 nM lactacystin and 100 nM concanamycin inhibitors for 1 hr before chilling on ice and biotinylated for recycling assay as described previously[298]. After biotinylation, cells were stimulated with 0.5 nM HGF at 37°C in the presence of inhibitors for 7 min to allow internalization. Cells were placed on ice, stripped with reducing reagent (100mM sodium 2-mercaptoethanesulfonic acid [MESNA] in 50 mM Tris-HCl [pH 8.6], 100 mM NaCl, 1 mM EDTA, and 0.2% BSA) to remove noninternalized biotinylated proteins, followed by returning cells to 37°C. To determine percentage of internalized proteins that recycled, cells were returned to ice, subjected to a second reduction with MesNa prior to lysis and recovery with NeutrAvidin-agarose beads, and immunoblot for detection of Met levels. Percent recycled Met was determined by quantifying IB and subtracting the amount recovered from a similarly processed sample that did not undergo a second round of reduction (representing total pool of internalized Met) divided by the total pool of internalized Met.

IF assay was performed as described previously[472]. Cells grown on glass coverslips were pulsed with prewarmed (37°C) 0.5 nM HGF for 5 min, washed

five times with Leibovitz-15 Medium containing 0.2% BSA at 4°C, and chased at 37°C for 20 min, fixed, and processed for IF. Cells were scored on ratio of endosomal (EN) over plasma membrane staining of Met and reported as mean ± SEM (n = 4). In each experiment a minimum of 20 fields was scored.

**siRNA Transfection**

HeLa cells were seeded at $2.0x10^5$ in 6-well dishes and transfected with 50nM siRNA using HiPerFect as per manufacturer's instructions (QIAGEN). All experiments were performed 72 hr posttransfection. siRNA sequences are described in Appendix Supplemental Experimental Procedures.

**Arf-GTP Assay**

A total of $1.0x10^6$ HeLa cells was serum starved overnight, then stimulated with 0.5 nM HGF for indicated times and subjected to pull-down assays using GST-GGA3 (1–316) domain as described previously [490].

**Migration Assay**

Equal number of HeLa cells ($5x10^4$) was seeded directly onto 6.5mm Corning Costar transwell chambers for migration assays as described previously[491]. All bar graphs represent mean ± SEM.

**Live-Cell Imaging**

Imaging was performed as described previously[470] using a Zeiss Axiovert 200 microscope and Olympus 150x/1.45 NA objective. Additional details can be found in Appendix Supplemental Experimental Procedures.

## 3.7. ACKNOWLEDGEMENTS

We thank Peter McPherson, Michael Way, Stephane Laporte, and members of the Park laboratory for critically reading the manuscript; Genetech Inc. for HGF; Juan Bonifacino for GGA3 constructs; Dongmei Zuo for labeling HGF; Claire

Brown and the McGill LCS Imaging Facility for MetaMorph analysis assistance; and Ken McDonald for FACS assistance. This research was supported by a Canada Graduate Scholarship Doctoral Award to C.A.P. from the CIHR (Canadian Institutes of Health Research), CIHR operating grants to M.P. (MOP-11545 and 106635), and NIH Grant GM-49217 to J.H.K. M.P. holds the Diane and Sal Guerrera Chair in Cancer Genetics.

## 3.8. FIGURES AND FIGURE LEGENDS

**Figure 3.1. HGF Regulates Recruitment of GGA3 to the Met RTK**

(A) A total of 500 mg of HGF-stimulated HeLa lysates was immunoprecipitated (IP) with anti-Met, and IB was as shown. 50μg of cell lysate (Input) was similarly detected. (B) HeLa cells pretreated with cycloheximide (CHX) for 2 hr were left unstimulated or stimulated 15 min with HGF and processed for IF to localize Met (red) and GGA3 (green). Scale bar, 10 mm. Inset shows region of higher magnification. (C) HeLa cells transfected with GFP-Rab4 and stimulated 15 min HGF followed by IF processing. Scale bar, 10 mm. ‘‘a’’ and ‘‘b’’ represent insets showing higher magnification of intracellular vesicles (arrowheads indicate regions of colocalization). (D) Colocalization quantification of Met and GFP-Rab4 and GFP-Rab5 ± 15 min HGF. (E) Colocalization quantification of GGA3 and GFP-Rab4 and GFP-Rab5 ± 15 min HGF. (F) Quantification of GGA3 vesicles ± 15 min HGF. All values are from three independent experiments (n = 15). Student’s t test, *$p < 0.02$. See also Figure S3.1.

## Figure 3.1

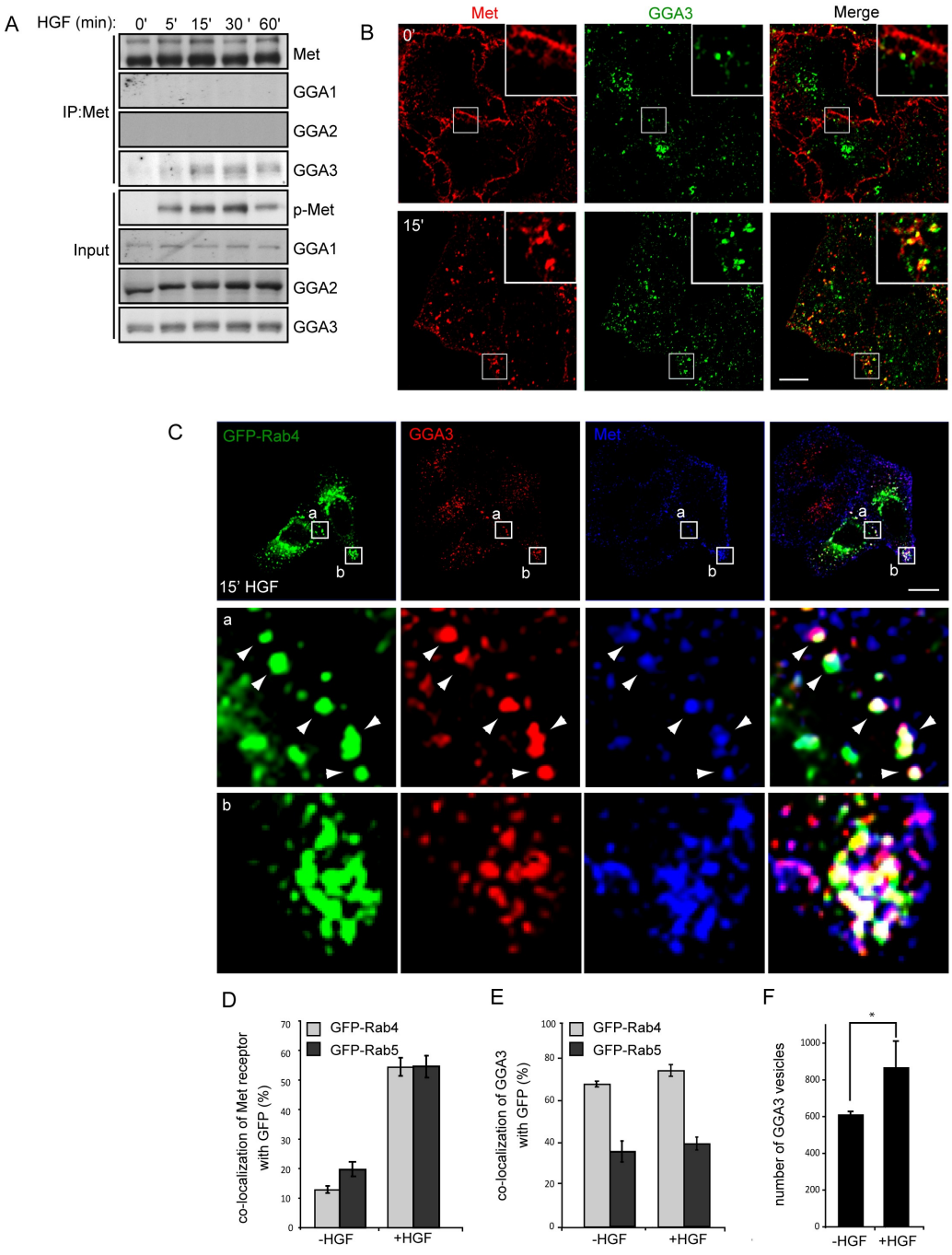
A
HGF (min): 0' 5' 15' 30 ' 60'
Met
GGA1
GGA2
GGA3
IP:Met
p-Met
GGA1
GGA2
GGA3
Input
B
Met
GGA3
Merge
0'
15'
C
GFP-Rab4
GGA3
Met
15' HGF
a
b
D
co-localization of Met receptor with GFP (%)
GFP-Rab4
GFP-Rab5
-HGF
+HGF
E
co-localization of GGA3 with GFP (%)
GFP-Rab4
GFP-Rab5
-HGF
+HGF
F
number of GGA3 vesicles
*
-HGF
+HGF

**Figure 3.2. GGA3 KD Enhances HGF-Induced Met Protein Degradation**

(A) HeLa control (CTL) or GGA3 knockdown (KD) cells were stimulated with HGF in the presence of cycloheximide (CHX) as indicated. IB was as shown. See also Figure S1. (B) Densitometric analysis of Met blots from four independent experiments like those shown in (A). Values were used to fit to an exponential decay, and half-life value ($t_{1/2}$) was calculated (Microsoft Excel). Results are expressed as mean ± SEM. (C) A total of 500 mg HGF-stimulated CTL and GGA3 KD HeLa cell lysates was immunoprecipitated (IP) with anti-Met, and IB was as shown for IP and 50 mg for input. Densitometric ratio of Ub/Met levels is indicated below blot. (D) CTL and KD cells transfected with GFP-Rab7 stimulated 15 min with HGF and processed for IF using anti-Met. Insets show region of higher magnification. Quantification of Met and Rab7 colocalization from at least three independent experiments (n = 30). Student's t test, *$p < 0.02$. Scale bar, 10 mm. See also Figures S2 and S3.

**Figure 3.2**

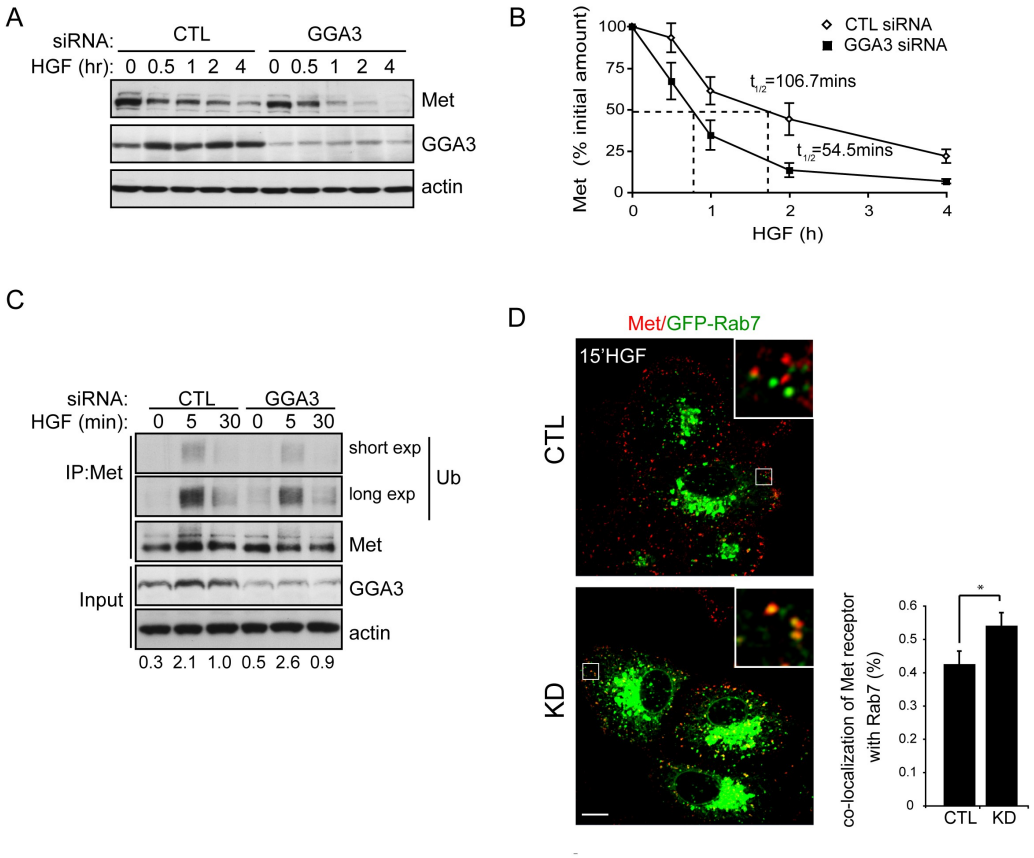
A
siRNA: CTL GGA3
HGF (hr): 0 0.5 1 2 4 0 0.5 1 2 4
Met
GGA3
actin
B
Met (% initial amount)
CTL siRNA
GGA3 siRNA
t1/2=106.7mins
t1/2=54.5mins
HGF (h)
C
siRNA: CTL GGA3
HGF (min): 0 5 30 0 5 30
IP:Met
short exp
long exp
Ub
Met
Input
GGA3
actin
0.3 2.1 1.0 0.5 2.6 0.9
D
Met/GFP-Rab7
15'HGF
CTL
KD
co-localization of Met receptor with Rab7 (%)
CTL KD

**Figure 3.3. GGA3 Mediates Recycling of the Met RTK** (A) CTL and GGA3 KD cells were surface labeled on ice with Sulfo-NHS-SS-biotin, stimulated 7 min with HGF at 37°C, and biotin from remaining cell surface receptors was removed by MesNa treatment at 4°C. Cells were then rewarmed to 37°C for the indicated times to allow recycling, followed by a second reduction with MesNa. The amount of recycled Met receptor is expressed as the percentage of the pool of biotinylated Met during the internalization period as described in Experimental Procedures. Values are mean ± SEM of five independent experiments. Student's t test, $^{**}p < 0.006$, $^{*}p < 0.05$. Representative IB is indicated below graph. (B) IF of CTL or KD cells pulsed for 5 min with HGF at 37°C to internalize Met receptors in early endosomes (00 chase), rapidly washed at 4°C to remove unbound ligand, and chased for 20 min to allow recycling. Met (white) and DAPI (blue). Scale bar, 10 mm. (C) Quantification of (B). Bar graph represents cells showing a greater ratio of endosomal (EN) over plasma membrane staining of Met. Student's t test, $^{*}p < 0.01$. KD levels as assessed by IB. See also Figure S4. (D) Live-cell imaging of association of GFP-GGA3 structures (green) with internalized Alexa 555-HGF (red). Continuous image streams of the boxed regions (see Movie S1) display examples of internalized HGF with one or more surrounding dynamic GGA3 structures. See also Movie S2. (E) Quantitation of Alexa 555-HGF signal intensity during a chase period (15 min load, 4–6 min chase) in structures with or without nearby dynamic GFP-GGA3 (16 spots each from four different experiments); slope of decrease in structures with nearby GFP-GGA3 is -0.34 ± 0.13 SEM.

## Figure 3.3

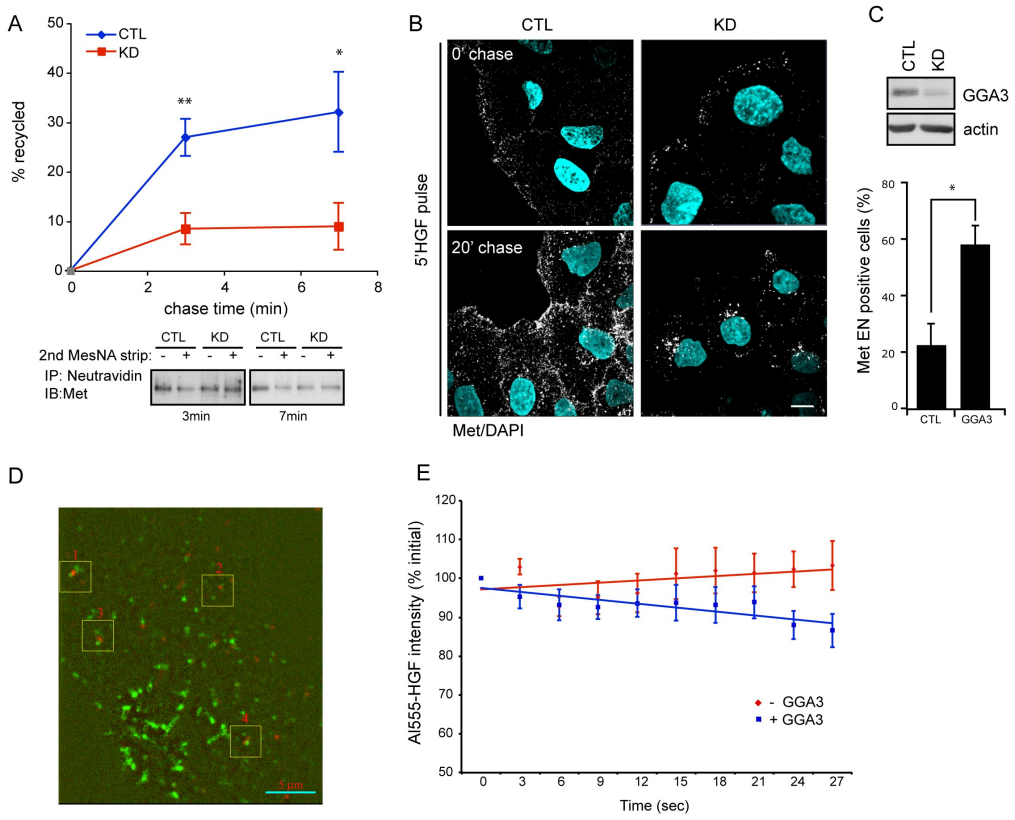
A
CTL
KD
% recycled
chase time (min)
**
*
2nd MesNA strip:
IP: Neutravidin
IB:Met
3min
7min
B
CTL
KD
0' chase
20' chase
5'HGF pulse
Met/DAPI
C
GGA3
actin
Met EN positive cells (%)
D
5 μm
E
AI555-HGF intensity (% initial)
- GGA3
+ GGA3
Time (sec)

**Figure 3.4. Loss of GGA3 Attenuates HGF-Induced ERK Signaling and Migration of HeLa Cells** (A) CTL and KD cells treated with HGF and CHX as indicated. IB was as shown. (B) Representative Odyssey IR analysis of p-ERK1/2 levels (top panel) and p-Akt levels (bottom panel). (C) CTL and KD treated 60 min with HGF, then fixed and stained for p-ERK1/2 (white) and DAPI (blue). Scale bars, 10 mm. (D) Representative phase-contrast images (10x) of migration assays using CTL and KD cells ± HGF. (E) Quantification of experiments (n = 3) shown in (D) using Scion Image. Student's t test, *p < 0.007. Inset shows typical IB of GGA3 expression levels. (F) CTL and GGA3 KD cells either left untreated (left) or stimulated with HGF 60 min, then stained for Met, phalloidin (actin), and DAPI. Arrowheads point to leading edge. Scale bar, 10 mm.

## Figure 3.4

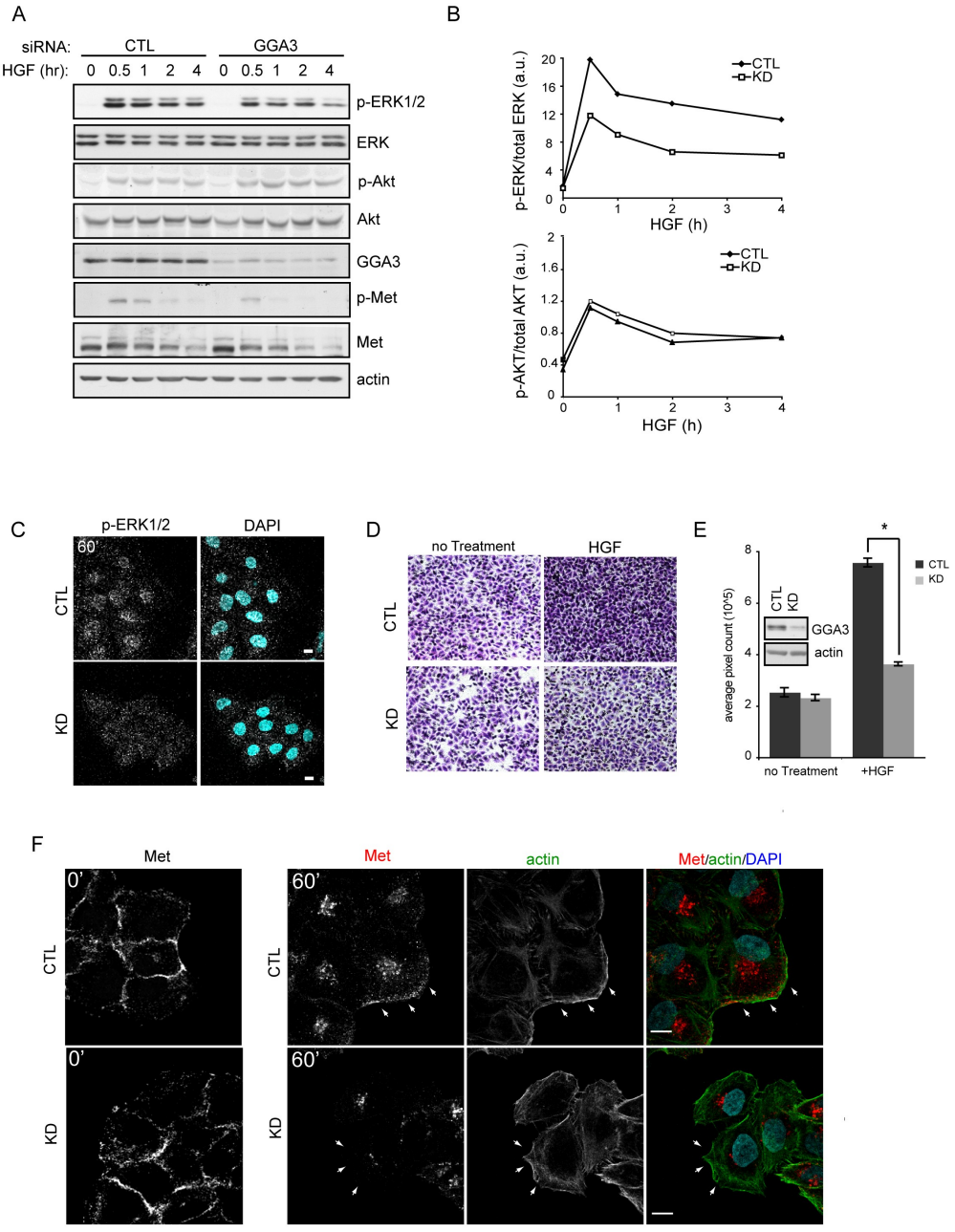
A
siRNA:
CTL
GGA3
HGF (hr):
0 0.5 1 2 4 0 0.5 1 2 4
p-ERK1/2
ERK
p-Akt
Akt
GGA3
p-Met
Met
actin
B
p-ERK/total ERK (a.u.)
CTL
KD
HGF (h)
p-AKT/total AKT (a.u.)
CTL
KD
HGF (h)
C
p-ERK1/2
DAPI
60'
CTL
KD
D
no Treatment
HGF
CTL
KD
E
*
CTL
KD
average pixel count (10^5)
CTL
KD
GGA3
actin
no Treatment
+HGF
F
Met
0'
CTL
0'
KD
Met
actin
Met/actin/DAPI
60'
CTL
60'
KD

**Figure 3.5. GGA3-Mediated Met Recycling Requires Arf6**

(A) Stable HeLa cell lines expressing siRNA-resistant GFP-GGA3 (WT) or GFP-GGA3 N194A left untreated or pulse/chased with HGF were processed for IF using anti-Met. Scale bars, 10mm. Arrowheads point to endosomal Met staining. (B) IB of KD and rescue levels of stable HeLa cell lines compared to parental cells. Bar graph represents cells showing a greater ratio of endosomal (EN) over plasma membrane staining of Met for CTL, GGA3 KD (KD), GGA3 WT rescue (WT) or GGA3-N194A rescue (N194A) following IF recycling assay. Student's t test, *$p < 0.0001$. (C) The top panel shows that CTL, KD, WT, and N194A cells were stimulated with HGF and used for IB as indicated. The bottom panel is a representative Odyssey IR imaging quantification of levels shown in top panel. (D) Migration assay of CTL, KD, WT, and N194A cells ± HGF ($n = 3$). See also Figure S5A. (E) HeLa cells stimulated with HGF used for GGA pull-down assay (GGA-PD) followed by IB for Arf6 to assess GTP-loaded Arf6. 10% input is shown. (F) HeLa cell lysates stimulated with HGF for 15 min were used in GGA3 pull-downs using either WT or N194A GST-GGAs, followed by IB for Arf6 and GST levels. 10% input is shown.

# Figure 3.5

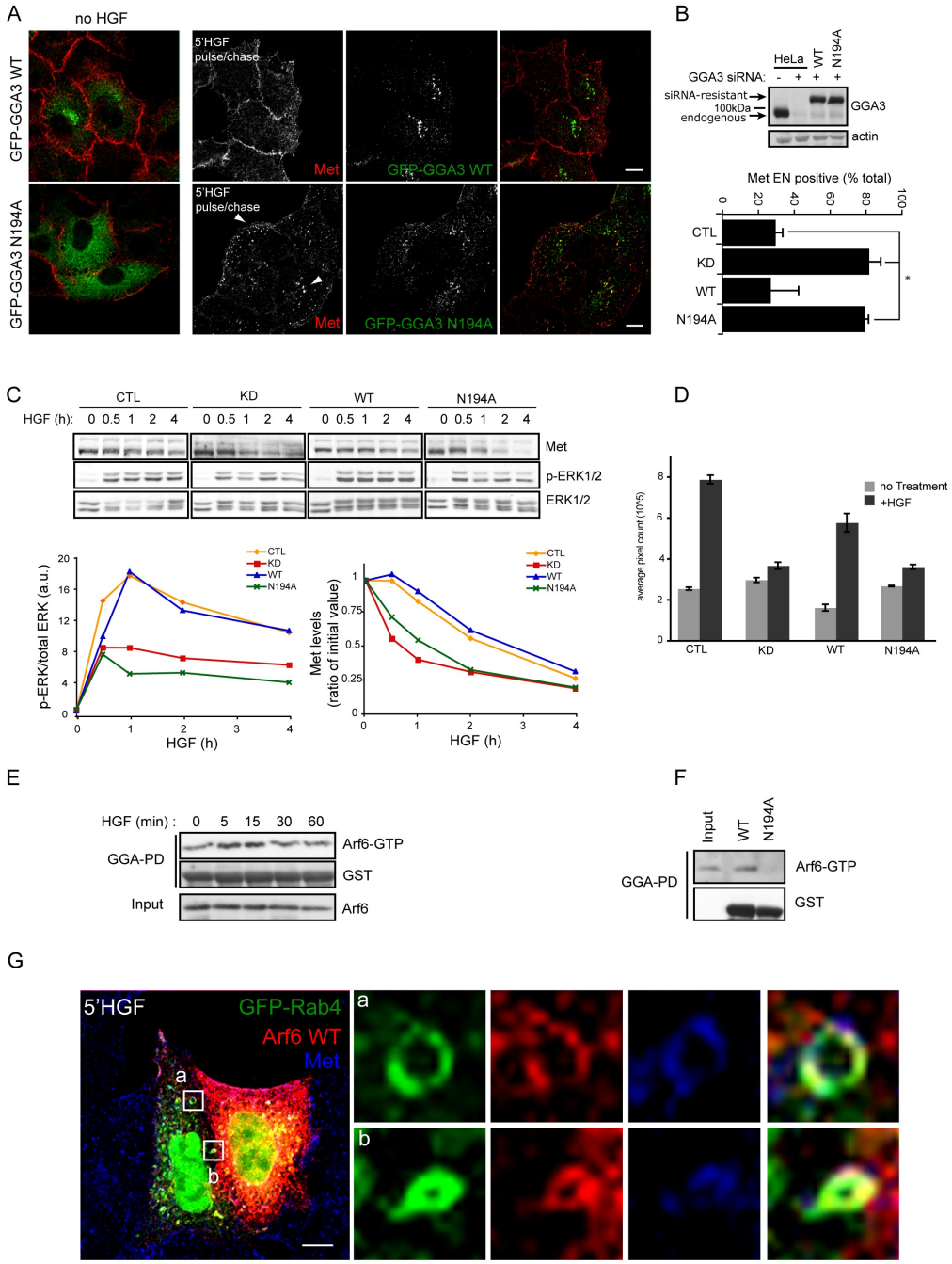
A
no HGF
5'HGF pulse/chase
GFP-GGA3 WT
GFP-GGA3 N194A
Met
GFP-GGA3 WT
GFP-GGA3 N194A
B
HeLa
WT
N194A
GGA3 siRNA: - + + +
siRNA-resistant
100kDa
endogenous
GGA3
actin
Met EN positive (% total)
0 20 40 60 80 100
CTL
KD
WT
N194A
*
C
CTL KD WT N194A
HGF (h): 0 0.5 1 2 4
Met
p-ERK1/2
ERK1/2
p-ERK/total ERK (a.u.)
Met levels (ratio of initial value)
HGF (h)
D
average pixel count (10^5)
no Treatment
+HGF
CTL KD WT N194A
E
HGF (min) : 0 5 15 30 60
GGA-PD
Arf6-GTP
GST
Input
Arf6
F
Input WT N194A
GGA-PD
Arf6-GTP
GST
G
5'HGF
GFP-Rab4
Arf6 WT
Met
a
b

**Figure 3.6. Crk Association with GGA3 Is Required for Met Association and Downstream Biological Processes**

(A) Schematic diagram of GGA3 protein domains and putative proline-rich Crk SH3-binding sites. (B) A total of 1 mg protein lysate from HeLa cells ± 15 min HGF was used for IP using anti-Crk (IP:Crk; Ab, antibody present), and 50 µg lysate was used for input. See also Figure S6. (C) Coimmunoprecipitation (co-IP) of HA-Crk from 500 µg HEK293 cells transfected with HA-Crk and GFP-tagged GGA3 constructs as indicated, followed by IB. 50µg of input is shown. (D) HeLa cells transfected with CTL or Crk siRNA, ± 15 min HGF and used to IP (1 mg) using anti-Met. 50µg of input is shown. (E) IB of GGA3ΔCrk stable expression levels. (F) Top panels show control, GGA3 KD, or GGA3ΔCrk stable cells stimulated with HGF. Bottom panels illustrate representative Odyssey IR imaging quantification. (G) Migration assay shown in (F) ± HGF (n = 3). See also Figure S6C.

## Figure 3.6

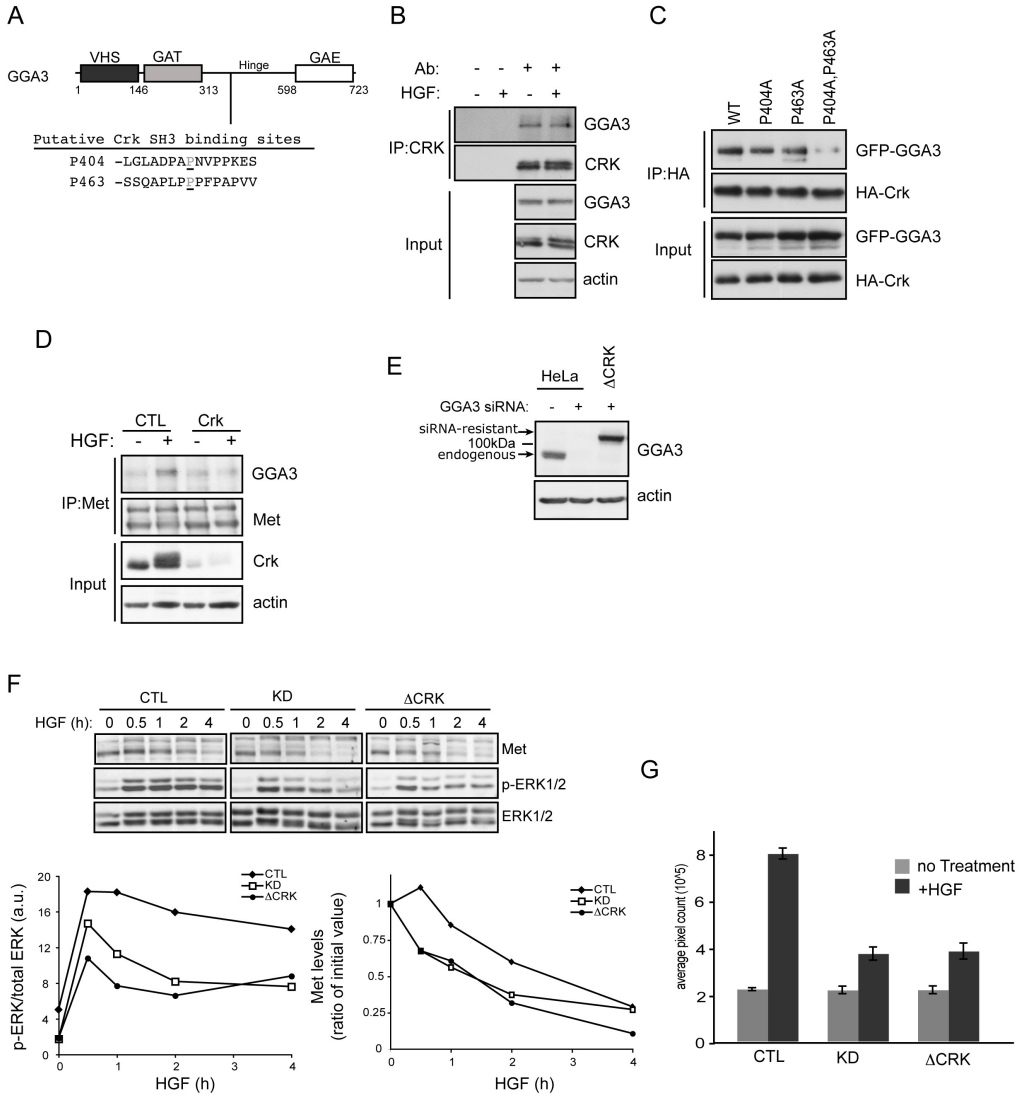
A
GGA3
VHS
GAT
Hinge
GAE
1
146
313
598
723
Putative Crk SH3 binding sites
P404 -LGLADPAPNVPPKES
P463 -SSQAPLPPPFPAPVV
B
Ab:
HGF:
IP:CRK
GGA3
CRK
Input
GGA3
CRK
actin
C
WT
P404A
P463A
P404A,P463A
IP:HA
GFP-GGA3
HA-Crk
Input
GFP-GGA3
HA-Crk
D
CTL
Crk
HGF:
IP:Met
GGA3
Met
Input
Crk
actin
E
HeLa
ΔCRK
GGA3 siRNA:
siRNA-resistant
100kDa
endogenous
GGA3
actin
F
CTL
KD
ΔCRK
HGF (h): 0 0.5 1 2 4 0 0.5 1 2 4 0 0.5 1 2 4
Met
p-ERK1/2
ERK1/2
p-ERK/total ERK (a.u.)
HGF (h)
CTL
KD
ΔCRK
Met levels (ratio of initial value)
HGF (h)
CTL
KD
ΔCRK
G
average pixel count (10^5)
no Treatment
+HGF
CTL
KD
ΔCRK

**Figure 3.7. Arf6 and Crk Cooperate to Recruit GGA3 to HGF-Induced Endosomal Membranes**

(A) HeLa cells transfected with the indicated GFP-GGA3 constructs were pretreated with CHX (2 hr), then stimulated with HGF (15 min) and processed for IF. Scale bar, 10 mm. Box region was used to perform line scan analysis of fluorescence intensity versus distance. (B) Quantification of cells exhibiting endosomal (EN) colocalization of GFP and Met, from three independent experiments (n = 75). Student's t test, **p < 0.005. (C) Model for GGA3-mediated recycling of Met RTK. Inset shows higher magnification of proposed Met-GGA3 protein complexes recruited to endosomes.

**Figure 3.7**

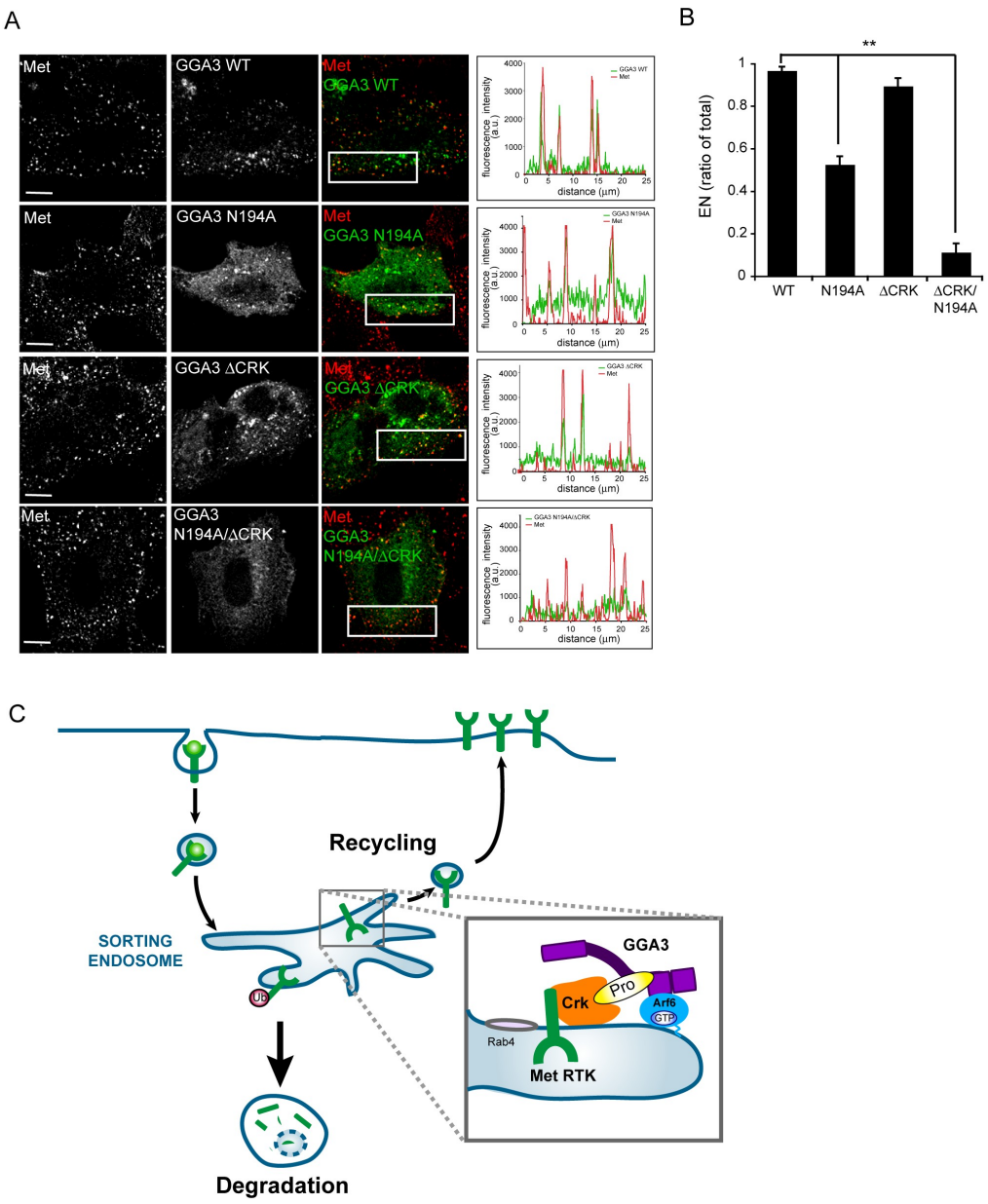
A
Met
GGA3 WT
Met
GGA3 WT
GGA3 N194A
Met
GGA3 N194A
GGA3 ΔCRK
Met
GGA3 ΔCRK
GGA3
N194A/ΔCRK
Met
GGA3
N194A/ΔCRK
fluorescence intensity (a.u.)
distance (μm)
B
EN (ratio of total)
**
WT
N194A
ΔCRK
ΔCRK/
N194A
C
Recycling
SORTING
ENDOSOME
Ub
Degradation
GGA3
Pro
Crk
Arf6
GTP
Rab4
Met RTK

**Supplemental Figures**

**Figure S3.1, Related to Figure 1. GGA3 Preferentially Colocalizes with Rab4 at Steady-State and Met Colocalizes with Rab4 upon HGF Stimulation**

(A) HeLa cells transfected with GFP-Rab4, GFP-Rab5, GFP-Rab7 or GFP-Rab11 were processed for IF and stained using anti-GGA3 antibodies. Bar = 10μm. Colocalization of GGA3-positive endosomes with GFP-Rabs from at least three independent experiments (N=30) was assessed using Metamorph software as described in experimental procedures and is indicated in merged image and graphed to the right. (B) HeLa cells were transfected with GFP-Rab4 and left unstimulated (-HGF) or stimulated 15 min with HGF (+HGF) followed by processing for IF using anti-Met (red). Bar = 10μm. Percent colocalization assessed as described in the text, is indicated in merged image. (C) Colocalization quantification of GGA3 and GFP-Rab4 and GFP-Rab5 in the absence or presence of 15 min HGF. Values are mean ± SEM from three independent experiments (N=15).

**Figure S3.1**

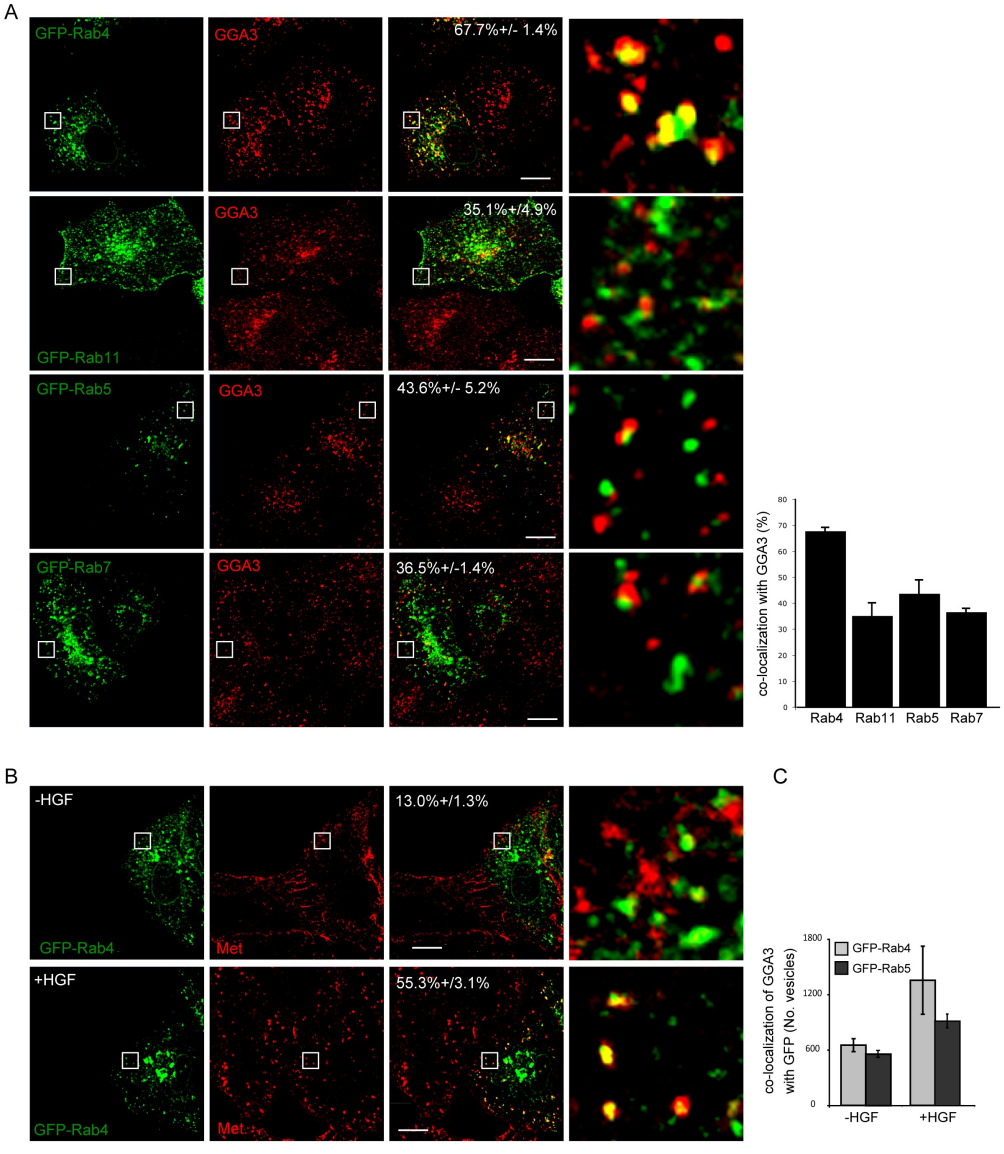
A
GFP-Rab4
GGA3
67.7%+/- 1.4%
GFP-Rab11
35.1%+/4.9%
GFP-Rab5
43.6%+/- 5.2%
GFP-Rab7
36.5%+/-1.4%
co-localization with GGA3 (%)
Rab4
Rab11
Rab5
Rab7
B
-HGF
GFP-Rab4
Met
13.0%+/1.3%
+HGF
55.3%+/3.1%
C
GFP-Rab4
GFP-Rab5
co-localization of GGA3 with GFP (No. vesicles)
-HGF
+HGF

**Figure S3.2, Related to Figure 2. GGA3 siRNA Duplexes Have an Opposite Effect to Tsg101 siRNA on Met Degradation**

(A) Bar graph of Met protein levels expressed as percent of initial values from HeLa cells transfected with control (CTL) siRNA or one of three siRNA duplexes against GGA3 after 1h treatment with HGF. Data represent the mean ± SEM from three independent experiments. (B) Mixed population of GGA3 siRNA-treated cells were pretreated with CHX, then stimulated with HGF as indicated before processing for IF (anti-Met; red, anti-GGA3; green in merge). Arrows indicate cells with good GGA3 KD as assessed by GGA3 staining. Note that after 15 min of HGF treatment, Met localization appears similar in both control and GGA3 KD cells. At 60 min, nearly all Met signal is lost in GGA3 KD cells, in contrast to control cells where signal persists. Cell outlines drawn using Zen software. Bar = 10μm. (C) CTL or Tsg101 KD cells were treated with HGF in the presence of CHX for the indicated amount of time and analyzed by IB.

**Figure S3.2**

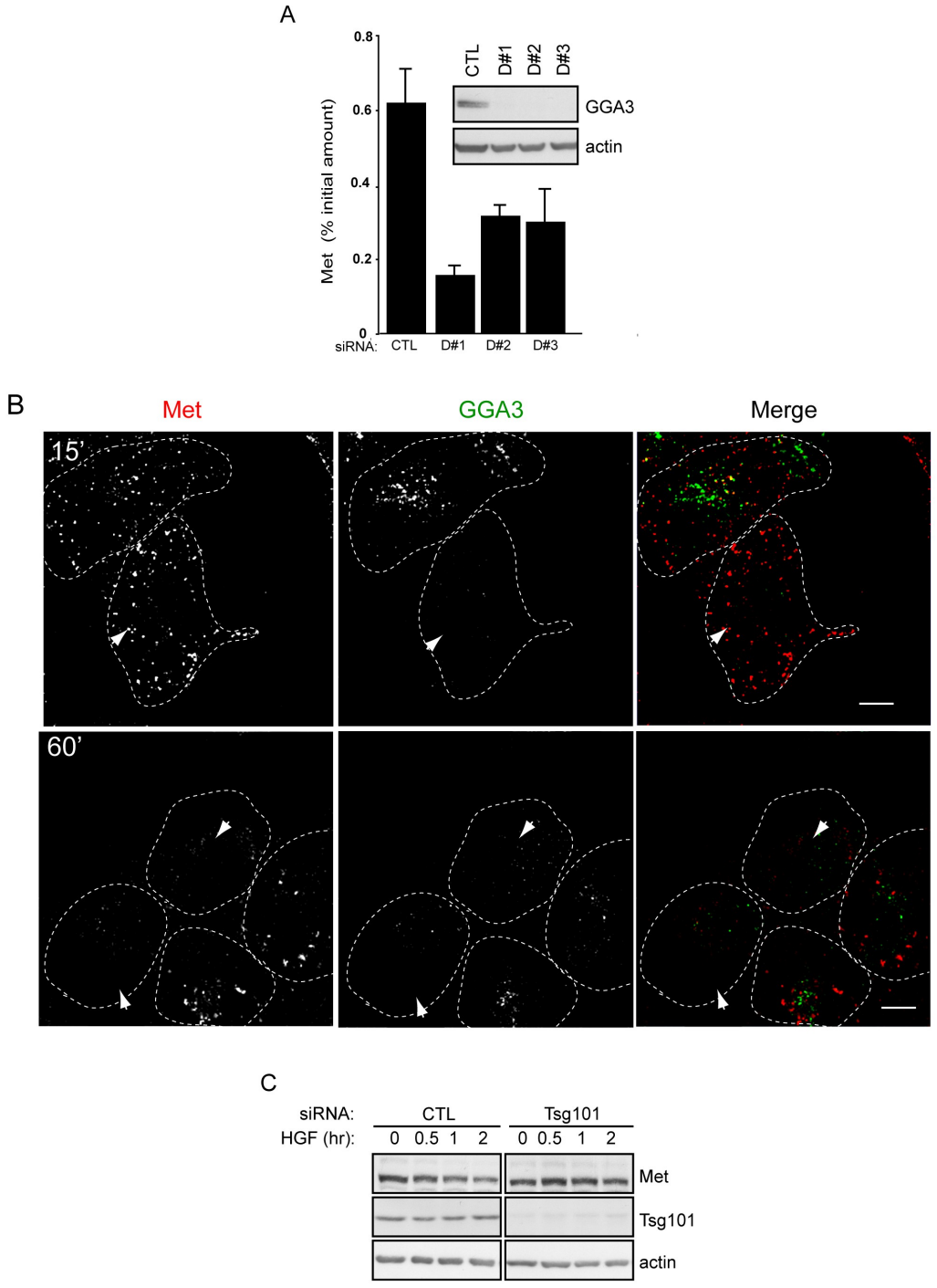
A
0.8
0.6
0.4
0.2
0
Met (% initial amount)
siRNA: CTL D#1 D#2 D#3
CTL
D#1
D#2
D#3
GGA3
actin
B
Met
GGA3
Merge
15'
60'
C
siRNA:
HGF (hr):
CTL
Tsg101
0 0.5 1 2
0 0.5 1 2
Met
Tsg101
actin

**Figure S3.3, Related to Figure 2. GGA3 KD Specifically Targets Met Degradation Independent of the Biosynthetic Pathway**

(A) HeLa cells transfected with CTL (top panels) or GGA3 siRNA (bottom panels) were analyzed for TGN export by incubating cells at 20ºC (top) then shifting back to 37ºC (lower) as described in experimental procedures. See also, (Matlin and Simons, 1983). Note, under these conditions, the distribution of M6PR in GGA3 KD cells was found to relocalize from predominantly TGN/late endosomes to early endosomes, indicative of impaired TGN export as described previously (Puertollano and Bonifacino, 2004). Cells were stained for Mannose-6-phosphate receptor (M6PR, green in merge), Giantin (red in merge), and Met (blue in merge). Bar = 10μm.

**Figure S3.3**

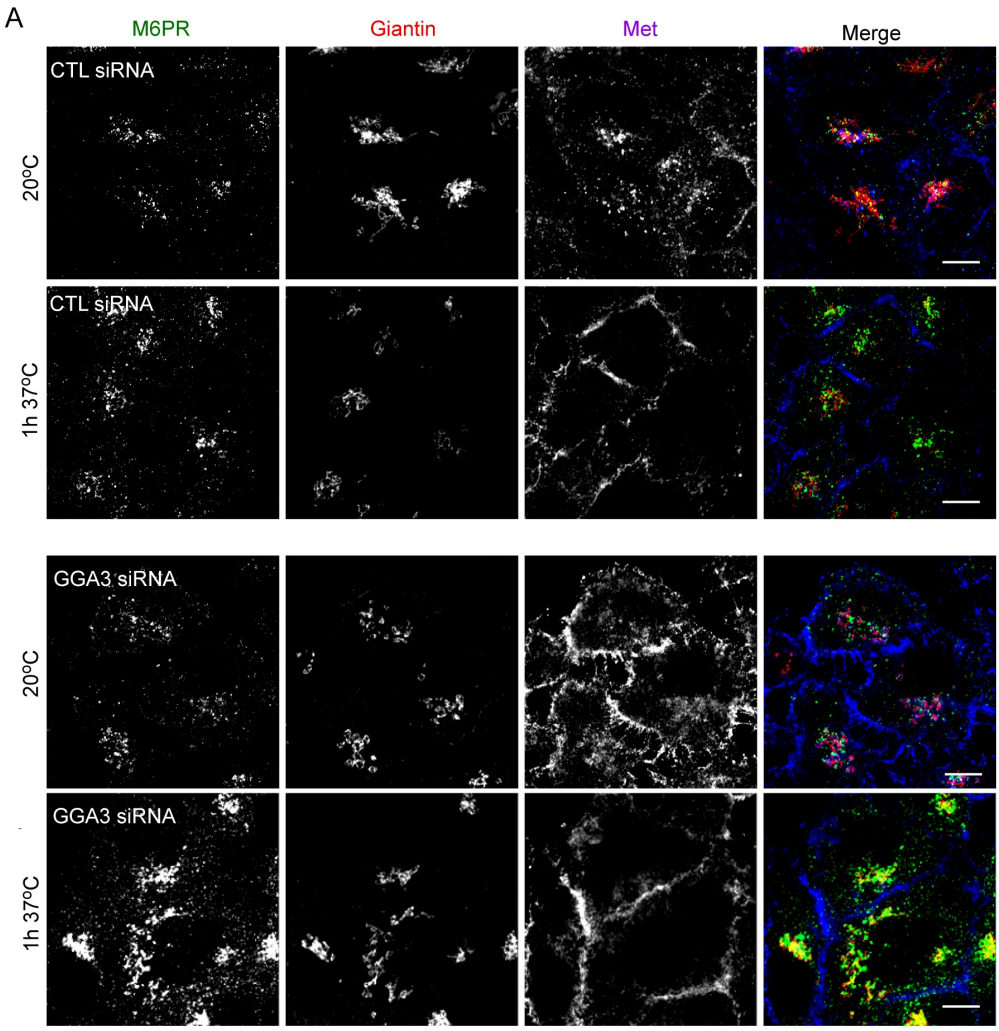
A
M6PR
Giantin
Met
Merge
CTL siRNA
20°C
CTL siRNA
1h 37°C
GGA3 siRNA
20°C
GGA3 siRNA
1h 37°C

**Figure S3.4, Related to Figure 3. Met Recycling Occurs Through a Rab4-Dependent Pathway**

(A) Bar graph representing the mean fluorescence of Met receptor expressed on the cell surface after HGF pulse/chase (±SEM, N=4) normalized and expressed as percentage of unstimulated samples as assessed by flow cytometry. Statistical analysis assessed by student's t-test; * $P < 0.05$. (B) HeLa cells treated with control or Rab4A siRNA were pulse/chased with HGF then processed for IF using antibodies against Met (shown in white). Nucleus stained with DAPI (blue). Bar = 10μm. (Right panel) IB of Rab4A KD levels achieved. (C) HeLa cells were transfected with GFP-Rab4, GFP-Rab11 or left untransfected were pulse/chased with HGF and processed for IF for the indicated antibodies. Bar = 10μm. (Right panel) Quantification of percentage of transfected cells exhibiting colocalization of endosomal (EN) Met with GFP-Rab after pulse/chase. Values are mean ± SEM from three independent experiments. Statistical significance assessed by student's t-test; *$P< 0.0005$.

**Figure S3.4**

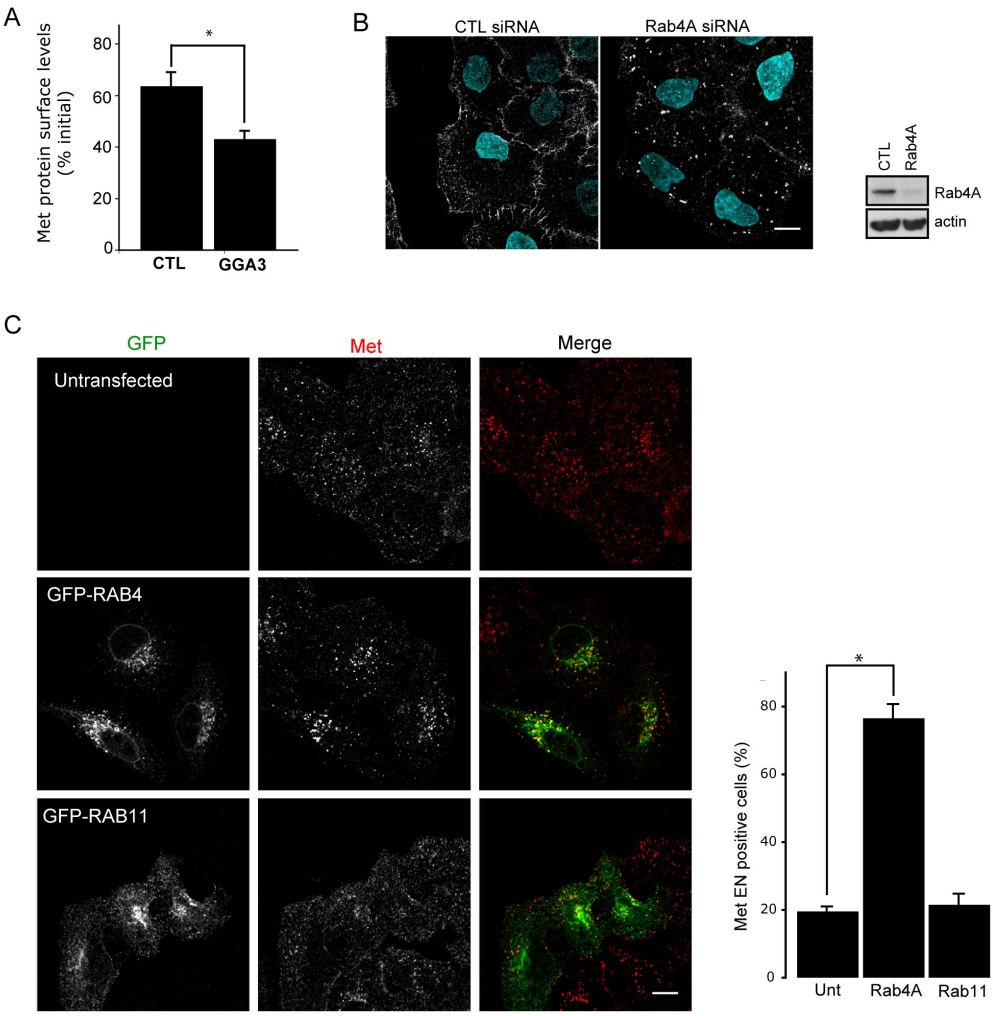
A
Met protein surface levels (% initial)
80
60
40
20
0
*
CTL
GGA3
B
CTL siRNA
Rab4A siRNA
CTL
Rab4A
Rab4A
actin
C
GFP
Met
Merge
Untransfected
GFP-RAB4
GFP-RAB11
Met EN positive cells (%)
80
60
40
20
0
*
Unt
Rab4A
Rab11

**Figure S3.5, Related to Figure 5. Met Displays Altered Localization with Arf6 KD or Arf6Q67L and Partially Colocalizes with WT-Arf6**

(A) Representative phase-contrast images (10x) of migration assays using CTL, KD, WT or N194A cells plated onto modified Boyden chambers and analyzed for their ability to migrate towards serum (no treatment) or HGF.

(B) HeLa cells treated with control or Arf1, Arf3 or Arf6 siRNA left untreated (no HGF) or pre-treated with CHX then pulse/chased with HGF were processed for IF using antibodies against Met (shown in white). Nucleus stained with DAPI (blue). Arrows point to regions of intracellular accumulation of Met located. Bar = 10μm. (C) IB of Arf KD levels achieved. (D) HeLa cells transfected with HA-Arf6 WT and treated for 5 min with HGF (top) or HA-Arf6Q67L (bottom) were processed for IF using anti-Met and anti-HA antibodies. Bar = 10μm.

## Figure S3.5

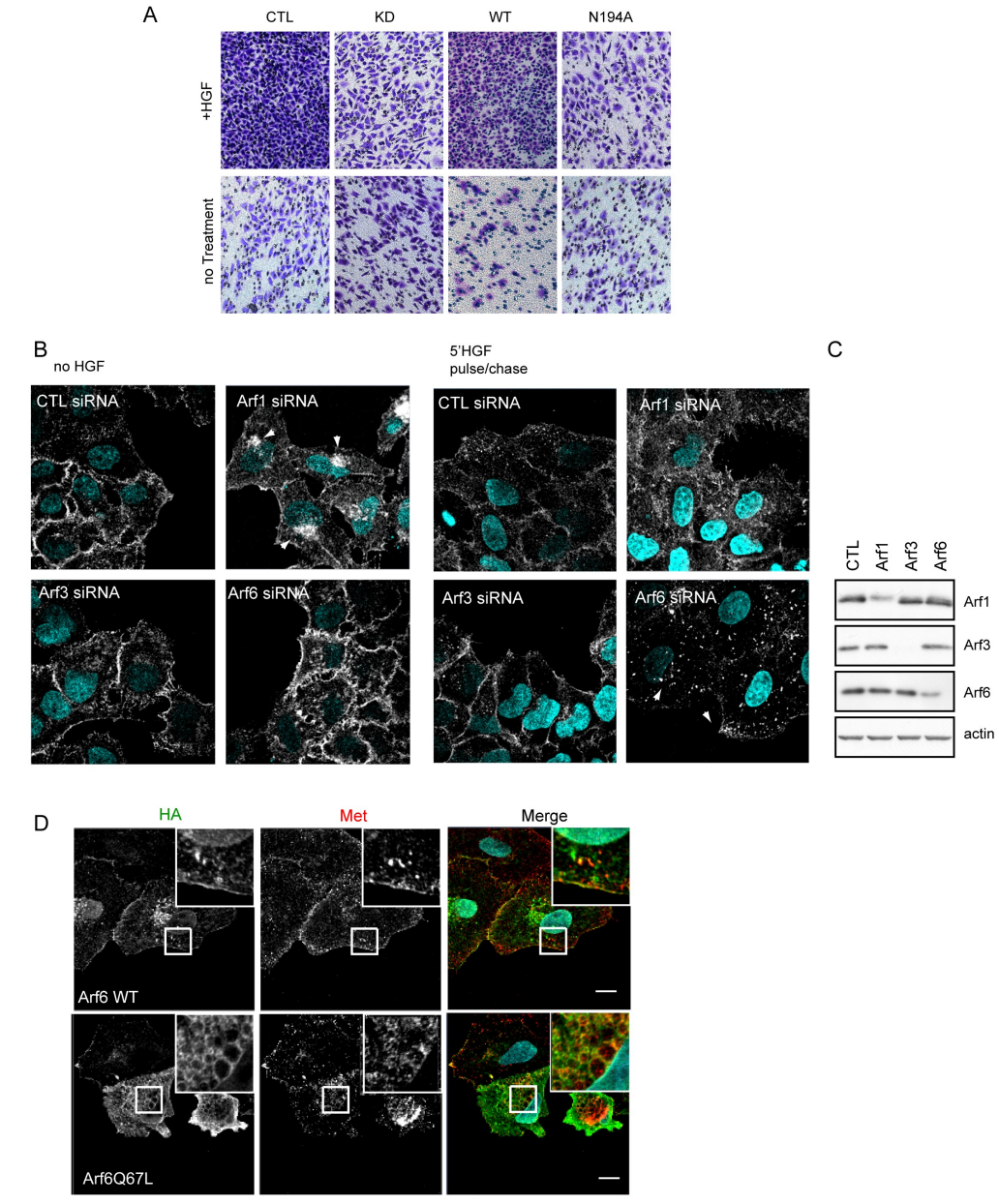
A
CTL
KD
WT
N194A
+HGF
no Treatment
B
no HGF
5'HGF
pulse/chase
CTL siRNA
Arf1 siRNA
Arf3 siRNA
Arf6 siRNA
C
CTL
Arf1
Arf3
Arf6
Arf1
Arf3
Arf6
actin
D
HA
Met
Merge
Arf6 WT
Arf6Q67L

**Figure S3.6, Related to Figure 6. Crk and GGA3 Associate and Are Required for Cell Migration**

(A) Eluted Myc-GGA3 recombinant protein was loaded onto GST or GST CRK proteins and used for pulldowns. 5% total pulldown input was loaded on gel. (B) Purified GST-tagged proteins (as indicated on top) were coupled to glutathione sepharose beads then incubated with HEK293 cell lysates transfected with GFP-GGA3 WT or GFP-GGA3ΔCrk constructs for GST pulldown assays. Samples were analyzed by IB with the indicated antibodies. 10% Input loaded as indicated. (C) Representative phase-contrast images (10x) of migration assays using CTL, KD or ΔCrk cells plated onto modified Boyden chambers and analyzed for their ability to migrate towards serum (no treatment) or HGF.

**Figure S3.6**

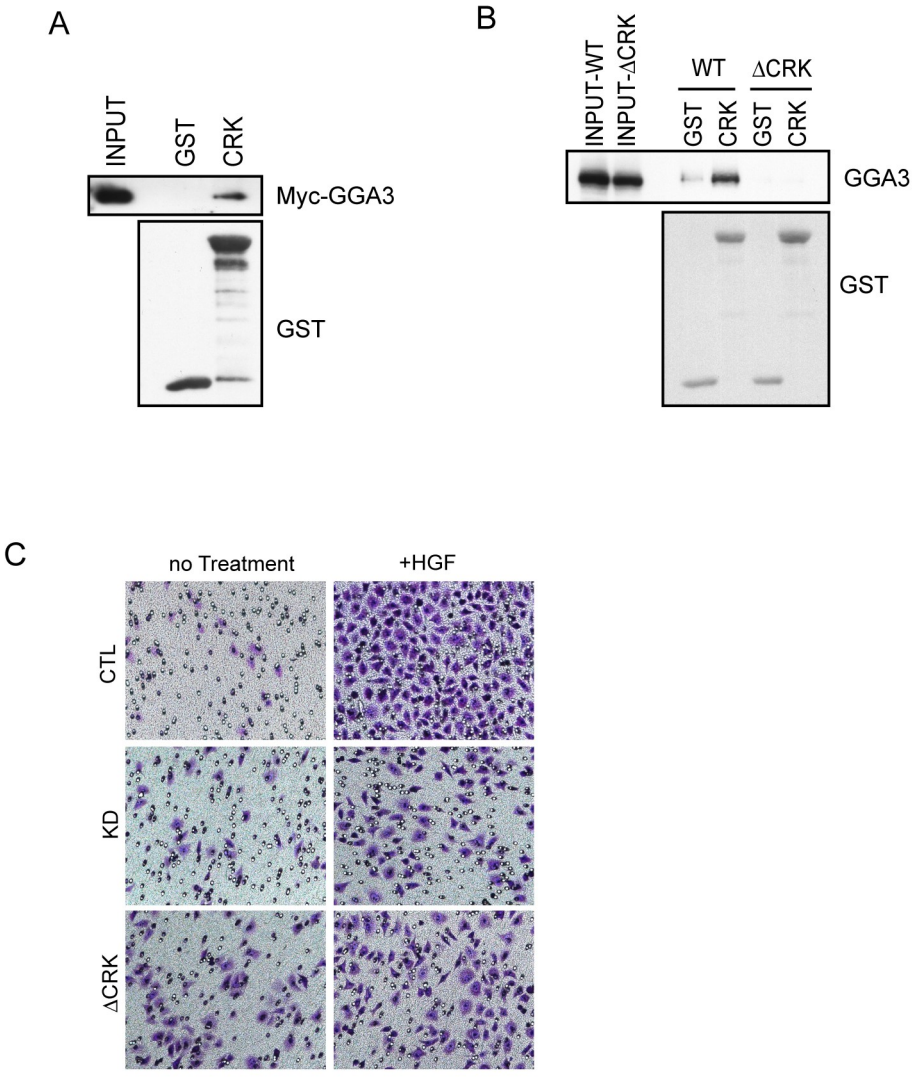
A
INPUT
GST
CRK
Myc-GGA3
GST
B
INPUT-WT
INPUT-ΔCRK
WT
ΔCRK
GST
CRK
GST
CRK
GGA3
GST
C
no Treatment
+HGF
CTL
KD
ΔCRK

**Supplemental Movie Legends**

**Movie S3.1, related to Figure 3. Dynamics of internalized Alexa555-HGF and GFP-GGA3 structures in live cells**. Continuous image streams taken with 30 ms exposures showing that the GFP-GGA3 structures are highly dynamic, and that multiple GGA3 structures frequently surround and repeatedly interact with internalized Alexa555-HGF. Numbers correspond to boxed areas (3.2 μm square) in Figure 3D. Playback at real-time (30 Hz).

**Movie S3.2, related to Figure 3. Dynamics of GFP-GGA3 and mCherry-Clathrin**. Movie showing dynamics and colocalization of GFP-GGA3 (green) and mCherry-Clathrin (red) in four fields (each 5.3μm square) in COS-1 cells. Playback at real-time (30 Hz).

# Chapter 4

## 4. CLIP-170 Links HGF-dependent Vesicle Motility to Microtubules During Cell Migration

Christine A. Parachoniak*, Kossay Zaoui* and Morag Park

*authors contributed equally to this work.

## 4.1. PREFACE

In Chapter 3, I demonstrated that in response to HGF, the Met receptor is recycled through a GGA3 and Rab4-dependent pathway to actin-rich membrane ruffles. This polarized delivery of the Met receptor suggests that this localization may be an important determinant for maintaining the spatial and temporal dynamics of signaling during HGF-mediated cell migration. In this Chapter, we have examined more closely the mechanistic basis for regulating Met recycling to lamellipodia and its impact on cellular migration. We provide evidence that the microtubule plus-end interacting protein, CLIP-170, regulates trafficking of Met-positive recycling vesicles to lamellipodia of motile cells and is required for cell migration.

## 4.2. ABSTRACT

Initiation of cell migration in response to activation of a receptor tyrosine kinase (RTK) is a complex process involving the coordinate and spatially restricted assembly of RTK signalling complexes. Here we report that the initiation of cell migration in response to hepatocyte growth factor (HGF) is dependent on the microtubule-directed trafficking of the HGF receptor, Met, to lamellipodia. The Met RTK is targeted to Rab4 vesicles following HGF-stimulation and rapidly recycles to the plasma membrane. This process is required for sustained Met signalling[492]. We find that the microtubule plus end binding protein, CLIP-170, is a key regulator in capturing Rab4 vesicles for microtubule-based transport of Met-positive endosomes to lamellipodia. CLIP-170 recruitment to activated Met occurs independent of microtubule interaction, and requires the coiled-coil domain of CLIP-170. Both CLIP-170 and microtubule integrity significantly contribute to the efficiency of Met receptor trafficking to lamellipodia and are essential for lamellipodial stability, nascent adhesion formation and cell migration, post-HGF stimulation. These results identify a function for microtubule and CLIP-170 interactions in the trafficking of the Met RTK, through regulation of Rab4-mediated recycling, essential for HGF mediated cell migration.

## 4.3. INTRODUCTION

Cells undergo dynamic remodelling of their cytoskeleton in response to growth factor stimuli. Cycles of cell protrusion, extracellular matrix adhesion, cell body translocation and rear retraction result in cellular movement[380]. In general, cells initially alter their shape by polymerizing actin into a dense network of branched filaments called the lamellipodium which protrudes in the direction of migration[383]. This polarization includes the asymmetric distribution of signalling and cytoskeleton proteins, which contributes to productive, directed movement[388]. Multiple RTKs regulate cell migration in response to ligand activation. How

RTK-dependent signals become spatially restricted in lamellipodia is poorly understood.

Following ligand stimulation, activated RTKs are rapidly internalized and either targeted for degradation or recycled back to the plasma membrane. Whether a RTK undergoes a degradative or recycling fate can greatly influence the strength and duration of RTK signalling[201,426]. In general, vesicle trafficking is controlled by members of the Rab family of small GTPases [277]. Rab11 regulates slow recycling of cargo transitioning through the recycling endosome, while Rab4 mediates fast recycling of cargo passing directly from the early endosome[277]. Exactly how these Rabs coordinate RTK-mediated cell migration is still unclear.

Growth factor signalling through the hepatocyte growth factor (HGF)/Met receptor axis coordinates essential cellular processes including proliferation, motility and epithelial to mesenchymal transitions (EMT)[462]. During development, Met signalling is indispensable for the growth and survival of placental trophoblasts, outgrowth of motor neurons, and migration of muscle precursor cells[46,47,49,456]. Likewise, during adulthood, Met regulates wound healing in several organs including the liver, heart and kidney[458-461]. Importantly, several studies have associated Met receptor trafficking in the regulation of Met RTK signal transduction and have linked impaired Met receptor endocytosis to tumorigenesis[9,106,108,492,493]. Thus understanding the molecular mechanisms regulating Met RTK trafficking is paramount to our ability to develop novel targeted therapeutics against the Met receptor.

Microtubules (MT) are cytoskeletal structures composed of protofilaments assembled from alpha and beta tubulin dimers. MTs are polarized; the minus end contacts the Microtubule-organizing center (MTOC) while the plus ends of microtubules radiate outward[393]. During cell migration plus ends are captured and stabilized at the leading edge, and are likely to aid in vesicle transport to the lamellipodia[392]. A group of plus-end-tracking proteins (+TIPs) preferentially accumulate at the plus ends of growing MTs and serve to regulate their stability and capture[393,494]. CLIP-170 is a prototypical +TIP, shown to positively regulate microtubule growth[495]. CLIP-170 has also been implicated in the attachment of

endosomes to MTs[406]. Nonetheless experimental evidence demonstrating a direct link between CLIP-170 in promoting the capture of a specified endocytic cargo to microtubules is lacking. Furthermore, the physiological function of CLIP-170 in regulating endosomal dynamics has not been fully addressed.

Regulators of actin polymerization, including the actin related protein 2/actin related protein 3 (Arp2/3) complex, nucleate actin monomers within the lamellipodia to drive protrusion[496,497]. Actin polymerization thus serves as both a mechanical support and the driving force required for cellular migration[497]. During lamellipodial advancement, small nascent adhesions form just below the plasma membrane and turnover at a frequency proportional to the rate of protrusion[498]. These multiprotein complexes, regulate contact of the cell body with the extracellular matrix and actin[391]. At the boundary between the lamellipodia/lamella, adhesions either disassemble or mature and elongate into larger adhesions to provide traction support[498]. While several adaptors, kinases and phosphatases have been reported to associate with focal adhesions[388], the mechanisms governing their regulation are still poorly understood.

We have investigated the role of CLIP-170 and microtubules in Met receptor trafficking and HGF-mediated cell migration. We show that CLIP-170 is essential for coupling Rab4 motility and microtubules. Loss of CLIP-170 results in defects in the recruitment of proteins to the lamellipodia, including Arp3, VASP, Paxillin and the Met receptor. Taken together, these results indicate that CLIP-170 affects HGF-mediated cell motility by regulating Met and Rab4 vesicle motility to lamellipodia and identify a role for CLIP-170 in a Met receptor-linked signalling pathway.

## 4.4. RESULTS

### 4.4.1. Microtubules and the plus-end protein CLIP-170 are required for Met trafficking to lamellipodia

In order to better understand the role of endocytosis in HGF-mediated cell migration, we sought to determine the subcellular localization of the Met receptor

in the breast cancer cell line SKBr-3 which in response to HGF, become asymmetrically polarized and form large lamellipodial extensions. Upon HGF stimulation, the receptor for HGF, Met, also becomes enriched at the lamellipodia (Fig. 1**a** also Supplemental Figure S4.1**a**). This ligand-dependent redistribution of the Met receptor is reliant on an intact microtubule network, as treatment with the microtubule depolymerizing drug, nocodazole, severely reduced this localization (Fig. 4.1**a**). The Met receptor recycles to lamellipodia through a Rab4-dependent recycling pathway[492]. Similarly, treatment of cells with nocodazole severely inhibited HGF-dependent Met recycling in HeLa cells, where localization of Met RTKs was enhanced in endosomes and evidence of Met recycling was reduced from 81.6% ($n$ = 48 cells) to 1.5% ($n$ = 74 cells; Fig. 1**b**, and S1**b**). Taken together, these results indicate that microtubules are required for HGF-dependent localization and recycling of the Met receptor to the leading edge.

The interaction of organelles and microtubules can occur through a class of microtubule plus-end interacting proteins (+TIPs), for which the prototypical protein is CLIP-170[398,405]. Using a candidate-based approach, we tested whether CLIP-170 is required for Met localization to lamellipodia, by performing short interfering RNA (siRNA)-mediated knockdown of CLIP-170. Under these conditions, reduced localization of Met in lamellipodia was observed in CLIP-170 knockdown versus control cells (Fig. 4.1**c**). A corresponding reduction in the ability to recycle the Met receptor was also observed following CLIP-170 knockdown (reduced from 80.0% to 10.7%, $P$ = 0.004, Fig. 4.1**d** and S4.1**c**). In order to confirm a requirement for CLIP-170/microtubule interactions in Met recycling, we took advantage of a dominant-negative EB3-GFP construct that functions by inhibiting CAP-Gly-EEY/F interactions and occludes the plus-end binding of CLIP-170, as well as any indirect recruitment through end-binding (EB) protein, EB1[421] (Fig. 4.1**e**). Over-expression of EB3-GFP was verified to disrupt association with CLIP-170 to microtubules, as shown previously (results not shown). When over-expressed, EB3-GFP resulted in a failure to efficiently recycle the Met receptor (Fig. 4.1**e** and S4.1**d**). Therefore, the recruitment of plus-end proteins, specifically CLIP-170, to microtubules is required for the efficient

recycling of the Met receptor.

### 4.4.2. CLIP-170 localizes to Met-positive endosomes independent of its microtubule interaction

To investigate the role of CLIP-170 in Met trafficking, we next used fluorescence microscopy to visualize the subcellular localization of CLIP-170 with respect to Met in response to ligand stimulation. In unstimulated cells, CLIP-170 was found in punctate structures, as previously described[406] and showed little co-localization with the Met receptor (Fig. 4.2**a**,**b**; 12.8%, *n* = 53 cells). HGF-induces the internalization and trafficking of the Met receptor into early endosomes[108]. Upon HGF treatment, a pronounced co-localization of the Met receptor with endogenous CLIP-170 was observed (Fig. 4.2**a**,**b**; 61.1%; *n* = 40 cells). This punctate staining was confirmed to be early endosomes, as both Met and CLIP-170 localized with GFP-Rab5 (Fig. S4.2**a**). Upon over-expression, CLIP-170 accumulates specifically to the plus ends of microtubules[499]. Under these conditions, we observed that the majority of HGF-induced Met-positive vesicles were in contact with CLIP-170 as visualized through 3D reconstruction across multiple cells (Fig. 4.2**c**,**d**; 78%, *n* = 164 spots). Consistent with this interaction, GFP-CLIP-170 co-immunoprecipitated (co-IP) with Met by 20 mins of HGF treatment (Fig. 4.2**e**) but not in unstimulated cells. Taken together these results support recruitment of CLIP-170 to a Met signalling complex in an HGF-dependent manner.

As CLIP-170 has not previously been implicated in recycling of RTKs, we utilized a structure-function approach to determine the region of CLIP-170 responsible for recruitment to a Met complex. To this end, various GFP-CLIP-170 mutants were expressed in HeLa cells, cells were then stimulated with HGF, and the ability of mutant CLIP-170 proteins to co-IP with the Met receptor was tested (Fig. 4.2**f**). Removal of the microtubule-binding domain (ΔH) did not disrupt the association with Met, and in fact resulted in a greater association with Met (Fig. 4.2**g**). Consistent with this observation, treatment with nocodazole did not abrogate co-localization of endogenous CLIP-170 with the Met receptor in

endosomes (Fig. 4.2**h**). Thus, association of CLIP-170 and the Met receptor can occur independently of the association of CLIP-170 with microtubules. Similarly, deletion of the c-terminal region (ΔC) of CLIP-170 had little effect on the association of CLIP-170 with the Met receptor and expression of the c-terminus of CLIP-170 alone (C1) was insufficient for association with Met (Fig. 4.2**i**). In contrast, expression of the central coiled-coil region (CC) of CLIP-170 was sufficient for association with a Met receptor complex (Fig. 4.2**i**). Together, this data indicates that HGF-dependent recruitment of CLIP-170 to the Met receptor can occur independently of its microtubule-interaction through a mechanism dependent on its coiled-coil domain.

### 4.4.3. CLIP-170 is required for HGF-dependent Rab4-positive vesicle motility

We have previously characterized a rapid Rab4-dependent recycling pathway involved in the trafficking of the Met receptor to the lamellipodia[492]. We confirmed that Met-positive endosomes in contact with GFP-CLIP-170-loaded microtubule plus-ends were positive for mCherry-Rab4 vesicles (Fig. 4.3**a**). Moreover, Alexa-555 labeled HGF was visualized to enter GFP-Rab4-positive structures after 20 min of stimulation (Fig. 4.3**b**). Consistent with these results, using live cell microscopy, we observed mCherry-Rab4-positive vesicles to track along growing microtubules in response to HGF treatment (Fig. 4.3**c** and Supplementary movie 4.1). To examine whether CLIP-170 is required for mobility of Rab4 vesicles in response to HGF, we depleted CLIP-170 using siRNA. In control cells, the majority of GFP-Rab4 vesicles were seen to move rapidly within the cell in response to HGF treatment (Fig.4.3**d** and 4.3**e**; 79.3% motile). In contrast, the mobility of GFP-Rab4 vesicles was detectably decreased by siRNA knockdown of CLIP-170 (Fig. 4.3**d** and 3**e**; 43.3% mobile). Indicating an overall reduction of 37.1% in Rab4 vesicle movement, under CLIP-170 knockdown conditions (Fig.4.3**e**). A corresponding reduction in the average speed of GFP-Rab4-positive vesicles was also observed in CLIP-170 knockdown cells (Fig. 4.3**e**; control = 0.35μm/s, CLIP-170 KD = 0.195μm/s). The majority of

moving GFP-Rab4 vesicles in response to HGF treatment, were found within the lamella of the cell, and it was this population of Rab4-positive vesicles which displayed a statistically significant reduction in vesicle speed following CLIP-170 knockdown (Fig. 4.3**e**; 0.18μm/s, $P = 0.00025$). Additionally, in support of our previous findings, Rab4 vesicle dynamics, could be rescued by expression of a siRNA-resistant CLIP-170 ΔC construct, but not by CLIP-170 constructs lacking the ability to bind to microtubules (ΔH, CC, C1) (Fig. 4.3**e**). Interestingly, the CC domain of CLIP-170, which was found to be sufficient for association with the Met receptor, also failed to rescue Rab4 dynamics (Fig. 4.3**e**), indicating that the association between CLIP-170 and the Met receptor alone is also insufficient. Taken together, these results support a requirement for both CLIP-170 and microtubule-binding of CLIP-170 in mediating HGF-induced Rab4 motility.

### 4.4.4. CLIP-170 KD alters actin remodeling and adhesion dynamics in response to HGF

HGF promotes lamellipodia formation and cell migration in epithelial cells[182]. Given our observation that the regulation of Rab4 vesicle movement through CLIP-170 is a critical component of Met receptor trafficking to lamellipodia, we next examined the impact of CLIP-170 on the formation of HGF-induced actin remodeling and adhesion complexes in developing lamellipodia. The actin related protein 2/actin related protein 3 (Arp2/Arp3) complex is a key regulator of actin dynamics in lamellipodia, as it controls branched actin nascent filament nucleation[500]. In response to HGF, GFP-Arp3 distinctly localized to lamellipodia in control cells (Fig. 4.4**a**). In contrast, GFP-Arp3 remained cytosolic and was only weakly detected at the edge of CLIP-170 depleted cells (Fig. 4.4**a**). In agreement with these results, actin-mCherry was visualized in well-defined, cortical networks of polymerized actin filaments at the leading edge of control cells stimulated with HGF (Fig. 4.4**b** and Supplemental movie 4.2). In CLIP-170 knockdown cells, actin-mCherry was found predominantly in stress fibers within the cell following HGF treatment (Fig. 4.4**b** and Supplemental movie 4.3). In a similar manner, the cytoskeleton protein

vasodilator-stimulated phosphoprotein (VASP), which localizes to regions of dynamic actin reorganization[501], accumulates in adhesions and at the leading edge of control cells, but not in CLIP-170 knockdown cells, where GFP-VASP chiefly localizes to adhesions (Fig. 4.4**c**).

Formation of nascent and focal adhesions is key to the ability of cells to efficiently migrate. Consistent with previous reports[502], two populations of adhesions were distinguishable upon HGF treatment; smaller, nascent adhesions located just beneath the leading edge and larger, more stable focal adhesions further within the lamella (Fig. 4.4**d**). Nascent adhesions serve to stabilize the lamellipodium by forming attachments to the extracellular matrix[383]. To investigate adhesion dynamics, we used live-cell microscopy using GFP-paxillin as a marker for adhesions. This revealed that in response to HGF, depletion of CLIP-170 reduced the percentage of cells able to form nascent adhesions from 81.8% to 19.98% while increasing the percentage of cells with larger focal adhesions from 18.15% to 80.1% in response to HGF (Fig. 4.4**e** and Supplemental movie 4.4 and 4.5). These changes were accompanied with a decrease in the total number of nascent adhesions and an increase in the total number of focal adhesions in CLIP-170 knockdown cells (Fig. 4.4**f**), along with an increase from 1.65 μm to 2.38μm in the average size per adhesion (Fig. 4.4**f**). Importantly, all of the siRNA-mediated changes in actin and actin related protein localization could be rescued by re-introduction of siRNA-resistant CLIP-170 (Fig. S4.3**a**) and were in accordance with results obtained for endogenous protein localization (Fig. S4.3**b**). Collectively, the aberrant actin structure and accompanied changes in adhesion dynamics observed in CLIP-170 depleted cells indicate a defect in both formation of nascent adhesions and turnover of established adhesions.

### 4.4.5. CLIP170 is required for HGF-mediated lamellipodial stability and cell migration

In order to test the hypothesis that CLIP-170 is required for HGF-mediated cell migration, we examined lamellipodia formation and cell migration, in cells depleted of CLIP-170. We first measured lamellipodial membrane dynamics of

CLIP-170 knockdown cells using distance-versus-time kymographs. In control cells, lamellipodia extended in a smooth and constant speed, with little fluctuations (Fig. 4.5**a**). However, in CLIP-170 knockdown cells, lamellipodia extensions were less regular, and frequently retracted (Fig. 4.5**a**). The less stable lamellipodia observed in CLIP-170 knockdown cells corresponded to a quantitative reduction of ~45% in the half-life of lamellipodia ($P = 1.64x10^{-5}$, Fig. 4.5**b**) and overall reduced size of lamellipodia size (Fig. 4.4**c**; width $P = 0.0006$, length $P = 0.008$). Thus CLIP-170 depleted cells extend smaller, less stable lamellipodia compared to control cells. Consistent with these findings, CLIP-170 depletion reduced the ability of cells to move in response to HGF, as visualized through time-lapse microscopy (Fig. 4.5**d**,**e** and supplemental movies 4.6 and 4.7). Furthermore, only 10.24% of CLIP-170 depleted cells were able to migrate in response to HGF, compared to 90.15% of control cells (Fig. 4.5**e**). Of those that did respond, the net speed of migration was severely reduced from 0.30μm/min down to 0.07μm/min (Fig. 4.5**f**). Given that the CLIP-170/microtubule interaction is required to achieve appropriate HGF/Met-dependent Rab4 vesicle trafficking, we used live-cell microscopy to assess the impact of this interaction on the overall ability of HGF to elicit cell migration. Importantly, while the speed of migration could be restored by re-expression of WT CLIP-170 or CLIP-170 ΔC, re-expression of either of the CLIP-170 ΔH, CC or C1 mutants failed to re-establish cell migration (Fig. 4.5**f**). These data argue that CLIP-170 is required to establish HGF-mediated cell migration, together with microtubule-mediated Met receptor trafficking.

## 4.5. DISCUSSION

Microtubules (MT) play important roles in the transport of vesicles at several distinct intracellular locations, including late and early endosomes[401,503]. Recently, microtubules have been identified to function in rapid recycling pathways involving the Transferrin receptor[504], although it remains unclear to what extent other receptors utilize a similar mechanism. Here, we show that microtubule

integrity is required for recycling of the Met receptor to lamellipodia in response to HGF. The Met receptor undergoes PKC-controlled microtubule-dependent trafficking to a perinuclear compartment[505]. Interestingly, while perinuclear trafficking was found to be dependent on the PKCα isoform of PKC, a separate upstream pathway involving PKCε, was postulated to regulate Met receptor recycling to the plasma membrane, although a role for microtubules was not investigated[506]. Hence two distinct microtubule-based pathways appear to control Met receptor trafficking. In line with these results, using a combination of biochemistry and live-cell imaging techniques, we specifically demonstrate that the microtubule plus end binding protein, CLIP-170, is a critical regulator of Met receptor recycling to lamellipodial leading edges.

Although CLIP-170 has historically been identified as an endosome to microtubule adaptor[406], experimental support for this function for CLIP-170 have been lacking. Our results position CLIP-170 as a linker enabling the capture of Rab4-positive Met cargo to microtubule plus-ends. The observation that endogenous CLIP-170 localizes with the Met receptor on early endosomes, independent of microtubules indicates that CLIP-170 can associate with the Met receptor independent of its microtubule association. In agreement with this, CLIP-170 mutants unable to associate with microtubules are still able to co-IP with the Met receptor and depolymerization of microtubules through nocodazole-treatment does not inhibit recruitment of CLIP-170 to Met-positive endosomes. As expression of the coiled-coil domain of CLIP-170 alone was sufficient for association with the Met receptor, this suggests differential requirements for CLIP-170 domains in the recruitment of CLIP-170 to Met and MTs, respectively. Interestingly, the BIN-amphiphysin-RVS (BAR) domain-containing protein amphiphysin interacts with CLIP-170 through the coiled-coil domain of CLIP-170[507]. As the BAR domain of amphiphysin binds lipid membranes[508,509], association of CLIP-170 with amphiphysin may aid in conveying CLIP-170 into close proximity to membrane-bound Met receptor complexes on early endosomes. Additionally, phosphorylation regulates autoinhibition of CLIP-170 through intramolecular interactions[510] as well as its binding to microtubules[417]. As several

phosphorylation sites have been identified within the head domain of CLIP-170, it is conceivable that the head domain, in addition to mediating the interaction of CLIP-170 with microtubules, is also responsible for inhibiting association of CLIP-170 with Met. This may account for the apparent increase in association between Met and CLIP-170 ΔH mutant. Thus, HGF-dependent recruitment of CLIP-170 to Met may occur via two non-mutually-exclusive mechanisms; through association with amphiphysin or through a phosphorylation-dependent process.

As CLIP-170 was found to associate with a Met receptor complex upon HGF stimulation, recruitment of CLIP-170 may serve as a critical step for loading of Met receptor-positive vesicles onto plus-ends of microtubules destined for the plasma membrane. We observed that the motility of Rab4+ recycling vesicles in the cell lamella is disrupted following CLIP-170 knockdown. This is in accord with earlier studies which localized CLIP-170 to transferrin-positive endosomes[406], which are known to partially accumulate on Rab4 endosomes[478], as well as our previous report that the Met receptor also localizes to Rab4+ vesicles[492]. As Rab4 vesicle motility could only be restored when both the head and coiled-coil domain of CLIP-170 were expressed together, this implicates both microtubule and Met receptor associations with CLIP-170 in the regulation of HGF-dependent Rab4 recycling. Additionally, we show that co-operation of these two domains of CLIP-170 are required for the formation of lamellipodia, cell adhesions and cell migration in response to HGF. These findings therefore mechanistically link the process of Rab4-positive vesicle recycling with cell migration and demonstrate that CLIP-170 is a major determinant in HGF-mediated cell migration. Several lines of evidence have demonstrated a requirement for Met endocytosis for cellular migration and *in vivo* transformation[9,108,493]. Our results extend these conclusions, providing new mechanistic understanding involving microtubule-mediated recycling of the Met receptor.

CLIP-170-mediated Met RTK trafficking also bears central implications for cell signalling, as this indicates that microtubule regulation serves a critical role in

Met receptor recycling linked to cell migration. Since multiple RTKs regulate cell migration and invasion, this raises the possibility that other microtubule binding proteins such as CLIP-170 may play a significant role in these processes.

## 4.6. EXPERIMENTAL PROCEDURES

### Cell culture, cDNA constructs and transfection

HeLa and HEK293 cells were cultured in DMEM containing 10% FBS. SKBr-3 cells were cultured in RPMI containing 10% FBS. Transient transfections in HEK293 and HeLa cells were performed using Lipofectamine Plus according to manufacturer's instructions (Invitrogen). SKBr-3 cells were transfected using Lipofectamine 2000 according to manufacturer's instructions (invitrogen) or by nucleofection (Amaxa). A detailed list of all reagents, constructs can be found in the Appendix: Supplemental Experimental Procedures.

### siRNA transfections

For siRNA experiments in HeLa cells, cells were seeded at $2.0x10^5$ in 6-well dishes coated with collagen and transfected with 50 nM siRNA using HiPerFect as per manufacture's instructions (Qiagen). SKBr-3 cells were seeded at $2.0x10^5$ in collagen-coated 6-well dishes and transfected using Liofectamine 2000 72h later or directing using nucleofection (Amaxa). All experiments were performed 72 hr post-transfection. control: Allstars negative control siRNA (Qiagen) for CLIP-170: siGENOME SMARTpool M-005294 (Dharmacon) and for rescue experiments : CLIP-170 (nt 4,472–4,495; within the 3`untranslated region) (Dharamacon).

### Immunoprecipitation and western blotting

Lysis and immunoblotting (IB) were as described previously[511]. Cells were harvested in 1% Trition lysis buffer (150mM NaCl, 20nMTris.HCl, 1mM EDTA, 1mM EGTA, 1% TritonX-100, 1% deoxycholate and PH 7.4). All lysis buffers were supplemented with 1 mM phenylmethylsulfonyl fluoride (PMSF), 1 mM

sodium vanadate, 1 mM sodium fluoride, 10μg/ml aprotinin and 10 μg/ml leupeptin. Samples were resolved by sodium dodecyl sulfate-polyacrylamide gel electrophoresis (SDS-PAGE) and transferred to nitrocellulose. Membranes were blocked with 5% bovine serum albumin and probed with appropriate antibodies, and then inculabed with horseradish peroxidase-conjugated secondary antibodies. All immunoblots were visualized by enhanced chemiluminescence (Amersham Biosciences, Piscataway, NJ).

**Immunofluorescence microscopy**

Cells grown on collagen–coated coverslips were fixed in 4% formaldehyde or 100 % Methanol at (-20°C) and permeabilized in 0.2% Triton X-100 before the addition of antibodies. Images were recorded with a scanning confocal microscope (LSM 510 Meta laser; Carl Zeiss, Inc.) with a 100 × plan Apo 1.4 NA objective and driven by ZEN LE software (Carl Zeiss, Inc.).

**Quantification of immunofluorescence**

Quantification of co-localization was as described previously[492]. Briefly, MetaMorph software was used for object-based colocalization measurements. Images were smoothed with a 3 x 3 low-pass filter, and endosomes were identified and counted using size estimates and intensity thresholds in each image set using the ‘‘Count Nuclei’’ application. Binary images were created for each set of endosomal spots and combined pairwise using logical AND operation to give only the ‘‘colocalized’’ spots. These spots were then counting using the ‘‘Count Nuclei’’ module. The minimum spot size was set so as to remove any small spots due to partial, and likely random, overlap of spots. Results were logged into Excel for analysis. Values for all analyses including colocalization and vesicle counting represent mean value ± standard error of the mean (SEM).

**3D imaging and quantification**

Images were generated from a three-dimensional reconstruction (volume image) of a confocal image stack using the Imaris software suite (Bitplane, Switzerland). Met spots were scored for contact with CLIP-170 positive structures ($n$ = 5).

**IF recycling assay**

Quantification of co-localization was as described previously[492]. Briefly, Cells grown on glass coverslips were pulsed with prewarmed (37°C) 0.5 nM HGF for 5 min, washed five times with Leibovitz-15 Medium containing 0.2% BSA at 4°C, and chased at 37°C for 20 min, fixed, and processed for IF. Cells were scored on ratio of endosomal (EN) over plasma membrane staining of Met and reported as mean ± SEM (n = 4). In each experiment a minimum of 20 fields was scored.

**Live-cell imaging**

Cells grown on collagen-coated glass coverslips (35mm, Ibidi GmbH Germany), after 20 min HGF stimulation (34ng/ml) they were positioned on the motorized stage on the inverted microscope Axiovert 200 M (Carl Zeiss, Inc), equipped with 100x plan Apochromat  NA 1.4 objective, AxioCam HRM [Carl Zeiss, Inc.] digital camera and equipped with a small transparent environmental chamber Climabox (Carl Zeiss, Inc) with 5% (v/v) CO2 in air at 37°C. The microscope was driven by the AxioVision LE software (Carl Zeiss, Inc). The motorized stage advanced to pre-programmed locations and photographs were collected for 2 min at 4 s intervals.

**Quantification of vesicle speed and adhesion sites**

Cells were observed as described in the previous paragraph except that images of paxillin-expressing cells were acquired at 4 s intervals for 2 min. Background-corrected fluorescence intensity images were used to measure small adhesion sites and FA size and number[502]. For the movement of vesicles, the images in 3D (X, Y, Z) of Rab4 expressing cells were acquired at 4 s intervals for 2 min and were kept at 37°C and 5% CO2 during the course of these experiments. The vesicle tracks were analyzed with Imaris software (Bitplane, Inc).

**Motility assay**

Live-cell motility was analyzed as described previously[502] except that pictures

were collected for 350 min at 5 min intervals. Motility parameters including rates of migration, migration paths and kymographs were obtained from time lapse movies. Means of velocity and kymograph analysis of membrane protrusions were calculated using MetaMorph and Excel (Microsoft) software.

**Statistics**

All results are presented as mean ± s.e.m. based on data averaged across multiple independent experiments. The *n* value of an experiment represents experiments done on different days unless otherwise noted. To assign significance, results were compared with control experiments by means of an unpaired *t* -test using Excel (Microsoft Office).

## 4.7. ACKNOWLEDGEMENTS

We thank Shawn Ferguson, Yulia Komarova, Kozo Kaibuchi, Anna Akhmanova, Niels Galjart, L. Welch, Victor Small, A.R. Horwitz and J. Wehland for generously providing constructs and Genetech Inc. for generously providing HGF. This research was supported by a McGill MICRTP Fellowship to K.Z., by a Canada Graduate Scholarship Doctoral Award to C.A.P. from the CIHR (Canadian Institutes of Health Research), CIHR operating grants to M.P. (MOP-11545 and 106635. M.P. holds the Diane and Sal Guerrera Chair in Cancer Genetics.

## 4.8. FIGURES AND FIGURE LEGENDS

**Figure 4.1. Microtubules and microtubule associating protein, CLIP-170, are required for Met receptor trafficking**. (**a**) Left, representative immunofluorescence (IF) images of SKBr-3 cells treated with DMSO or nocodazole and stimulated 20 min with HGF stained for Met (red) and alpha-tubulin (green). Insets show higher magnification, scale bar = 10μm. Right, fluorescence intensity line scan of Met fluorescence intensity versus distance from line shown in insets to the left. (**b**) Quantification of IF images from cells pre-treated with DMSO or nocodazole, pulsed for 5 min with HGF at 37ºC to allow internalization of Met receptors into early endosomes, then rapidly washed at 4ºC to remove unbound ligand and chased for 20 min to allow recycling. Data points are the mean ± s.e.m. from three independent experiments. Immunoflurescence images are shown in supplementary Fig. S4.1. (**c**) Left, representative IF image of cells treated with control (CTL) or CLIP-170 siRNA and stimulated 20 min with HGF, Met (red) and DAPI (blue). Insets show higher magnification, scale bar = 10μm. Right, fluorescence intensity line scan of Met fluorescence intensity versus distance from line in inset. Typical immunoblot (IB) of knockdown levels indicated above plot. (**d**) Quantification of IF recycling assay, performed as in **b**, from cells treated with CTL or CLIP-170 siRNA. (**e**) Left, schematic of EB3-GFP inhibition on plus-end binding. Right, Quantification of IF recycling assay, performed as in **b** in cells expressing GFP-vector or EB3-GFP.

## Figure 4.1

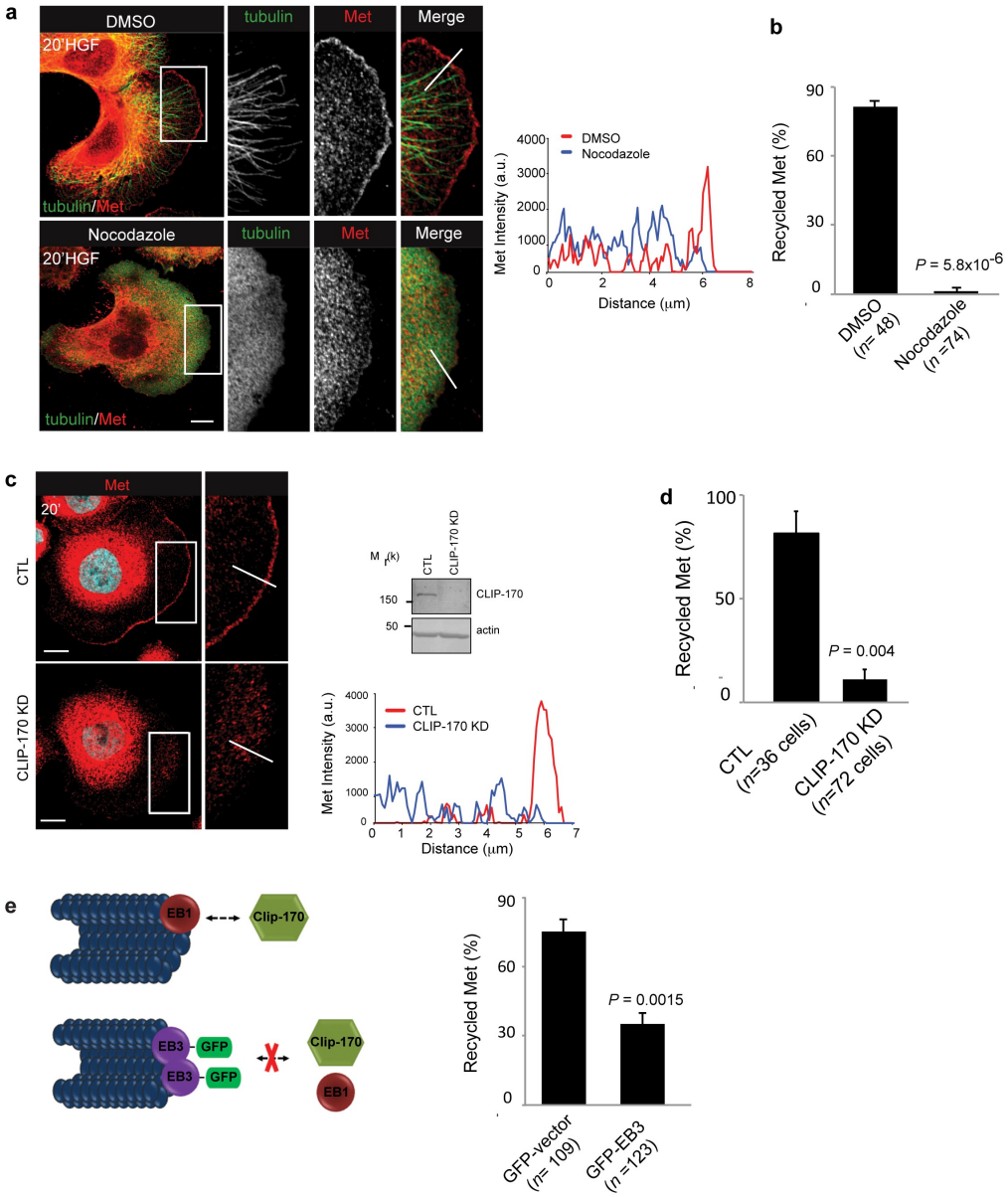
a
DMSO
20'HGF
tubulin
Met
Merge
tubulin/Met
Nocodazole
20'HGF
Met Intensity (a.u.)
DMSO
Nocodazole
Distance (μm)
b
Recycled Met (%)
P = 5.8x10-6
DMSO (n= 48)
Nocodazole (n =74)
c
Met
20'
CTL
CLIP-170 KD
M r(k)
CLIP-170
actin
Met Intensity (a.u.)
Distance (μm)
d
Recycled Met (%)
P = 0.004
CTL (n=36 cells)
CLIP-170 KD (n=72 cells)
e
EB1
Clip-170
EB3
GFP
Recycled Met (%)
P = 0.0015
GFP-vector (n= 109)
GFP-EB3 (n =123)

**Figure 4.2. The Met receptor associates with CLIP-170.** (**a**) Representative images of HeLa cells pre-treated with cycloheximide (CHX) for 2h were left unstimulated or stimulated 20 minutes with HGF and processed for IF to localize Met (red) and CLIP-170 (green). Bar = 10μm. (**b**) Top, quantification of colocalization of Met and CLIP-170 ± 20 min HGF. Values are mean ± s.e.m from 3 independent experiments. Bottom, line scan analysis of Met and CLIP-170 from region shown in **a**. (**c**) Representative IF of HeLas transfected with GFP-CLIP-170, pretreated with CHX, stimulated with HGF (20min) and stained for Met (red) and GFP-CLIP-170 (green). Boxed region of interest (ROI) shown at higher magnification (middle) and used to generate a, three-dimensional reconstruction, volume image, (Merge 3D). Arrows point to vesicles in close association with CLIP-170. Bar = 10μm. (**d**) Quantification of 3D-generated Met spots in contact with CLIP-170 structures, (*n* = 164 spots). (**e**) Representative immunoblots from HeLas transfected with GFP-CLIP-170 and stimulated for the indicated times with HGF were used for immunoprecipitations (IP) with Met or control IgG antibodies and blotted as shown. 10% of total cell lysate levels. (**f**) Schematic of CLIP-170 constructs. (**g**) HeLas transfected with GFP-CLIP-170 constructs and stimulated 20 mins with HGF were used for IPs with anti-Met and immunoblotted as shown. 10% of total cell lysate levels. (**h**) Representative IF images from cells pretreated with DMSO or nocodazol, stimulated for 20 min with HGF and stained for Met (red) and CLIP-170 (green). Scale bar = 10μm (**i**) Representative IBs from HeLa cell lysates transfected with GFP-CLIP170 constructs, stimulated with HGF for 20 mins and used for IPs using antibodies against Met. 10% of total cell lysate levels.

## Figure 4.2

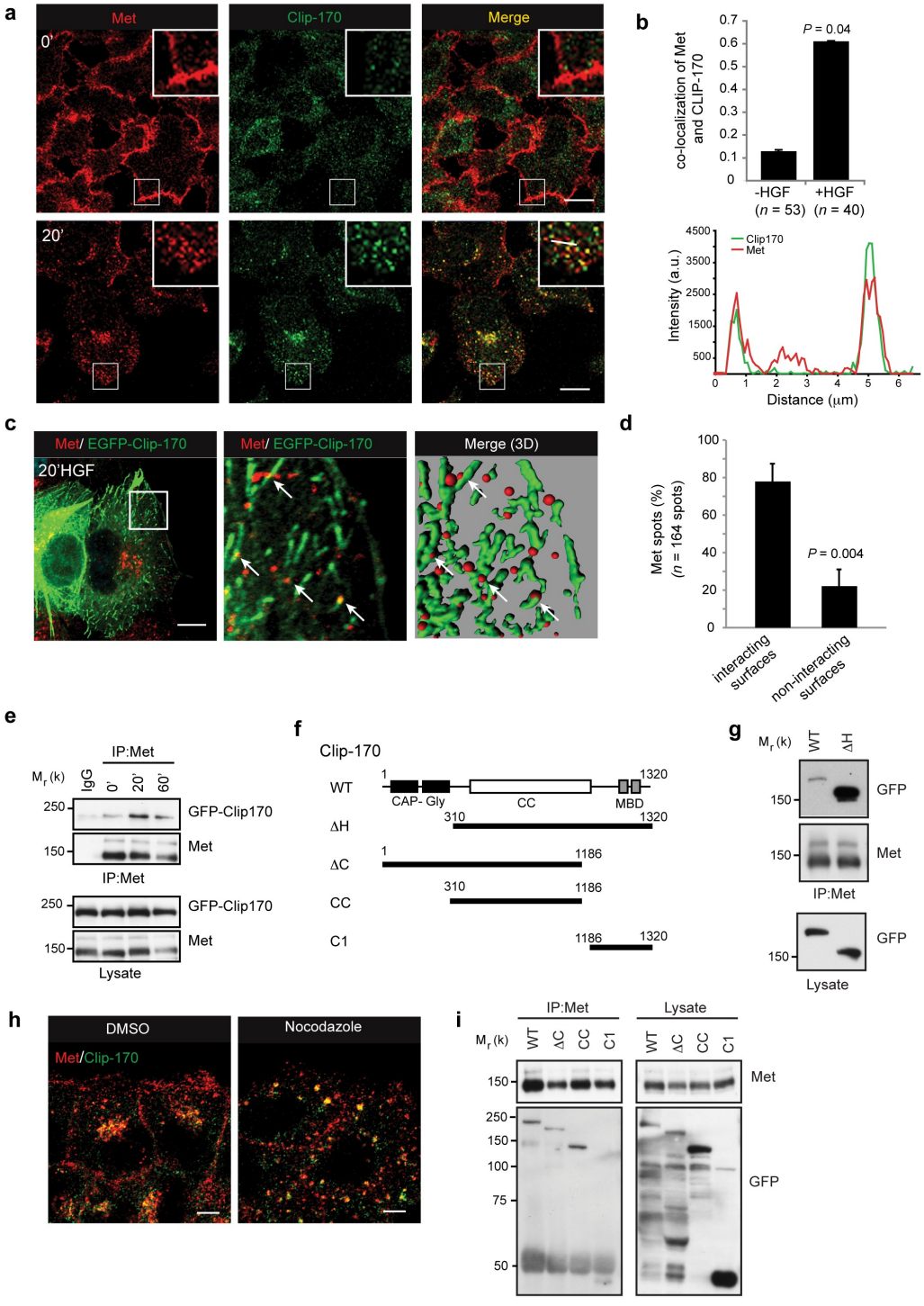
a
Met
Clip-170
Merge
0'
20'
b
co-localization of Met and CLIP-170
P = 0.04
-HGF (n = 53)
+HGF (n = 40)
Clip170
Met
Intensity (a.u.)
Distance (μm)
c
Met/ EGFP-Clip-170
20'HGF
Merge (3D)
d
Met spots (%) (n = 164 spots)
P = 0.004
interacting surfaces
non-interacting surfaces
e
IP:Met
IgG
0'
20'
60'
GFP-Clip170
Met
Lysate
f
Clip-170
WT
ΔH
ΔC
CC
C1
CAP- Gly
MBD
g
WT
ΔH
GFP
Met
IP:Met
Lysate
h
DMSO
Nocodazole
Met/Clip-170
i
IP:Met
Lysate
WT
ΔC
CC
C1
Met
GFP

**Figure 4.3. CLIP-170 regulates HGF-dependent Rab4 vesicle motility.** (**a**) Representative IF image of HeLa cells transfected with GFP-CLIP-170 and mCherry-Rab4, stimulated for 20 mins with HGF and processed for IF. GFP-CLIP-170 (green), mCherry-Rab4 (red), Met (blue). Scale bar = 10μm. ROI 1 and 2 shown at higher magnification to the right. (**b**) Representative live-cell image from SKBr-3 cells containing GFP-Rab4 and Alexa-555 HGF. Scale bar = 10μm. Inset shown at higher magnification to the right. (**c**) Montage of live-cell images taken every 4 s of SKBR-3 cells following stimulation for 20 min of HGF to track fluorescence from GFP-tubulin and mCherry-Rab4. Arrow indicates Rab4 vesicle tracking along a microtubule. (**d**) Representative images from live-cell imaging of GFP-Rab4 following 20 min of HGF treatment of cells treated with control of CLIP-170 siRNA. ROI shows inset at higher magnification with overlay of 3D tracks of Rab4 vesicles acquired for 2 min, every 4 s. (**e**) Quantification of 3D tracking of Rab4 vesicles, from movies as shown in **d** from cells treated with control or CLIP-170 siRNA and transfected with GFP-Rab4 and incubated with HGF for 20 min. Co-expression of CLIP-170 siRNA-resistant constructs were used in the lanes indicated.

## Figure 4.3

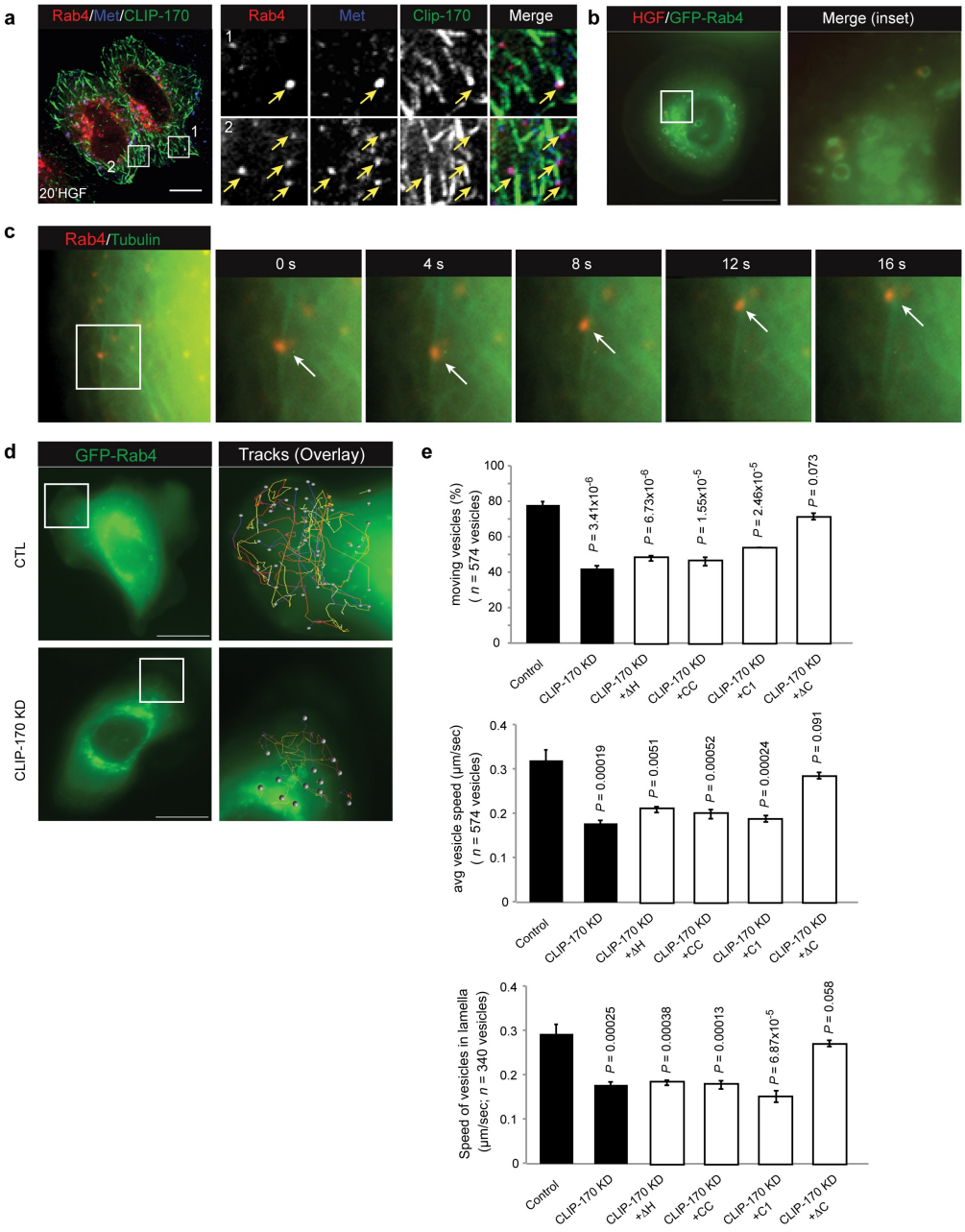
a
Rab4/Met/CLIP-170
Rab4
Met
Clip-170
Merge
20'HGF
b
HGF/GFP-Rab4
Merge (inset)
c
Rab4/Tubulin
0 s
4 s
8 s
12 s
16 s
d
GFP-Rab4
Tracks (Overlay)
CTL
CLIP-170 KD
e
moving vesicles (%) ( n = 574 vesicles)
P = 3.41x10-6
P = 6.73x10-6
P = 1.55x10-5
P = 2.46x10-5
P = 0.073
avg vesicle speed (μm/sec) ( n = 574 vesicles)
P = 0.00019
P = 0.0051
P = 0.00052
P = 0.00024
P = 0.091
Speed of vesicles in lamella (μm/sec; n = 340 vesicles)
P = 0.00025
P = 0.00038
P = 0.00013
P = 6.87x10-5
P = 0.058
Control
CLIP-170 KD
CLIP-170 KD +ΔH
CLIP-170 KD +CC
CLIP-170 KD +C1
CLIP-170 KD +ΔC

**Figure 4.4. CLIP-170 KD alters Arp3, actin and paxillin localization in response to HGF.** (**a**, **b**, **c**, **d**) Representative live-cell images of control and CLIP-170 siRNA treated cells following 20 min of HGF stimulation. Cell transfected with either (**a**) GFP-Arp3 (black) (**b**) Actin-mCherry (black) (**c**) GFP-VASP (black) or (**d**) GFP-paxillin (white). Scale bar = 10μm. (**e**,**f**) Quantification of imaging results from experiments performed as in **d**. (**e**) Mean values of percentage of cells forming nascent (black) or focal adhesions (white). (**f**) Left, mean values of number of cells forming nascent (black) or focal adhesions (white). Right, mean values of average focal adhesion size.

## Figure 4.4

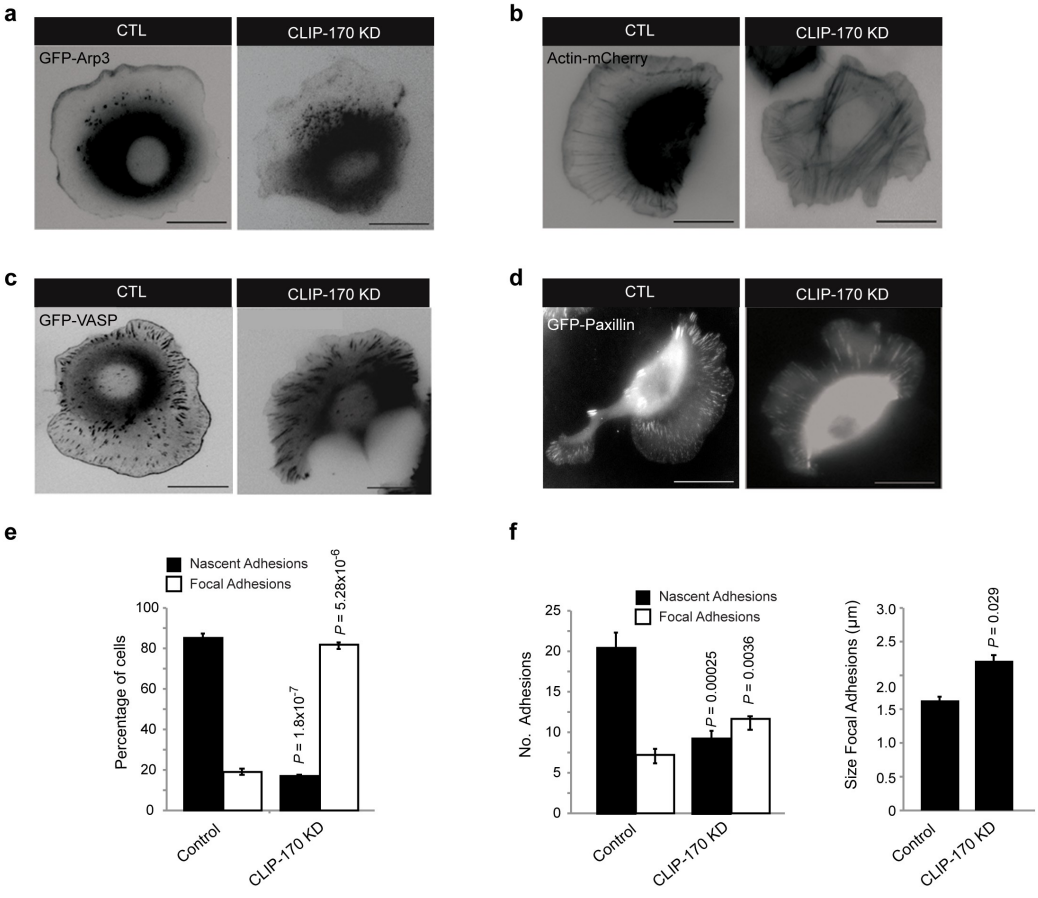
a
CTL
CLIP-170 KD
GFP-Arp3
b
CTL
CLIP-170 KD
Actin-mCherry
c
CTL
CLIP-170 KD
GFP-VASP
d
CTL
CLIP-170 KD
GFP-Paxillin
e
Nascent Adhesions
Focal Adhesions
Percentage of cells
P = 1.8x10-7
P = 5.28x10-6
Control
CLIP-170 KD
f
Nascent Adhesions
Focal Adhesions
No. Adhesions
P = 0.00025
P = 0.0036
Control
CLIP-170 KD
Size Focal Adhesions (µm)
P = 0.029
Control
CLIP-170 KD

**Figure 4.5. CLIP170 regulates HGF-mediated lamellipodial stability and cell migration.** (**a**) Representative kymographs of extending lamellipodia from control and CLIP170 KD cells after 20 min of HGF treatment. Average (**b**) Half-life, (**c**) width and length of lamellipodia quantified from live cell images, performed as shown in **a**. (**d**,**e**,**f**) Live-cell movies from cells treated with HGF overnight were tracked and quantified. (**d**) Displacement plots of 10 representative control and CLIP-170 KD cells. (**e**) Percentage of moving cells from control or CLIP-170 siRNA treated cells along with rescue CLIP-170 constructs. (**f**) Velocity of control of CLIP-170 siRNA-treated cells along with rescue CLIP-170 constructs.

## Figure 4.5

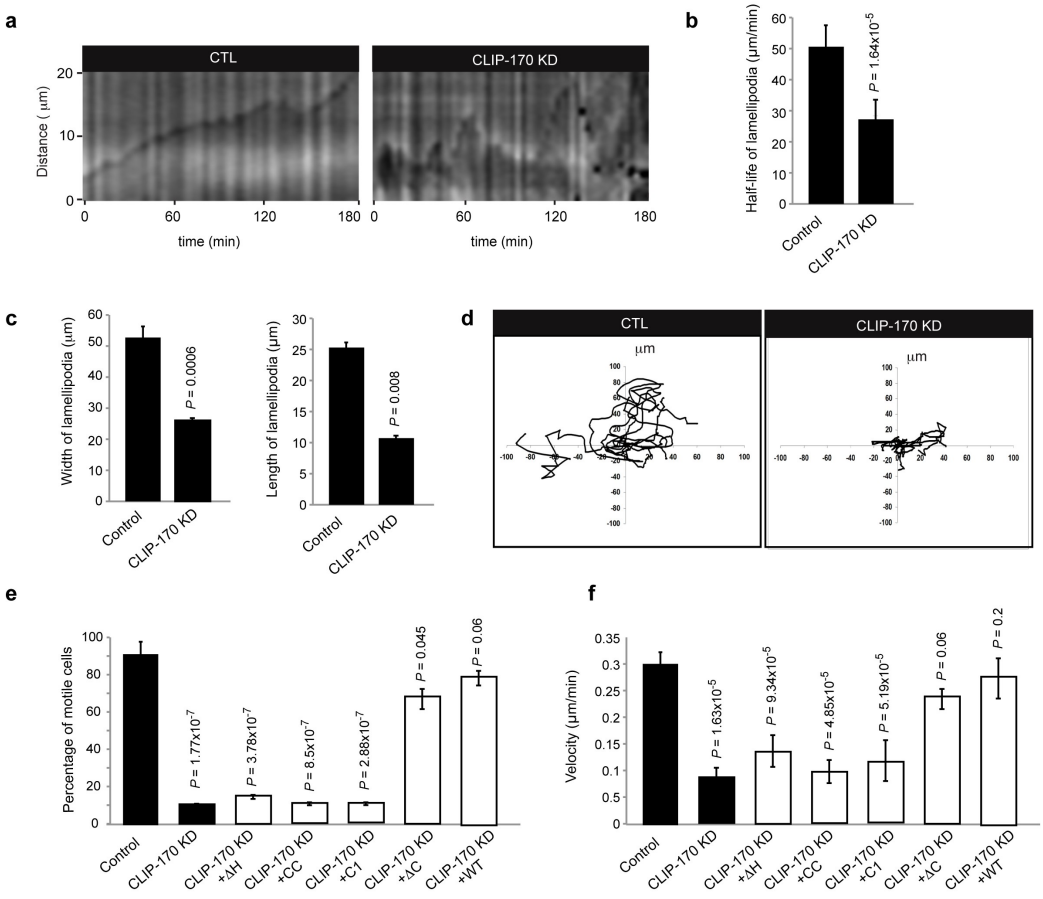
a
CTL
CLIP-170 KD
Distance ( μm)
time (min)
b
Half-life of lamellipodia (μm/min)
P = 1.64x10-5
Control
CLIP-170 KD
c
Width of lamellipodia (μm)
P = 0.0006
Length of lamellipodia (μm)
P = 0.008
d
CTL
CLIP-170 KD
μm
e
Percentage of motile cells
P = 1.77x10-7
P = 3.78x10-7
P = 8.5x10-7
P = 2.88x10-7
P = 0.045
P = 0.06
Control
CLIP-170 KD
CLIP-170 KD +ΔH
CLIP-170 KD +CC
CLIP-170 KD +C1
CLIP-170 KD +ΔC
CLIP-170 KD +WT
f
Velocity (μm/min)
P = 1.63x10-5
P = 9.34x10-5
P = 4.85x10-5
P = 5.19x10-5
P = 0.06
P = 0.2

**Figure S4.1. Microtubules and +TIPs are required for Met localization and recycling.** (**a**) Left, representative immunofluorescence (IF) images of SKBR-3 cells treated with DMSO or nocodazole stained for Met (red) and alpha-tubulin (green). Insets show higher magnification, scale bar = 10μm. Right, fluorescence intensity line scan of Met fluorescence intensity versus distance from line shown in insets to the left. (**b**,**c**,**d**) Representative IF images from cells pulsed for 5 min with HGF at 37ºC to allow internalization of Met receptors into early endosomes, then rapidly washed at 4ºC to remove unbound ligand and chased for 20 min to allow recycling. Data points are the mean ± s.e.m. from three independent experiments. (**b**) cells pre-treated with DMSO or nocodazole, (**c**) CTL and CLIP-170 knockdown cells (**d**) cells transfected with GFP-vector or EB3-GFP.

**Figure S4.1**

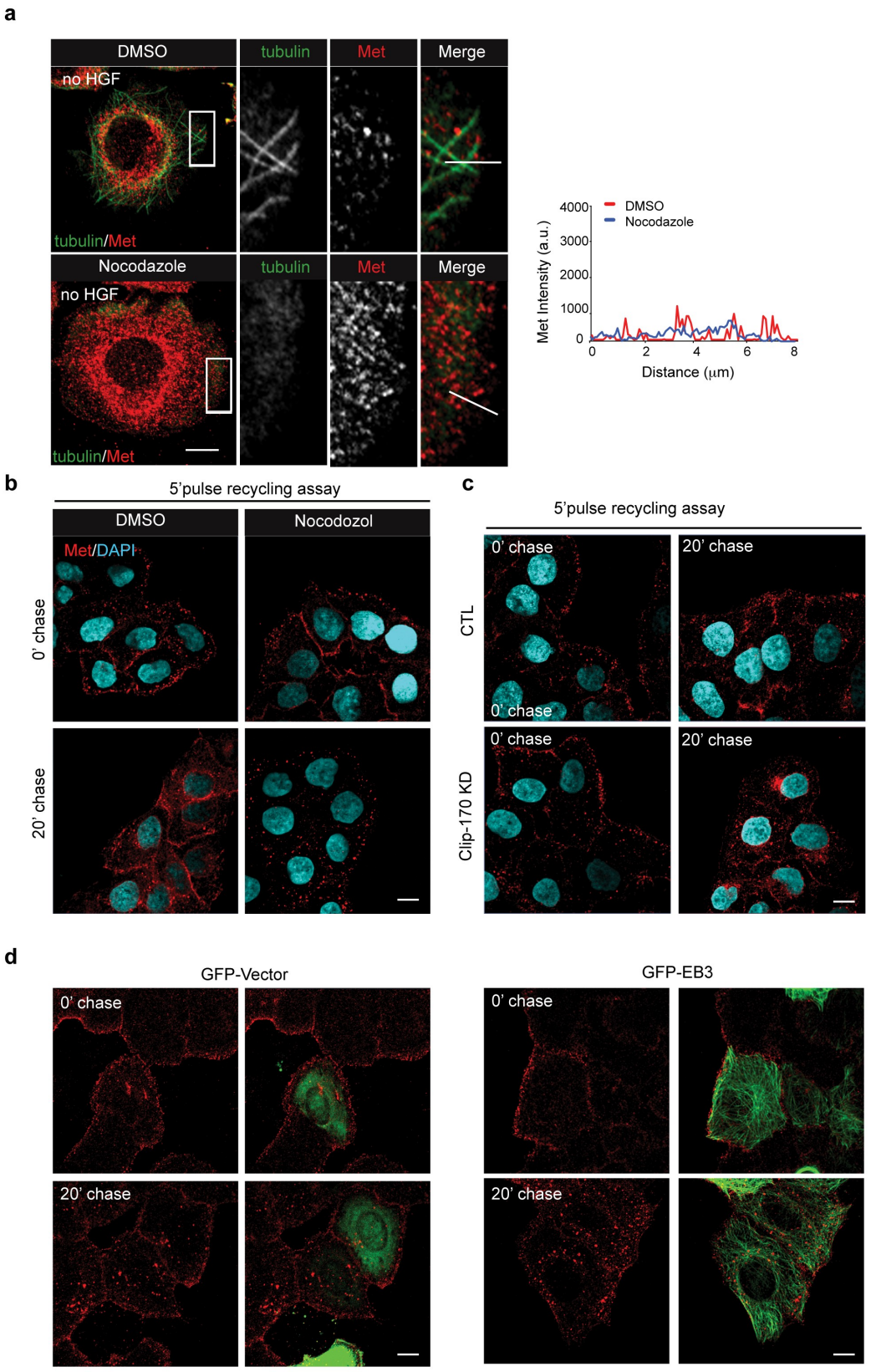
a
DMSO
tubulin
Met
Merge
no HGF
tubulin/Met
Nocodazole
tubulin
Met
Merge
no HGF
tubulin/Met
DMSO
Nocodazole
Met Intensity (a.u.)
4000
3000
2000
1000
0
0
2
4
6
8
Distance (μm)
b
5'pulse recycling assay
DMSO
Nocodozol
Met/DAPI
0' chase
20' chase
c
5'pulse recycling assay
0' chase
20' chase
CTL
Clip-170 KD
0' chase
20' chase
d
GFP-Vector
GFP-EB3
0' chase
20' chase
0' chase
20' chase

**Figure S4.2. Met and CLIP-170 localize to GFP-Rab5-positive endosomes**. (**a**)Representative IF images of HeLa cells transfected with GFP-Rab5, were pre-treated with cycloheximide then stimulated with HGF for 20 min before fixation. GFP-Rab5 (green), Met (red), CLIP-170 (blue). Scale bar = 10 μm.

**Figure S4.3. Rescue of CLIP-170 knockdown and localization of endogenous Met, actin and vinculin proteins**. (a) Representative live cell images of SKBr-3 cells transfected with GFP-Arp3, Actin-mCherry, GFP-VASP and GFP-Paxillin treated with CLIP-170 siRNA and rescued with CLIP-170 WT. Images captured after 20 min HGF-treatment. Scale bar = 10μm. (b) Representative IF of SKBr-3 cells treated with control of CLIP-170 siRNA and stimulated for 20 min with HGF followed by fixing and staining for Met (red), phallodin (green), vinculin (purple). Scale bar = 10 μm.

## Figure S4.2

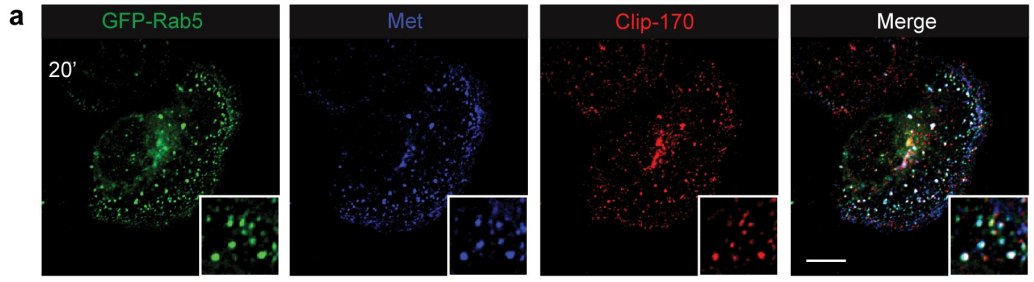


## Figure S4.3

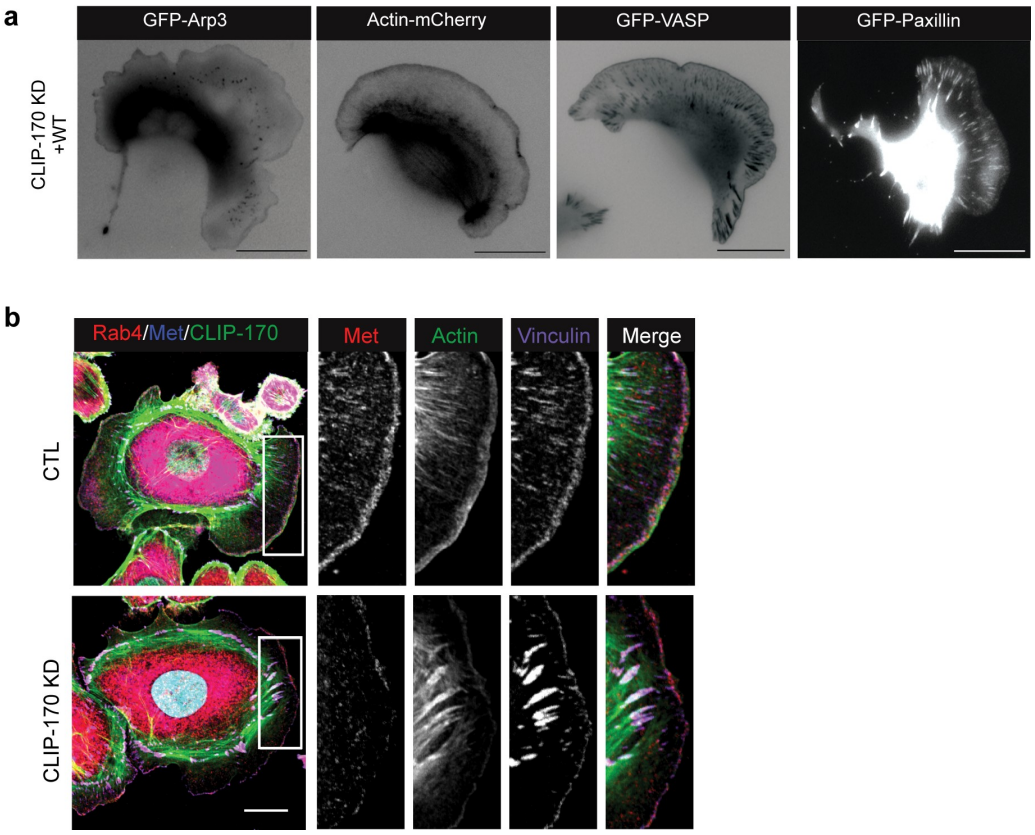

**Supplemental Movie Legends**

**Supplemental Movie 4.1. Rab4 vesicles move along MTs**. Representative movie of mCherry-Rab4 (red) and GFP-tubulin (green) in SKBr-3 cells stimulated with HGF for 20 min prior to imaging. Images were collected every 4 s for 2 min.

**Supplemental Movie 4.2. Actin Dynamics in control knockdown SKBr-3 cells.** Representative movie of Actin-mCherry in control siRNA-treated SKBr-3 cells imaged after 20 min of HGF stimulation. Images were collected every 4 s for 2 min.

**Supplemental Movie 4.3. Actin Dynamics in CLIP-170-depleted SKBr-3 cells.** Representative movie of Actin-mCherry in CLIP-170 siRNA-treated SKBr-3 cells imaged after 20 min of HGF stimulation. Images were collected every 4 s for 2 min.

**Supplemental Movie 4.4. Adhesion Dynamics in control knockdown SKBr-3 cells.** Representative movie of GFP-paxillin in control siRNA-treated SKBr-3 cells imaged after 20 min of HGF stimulation. Images were collected every 4 s for 2 min.

**Supplemental Movie 4.5. Adhesion Dynamics in CLIP-170 knockdown SKBr-3 cells.** Representative movie of GFP-paxillin in CLIP-170 siRNA-treated SKBr-3 cells imaged after 20 min of HGF stimulation. Images were collected every 4 s for 2 min.

**Supplemental Movie 4.6. Time-lapse movie of control SKBr-3 cells.** Representative movie of control siRNA-treated SKBr-3 cells imaged after 20 min of HGF stimulation. Images acquired for 350 min at 5 min intervals.

**Supplemental Movie 4.7. Time-lapse movie of CLIP-170 depleted SKBr-3 cells.** Representative movie of CLIP-170 siRNA-treated SKBr-3 cells imaged after 20 min of HGF stimulation for 16h. Playback at real-time (30 Hz). Images acquired for 350 min at 5 min intervals.

# Chapter 5

5. General Discussion

Upon commencement of this thesis, the role of ubiquitination in mediating the downregulation of RTKs had established precedence for investigating mechanisms that control trafficking of RTKs. However these findings highlighted the need to understand other steps in RTK trafficking. If degradation of RTKs in the lysosome is a critical step to turn off RTK signalling, are other steps along the endocytic pathway just as critical? If so, how? Are these mechanisms conserved among RTKs or do divergent pathways exist and how do these contribute to biological response? I have addressed these questions specifically for the Met RTK.

## 5.1. EPS15 RECRUITMENT TO RTKS

In Chapter 2, I investigated the role of an endocytic adaptor, Eps15, previously characterised downstream of the EGF RTK. I addressed the involvement of Eps15 downstream of the Met receptor and established that the mode of recruitment of Eps15 to Met is distinct from that of Eps15 recruitment to the EGFR. Downstream of Met, Eps15 recruitment requires the coiled-coil domain of Eps15 and a Grb2 binding site located in the third domain of Eps15 (Parachoniak and Park 2009, Chapter 2)[511]. This is in contrast to the EGFR, which associates with Eps15 through the c-terminal UIM domains of Eps15[259]. However in a similar manner to the EGFR[437,438], I show that Eps15 becomes tyrosine phosphorylated at Y850, and is monoubiquitinated downstream of HGF. Why might an endocytic adaptor such as Esp15, be similarly recruited to two RTKs, via distinct mechanisms of recruitment?

One hypothesis is that distinct mechanisms of recruitment may reflect variations in the trafficking routes taken by these two RTKs. Among the most prominent differences between the Met and EGF receptors is the ability of HGF to induce prolonged activation of MAPK (3-12h) compared to a more transient signal elicited by EGF (~20mins)[182,512,513]. Additionally, HGF, but not EGF, induces dorsal ruffle formation, cell scatter and branching morphogenesis in MDCK cells[149,187], even though the EGFR is highly phosphorylated and can

activate similar downstream signalling pathways to the Met RTK. Besides these biological differences, the EGFR readily co-localizes with the late endosomal/lysosomal marker LAMP-1[514], while the Met RTK does not show significant co-localization with LAMP-1 (Abella, unpublished results). Thus these RTKs may be preferentially targeted to distinct compartments in the endocytic pathway, which may contribute to the observed differences in their biological responses.

The finding that Eps15 co-immunoprecipitates with Grb2 (Parachoniak and Park, Chapter 2)[511], also suggests that other signalling adaptor molecules may associate with Eps15. To this end, a screen to identify SH2 domains that bind to a phosphopeptide surrounding Y850 in Eps15, phosphorylated downstream of Met and EGFR, was used to identify potential binding proteins (Parachoniak *et al.* unpublished; see Figure 5.1). Indeed, the SH2 domains of several kinases, including Fyn, Abl and the adaptor Gads, were detected to bind to the Y850 phosphopeptide in a dose-dependent manner, with Z-scores above 3.0 (Table 5.1). c-Abl, the cellular homologue of the Abelson murine leukaemia virus, for example, is a non-receptor tyrosine kinase that regulates cell cycle regulation, cell adhesion and stress response[515]. Abl interacts with Cbl[516] and Crk[517], two other adaptor proteins, critical for Met receptor function. The intricate Eps15 protein interaction network may thus serve to integrate multiple signalling events downstream of RTKs. Whether these Eps15 associated proteins contribute to Met receptor trafficking and/or signalling awaits further investigation.

**Figure 5.1**

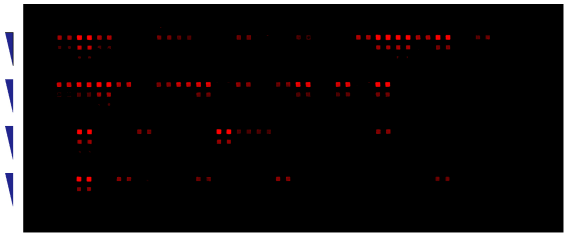

| | | | | | | | | | | | | | | | | | | | | | | | |
|---|---|---|---|---|---|---|---|---|---|---|---|---|---|---|---|---|---|---|---|---|---|---|---|
| BSA-b | ABL1 | ABL2 | APS | BLK | BLNK | BMX | BRDG1 | BRK | CRK | CRKL | CSK | FER | FES | FGR | FRK | FYN | GADS | GRAP | GRB10 | Buffer | His-ABL2 | His-PLCG1C | His-SH2D4A |
| GRB14 | GRB2 | GRB7 | HCK | HSH2D | ITK | LCK | LYN | MATK | NCK1 | NCK2 | PIK3R1_C | PIK3R1_N | PIK3R2_C | PIK3R2_N | PIK3R3_C | PIK3R3_N | PLCg1-N | PTPN11-C | PTPN11-N | Buffer | His-CBLB | His-PLCG2C | His-ZAP70-Tandem |
| PTPN6-C | RASA1_N | RASA1_C | SH2B | SH2D1A | SH2D1B | SH2D2A | SH3BP2 | SHB | SHC1 | SHC3 | SHC4 | SHD | SHE | SHF | SHIP1 | SHIP2 | SLNK | SUPT6H | SYK-C | Buffer | His-CSK | His-PLCg2N | His-PLCG1-Tandem |
| SYK-N | SRC | SRMS | TEC | TNS1 | TNS2 | TNS4 | TXK | Vav1 | VAV2 | VAV3 | YES | ZAP70-N | SOCS6 | SOCS2 | SOCS4 | SOCS7 | CIS-E | GST | BSA-b | Buffer | His-DAPP1 | His-SH2D3A | His-PTPN11-Tandem |

**Figure 5.1. Eps15 phosphopeptide SH2 array.** A. SH2 array was probed with 5μM biotinylated EPS15 peptide and detected with fluorescently labeled streptavidin. All SH2s are printed in duplicate (in the x-dimension) and at three different concentrations in the Y-dimension. At the bottom of the figure is a map of the locations of the SH2 domains. The majority of the SH2s are expressed and purified as GST -fusions, but it should be noted that on this batch of arrays, there were some experimental His-tagged SH2s (on the right hand side of the array). Only the GST tagged proteins, however, were used in the analysis. Eps15 phosphopeptide NFANFSApYPSEEDM. Array and analysis performed by Dr. Shawn Li's lab (University of Western Ontario, Canada).

| 40uM SH2 | Z-score | 10uM SH2 | Z-score | 2.5uM SH2 | Z-score |
|---|---|---|---|---|---|
| FYN | 4.6 | **ABL1** | 4.8 | **ABL1** | 4.6 |
| ABL1 | 3.2 | **GADS** | 3.6 | **GRB7** | 4.6 |
| SRC | 2.9 | **GRB7** | 3.0 | **GADS** | 3.9 |
| RASA1_N | 2.7 | **FYN** | 2.8 | **RASA1_N** | 3.6 |
| GRB7 | 2.6 | **RASA1_N** | 2.6 | **SHB** | 1.6 |
| SHB | 2.3 | **SHB** | 2.5 | **FYN** | 1.6 |
| GADS | 2.3 | **GRB10** | 1.6 | **PIK3R2_N** | 1.2 |
| GRB10 | 1.8 | **SRC** | 1.6 | **PIK3R3_N** | 1.0 |
| PIK3R3_N | 1.7 | **PIK3R3_N** | 1.4 | | |
| GRB2 | 1.3 | **LYN** | 1.2 | | |
| PIK3R1_N | 1.2 | | | | |

**Table 5.1. Summary of SH2 rankings from three concentrations.** The ranking was done using a Z-score, which normalizes the data across the slide and between slides. Correlation between array score and solution binding Kd is approximately a R-squared value of 0.8.

## 5.2. GGA3 AS A RECYCLING ADAPTOR

In Chapter 3, we uncover a role for GGA3 as a recycling adaptor for the Met receptor. Previous data had implicated GGA3 as a ubiquitin adaptor[324,518] based on direct evidence for sorting the TGN yeast protein Gap1[519] and indirect evidence in mammalian cells with the EGFR[324]. However, in yeast, only two GGA proteins exist, Gga1 and Gga2, which are only 25% identical to their human counterparts[520]. Additionally, unlike recruitment in mammalian cells, yeast Gga proteins do not require Arf for membrane localization[520], suggesting a divergence in GGA function within eukaryotic organisms.

The high degree of co-localization between GGA3 with the fast recycling marker, Rab4 indicated that functionally, GGA3 may serve as a recycling adaptor for Met. Although GGA3 was previously localized to 'peripherial region(s)' of the cell[476] and in transferrin-positive early endosomes[324], GGA3 had not formally been implicated in recycling. In addition to its subcellular localization, GGA3 has also been shown *in vitro* and through co-immunoprecipitation experiments to associate with the Rab4/Rab5 effector, Rabaptin-5[233,479,521] through its GAE domain[522]. Rabaptin-5 stabilizes Rab5-GTP in part through forming a complex with the Rab5 GEF, Rabex-5[523] and is thought to function in mediating membrane fusion events[279,281,523]. In an analogous manner, the endocytic protein, Rabenosyn-5 interacts with both Rab4 and Rab5 and has been implicated in coordinating the movement of cargo between the Rab4 and Rab5 sub-domains of early endosomes[317]. This data suggests that GGA3 could serve as an important link between cargo and Rab proteins for subsequent packaging and transport within early endosomes.

Further evidence in support of GGA3 as a recycling adaptor, comes from one report documenting the family member, GGA1 in clathrin-positive rapid recycling structures[470]. These structures were described as coated membrane tubules, positive for clathrin and GGA1, moving with rapid kinetics (average velocity of 3.73μm/s ± 0.53 S.D.)[470]. In a similar manner, we observed GGA3 in clathrin-

positive, rapidly moving structures, which we show associate with Alexa 555-labelled HGF (Parachoniak *et al.* 2011, Chapter 3)[492].

Previous reports on early recycling have focused on the constitutively cycling transferrin receptor[314]. This receptor has been linked with default recycling, which for the most part, is unregulated and highly dependent on endosome geometry[282]. However, in recent years, our knowledge of recycling pathways has been extended to include several additional mechanisms. MHC class II proteins recycle via Rab35/EHD1-positive tubules on early endosomes[524]. Theses tubules also recycle MHC class I but not the transferrin or β1 integrin receptor, although the latter proteins can also pass through early endosomes[525]. Likewise, G-protein coupled receptors, also segregate in their itineraries; the β2 adrenergic receptor is sorted through a Rab4-dependent pathway, while the delta-opioid GPCR is not recycled[318]. These studies illustrate a sophisticated and complex endocytic system whereby subsets of cargo can be shunted through different pathways. Importantly, these studies, in agreement with our data, support a mechanism by which cargo-dependent recruitment of the endocytic machinery, such as GGA3, dictates the trafficking route taken by cargo proteins.

In Chapters 3 and 4, we show that in response to HGF, the Met receptor is recycled to specific actin-rich regions of the plasma membrane, the lamellipodia. In an analogous manner, several other studies have shown spatially restricted trafficking of cell surface proteins. In ovarian cancer cells, α5β1 integrin heterodimers are recycled towards the edge of invading pseudopods[352]. During *Drosophila* oogenesis, EGFR and PVR (PDGF/VEGF) receptors localize to the cell front of border cells[487]. Trafficking of these receptors has been linked with the ability to undergo growth-factor induced cellular migration, tumor cell invasion, and guided border cell migration, in their respective systems. Importantly, these studies correlate loss of spatial trafficking with an inability to undergo biological response. Thus, by ensuring localized receptor signaling, we would predict that the target site of recycling is physiologically pertinent.

## 5.3. GGA RECRUITMENT

### 5.3.1. Proline Motifs

GGA3 was previously shown to engage cargo through VHS-DXXLL motif interactions[321]. However, due to a lack of traditional DXXLL motifs in the Met receptor, we explored other mechanisms of GGA3 recruitment to Met.

Proline motifs that are binding sites for SH3 domains are prevalent not only in signalling proteins[449,526,527], but also in trafficking proteins. The ESCRT proteins, which recognize and sort ubiquitinated cargo proteins into the internal vesicles of MVBs, for instance are a class of endocytic proteins which contain several regions rich in proline motifs[528]. The ESCRT-interacting protein, Alg-2 Interacting protein X/AIP (ALIX) contains over five proline-rich regions in its 150 amino acid c-terminus region alone; equivalent to a 33% proline content[528]. Thus our observation that GGA3 contains a proline rich region in the hinge domain is in agreement with previous reports on the function of proline interaction domains as a mechanism to build protein-protein complexes. Although SH3-domain-proline interaction affinities can differ depending on the residues surrounding the recognition motif, and also the orientation of binding[529-531], SH3-domain-proline interactions are typically of low affinity (Kd values typically range from 1 μM to approximately 10 μM)[532]. Thus the presence of multiple proline-mediated interactions may serve to enhance the stability of protein-protein interactions. We identified two proline rich motifs required for the association of GGA3 with the Crk adaptor, however, additional proline-rich motifs that may bind SH3-domain containing proteins are present within the central region of GGA3[445] (Parachoniak, unpublished observation). These include putative binding sites for Abl, p85, intersectin, cortactin and Cbl-associated protein (Sorbs1). Whether these proteins associate with GGA3 *in vivo* awaits experimental confirmation.

Surprisingly, although GGA1 was observed in rapid clathrin-structures in a manner similar to GGA3; I did not observe co-immunoprecipation of GGA1 with Met. In contrast to GGA3, GGA1 and GGA2 do not contain a proline-rich region in their hinge domain and therefore do not contain proline motifs with consensus binding sites for Crk (Parachoniak, unpublished observations). Hence, consistent

with their inability to engage with the Met receptor, GGA1 and GGA2 do not associate with Crk (Parachoniak, unpublished observation). Thus, we reason that GGA3 may play an important role in recycling of the Met receptor or other RTKs that recruit Crk, while GGA1 may serve a similar role downstream of other RTKs, through alternative mechanisms.

### 5.3.2. Association with Crk Proteins

Numerous examples document the involvement of Crk in signaling pathways located downstream of RTKs including the PDGF[533,534], Ret[535] and insulin[534] and EphB4[536] receptors. Yet no studies have examined Crk in RTK trafficking. While the precise mechanism(s) of Crk recruitment and function downstream of RTKs has not fully been determined, differences between RTK-dependent Crk function have been reported[534]. Thus, we may predict that RTKs that robustly recruit Crk, (such as through Gab1, as is the case for Met), may also efficiently recruit GGA3. Recruitment of GGA3 would then be predicted to promote recycling and hence, prolong the signaling of these RTKs.

## 5.4. ARF GTPASES IN MEMBRANE TRAFFICKING

Arf family members are small (20kDa) in size and highly similar; class I Arfs (Arf1-Arf3) are >96% identical, class II (Arf4 and Arf5) are 90% identical to each other and 80% identical to class I, and finally class III, Arf6, harbours the least similarity by sharing 64-69% homology to the other Arfs[537]. Additionally several effectors have been shown to bind to more than one Arf family member[467]. How specificity is achieved between Arf family members is still unclear, although one explanation is likely associated with the distinct intracellular distribution of each Arf[538]. In this regard, Arf1 localizes to the Golgi and regulates Golgi dynamics, whereas Arf6 does not localize to nor regulates Golgi transport and instead, localizes to the plasma membrane and endosomes[467]. Interestingly, we also observed GFP-tagged Arf3 WT and constitutively active (Q71L) proteins to partially localize with the Met receptor in response to HGF. (Parachoniak,

unpublished results Figure 5.2). Thus, Arf3 may also play a role downstream of Met. Although characterized to localize to the TGN, Arf3 has distinct properties from Arf1[539] which makes it an interesting candidate for further studies. Additionally, Arf-specific GAP and GEFs have been observed *in vivo* [540,541], which may also serve to regulate the unique intracellular function of each Arf. Of note, the Arf-GAP, GEP100 specifically activates Arf6 to promote EGF-mediated invasion of breast cancer cells[542] and is preferentially co-expressed with the EGFR in malignant primary breast ductal carcinomas[542]. This Arf-GEF binds directly to tyrosines Y1068/Y1086 of the EGFR through a PH domain[542]. Interestingly, these tyrosines also directly recruit Grb2[543]. As the Met receptor interacts with Grb2 through Y1356[119], GEP100 may also be recruited to the Met receptor, through a similar tyrosine-mediated interaction. Which Arf GEFs and GAPs function downstream of Met is currently unknown.

Besides sharing the least similarity to the other Arf family members, Arf6 is arguably the best studied amongst the Arfs. The extent to which Arf6 regulates cell surface receptors, however, is still controversial, owing perhaps to differences in cellular context[544]. Likewise, differences in expression and intracellular distribution of Arf6 have been reported for differing tissues and cell types, which may account for some of the observed discrepancies[545]. Nonetheless, a role for Arf6 has been observed downstream of HGF in modulating Rac1 activation, cell scatter and tubule development[468,483,546,547]. In agreement with these results, we find that Arf6 positively regulates Met receptor recycling (Chapter 3). Our interpretation that Met receptor recycling modulates signalling pathways downstream of HGF, could therefore be extrapolated to include pathways which induce Rac activation, cell scatter and tubule development. Additionally, previous studies have implicated Arf6 in the internalization of the β2 Adrenergic receptor[548] and leutinizing hormone receptor[549] and in recycling of the transferrin receptor[550]. Thus, we extend these finding to include the Met receptor. Which function Arf6 has on any particular cargo is likely to be governed by which Arf6 effector protein is activated. For example, Arf6 may promote internalization of cargo through its ability to activate phospholipase D at the plasma membrane[314], while activation of

phosphatidylinositol-4-phosphate 5-kinase[314] or recruitment of GGA3 (Chapter 3)[492], may promote cargo recycling from the late or early recycling compartments, respectively.

One particularly interesting example of Arf6-regulated trafficking, is the β1 integrin receptor. Arf6 regulates stimulation-dependent β1 recycling through a Rab11-dependent pathway[551] via a mechanism whereby serum stimulation activates Akt to phosphorylate ACAP1, an Arf6-GAP[552]. Notably, Arf6 is required for serum and EGF-dependent cell migration and invasion[551-553], and expression levels of Arf6 correlate with invasiveness of breast cancer cells[553]. As Arf6 has been shown to be required for the disassembly of adherens junctions[468], it appears that Arf6 can regulate several pathways required for cell migration. In line with this, we have observed changes in focal adhesion phospho-proteins downstream of HGF in the presence of Arf6 siRNA (Parachoniak *et al.*, unpublished results). Thus, Arf6 appears to be a pivotal regulator of a complex signalling circuit, which warrants further investigation.

**Figure 5.2**

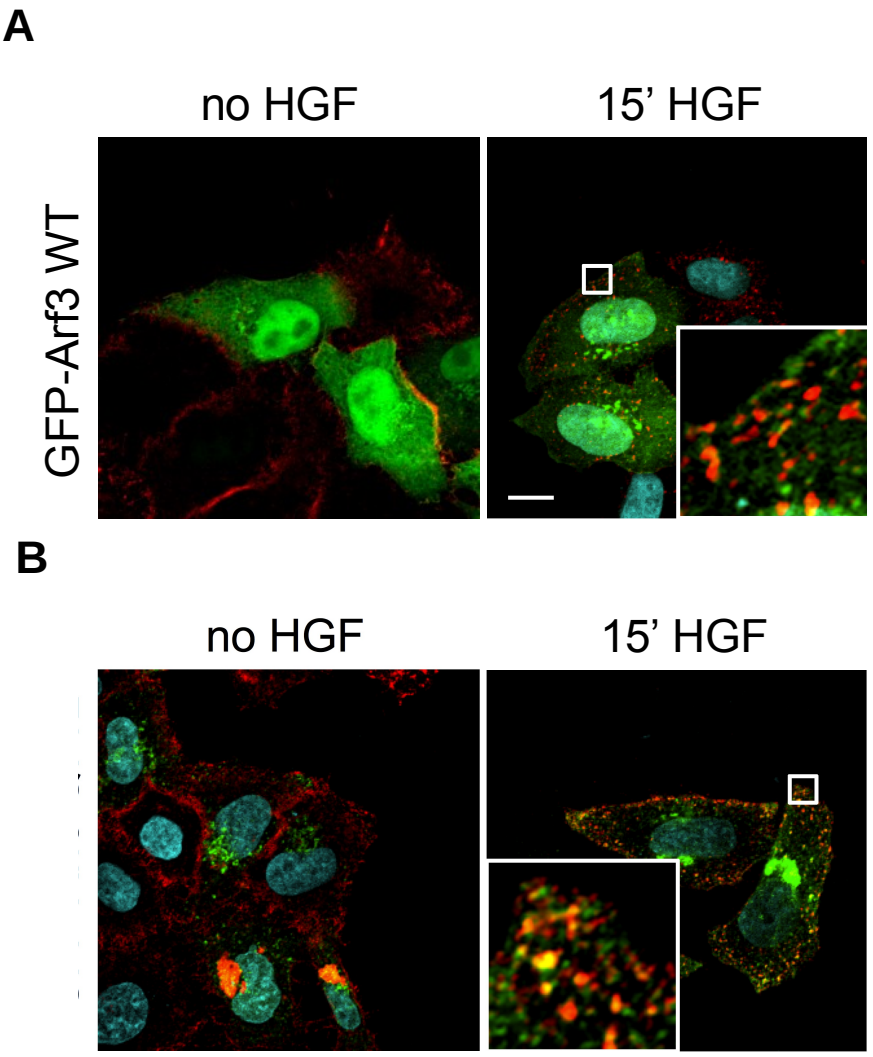


**Figure 5.2. Arf3 localizes with the Met receptor**. HeLa cells transfected with (A) GFP-Arf3 WT or (B) Arf3Q71L were CHX treated for 2hr then left untreated (no HGF) or stimulated with HGF for 15 min. Cells were then fixed and stained for Met (red). Scale bar = 10μm.

## 5.5. GGA3 IN INTEGRIN TRAFFICKING AND MIGRATION

Integrin receptors are important heterodimers involved in forming attachments to the extracellular matrix in the leading edge of cells during cell migration[554]. Importantly, the trafficking fate of integrins is now known to influence their function in cell migration[555-557].

The endocytic protein, Rab-coupling protein (RCP), has been documented to coordinate the recycling of the EGFR with α5/β1 integrin to promote cell migration in 3D[353]. In an analogous manner, it is conceivable that GGA3 may coordinate the recycling of the Met receptor with integrins. In support of this hypothesis, several studies have linked the Met receptor with integrin activation. For example, during early innate immune response, co-stimulatory signals from both α2/β1 integrin and the Met receptor contributes to mast cell activation[558]. Additionally, cells adhering to fibronectin activate Met in a ligand-independent manner[559] through an α5/β1 integrin-mediated Src/FAK pathway in breast epithelial and carcinoma cells[560]. Further evidence for crosstalk between the Met receptor and α3/β1[561], α5/β1[562] and α6/β4[563] have also been reported.

Interestingly, HGF-dependent cell invasion through collagen or matrigel is decreased in GGA3-depleted cells, and in "wound healing" assays, GGA3 knockdown severely inhibits wound closure (Parachoniak, unpublished data, Figure 5.3). These results correlate with defects in maintaining a robust lamellipodial actin network and lack of nascent focal adhesions as observed in response to HGF treatment (Parachoniak, unpublished data, Figure 5.4). During wound healing, new attachments may promote ligand-independent activation of Met and co-trafficking of Met and β1-integrin to the wound edge, through a GGA3-mediated recycling pathway. Conversely, in response to HGF integrins may lie downstream of the Met receptor. Whether such mechanisms exist awaits experimental validation.

Thus, taken together, a function for a synergistic relationship between the Met receptor and integrins merits further exploration in the context of GGA3-mediated trafficking.

**Figure 5.3**

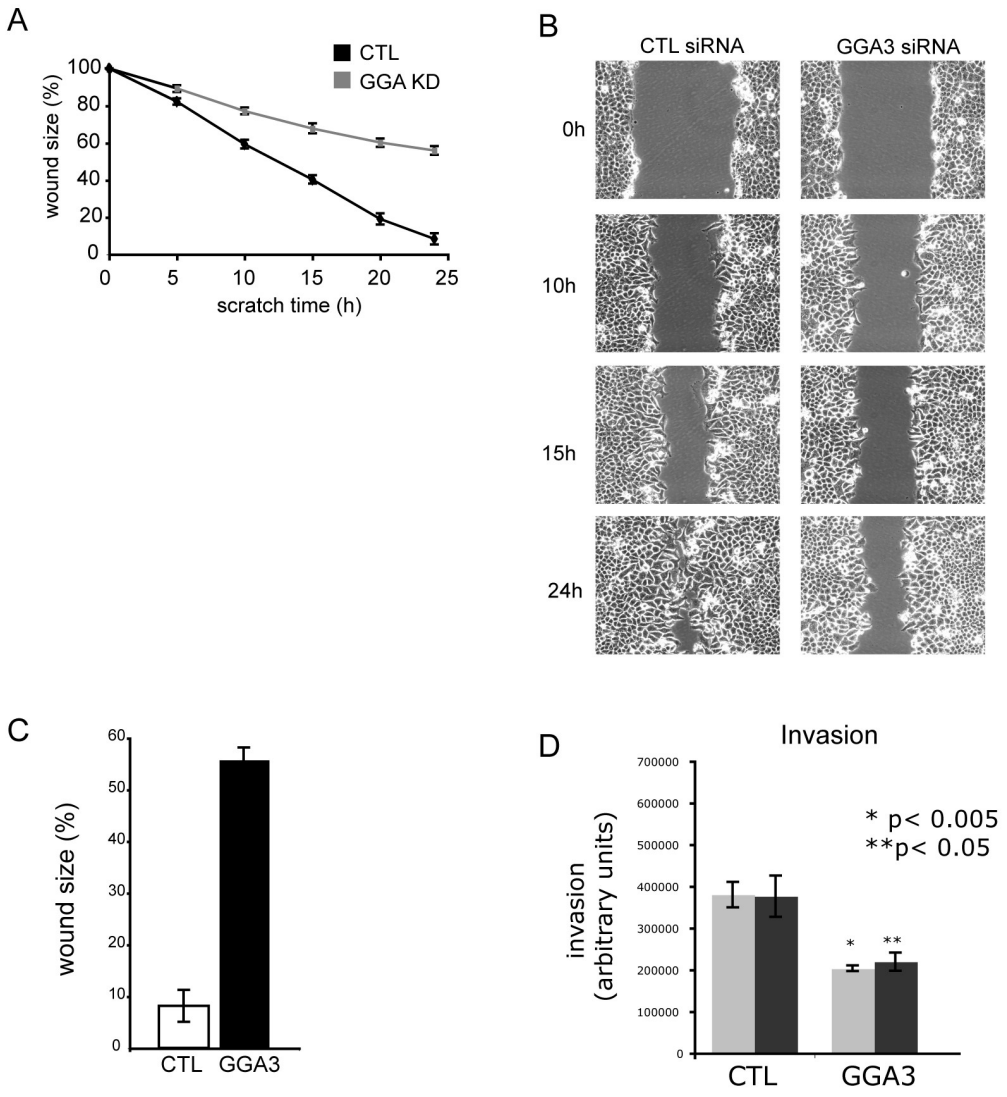


**Figure 5.3. GGA3-depletion reduces wound closure and invasion.** (A-C) HeLa cells treated with control of GGA3 siRNA were grown to confluence for 72h. A pipette tip was then used to make a scratch and phase contrast images of cells were acquired every 5 mins for 24h, using live cell imaging. Size of wound was then measured and quantified. Results shown from five separate wounds per experiment, N=3. (D) Invasion assay results from boyden chambers coated with collagen I (grey bars) or matrigel (dark grey bars) in response to HGF for HeLa cells treated with control or GGA3 siRNA.

## Figure 5.4

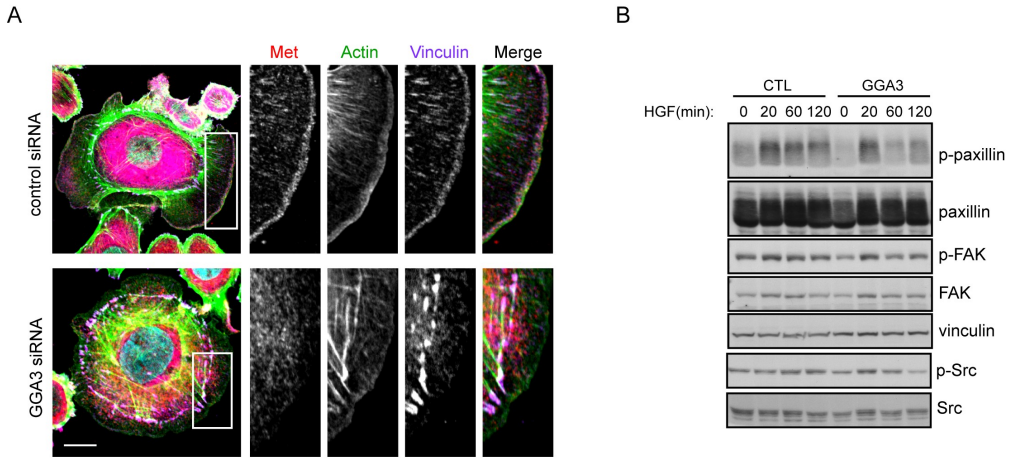


**Figure 5.4. GGA3-depletion alters lamellipodial actin and adhesion dynamics.** (A) IF images of SKBr3 cells treated with control or GGA3 siRNA were plated on collagen IV and stimulated with HGF 20 min. Cells were stained for Met (red), phallodin (green) and vinculin (purple). Scale bar = 10μm. (B) Lysates from control and GGA3 siRNA treated cells and stimulated for the indicated amounts of time with HGF and probed for phospho-paxillin (Y118), paxillin, p-FAK (Y397), FAK, p-Src (Y416) and Src.

## 5.6. DEGRADATION AS A CONSEQUENCE OF LOSS OF RECYCLING

In addition to attenuating HGF-mediated Met receptor recycling, when GGA3 is depleted from cells using siRNA, we observed a striking enhancement of Met receptor degradation. We interpreted this as a consequence of loss of recycling, whereby the Met receptor is targeted to the degradative pathway through ubiquitin-dependent mechanisms, by default. Indeed, a similar increase in degradation was recently reported for the β2 adrenergic receptor when integral components of its recycling pathway, VPS35 were depleted[564]. Importantly, the β2 adrenergic receptor also enters a Rab4 positive compartment[318,565]. Hence a degradative pathway may result as a default pathway for receptor cargo that fail to activate and recruit Rab4 for entry into the recycling tubule network. In agreement with this, expression of dominant negative Rab4 (S22N) leads to a reduction in recycling and enhanced degradation of the transferrin, LDL and EGF receptors[566].

## 5.7. MICROTUBULE TRANSPORT IN THE SPATIAL REGULATION OF SIGNALING COMPLEXES

Intracellular vesicles can move with a broad range of velocities over both short and long distances in a bidirectional manner[401,567,568]. Actin and myosin-based motors have been shown to function in the initial transport of clathrin-coated vesicles to early endosomes[569]. The mode of transportation involved in other trafficking steps, however, is less well defined, and may be dependent on the context and cargo under examination.

In Chapter 4, we show that Met receptor trafficking within Rab4-positive vesicles to the plasma membrane requires a microtubule-based transport mechanism. Furthermore, we identify the plus-end binding protein, CLIP-170 as a critical regulator of this process. Remarkably, Arf6 has recently been implicated in microtubule-based, rapid recycling of the transferrin receptor[570]. This is

consistent with our requirement for Arf6-dependent recruitment of GGA3 to a Met endosomal complex (Chapter 3).

A protein complex involving the class II PI3K, PI3K-C2α, and dynactin is also involved in mediating rapid motility of vesicles along microtubules[571]. These are similar to the structures described to involve rapid, 'gyrating' clathrin[470] which we documented in Chapter 3 and raise the possibility that this coupling may also be involved with Met.

Met endocytic trafficking has previously been characterized to be microtubule-dependent. Two isotypes of PKC, PKCε and PKCα, have been implicated in early and late trafficking steps of the Met receptor, respectively[320]. Of the two, PKCα mediates perinuclear trafficking of Met in a microtubule-dependent manner[319,320]. Although PKCε was shown to be required for ERK localization to focal adhesions in response to HGF[320], recycling of Met to lamellipodia was not addressed. Given that we observe recycling of Met to lamellipodia, it is highly likely that Met recycling is also PKCε -dependent and that the observed focal adhesion localization of ERK is a consequence of disrupted Met recycling.

Consistent with our assignment of CLIP-170 and microtubules in HGF/Met function, a role for motor proteins is starting to be appreciated in signalling. In neurons, the dynein motor complex functions in transport of Nerve growth factor (NGF) and its receptor, TrkA from the synapse to the cell body[572] during signal propagation[403]. Additionally, the JNK/MAPK binding scaffold proteins, c-jun $NH_2$-terminal kinase (JNK)–interacting proteins (JIP1/2)[573] and JIP3/SYD[573,574] link kinesins to vesicles carrying signalling molecules[403].

Microtubules and associated motor proteins have also been described downstream of other receptors. Myosin VI, an unconventional minus-end directed actin motor protein has been characterized to function in concert with its binding partner, optineurin, in the delivery of EGFR to the leading edge[575]. Loss of EGFR from the leading edge correlates with reduced EGF-directed cell migration and defective lamellipodia formation[575]. As it was not determined whether myosin VI/optineurin operates in the delivery of TGN-derived or endocytic carrier

vesicles containing EGFR *per se*, it remains unclear how myosin VI functions in anterograde trafficking. One possibility however, is that myosin VI may help deliver cargo from the actin to microtubule-based transport system[399]. In agreement with this study, we also find transport of the Met RTK to the leading edge to play an important role in cell migration. Thus, motor proteins and vesicle transport contribute to the spatial regulation of signal transduction. In regards to the Met receptor, the exact kinesins involved in Met transport remain to be investigated.

## 5.8. COMPARTMENTALIZATION OF SIGNALLING COMPLEXES

The participation of endosomes in RTK trafficking is not limited only to carrier functions. Current views now support that endosomes serve as 'multifunctional platforms' on which protein complexes can assemble[201].

Seminal work by Bergeron's group demonstrated that signalling molecules such as Shc, Grb2 and mSOS can be found within isolated endosomal fractions from liver after EGF treatment[576]. Additional studies performed in the mid 90's using dominant-negative dynamin (K44A) to inhibit EGFR internalization, demonstrated dramatic reductions in EGF-dependent MAPK and PI3K signalling[577]. Similar results have since been found for other receptors[578-580], providing evidence that internalization is required for full activation of signalling molecules/pathways downstream from receptors. Using experimental strategies to analyze post-internalization effects, the EGF, PDGF and Met receptors, have all been demonstrated to induce recruitment and activation of signalling molecules in endosomes[196,580,581]. (A summary table of signalling proteins observed in endosomal compartments can be found in reference[426]). For example, the MAPK scaffold complex, MP1-p14 assembles on late endosomes, and is required for maximal EGF-induced MAPK activation[582]. In agreement with these results, by inhibiting the duration of the Met receptor in the endocytic pathway, through GGA3 knockdown, we show that MAPK phosphorylation is significantly

attenuated compared to control cells. Given the previous findings that components of the MAPK pathway are recruited to endosomes, including MAPK scaffolding complexes such as MP1-p14, these findings support the existence of endosomally localized MAPK scaffolding complexes downstream from the Met receptor, similar to what has been reported for the EGFR.

Alternative mechanisms that affect RTK engagement with endosomal signalling complexes also exist. For example, the EGFR is internalized both through the clathrin-mediated pathway where EGFRs are preferentially recycled back to the plasma membrane and clathrin-independent mechanisms where EGFRs are targeted for degradation[583]. Importantly, this difference in EGFR trafficking is reflected in signalling, where clathrin-mediated endocytosis, and enhanced recycling, of EGFRs correlates with sustained PI3K and MAPK phosphorylation[583]. One interpretation of these results is that while initial signalling (approximately for the first 5min) occurs almost exclusively at the plasma membrane and (is not significantly altered by the mode of internalization), signalling at later times may rely more heavily on endosomes for assembly of signalling complexes. Hence, endosomal signalling would be attenuated in receptors targeted for degradation through the clathrin-independent pathway.

Additionally, delivery of receptors to recycling pathways also protects receptors against degradation and promotes targeting of receptors to specialized microdomains of the plasma membrane, such as lamellipodia, as demonstrated for the Met RTK in Chapters 3 and 4. Met receptors restricted to this region of the cell could maintain an active signalling microenvironment, required for cell migration. Indeed, other signalling receptors, most notably integrins[340,555,584,585] and the EGFR[353,575] have been observed to traffic to the lamellipodia.

In polarized MDCK cells, HGF-treatment leads to specialized apical protrusions called dorsal ruffles[586], which also become enriched in the Met receptor and both ERK1/2 isoforms[187]. Additional signalling molecules have also been reported in dorsal ruffles, downstream of other growth-factor receptors[587,588]. Thus, specialized RTK-mediated membrane signalling microenvironments may be

a common feature of RTK signalling that leads to remodelling of the actin cytoskeleton.

## 5.9. LIGAND-MEDIATED RECYCLING IN TUMORIGENESIS

Several modes of internalization exist[212,589], and it appears from my work and others that a similar complexity in recycling pathways also exists[282,314]. The presence of "cargo-selective" recycling pathways[525] provides an additional level of stringency on receptor signalling and may account for differences in receptors that activate similar downstream signalling pathways. This complexity is highlighted for the EGF receptor family.

Unlike the Met receptor, which has only one known ligand, HGF, the EGFR has seven known ligands[590] which have recently been characterized to impose different trafficking fates on the EGFR[591].

In contrast to EGF, addition of TGFα ligand results in preferential targeting of the EGFR to the recycling pathway over the lysosomal-degradative pathway[592-594]. This correlates with TGFα being a more potent mitogen than EGF ligand [594-597]. In connection with the above results, previous studies have reported differential expression of EGFR ligands in breast, bladder, ovarian and prostate tumors[598-601]. Of note, where investigated, the more highly aggressive tumours express higher levels of TGFα, and other ligands that induce EGFR recycling[591,598]. One might then predict that tumours expressing ligands that promote EGFR recycling may be heavily dependent on EGFR signalling and would be more sensitive to anti-EGFR therapies than tumours lacking these ligands. Indeed, colorectal and non-small cell lung cancer patients whose tumours express ligands that induce recycling, have been reported to respond better to gefitinib and cetuximab EGFR-treatments than those not expressing these ligands[602,603].

Although the underlying mechanism is likely to be different, akin to TGFα, HGF leads to a more sustained MAPK signal, compared to EGF[182] and also promotes recycling. Given the known role of Met in various cancers, it will be

interesting to determine the extent to which Met receptor recycling contributes to pathogenesis *in vivo*.

## 5.10. SUMMARY

During the past several years, endocytic trafficking of RTKs has emerged as a critical component of RTK biology. Throughout the course of this thesis several aspects of Met RTK trafficking have been explored. In the first part, I have characterised the role of Eps15 in Met receptor trafficking and determined that unlike the EGF RTK, the Met receptor utilizes a distinct mechanism of recruitment of Eps15. In addition, I have extended previous studies on Met receptor trafficking to include a rapid Rab4-dependent recycling pathway. These studies have led to the attribution of a recycling function to GGA3 at early endosomes. Furthermore, by characterizing the molecular pathway, we have extended the current body of knowledge on RTK trafficking.

Importantly, these studies highlight the substantial control endocytic trafficking proteins play in Met RTK signalling and cell migration. This is highlighted by the discovery that microtubules provide the physical transport of HGF-dependent Rab4+ vesicles to the leading edge and are required for the transport of Met to lamellipodia. During cell migration, localization of the Met receptor to lamellipodia provides a unique signalling microenvironment. This localization is required for maintaining proper lamellipodia and adhesion dynamics to support cell migration. The involvement of RTK endocytosis and recycling in cancer progression is still in the beginning stages of our understanding. Considering the large number of endocytic proteins, it seems likely that additional mechanisms of regulating receptor trafficking will be identified in the future. Thus by studying the pathways of how RTKs such as the Met receptor normally traffic, we may gain greater knowledge on developing better, novel therapeutic strategies.

# 6. BIBLIOGRAPHY


1. Blume-Jensen, P. & Hunter, T. Oncogenic kinase signalling. *Nature* **411**, 355-365 (2001).
2. Lemmon, M.A. & Schlessinger, J. Cell Signaling by Receptor Tyrosine Kinases. *Cell* **141**, 1117-1134 (2010).
3. Gschwind, A., Fischer, O.M. & Ullrich, A. The discovery of receptor tyrosine kinases: targets for cancer therapy. *Nat Rev Cancer* **4**, 361-370 (2004).
4. Ullrich, A.*, et al.* Human epidermal growth factor receptor cDNA sequence and aberrant expression of the amplified gene in A431 epidermoid carcinoma cells. *Nature* **309**, 418-425 (1984).
5. Carpenter, G., Lembach, K.J., Morrison, M.M. & Cohen, S. Characterization of the binding of 125-I-labeled epidermal growth factor to human fibroblasts. *Journal of Biological Chemistry* **250**, 4297-4304 (1975).
6. Carpenter, G., King, L. & Cohen, S. Epidermal growth factor stimulates phosphorylation in membrane preparations in vitro. *Nature* **276**, 409-410 (1978).
7. Schlessinger, J. Cell Signaling by Receptor Tyrosine Kinases. *Cell* **103**, 211-225 (2000).
8. Peschard, P. & Park, M. Escape from Cbl-mediated downregulation: A recurrent theme for oncogenic deregulation of receptor tyrosine kinases. *Cancer Cell* **3**, 519-523 (2003).
9. Peschard, P.*, et al.* Mutation of the c-Cbl TKB Domain Binding Site on the Met Receptor Tyrosine Kinase Converts It into a Transforming Protein. *Molecular Cell* **8**, 995-1004 (2001).
10. Wagh, P.K., Peace, B.E. & Waltz, S.E. Met[hyphen (true graphic)]Related Receptor Tyrosine Kinase Ron in Tumor Growth and Metastasis. in *Advances in Cancer Research*, Vol. Volume 100 (eds. George, F.V.W. & George, K.) 1-33 (Academic Press, 2008).
11. Birchmeier, C., Birchmeier, W., Gherardi, E. & Woude, G.F.V. Met, Metastasis, Motility and More. *Nature Reviews* **4**, 915-925 (2003).
12. Huff, J.L., Jelinek, M.A., Borgman, C.A., Lansing, T.J. & Parsons, J.T. The protooncogene c-sea encodes a transmembrane protein-tyrosine kinase related to the Met/hepatocyte growth factor/scatter factor receptor. *Proceedings of the National Academy of Sciences* **90**, 6140-6144 (1993).
13. Smith, D.R., Vogt, P.K. & Hayman, M.J. The v-sea oncogene of avian erythroblastosis retrovirus S13: another member of the protein-tyrosine kinase gene family. *Proceedings of the National Academy of Sciences* **86**, 5291-5295 (1989).
14. Weidner, K.M., Sachs, M. & Birchmeier, W. The Met receptor tyrosine kinase transduces motility, proliferation, and morphogenic signals of scatter factor/hepatocyte growth factor in epithelial cells. *The Journal of*

*Cell Biology* **121**, 145-154 (1993).
15. Zhu, H., Naujokas, M.A. & Park, M. Receptor chimeras indicate that the met tyrosine kinase mediates the motility and morphogenic responses of hepatocyte growth/scatter factor. *Cell Growth Differ* **5**, 359-366 (1994).
16. Birchmeier, C. & Gherardi, E. Developmental roles of HGF/SF and its receptor, the c-Met tyrosine kinase. *Trends in Cell Biology* **8**, 404-410 (1998).
17. Stoker, M., Gherardi, E., Perryman, M. & Gray, J. Scatter factor is a fibroblast-derived modulator of epithelial cell mobility. *Nature* **327**, 239-242 (1987).
18. Miyazawa, K.*, et al.* Molecular cloning and sequence analysis of cDNA for human hepatocyte growth factor. *Biochem Biophys Res Commun.* **163**, 967-973 (1989).
19. Zarnegar, R. & Michalopoulos, G. Purification and Biological Characterization of Human Hepatopoietin A, a Polypeptide Growth Factor for Hepatocytes. *Cancer Research* **49**, 3314-3320 (1989).
20. Nakamura, T.*, et al.* Molecular cloning and expression of human hepatocyte growth factor. *Nature* **342**, 440-443 (1989).
21. Weidner, K.M.*, et al.* Evidence for the identity of human scatter factor and human hepatocyte growth factor. *Proceedings of the National Academy of Sciences of the United States of America* **88**, 7001-7005 (1991).
22. Gherardi, E. & Stoker, M. Hepatocytes and scatter factor. *Nature* **346**, 228-228 (1990).
23. Bottaro, D.P.*, et al.* Identification of the Hepatocyte Growth Factor Receptor as the c-*met* Proto-Oncogene Product. *Science* **251**, 802-804 (1991).
24. Goldoni, S.*, et al.* Decorin is a novel antagonistic ligand of the Met receptor. *The Journal of Cell Biology* **185**, 743-754 (2009).
25. Shen, Y., Naujokas, M., Park, M. & Ireton, K. InlB-Dependent Internalization of Listeria Is Mediated by the Met Receptor Tyrosine Kinase. *Cell* **103**, 501-510 (2000).
26. Mars, W.M., Zarnegar, R. & Michalopoulos, G.K. Activation of hepatocyte growth factor by the plasminogen activators uPA and tPA. *Am J Pathol.* **143**, 949-958 (1993).
27. Gherardi, E.*, et al.* Structural basis of hepatocyte growth factor/scatter factor and MET signalling. *Proceedings of the National Academy of Sciences of the United States of America* **103**, 4046-4051 (2006).
28. JE, T. & JP., Q. The role of urokinase-type plasminogen activator in aggressive tumor cell behavior. *Cancer Metastasis Rev.* **9**, 353-367 (1990).
29. Michalopoulos, G.K. & DeFrances, M.C. Liver Regeneration. *Science* **276**, 60-66 (1997).
30. Bhowmick, N.A., Neilson, E.G. & Moses, H.L. Stromal fibroblasts in cancer initiation and progression. *Nature* **432**, 332-337 (2004).
31. Lokker, N.A.*, et al.* Structure-function analysis of hepatocyte growth factor: identification of variants that lack mitogenic activity yet retain high affinity receptor binding. *EMBO J.* **11**, 2503-2510 (1992).

32. Funakoshi, H. & Nakamura, T. Hepatocyte growth factor: from diagnosis to clinical applications. *Clinica Chimica Acta* **327**, 1-23 (2003).
33. Holmes, O.*, et al.* Insights into the Structure/Function of Hepatocyte Growth Factor/Scatter Factor from Studies with Individual Domains. *Journal of Molecular Biology* **367**, 395-408 (2007).
34. Basilico, C., Arnesano, A., Galluzzo, M., Comoglio, P.M. & Michieli, P. A High Affinity Hepatocyte Growth Factor-binding Site in the Immunoglobulin-like Region of Met. *Journal of Biological Chemistry* **283**, 21267-21277 (2008).
35. Youles, M.*, et al.* Engineering the NK1 Fragment of Hepatocyte Growth Factor/Scatter Factor as a MET Receptor Antagonist. *Journal of Molecular Biology* **377**, 616-622 (2008).
36. Raiber, E.-A.*, et al.* Novel heparin/heparan sulfate mimics as inhibitors of HGF/SF-induced MET activation. *Bioorganic & Medicinal Chemistry Letters* **17**, 6321-6325 (2007).
37. Pizarro-Cerd, J., Sousa, S. & Cossart, P. Exploitation of host cell cytoskeleton and signalling during Listeria monocytogenes entry into mammalian cells. *Comptes Rendus Biologies* **327**, 523-531 (2004).
38. Serge, M. & Pascale, C. Cytoskeleton rearrangements during Listeria infection: Clathrin and septins as new players in the game. *Cell Motility and the Cytoskeleton* **[E-pub ahead of print]**(2009).
39. Niemann, H.H. Structural insights into Met receptor activation. *European Journal of Cell Biology* **In Press, Corrected Proof**.
40. Stamos, J., Lazarus, R.A., Yao, X., Kirchhofer, D. & Wiesmann, C. Crystal structure of the HGF beta-chain in complex with the Sema domain of the Met receptor. *EMBO Journal* **23**, 2325–2335 (2004).
41. Niemann, H.H.*, et al.* Structure of the Human Receptor Tyrosine Kinase Met in Complex with the Listeria Invasion Protein InlB. *Cell* **130**, 235-246 (2007).
42. Banerjee, M.*, et al.* GW domains of the Listeria monocytogenes invasion protein InlB are required for potentiation of Met activation. *Molecular Microbiology* **52**, 257-271 (2004).
43. Jung, C.*, et al.* Involvement of CD44v6 in InlB-dependent Listeria invasion. *Molecular Microbiology* **72**, 1196-1207 (2009).
44. Orian-Rousseau, V., Chen, L., Sleeman, j.P., Herrlich, P. & Ponta, H. CD44 is required for two consecutive steps in HGF/c-Met signaling. *Genes and Development* **16**, 3074-3086 (2002).
45. Schmidt, L.*, et al.* Germline and somatic mutations in the tyrosine kinase domain of the MET proto-oncogene in papillary renal carcinomas. *Nat Genet* **16**, 68-73 (1997).
46. Uehara, Y.*, et al.* Placental defect and embryonic lethality in mice lacking hepatocyte growth factor/scatter factor. *Nature* **373**, 702-705 (1995).
47. Bladt, F., Riethmacher, D., Isenmann, S., Aguzzi, A. & Birchmeier, C. Essential role for the c-met receptor in the migration of myogenic precursor cells into the limb bud. *Nature* **376**, 768-771 (1995).
48. Dietrich, S.*, et al.* The role of SF/HGF and c-Met in the development of

skeletal muscle. *Development* **126**, 1621-1629 (1999).
49. Maina, F. & Klein, R. Hepatocyte growth factor, a versatile signal for developing neurons. *Nat Neurosci* **2**, 213-217 (1999).
50. Yang, X. & Park, M. xpression of the hepatocyte growth factor/scatter factor receptor tyrosine kinase is localized to epithelia in the adult mouse. *Laboratory Investigation* **73**, 483-491 (1995).
51. Borowiak, M.*, et al.* Met provides essential signals for liver regeneration. *Proc. Natl. Acad. Sci. U.S.A.* **101**, 10608-10613 (2004).
52. Huh, C.-G.*, et al.* Hepatocyte growth factor/c-met signaling pathway is required for efficient liver regeneration and repair. *Proc. Natl. Acad. Sci. U.S.A.* **101**, 4477-4482 (2004).
53. Nakamura, T.*, et al.* Myocardial protection from ischemia/reperfusion injury by endogenous and exogenous HGF. *J Clin Invest* **106**, 1511-1519 (2000).
54. Kawaida, K., Matsumoto, K., Shimazu, H. & Nakamura, T. Hepatocyte growth factor prevents acute renal failure and accelerates renal regeneration in mice. *Proceedings of the National Academy of Sciences* **91**, 4357-4361 (1994).
55. Homsia, E., Janinoa, P., Amanob, M. & Camara, N.O.S. Endogenous Hepatocyte Growth Factor Attenuates Inflammatory Response in Glycerol-Induced Acute Kidney Injury. *American Journal of Nephrology* **29**, 283-291 (2009).
56. RABKIN, R.*, et al.* Hepatocyte Growth Factor Receptor in Acute Tubular Necrosis. *Journal of the American Society of Nephrology* **12**, 531-540 (2001).
57. Roos, F., Ryan, A.M., Chamow, S.M., Bennett, G.L. & Schwall, R.H. Induction of liver growth in normal mice by infusion of hepatocyte growth factor/scatter factor. *American Journal of Physiology - Gastrointestinal and Liver Physiology* **268**, G380-G386 (1995).
58. Cooper, C.S.*, et al.* Molecular cloning of a new transforming gene from a chemically transformed human cell line. *Nature* **311**, 29-33 (1984).
59. Park, M.*, et al.* Mechanism of *met* Oncogene Activation. *Cell* **45**, 895-904 (1986).
60. Park, M.*, et al.* Sequence of MET protooncogene cDNA has features characteristic of the tyrosine kinase family of growth-factor receptors. *Proceedings of the National Academy of Sciences* **84**, 6379-6383 (1987).
61. M, D.*, et al.* The human met oncogene is related to the tyrosine kinase oncogenes. *Nature* **318**, 385-388 (1985).
62. Rodrigues, G.A. & Park, M. Dimerization mediated through a leucine zipper activates the oncogenic potential of the met receptor tyrosine kinase. *Mol. Cell. Biol.* **13**, 6711-6722 (1993).
63. Rong, S., Segal, S., Anver, M., Resau, J.H. & Vande Woude, G.F. Invasiveness and metastasis of NIH 3T3 cells induced by Met-hepatocyte growth factor/scatter factor autocrine stimulation. *Proceedings of the National Academy of Sciences* **91**, 4731-4735 (1994).
64. Abounader, R.*, et al.* In vivo targeting of SF/HGF and c-met expression

via U1snRNA/ribozymes inhibits glioma growth and angiogenesis and promotes apoptosis. *The FASEB Journal* **16**, 108-110 (2002).
65. Furge, K.A.*, et al.* Suppression of Ras-mediated tumorigenicity and metastasis through inhibition of the Met receptor tyrosine kinase. *Proceedings of the National Academy of Sciences* **98**, 10722-10727 (2001).
66. Ivan, M., Bond, J.A., Prat, M., Comoglio, P.M. & Wynford-Thomas, D. Activated ras and ret oncogenes induce over-expression of c-met (hepatocyte growth factor receptor) in human thyroid epithelial cells. *Oncogene* **14**, 2417-2423 (1997).
67. Takayama, H.*, et al.* Diverse tumorigenesis associated with aberrant development in mice overexpressing hepatocyte growth factor/scatter‚Äâfactor. *Proceedings of the National Academy of Sciences* **94**, 701-706 (1997).
68. Ponzo, M.G.*, et al.* Met induces mammary tumors with diverse histologies and is associated with poor outcome and human basal breast cancer. *Proceedings of the National Academy of Sciences* **106**, 12903-12908 (2009).
69. Graveel, C.R.*, et al.* Met induces diverse mammary carcinomas in mice and is associated with human basal breast cancer. *Proceedings of the National Academy of Sciences* **106**, 12909-12914 (2009).
70. Ponzo, M.G.*, et al.* Met induces mammary tumors with diverse histologies and is associated with poor outcome and human basal breast cancer. *Proc. Natl Acad. Sci. USA*, E-pub (2009).
71. Lengyel, E.*, et al.* C-Met overexpression in node-positive breast cancer identifies patients with poor clinical outcome independent of Her2/neu. *International Journal of Cancer* **113**, 678-682 (2005).
72. Ghoussoub, R.A.D.*, et al.* Expression of c-met is a strong independent prognostic factor in breast carcinoma. *Cancer* **82**, 1513-1520 (1998).
73. Jeffers, M.*, et al.* Activating mutations for the Met tyrosine kinase receptor in human†cancer. *Proceedings of the National Academy of Sciences* **94**, 11445-11450 (1997).
74. Park, W.S.*, et al.* Somatic Mutations in the Kinase Domain of the Met/Hepatocyte Growth Factor Receptor Gene in Childhood Hepatocellular Carcinomas. *Cancer Res* **59**, 307-310 (1999).
75. Schmidt, L.*, et al.* Novel mutations of the MET proto-oncogene in papillary renal carcinomas. *Oncogene* **18**, 2343-2350 (1999).
76. Lee, J.-H.*, et al.* A novel germ line juxtamembrane Met mutation in human gastric cancer. *Oncogene* **19**, 4947-4953 (2000).
77. Renzo, M.F.D.*, et al.* Somatic mutations of the MET oncogene are selected during metastatic spread of human HNSC carcinomas. *Oncogene* **19**, 1547-1555 (2000).
78. Tengs, T.*, et al.* A transforming MET mutation discovered in non-small cell lung cancer using microarray-based resequencing. *Cancer Letters* **239**, 227-233 (2006).
79. Jeffers, M.*, et al.* Activating mutations for the Met tyrosine kinase receptor

in human cancer. *PNAS* **94**, 11445-11450 (1997).
80. Jeffers, M.*, et al.* The mutationally activated Met receptor mediates motility and metastasis. *Proceedings of the National Academy of Sciences* **95**, 14417-14422 (1998).
81. Rong, S.*, et al.* Met Expression and Sarcoma Tumorigenicity. *Cancer Research* **53**, 5355-5360 (1993).
82. T, F.*, et al.* Coexpression of HGF and c-Met/HGF receptor in human bone and soft tissue tumors. *Pathol Int.* **48**, 757-762 (1998).
83. Arihiro, K. & Inai, K. Expression of CD31, Met/hepatocyte growth factor receptor and bone morphogenetic protein in bone metastasis of osteosarcoma. *Pathology International* **51**, 100-106 (2001).
84. Patane, S.*, et al.* MET Overexpression Turns Human Primary Osteoblasts into Osteosarcomas. *Cancer Research* **66**, 4750-4757 (2006).
85. Wu, C.W.*, et al.* Hepatocyte growth factor and Met/HGF receptors in patients with gastric adenocarcinoma. *Oncol Rep* **5**, 817-822 (1998).
86. Nakajima, M.*, et al.* The prognostic significance of amplification and overexpression of c-met and c-erb B-2 in human gastric carcinomas. *Cancer* **85**, 1894-1902 (1999).
87. Wang, J.-Y.*, et al.* Alterations of APC, c-met, and p53 genes in tumor tissue and serum of patients with gastric cancers. *Journal of Surgical Research* **120**, 242-248 (2004).
88. Inoue, T.*, et al.* Activation of c-Met (hepatocyte growth factor receptor) in human gastric cancer tissue. *Cancer Science* **95**, 803-809 (2004).
89. Wullich, B., Muller, H.-W., Fischer, U., Zang, K.D. & Meese, E. Amplified met gene linked to double minutes in human glioblastoma. *Eur J Cancer* **29A**, 1991-1993 (1993).
90. Arrieta, O.*, et al.* Hepatocyte growth factor is associated with poor prognosis of malignant gliomas and is a predictor for recurrence of meningioma. *Cancer* **94**, 3210-3218 (2002).
91. Koochekpour, S.*, et al.* Met and Hepatocyte Growth Factor/Scatter Factor Expression in Human Gliomas. *Cancer Research* **57**, 5391-5398 (1997).
92. Lamszus, K., Laterra, J., Westphal, M. & Rosen, E.M. Scatter factor/hepatocyte growth factor (SF/HGF) content and function in human gliomas. *International Journal of Developmental Neuroscience* **17**, 517-530 (1999).
93. Wondergem, R., Ecay, T.W., Mahieu, F., Owsianik, G. & Nilius, B. HGF/SF and menthol increase human glioblastoma cell calcium and migration. *Biochemical and Biophysical Research Communications* **372**, 210-215 (2008).
94. Ma, P.C.*, et al.* Functional Expression and Mutations of c-Met and Its Therapeutic Inhibition with SU11274 and Small Interfering RNA in Non‚ÄìSmall Cell Lung Cancer. *Cancer Research* **65**, 1479-1488 (2005).
95. Liang, J.*, et al.* Expression of scatter factor and c-met receptor in benign and malignant breast tissue. *Cancer* **79**, 749-760 (1997).
96. Edakuni, G., Sasatomi, E., Satoh, T., Tokunaga, O. & Miyazaki, K. Expression of the hepatocyte growth factor/c-Met pathway is increased at

the cancer front in breast carcinoma. *Pathology International* **51**, 172-178 (2001).
97. Jin , L.*, et al.* Expression of scatter factor and c-met receptor in benign and malignant breast tissue. *Cancer* **79**, 749-760 (1997).
98. Kang, J.Y.*, et al.* Tissue Microarray Analysis of Hepatocyte Growth Factor/Met Pathway Components Reveals a Role for Met, Matriptase, and Hepatocyte Growth Factor Activator Inhibitor 1 in the Progression of Node-negative Breast Cancer. *Cancer Research* **63**, 1101-1105 (2003).
99. Tuck, A.B., Park, M., Sterns, E.E., Boag, A. & Elliott, B.E. Coexpression of hepatocyte growth factor and receptor (Met) in human breast carcinoma. *Am J Pathol.* **148**, 225-232 (1996).
100. Yamashita, J.-i.*, et al.* Immunoreactive Hepatocyte Growth Factor Is a Strong and Independent Predictor of Recurrence and Survival in Human Breast Cancer. *Cancer Research* **54**, 1630-1633 (1994).
101. Lindemann, K.*, et al.* Differential expression of c-Met, its ligand HGF/SF and HER2/neu in DCIS and adjacent normal breast tissue. *Histopathology* **51**, 54-62 (2007).
102. R, F.*, et al.* The Met/HGF receptor is over-expressed in human osteosarcomas and is activated by either a paracrine or an autocrine circuit. *Oncogene* **10**, 739-749 (1995).
103. Sheen-Chen, S.-M., Liu, Y.-W., Eng, H.-L. & Chou, F.-F. Serum Levels of Hepatocyte Growth Factor in Patients with Breast Cancer. *Cancer Epidemiology Biomarkers & Prevention* **14**, 715-717 (2005).
104. Eichbaum, M.*, et al.* Serum levels of hepatocyte growth factor/scatter factor in patients with liver metastases from breast cancer. *Tumour Biol.* **28**, 36-44 (2007).
105. Camp, R.L., Rimm, E.B. & Rimm, D.L. Met expression is associated with poor outcome in patients with axillary lymph node negative breast carcinoma. *Cancer* **86**, 2259-2265 (1999).
106. Kong-Beltran, M.*, et al.* Somatic Mutations Lead to an Oncogenic Deletion of Met in Lung Cancer. *Cancer Res* **66**, 283-289 (2006).
107. Asaoka, Y.*, et al.* Gastric cancer cell line Hs746T harbors a splice site mutation of c-Met causing juxtamembrane domain deletion. *Biochemical and Biophysical Research Communications* **394**, 1042-1046 (2010).
108. Abella, J.V.*, et al.* Met/Hepatocyte Growth Factor Receptor Ubiquitination Suppresses Transformation and Is Required for Hrs Phosphorylation. *Mol. Cell. Biol.* **25**, 9632-9645 (2005).
109. Peschard, P. & Park, M. From Tpr-Met to Met, tumorigenesis and tubes. *Oncogene* **26**, 1276-1285 (2007).
110. Maroun, C.R.*, et al.* The Gab1 PH Domain Is Required for Localization of Gab1 at Sites of Cell-Cell Contact and Epithelial Morphogenesis Downstream from the Met Receptor Tyrosine Kinase. *Mol. Cell. Biol.* **19**, 1784-1799 (1999).
111. Schlessinger, J. & Ullrich, A. Growth factor signaling by receptor tyrosine kinases. *Neuron* **9**, 383-391 (1992).
112. Schiering, N.*, et al.* Crystal structure of the tyrosine kinase domain of the

hepatocyte growth factor receptor c-Met and its complex with the microbial alkaloid K-252a. *Proceedings of the National Academy of Sciences of the United States of America* **100**, 12654-12659 (2003).
113. Kong-Beltran, M., Stamos, J. & Wickramasinghe, D. The Sema domain of Met is necessary for receptor dimerization and activation. *Cancer Cell* **6**, 75-84 (2004).
114. Naldini, L.*, et al.* The tyrosine kinase encoded by the MET proto-oncogene is activated by autophosphorylation. *Mol. Cell. Biol.* **11**, 1793-1803 (1991).
115. Ferracini, R., Longati, P., Naldini, L., Vigna, E. & Comoglio, P.M. Identification of the major autophosphorylation site of the Met/hepatocyte growth factor receptor tyrosine kinase. *Journal of Biological Chemistry* **266**, 19558-19564 (1991).
116. Peschard, P., Ishiyama, N., Lin, T., Lipkowitz, S. & Park, M. A Conserved DpYR Motif in the Juxtamembrane Domain of the MET Receptor Family Forms an Atypical c-Cbl/Cbl-b Tyrosine Kinase Binding Domain Site Required for Suppression of Oncogenic Activation. *Journal of Biological Chemistry* **279**, 29565-29571 (2004).
117. Pawson, T. Protein modules and signalling networks. *Nature* **373**, 573-580 (1995).
118. Bork, P. & margolis, B. A phosphotyrosine interaction domain. *Cell* **80**, 693-694 (1995).
119. Ponzetto, C.*, et al.* A Multifunctional Docking Site Mediates Signaling and Transformation by the Hepatocyte Growth Factor.Scatter Factor Receptor Family. *Cell* **77**, 261-271 (1994).
120. Komada, M. & Kitamura, N. The cell dissociation and motility triggered by scatter factor/hepatocyte growth factor are mediated through the cytoplasmic domain of the c-Met receptor. *Oncogene* **8**, 2381-2390 (1993).
121. Saucier, C.*, et al.* Use of signal specific receptor tyrosine kinase oncoproteins reveals that pathways downstream from Grb2 or Shc are sufficient for cell transformation and metastasis. *Oncogene* **21**, 1800-1811 (2002).
122. Maina, F.*, et al.* Uncoupling of Grb2 from the Met Receptor In Vivo Reveals Complex Roles in Muscle Development. *Cell* **87**, 531-542 (1996).
123. Chol, K.-Y., Satterberg, B., Lyons, D.M. & Elion, E.A. Ste5 tethers multiple protein kinases in the MAP kinase cascade required for mating in S. cerevisiae. *Cell* **78**, 499-512 (1994).
124. Kornau, H., Schenker, L., Kennedy, M. & Seeburg, P. Domain interaction between NMDA receptor subunits and the postsynaptic density protein PSD-95. *Science* **269**, 1737-1740 (1995).
125. Printen, J.A. & Sprague-Jr., G.F. Protein-Protein Interactions in the Yeast Pheromone Response Pathway: Ste5p Interacts With All Members of the MAP Kinase Cascade. *Genetics* **138**, 609-619 (1994).
126. Therrien, M., Michaud, N.R., Rubin, G.M. & Morrison, D.K. KSR modulates signal propagation within the MAPK cascade. *Genes and*

*Development* **10**, 2684-2695 (1996).
127. Tsunoda, S.*, et al.* A multivalent PDZ-domain protein assembles signalling complexes in a G-protein-coupled cascade. *Nature* **388**, 243-249 (1997).
128. Zhang, W., Sloan-Lancaster, J., Kitchen, J., Trible, R.P. & Samelson, L.E. LAT: The ZAP-70 Tyrosine Kinase Substrate that Links T Cell Receptor to Cellular Activation. *Cell* **92**, 83-92 (1998).
129. Good, M.C., Zalatan, J.G. & Lim, W.A. Scaffold Proteins: Hubs for Controlling the Flow of Cellular Information. *Science* **332**, 680-686 (2011).
130. Zhu, H., Naujokas, M.A., Fixman, E.D., Torossian, K. & Park, M. Tyrosine 1356 in the carboxyl-terminal tail of the HGF/SF receptor is essential for the transduction of signals for cell motility and morphogenesis. *Journal of Biological Chemistry* **269**, 29943-29948 (1994).
131. Fixman, E.D., Naujokas, M.A., Rodrigues, G.A., Moran, M.F. & Park, M. Efficient cell transformation by the Tpr-Met oncoprotein is dependent upon tyrosine 489 in the carboxy-terminus. *Oncogene* **10**, 237-249 (1995).
132. Pelicci, G.*, et al.* The motogenic and mitogenic responses to HGF are amplified by the Shc adaptor protein. *Oncogene* **10**, 1631-1638 (1995).
133. Fixman, E.D., Fournier, T.M., Kamikura, D.M., Naujokas, M.A. & Park, M. Pathways Downstream of Shc and Grb2 Are Required for Cell Transformation by the Tpr-Met Oncoprotein. *Journal of Biological Chemistry* **271**, 13116-13122 (1996).
134. Koch, A., Mancini, A., El Bounkari, O. & Tamura, T. The SH2-domian-containing inositol 5-phosphatase (SHIP)-2 binds to c-Met directly via tyrosine residue 1356 and involves hepatocyte growth factor (HGF)-induced lamellipodium formation, cell scattering and cell spreading. *Oncogene* **24**, 3436-3447 (2005).
135. Stefan, M.*, et al.* Src Homology 2-containing Inositol 5-Phosphatase 1 Binds to the Multifunctional Docking Site of c-Met and Potentiates Hepatocyte Growth Factor-induced Branching Tubulogenesis. *Journal of Biological Chemistry* **276**, 3017-3023 (2001).
136. Weidner, K.M.*, et al.* Interaction between Gab1 and the c-Met receptor tyrosine kinase is responsible for epithelial morphogenesis. *Nature* **384**, 173-176 (1996).
137. Nguyen, L.*, et al.* Association of the Multisubstrate Docking Protein Gab1 with the Hepatocyte Growth Factor Receptor Requires a Functional Grb2 Binding Site Involving Tyrosine 1356. *Journal of Biological Chemistry* **272**, 20811-20819 (1997).
138. Lock, L.S., Royal, I., Naujokas, M.A. & Park, M. Identification of an Atypical Grb2 Carboxyl-terminal SH3 Domain Binding Site in Gab Docking Proteins Reveals Grb2-dependent and -independent Recruitment of Gab1 to Receptor Tyrosine Kinases. *Journal of Biological Chemistry* **275**, 31536-31545 (2000).
139. Fixman, E.D.*, et al.* Efficient Cellular Transformation by the Met Oncoprotein Requires a Functional Grb2 Binding Site and Correlates with

Phosphorylation of the Grb2-associated Proteins, Cbl and Gab1. *Journal of Biological Chemistry* **272**, 20167-20172 (1997).
140. Kholodenko, B.N., Hoek, J.B. & Westerhoff, H.V. Why cytoplasmic signalling proteins should be recruited to cell membranes. *Trends in Cell Biology* **10**, 173-178 (2000).
141. Wang, J.*, et al.* Grb10, a Positive, Stimulatory Signaling Adapter in Platelet-Derived Growth Factor BB-, Insulin-Like Growth Factor I-, and Insulin-Mediated Mitogenesis. *Mol. Cell. Biol.* **19**, 6217-6228 (1999).
142. Boccaccio, C.*, et al.* Induction of epithelial tubules by growth factor HGF depends on the STAT pathway. *Nature* **391**, 285-288 (1998).
143. Chen, S.-Y. & Chen, H.-C. Direct Interaction of Focal Adhesion Kinase (FAK) with Met Is Required for FAK To Promote Hepatocyte Growth Factor-Induced Cell Invasion. *Mol. Cell. Biol.* **26**, 5155-5167 (2006).
144. Schaaf, C.P.*, et al.* Novel interaction partners of the TPR/MET tyrosine kinase. *The FASEB Journal* (2004).
145. Lai, A.Z., Abella, J.V. & Park, M. Crosstalk in Met receptor oncogenesis. *Trends in Cell Biology* **19**, 542-551 (2009).
146. Lock, L.S., Frigault, M.M., Saucier, C. & Park, M. Grb2-independent Recruitment of Gab1 Requires the C-terminal Lobe and Structural Integrity of the Met Receptor Kinase Domain. *Journal of Biological Chemistry* **278**, 30083-30090 (2003).
147. Schaeper, U.*, et al.* Coupling of Gab1 to C-Met, Grb2, and Shp2 Mediates Biological Responses. *The Journal of Cell Biology* **149**, 1419-1432 (2000).
148. Paliouras, G.N., Naujokas, M.A. & Park, M. Pak4, a Novel Gab1 Binding Partner, Modulates Cell Migration and Invasion by the Met Receptor. *Molecular and Cellular Biology* **29**, 3018-3032 (2009).
149. Abella, J.V.*, et al.* The Gab1 scaffold regulates RTK-dependent dorsal ruffle formation through the adaptor Nck. *J Cell Sci* **123**, 1306-1319 (2010).
150. Gu, H. & Neel, B.G. The `Gab' in signal transduction. *Trends in Cell Biology* **13**, 122-130 (2003).
151. Sachs, M.*, et al.* Essential Role of Gab1 for Signaling by the C-Met Receptor in Vivo. *The Journal of Cell Biology* **150**, 1375-1384 (2000).
152. Marmor, M.D. & Yarden, Y. Role of protein ubiquitylation in regulating endocytosis of receptor tyrosine kinases. *Oncogene* **23**, 2057-2070.
153. Lee, P.S.W.*, et al.* The Cbl protooncoprotein stimulates CSF-1 receptor multiubiquitination and endocytosis, and attenuates macrophage proliferation. *EMBO J* **18**, 3616-3628 (1999).
154. Joazeiro, C.A.P.*, et al.* The Tyrosine Kinase Negative Regulator c-Cbl as a RING-Type, E2-Dependent Ubiquitin-Protein Ligase. *Science* **286**, 309-312 (1999).
155. Levkowitz, G.*, et al.* Ubiquitin Ligase Activity and Tyrosine Phosphorylation Underlie Suppression of Growth Factor Signaling by c-Cbl/Sli-1. *Molecular Cell* **4**, 1029-1040 (1999).
156. Penengo, L., Rubin, C., Yarden, Y. & Gaudino, G. c-Cbl is a critical

modulator of the Ron tyrosine kinase receptor. *Oncogene* **22**, 3669-3679 (0000).
157. Miyake, S., Lupher, M.L., Druker, B. & Band, H. The tyrosine kinase regulator Cbl enhances the ubiquitination and degradation of the platelet-derived growth factor receptor alpha. *Proceedings of the National Academy of Sciences* **95**, 7927-7932 (1998).
158. Goldstein, G.*, et al.* Isolation of a polypeptide that has lymphocyte-differentiating properties and is probably represented universally in living cells. *PNAS* **72**, 11-15 (1975).
159. Ciehanover, A., Hod, Y. & Hershko, A. A heat-stable polypeptide component of an ATP-dependent proteolytic system from reticulocytes. *Biochem Biophys Res Commun.* **81**, 1100-1105 (1978).
160. Hershko, A., Ciechanover, A., Heller, H., Haas, A.L. & Rose, I.A. Proposed role of ATP in protein breakdown: conjugation of protein with multiple chains of the polypeptide of ATP-dependent proteolysis. *PNAS* **77**, 1783-1786 (1980).
161. Ciechanover, A., Elias, S., Heller, H. & Hershko, A. "Covalent affinity" purification of ubiquitin-activating enzyme. *Journal of Biological Chemistry* **257**, 2537-2542 (1982).
162. Hershko, A., Heller, H., Elias, S. & Ciechanover, A. Components of ubiquitin-protein ligase system. Resolution, affinity purification, and role in protein breakdown. *Journal of Biological Chemistry* **258**, 8206-8214 (1983).
163. Regnier, D.C.*, et al.* Identification of two murine loci homologous to the v-cbl oncogene. *J. Virol.* **63**, 3678-3682 (1989).
164. Kolling, R. & Hollenberg, C.P. The ABC-transporter Ste6 accumulates in the plasma membrane in a ubiquitinated form in endocytosis mutants. *EMBO J.* **13**, 3261 -3271 (1994).
165. Yoon, C.H., Lee, J., Jongeward, G.D. & Sternberg, P.W. Similarity of sli-1, a Regulator of Vulval Development in C. elegans, to the Mammalian Proto-Oncogene c-cbl. *Science* **269**, 1102-1105 (1995).
166. Levkowitz, G.*, et al.* Coupling of the c-Cbl protooncogene product to ErbB-1/EGF-receptor but not to other ErbB proteins. *Oncogene* **12**, 1117-1125 (1996).
167. Fukazawa, T., Miyake, S., Band, V. & Band, H. Tyrosine Phosphorylation of Cbl upon Epidermal Growth Factor (EGF) Stimulation and Its Association with EGF Receptor and Downstream Signaling Proteins. *Journal of Biological Chemistry* **271**, 14554-14559 (1996).
168. Lupher, M.L., Songyang, Z., Shoelson, S.E., Cantley, L.C. & Band, H. The Cbl Phosphotyrosine-binding Domain Selects a D(N/D)XpY Motif and Binds to the Tyr292Negative Regulatory Phosphorylation Site of ZAP-70. *Journal of Biological Chemistry* **272**, 33140-33144 (1997).
169. Meisner, H.*, et al.* Interactions of Drosophila Cbl with epidermal growth factor receptors and role of Cbl in R7 photoreceptor cell development. *Mol. Cell. Biol.* **17**, 2217-2225 (1997).
170. Galan, J.-M. & Haguenauer-Tsapis, R. Ubiquitin Lys63 is involved in

ubiquitination of a yeast plasma membrane protein. *EMBO Journal* **16**, 5847–5854 (1997).
171. Odorizzi, G., Babst, M. & Emr, S.D. Fab1p PtdIns(3)P 5-Kinase Function Essential for Protein Sorting in the Multivesicular Body. *Cell* **95**, 847-858 (1998).
172. Katzmann, D.J., Babst, M. & Emr, S.D. Ubiquitin-Dependent Sorting into the Multivesicular Body Pathway Requires the Function of a Conserved Endosomal Protein Sorting Complex, ESCRT-I. *Cell* **106**, 145-155 (2001).
173. Petrelli, A.*, et al.* The endophilin-CIN85-Cbl complex mediates ligand-dependent downregulation of c-Met. *Nature* **416**, 187-190 (2002).
174. Soubeyran, P., Kowanetz, K., Szymkiewicz, I., Langdon, W.Y. & Dikic, I. Cbl-CIN85-endophilin complex mediates ligand-induced downregulation of EGF receptors. *Nature* **416**, 183-187 (2002).
175. Haglund, K.*, et al.* Multiple monoubiquitination of RTKs is sufficient for their endocytosis and degradation. *Nat Cell Biol* **5**, 461-466 (2003).
176. Mosesson, Y.*, et al.* Endocytosis of Receptor Tyrosine Kinases Is Driven by Monoubiquitylation, Not Polyubiquitylation. *Journal of Biological Chemistry* **278**, 21323-21326 (2003).
177. Xuejun, J. & Alexander, S. Epidermal Growth Factor Receptor Internalization through Clathrin-Coated Pits Requires Cbl RING Finger and Proline-Rich Domains But Not Receptor Polyubiquitylation. *Traffic* **4**, 529-543 (2003).
178. Geetha, T., Jiang, J. & Wooten, M.W. Lysine 63 Polyubiquitination of the Nerve Growth Factor Receptor TrkA Directs Internalization and Signaling. **20**, 301-312 (2005).
179. Huang, F., Kirkpatrick, D., Jiang, X., Gygi, S. & Sorkin, A. Differential Regulation of EGF Receptor Internalization and Degradation by Multiubiquitination within the Kinase Domain. *Molecular Cell* **21**, 737-748 (2006).
180. Huang, F., Goh, L.K. & Sorkin, A. EGF receptor ubiquitination is not necessary for its internalization. *Proc. Natl Acad. Sci. USA* **104**, 16904–16909 (2007).
181. Zarrinpar, A., Bhattacharyya, R.P., Lim, W.A. & Gough, N.R. Activation of Ras by Grb2-SOS: Demonstrating an Assembly Role of SH3 Domains. *Sci. STKE* **2003**, tr1- (2003).
182. Maroun, C.R., Naujokas, M.A., Holgado-Madruga, M., Wong, A.J. & Park, M. The Tyrosine Phosphatase SHP-2 Is Required for Sustained Activation of Extracellular Signal-Regulated Kinase and Epithelial Morphogenesis Downstream from the Met Receptor Tyrosine Kinase. *Mol. Cell. Biol.* **20**, 8513-8525 (2000).
183. Montagner, A.*, et al.* A Novel Role for Gab1 and SHP2 in Epidermal Growth Factor-induced Ras Activation. *Journal of Biological Chemistry* **280**, 5350-5360 (2005).
184. O'Brien, L.E.*, et al.* ERK and MMPs Sequentially Regulate Distinct Stages of Epithelial Tubule Development. *Developmental Cell* **7**, 21-32 (2004).

185. Bard-Chapeau, E.A.*, et al.* Concerted Functions of Gab1 and Shp2 in Liver Regeneration and Hepatoprotection. *Mol. Cell. Biol.* **26**, 4664-4674 (2006).
186. Frigault, M.M., Naujokas, M.A. & Park, M. Gab2 requires membrane targeting and the met binding motif to promote lamellipodia, cell scatter, and epithelial morphogenesis downstream from the met receptor. *Journal of Cellular Physiology* **214**, 694-705 (2008).
187. Abella, J.V., Parachoniak, C.A., Sangwan, V. & Park, M. Dorsal Ruffle Microdomains Potentiate Met Receptor Tyrosine Kinase Signaling and Down-regulation. *Journal of Biological Chemistry* **285**, 24956-24967 (2010).
188. Trusolino, L., Bertotti, A. & Comoglio, P.M. MET signalling: principles and functions in development, organ regeneration and cancer. *Nat Rev Mol Cell Biol* **11**, 834-848 (2010).
189. Rodrigues, G.A., Park, M. & Schlessinger, J. Activation of the JNK pathway is essential for transformation by the Met oncogene. *EMBO J.* **16**, 2634-2645 (1997).
190. Lamorte, L., Kamikura, D.M. & Park, M. A switch from p130Cas/Crk to Gab1/Crk signaling correlates with anchorage independent growth and JNK activation in cells transformed by the Met receptor oncoprotein. *Oncogene* **19**, 5973-5981 (2000).
191. Recio, J.A. & Merlino, G. Hepatocyte growth factor/scatter factor activates proliferation in melanoma cells through p38 MAPK, ATF-2 and cyclin D1. *Oncogene* **21**, 1000-1008 (2002).
192. Rasola, A.*, et al.* Hepatocyte Growth Factor Sensitizes Human Ovarian Carcinoma Cell Lines to Paclitaxel and Cisplatin. *Cancer Research* **64**, 1744-1750 (2004).
193. Coltella, N.*, et al.* p38 MAPK turns hepatocyte growth factor to a death signal that commits ovarian cancer cells to chemotherapy-induced apoptosis. *International Journal of Cancer* **118**, 2981-2990 (2006).
194. Cramer, A.*, et al.* Activation of the c-Met receptor complex in fibroblasts drives invasive cell behavior by signaling through transcription factor STAT3. *Journal of Cellular Biochemistry* **95**, 805-816 (2005).
195. Zhang YW, W.L., Jove R, Vande Woude GF. Requirement of Stat3 signaling for HGF/SF-Met mediated tumorigenesis. *Oncogene* **21**, 217-226 (2002).
196. Kermorgant, S. & Parker, P.J. Receptor trafficking controls weak signal delivery: a strategy used by c-Met for STAT3 nuclear accumulation. *J. Cell Biol.* **182**, 855-863 (2008).
197. Fan, S.*, et al.* Role of NF-[kappa]B signaling in hepatocyte growth factor//scatter factor-mediated cell protection. *Oncogene* **24**, 1749-1766 (2005).
198. Muller, M., Morotti, A. & Ponzetto, C. Activation of NF-{kappa}B Is Essential for Hepatocyte Growth Factor-Mediated Proliferation and Tubulogenesis. *Mol. Cell. Biol.* **22**, 1060-1072 (2002).
199. Tacchini, L., De Ponti, C., Matteucci, E., Follis, R. & Desiderio, M.A.

Hepatocyte growth factor-activated NF-ŒʃB regulates HIF-1 activity and ODC expression, implicated in survival, differently in different carcinoma cell lines. *Carcinogenesis* **25**, 2089-2100 (2004).
200. Bevan, P.A., Drake, P.G., Bergeron, J.J.M. & Posner, B.I. Intracellular signal transduction: The role of endosomes. *Trends in Endocrinology and Metabolism* **7**, 13-21 (1996).
201. Gould, G.W. & Lippincott-Schwartz, J. New roles for endosomes: from vesicular carriers to multi-purpose platforms. *Nat Rev Mol Cell Biol* **10**, 287-292 (2009).
202. Resat, H., Ewald, J.A., Dixon, D.A. & Wiley, H.S. An Integrated Model of Epidermal Growth Factor Receptor Trafficking and Signal Transduction. *Biophys J.* **85**, 730-743 (2003).
203. Roth, M.G. Clathrin-mediated endocytosis before fluorescent proteins. *Nat Rev Mol Cell Biol* **7**, 63-68 (2006).
204. Roth, T.F. & Porter, K.R. YOLK PROTEIN UPTAKE IN THE OOCYTE OF THE MOSQUITO AEDES AEGYPTI. L. *The Journal of Cell Biology* **20**, 313-332 (1964).
205. Kanaseki, T. & Kadota, K. THE "VESICLE IN A BASKET". *The Journal of Cell Biology* **42**, 202-220 (1969).
206. Heuser, J. Three-dimensional visualization of coated vesicle formation in fibroblasts. *The Journal of Cell Biology* **84**, 560-583 (1980).
207. Pearse, B.M. Coated vesicles from pig brain: purification and biochemical characterization. *J. Mol. Biol.* **97**, 93-98 (1975).
208. Pearse, B.M. Clathrin: a unique protein associated with intracellular transfer of membrane by coated vesicles. *Proc. Natl Acad. Sci. USA* **73**, 1255-1259 (1976).
209. Anderson, R.G., Goldstein, J.L. & Brown, M.S. A mutation that impairs the ability of lipoprotein receptors to localise in coated pits on the cell surface of human fibroblasts. *Nature* **270**, 695-699 (1977).
210. Goldstein, J.L., Anderson, R.G. & Brown, M.S. Coated pits, coated vesicles, and receptor-mediated endocytosis. *Nature* **279**, 679-685 (1979).
211. Pandey, K.N. Functional roles of short sequence motifs in the endocytosis of membrane receptors. *Frontiers in Bioscience* **14**, 5339-5360 (2009).
212. Mayor, S. & Pagano, R.E. Pathways of clathrin-independent endocytosis. *Nat Rev Mol Cell Biol* **8**, 603-612 (2007).
213. Borner, G.H.H., Harbour, M., Hester, S., Lilley, K.S. & Robinson, M.S. Comparative proteomics of clathrin-coated vesicles. *J. Cell Biol.* **175**, 571-578 (2006).
214. Bonifacino, J.S. & Traub, L.M. SIGNALS FOR SORTING OF TRANSMEMBRANE PROTEINS TO ENDOSOMES AND LYSOSOMES *. *Annual Review of Biochemistry* **72**, 395-447 (2003).
215. Kibbey, R.G., Rizo, J., Gierasch, L.M. & Anderson, R.G.W. The LDL Receptor Clustering Motif Interacts with the Clathrin Terminal Domain in a Reverse Turn Conformation. *The Journal of Cell Biology* **142**, 59-67 (1998).
216. Boll, W.*, et al.* The μ2 Subunit of the Clathrin Adaptor AP-2 Binds to

FDNPVY and YppØ Sorting Signals at Distinct Sites. *Traffic* **3**, 590-600 (2002).
217. Mishra, S.K.*, et al.* Disabled-2 exhibits the properties of a cargo-selective endocytic clathrin adaptor. *EMBO J* **21**, 4915-4926 (2002).
218. Williams, M.A. & Fukuda, M. Accumulation of membrane glycoproteins in lysosomes requires a tyrosine residue at a particular position in the cytoplasmic tail. *The Journal of Cell Biology* **111**, 955-966 (1990).
219. Harter, C. & Mellman, I. Transport of the lysosomal membrane glycoprotein lgp120 (lgp-A) to lysosomes does not require appearance on the plasma membrane. *The Journal of Cell Biology* **117**, 311-325 (1992).
220. Hunziker, W., Harter, C., Matter, K. & Mellman, I. Basolateral sorting in MDCK cells requires a distinct cytoplasmic domain determinant. *Cell* **66**, 907-920 (1991).
221. Rajasekaran, A.*, et al.* TGN38 recycles basolaterally in polarized Madin-Darby canine kidney cells. *Mol. Biol. Cell* **5**, 1093-1103 (1994).
222. Ohno, H.*, et al.* Interaction of tyrosine-based sorting signals with clathrin-associated proteins. *Science* **269**, 1872-1875 (1995).
223. Stephens, D.J., Crump, C.M., Clarke, A.R. & Banting, G. Serine 331 and Tyrosine 333 Are Both Involved in the Interaction between the Cytosolic Domain of TGN38 and the Œº2 Subunit of the AP2 Clathrin Adaptor Complex. *Journal of Biological Chemistry* **272**, 14104-14109 (1997).
224. Rapoport, I.*, et al.* Regulatory interactions in the recognition of endocytic sorting signals by AP-2 complexes. *EMBO J* **16**, 2240-2250 (1997).
225. Rous, B.A.*, et al.* Role of Adaptor Complex AP-3 in Targeting Wild-Type and Mutated CD63 to Lysosomes. *Mol. Biol. Cell* **13**, 1071-1082 (2002).
226. Fingerhut, A., von Figura, K. & H√∂ning, S. Binding of AP2 to Sorting Signals Is Modulated by AP2 Phosphorylation. *Journal of Biological Chemistry* **276**, 5476-5482 (2001).
227. Ricotta, D., Conner, S.D., Schmid, S.L., von Figura, K. & H√∂ning, S. Phosphorylation of the AP2 Œº subunit by AAK1 mediates high affinity binding to membrane protein sorting signals. *The Journal of Cell Biology* **156**, 791-795 (2002).
228. Rodionov, D.G. & Bakke, O. Medium Chains of Adaptor Complexes AP-1 and AP-2 Recognize Leucine-based Sorting Signals from the Invariant Chain. *Journal of Biological Chemistry* **273**, 6005-6008 (1998).
229. Bremnes, T., Lauvrak, V., Lindqvist, B.r. & Bakke, O. A Region from the Medium Chain Adaptor Subunit (Œº) Recognizes Leucine- and Tyrosine-based Sorting Signals. *Journal of Biological Chemistry* **273**, 8638-8645 (1998).
230. Rapoport, I., Chen, Y.C., Cupers, P., Shoelson, S.E. & Kirchhausen, T. Dileucine-based sorting signals bind to the [beta] chain of AP-1 at a site distinct and regulated differently from the tyrosine-based motif-binding site. *EMBO J* **17**, 2148-2155 (1998).
231. Kelly, B.T.*, et al.* A structural explanation for the binding of endocytic dileucine motifs by the AP2 complex. *Nature* **456**, 976-979 (2008).
232. Puertollano, R., Aguilar, R.C., Gorshkova, I., Crouch, R.J. & Bonifacino,

J.S. Sorting of Mannose 6-Phosphate Receptors Mediated by the GGAs. *Science* **292**, 1712-1716 (2001).
233. Zhu, Y., Doray, B., Poussu, A., Lehto, V.-P. & Kornfeld, S. Binding of GGA2 to the Lysosomal Enzyme Sorting Motif of the Mannose 6-Phosphate Receptor. *Science* **292**, 1716-1718 (2001).
234. Misra, S., Puertollano, R., Kato, Y., Bonifacino, J.S. & Hurley, J.H. Structural basis for acidic-cluster-dileucine sorting-signal recognition by VHS domains. *Nature* **415**, 933-937 (2002).
235. Kato, Y., Misra, S., Puertollano, R., Hurley, J.H. & Bonifacino, J.S. Phosphoregulation of sorting signal-VHS domain interactions by a direct electrostatic mechanism. *Nat Struct Mol Biol* **9**, 532-536 (2002).
236. Shiba, T.*, et al.* Structural basis for recognition of acidic-cluster dileucine sequence by GGA1. *Nature* **415**, 937-941 (2002).
237. Wan, L.*, et al.* PACS-1 Defines a Novel Gene Family of Cytosolic Sorting Proteins Required for trans-Golgi Network Localization. *Cell* **94**, 205-216 (1998).
238. Crump, C.M.*, et al.* PACS-1 binding to adaptors is required for acidic cluster motif-mediated protein traffic. *EMBO J* **20**, 2191-2201 (2001).
239. Laguette, N.*, et al.* Nef-induced CD4 endocytosis in human immunodeficiency virus type 1 host cells: role of the p56lck kinase. *J. Virol.*, JVI.01648-01608 (2009).
240. Traub, L.M. Tickets to ride: selecting cargo for clathrin-regulated internalization. *Nat Rev Mol Cell Biol* **10**, 583-596 (2009).
241. Dupre, S., Urban-Grimal, D. & Haguenauer-Tsapis, R. Ubiquitin and endocytic internalization in yeast and animal cells. *Biochimica et Biophysica Acta (BBA) - Molecular Cell Research* **1695**, 89-111 (2004).
242. Huang, K.M., D'Hondt, K., Riezman, H. & Lemmon, S.K. Clathrin functions in the absence of heterotetrameric adaptors and AP180-related proteins in yeast. *EMBO J* **18**, 3897-3908 (1999).
243. Rohrer, J., Benedetti, H., Zanolari, B. & Riezman, H. Identification of a novel sequence mediating regulated endocytosis of the G protein-coupled alpha-pheromone receptor in yeast. *Mol. Biol. Cell* **4**, 511-521 (1993).
244. Hicke, L. & Riezman, H. Ubiquitination of a Yeast Plasma Membrane Receptor Signals Its Ligand-Stimulated Endocytosis. *Cell* **84**, 277-287 (1996).
245. Weissman, A.M. Themes and variations on ubiquitylation. *Nat Rev Mol Cell Biol* **2**, 169-178 (2001).
246. Takeshi, T.*, et al.* Structural basis for distinct roles of Lys63- and Lys48-linked polyubiquitin chains. *Genes to Cells* **9**, 865-875 (2004).
247. Fazioli, F., Minichiello, L., Matoskova, B., Wong, W.T. & Fiore, P.P.D. eps15, a novel tyrosine kinase substrate, exhibits transforming activity. *Mol. Biol. Cell* **13**, 5814-5828 (1993).
248. Delft, S.v., Schumacher, C., Hage, W., Verkleij, A.J. & Henegouwen, P.M.P.v.B.e. Association and Colocalization of Eps15 with Adaptor Protein-2 and Clathrin
10.1083/jcb.136.4.811. *J. Cell Biol.* **136**, 811-821 (1997).

249. Tebar, F., Sorkina, T., Sorkin, A., Ericsson, M. & Kirchhausen, T. Eps15 Is a Component of Clathrin-coated Pits and Vesicles and Is Located at the Rim of Coated Pits
10.1074/jbc.271.46.28727. *J. Biol. Chem.* **271**, 28727-28730 (1996).
250. Benmerah, A.*, et al.* The tyrosine kinase substrate eps15 is constitutively associated with the plasma membrane adaptor AP-2
10.1083/jcb.131.6.1831. *J. Cell Biol.* **131**, 1831-1838 (1995).
251. Benmerah, A., Bègue, B., Dautry-Varsat, A. & Cerf-Bensussan, N. The Ear of alpha-Adaptin Interacts with the COOH-terminal Domain of the Eps15 Protein
10.1074/jbc.271.20.12111. *J. Biol. Chem.* **271**, 12111-12116 (1996).
252. Chen, H.*, et al.* Epsin is an EH-domain-binding protein implicated in clathrin-mediated endocytosis. *Nature* **394**, 793-797 (1998).
253. Bean, A.J.*, et al.* Hrs-2 Regulates Receptor-mediated Endocytosis via Interactions with Eps15
10.1074/jbc.275.20.15271. *J. Biol. Chem.* **275**, 15271-15278 (2000).
254. de Beer, T.*, et al.* Molecular mechanism of NPF recognition by EH domains. *Nat Struct Mol Biol* **7**, 1018-1022 (2000).
255. Naslavsky, N., Rahajeng, J., Chenavas, S., Sorgen, P.L. & Caplan, S. EHD1 and Eps15 Interact with Phosphatidylinositols via Their Eps15 Homology Domains. *J. Biol. Chem.* **282**, 16612-16622 (2007).
256. Benmerah, A., Bayrou, M., Cerf-Bensussan, N. & Dautry-Varsat, A. Inhibition of clathrin-coated pit assembly by an Eps15 mutant. *J Cell Sci* **112**, 1303-1311 (1999).
257. Cupers, P., ter Haar, E., Boll, W. & Kirchhausen, T. Parallel Dimers and Anti-parallel Tetramers Formed by Epidermal Growth Factor Receptor Pathway Substrate Clone 15 (EPS15)
10.1074/jbc.272.52.33430. *J. Biol. Chem.* **272**, 33430-33434 (1997).
258. Polo, S.*, et al.* A single motif responsible for ubiquitin recognition and monoubiquitination in endocytic proteins. *Nature* **416**, 451-455 (2002).
259. Sigismund, S.*, et al.* From the Cover: Clathrin-independent endocytosis of ubiquitinated cargos
10.1073/pnas.0409817102. *Proceedings of the National Academy of Sciences* **102**, 2760-2765 (2005).
260. de Melker, A.A., van der Horst, G. & Borst, J. c-Cbl directs EGF receptors into an endocytic pathway that involves the ubiquitin-interacting motif of Eps15
10.1242/jcs.01354. *J Cell Sci* **117**, 5001-5012 (2004).
261. Belleudi, F.*, et al.* Ligand-induced clathrin-mediated endocytosis of the keratinocyte growth factor receptor occurs independently of either phosphorylation or recruitment of eps15. *FEBS Letters* **553**, 262-270 (2003).
262. Loerke, D.*, et al.* Cargo and Dynamin Regulate Clathrin-Coated Pit Maturation. *PLoS Biol* **7**, e1000057 (2009).
263. Taylor, M.J., Perrais, D. & Merrifield, C.J. A High Precision Survey of the Molecular Dynamics of Mammalian Clathrin-Mediated Endocytosis.

*PLoS Biol* **9**, e1000604 (2011).
264. Kaksonen, M., Toret, C.P. & Drubin, D.G. A Modular Design for the Clathrin- and Actin-Mediated Endocytosis Machinery. *Cell* **123**, 305-320 (2005).
265. Simonsen, A., Wurmser, A.E., Emr, S.D. & Stenmark, H. The role of phosphoinositides in membrane transport. *Current Opinion in Cell Biology* **13**, 485-492 (2001).
266. Ferguson, S.*, et al.* Coordinated Actions of Actin and BAR Proteins Upstream of Dynamin at Endocytic Clathrin-Coated Pits. *Developmental Cell* **17**, 811-822 (2009).
267. Yarar, D., Waterman-Storer, C.M. & Schmid, S.L. A Dynamic Actin Cytoskeleton Functions at Multiple Stages of Clathrin-mediated Endocytosis. *Mol. Biol. Cell* **16**, 964-975 (2005).
268. Merrifield, C.J., Feldman, M.E., Wan, L. & Almers, W. Imaging actin and dynamin recruitment during invagination of single clathrin-coated pits. *Nat Cell Biol* **4**, 691-698 (2002).
269. Itoh, T.*, et al.* Dynamin and the Actin Cytoskeleton Cooperatively Regulate Plasma Membrane Invagination by BAR and F-BAR Proteins. *Developmental Cell* **9**, 791-804 (2005).
270. Frost, A., Unger, V.M. & De Camilli, P. The BAR Domain Superfamily: Membrane-Molding Macromolecules. *Cell* **137**, 191-196 (2009).
271. Evan, E. & Lois, E.G. Multiple Roles of Auxilin and Hsc70 in Clathrin-Mediated Endocytosis. *Traffic* **8**, 640-646 (2007).
272. Vanhaesebroeck, B., Leevers, S.J., Panayotou, G. & Waterfield, M.D. Phosphoinositide 3-kinases: A conserved family of signal transducers. *Trends in Biochemical Sciences* **22**, 267-272 (1997).
273. Stenmark, H., Aasland, R., Toh, B.-H. & D'Arrigo, A. Endosomal Localization of the Autoantigen EEA1 Is Mediated by a Zinc-binding FYVE Finger. *Journal of Biological Chemistry* **271**, 24048-24054 (1996).
274. Ohya, T.*, et al.* Reconstitution of Rab- and SNARE-dependent membrane fusion by synthetic endosomes. *Nature* **459**, 1091-1097 (2009).
275. Bourne, H.R., Sanders, D.A. & McCormick, F. The GTPase superfamily: conserved structure and molecular mechanism. *Nature* **349**, 117-127 (1991).
276. Vetter, I.R. & Wittinghofer, A. The Guanine Nucleotide-Binding Switch in Three Dimensions. *Science* **294**, 1299-1304 (2001).
277. Stenmark, H. Rab GTPases as coordinators of vesicle traffic. *Nat Rev Mol Cell Biol* **advanced online publication**(2009).
278. Bucci, C.*, et al.* The small GTPase rab5 functions as a regulatory factor in the early endocytic pathway. *Cell* **70**, 715-728 (1992).
279. Stenmark, H., Vitale, G., Ullrich, O. & Zerial, M. Rabaptin-5 is a direct effector of the small GTPase Rab5 in endocytic membrane fusion. *Cell* **83**, 423-432 (1995).
280. Zhu, H., Qian, H. & Li, G. Delayed Onset of Positive Feedback Activation of Rab5 by Rabex-5 and Rabaptin-5 in Endocytosis. *PLoS ONE* **5**, e9226 (2010).

281. Lippe, R., Miaczynska, M., Rybin, V., Runge, A. & Zerial, M. Functional Synergy between Rab5 Effector Rabaptin-5 and Exchange Factor Rabex-5 When Physically Associated in a Complex. *Mol. Biol. Cell* **12**, 2219-2228 (2001).
282. Maxfield, F.R. & McGraw, T.E. Endocytic recycling. *Nat Rev Mol Cell Biol* **5**, 121-132 (2004).
283. Poteryaev, D., Datta, S., Ackema, K., Zerial, M. & Spang, A. Identification of the Switch in Early-to-Late Endosome Transition. *Cell* **141**, 497-508 (2010).
284. Sachse, M., Urbe, S., Oorschot, V., Strous, G.J. & Klumperman, J. Bilayered Clathrin Coats on Endosomal Vacuoles Are Involved in Protein Sorting toward Lysosomes. *Mol. Biol. Cell* **13**, 1313-1328 (2002).
285. Felder, S.*, et al.* Kinase activity controls the sorting of the epidermal growth factor receptor within the multivesicular body. *Cell* **61**, 623-634 (1990).
286. Bowers, K. & Stevens, T.H. Protein transport from the late Golgi to the vacuole in the yeast Saccharomyces cerevisiae. *Biochimica et Biophysica Acta (BBA) - Molecular Cell Research* **1744**, 438-454 (2005).
287. Katzmann, D.J., Odorizzi, G. & Emr, S.D. Receptor downregulation and multivesicular-body sorting. *Nat Rev Mol Cell Biol* **3**, 893-905 (2002).
288. Raiborg, C.*, et al.* Hrs sorts ubiquitinated proteins into clathrin-coated microdomains of early endosomes. *Nat Cell Biol* **4**, 394-398 (2002).
289. Raiborg, C. & Stenmark, H. The ESCRT machinery in endosomal sorting of ubiquitylated membrane proteins. *Nature* **458**, 445-452 (2009).
290. Williams, R.L. & Urbe, S. The emerging shape of the ESCRT machinery. *Nat Rev Mol Cell Biol* **8**, 355-368 (2007).
291. Gruenberg, J. & Stenmark, H. The biogenesis of multivesicular endosomes. *Nat Rev Mol Cell Biol* **5**, 317-323 (2004).
292. Roxrud, I., Raiborg, C., Pedersen, N.M., Stang, E. & Stenmark, H. An endosomally localized isoform of Eps15 interacts with Hrs to mediate degradation of epidermal growth factor receptor. *J. Cell Biol.* **180**, 1205-1218 (2008).
293. Ren, X. & Hurley, J.H. VHS domains of ESCRT-0 cooperate in high-avidity binding to polyubiquitinated cargo. *EMBO J* **29**, 1045-1054 (2010).
294. Raiborg, C.*, et al.* FYVE and coiled-coil domains determine the specific localisation of Hrs to early endosomes. *Journal of Cell Science* **114**, 2255-2263 (2001).
295. Bache, K.G., Raiborg, C., Mehlum, A. & Stenmark, H. STAM and Hrs Are Subunits of a Multivalent Ubiquitin-binding Complex on Early Endosomes
10.1074/jbc.M210843200. *J. Biol. Chem.* **278**, 12513-12521 (2003).
296. Bilodeau, P.S., Urbanowski, J.L., Winistorfer, S.C. & Piper, R.C. The Vps27p-Hse1p complex binds ubiquitin and mediates endosomal protein sorting. *Nat Cell Biol* **4**, 534-539 (2002).
297. Hirano, S.*, et al.* Double-sided ubiquitin binding of Hrs-UIM in

endosomal protein sorting. *Nat Struct Mol Biol* **13**, 272-277 (2006).
298. Hammond, D.E.*, et al.* Endosomal Dynamics of Met Determine Signaling Output. *Mol. Biol. Cell* **14**, 1346-1354 (2003).
299. Bilodeau, P.S., Winistorfer, S.C., Kearney, W.R., Robertson, A.D. & Piper, R.C. Vps27-Hse1 and ESCRT-I complexes cooperate to increase efficiency of sorting ubiquitinated proteins at the endosome. *The Journal of Cell Biology* **163**, 237-243 (2003).
300. Katzmann, D.J., Stefan, C.J., Babst, M. & Emr, S.D. Vps27 recruits ESCRT machinery to endosomes during MVB sorting. *The Journal of Cell Biology* **162**, 413-423 (2003).
301. Lu, Q., Hope, L.W., Brasch, M., Reinhard, C. & Cohen, S.N. TSG101 interaction with HRS mediates endosomal trafficking and receptor down-regulation. *Proceedings of the National Academy of Sciences* **100**, 7626-7631 (2003).
302. Bache, K.G., Brech, A., Mehlum, A. & Stenmark, H. Hrs regulates multivesicular body formation via ESCRT recruitment to endosomes. *The Journal of Cell Biology* **162**, 435-442 (2003).
303. Slagsvold, T.*, et al.* Eap45 in Mammalian ESCRT-II Binds Ubiquitin via a Phosphoinositide-interacting GLUE Domain. *Journal of Biological Chemistry* **280**, 19600-19606 (2005).
304. Teo, H.*, et al.* ESCRT-I Core and ESCRT-II GLUE Domain Structures Reveal Role for GLUE in Linking to ESCRT-I and Membranes. *Cell* **125**, 99-111 (2006).
305. Babst, M., Katzmann, D.J., Estepa-Sabal, E.J., Meerloo, T. & Emr, S.D. Escrt-III: An endosome-associated heterooligomeric protein complex required for mvb sorting. *Developmental Cell* **3**, 271-282 (2002).
306. Teo, H., Perisic, O., Gonz·lez, B. & Williams, R.L. ESCRT-II, an Endosome-Associated Complex Required for Protein Sorting: Crystal Structure and Interactions with ESCRT-III and Membranes. *Developmental Cell* **7**, 559-569 (2004).
307. Wollert, T. & Hurley, J.H. Molecular mechanism of multivesicular body biogenesis by ESCRT complexes. *Nature* **464**, 864-869 (2010).
308. Clague, M.J. & UrbÈ, S. Endocytosis: the DUB version. *Trends in Cell Biology* **16**, 551-559 (2006).
309. Futter, C.E., Pearse, A., Hewlett, L.J. & Hopkins, C.R. Multivesicular endosomes containing internalized EGF-EGF receptor complexes mature and then fuse directly with lysosomes. *J. Cell Biol.* **132**, 1011-1023 (1996).
310. Schmid, S.L., Fuchs, R., Male, P. & Mellman, I. Two distinct subpopulations of endosomes involved in membrane recycling and transport to lysosomes. *Cell* **52**, 73-83 (1988).
311. Mayor, S., Presley, J.F. & Maxfield, F.R. Sorting of membrane components from endosomes and subsequent recycling to the cell surface occurs by a bulk flow process. *The Journal of Cell Biology* **121**, 1257-1269 (1993).
312. Hopkins, C.R. Intracellular routing of transferrin and transferrin receptors

in epidermoid carcinoma A431 cells. *Cell* **35**, 321-330 (1983).
313. Yamashiro, D.J., Tycko, B., Fluss, S.R. & Maxfield, F.R. Segregation of transferrin to a mildly acidic (pH 6.5) para-golgi compartment in the recycling pathway. *Cell* **37**, 789-800 (1984).
314. Grant, B.D. & Donaldson, J.G. Pathways and mechanisms of endocytic recycling. *Nat Rev Mol Cell Biol* **10**, 597-608 (2009).
315. S√∂nnichsen, B., De Renzis, S., Nielsen, E., Rietdorf, J. & Zerial, M. Distinct Membrane Domains on Endosomes in the Recycling Pathway Visualized by Multicolor Imaging of Rab4, Rab5, and Rab11. *The Journal of Cell Biology* **149**, 901-914 (2000).
316. Griffiths, G., Back, R. & Marsh, M. A quantitative analysis of the endocytic pathway in baby hamster kidney cells. *The Journal of Cell Biology* **109**, 2703-2720 (1989).
317. De Renzis, S., Sonnichsen, B. & Zerial, M. Divalent Rab effectors regulate the sub-compartmental organization and sorting of early endosomes. *Nat Cell Biol* **4**, 124-133 (2002).
318. Puthenveedu, M.A.*, et al.* Sequence-Dependent Sorting of Recycling Proteins by Actin-Stabilized Endosomal Microdomains. *Cell* **143**, 761-773 (2010).
319. Kermorgant, S., Zicha, D. & Parker, P.J. Protein Kinase C Controls Microtubule-based Traffic but Not Proteasomal Degradation of c-Met. *J. Biol. Chem.* **278**, 28921-28929 (2003).
320. Kermorgant, S., Zicha, D. & Parker, P.J. PKC controls HGF-dependent c-Met traffic, signalling and cell migration. *EMBO J.* **23**, 3721-3734 (2004).
321. Bonifacino, J.S. The GGA proteins: adaptors on the move. *Nat Rev Mol Cell Biol* **5**, 23-32 (2004).
322. Boman, A.L., Zhang, C.-j., Zhu, X. & Kahn, R.A. A Family of ADP-Ribosylation Factor Effectors That Can Alter Membrane Transport through the trans-Golgi. *Mol. Biol. Cell* **11**, 1241-1255 (2000).
323. Dell'Angelica, E.C.*, et al.* GGAs: A Family of ADP Ribosylation Factor-binding Proteins Related to Adaptors and Associated with the Golgi Complex. *J. Cell Biol.* **149**, 81-94 (2000).
324. Puertollano, R. & Bonifacino, J.S. Interactions of GGA3 with the ubiquitin sorting machinery. *Nat Cell Biol* **6**, 244-251 (2004).
325. Shiba, Y.*, et al.* GAT (GGA and Tom1) Domain Responsible for Ubiquitin Binding and Ubiquitination. *J. Biol. Chem.* **279**, 7105-7111 (2004).
326. Nielsen, M.S.*, et al.* The sortilin cytoplasmic tail conveys Golgi–endosome transport and binds the VHS domain of the GGA2 sorting protein. *EMBO J.* **20**, 2180–2190 (2001).
327. Mosesson, Y., Mills, G.B. & Yarden, Y. Derailed endocytosis: an emerging feature of cancer. *Nat Rev Cancer* **8**, 835-850 (2008).
328. Rao, D.S.*, et al.* Altered receptor trafficking in Huntingtin Interacting Protein 1-transformed cells. *Cancer Cell* **3**, 471-482 (2003).
329. Rao, D.S.*, et al.* Huntingtin-interacting protein 1 is overexpressed in prostate and colon cancer and is critical for cellular survival. *The Journal of Clinical Investigation* **110**, 351-360 (2002).

330. Gottfried, I., Ehrlich, M. & Ashery, U. HIP1 exhibits an early recruitment and a late stage function in the maturation of coated pits. *Cellular and Molecular Life Sciences* **66**, 2897-2911 (2009).
331. Li, L. & Cohen, S.N. tsg101: A Novel Tumor Susceptibility Gene Isolated by Controlled Homozygous Functional Knockout of Allelic Loci in Mammalian Cells. *Cell* **85**, 319-329 (1996).
332. Li, L., Liao, J., Ruland, J.r., Mak, T.W. & Cohen, S.N. A TSG101/MDM2 regulatory loop modulates MDM2 degradation and MDM2/p53 feedback control. *Proceedings of the National Academy of Sciences* **98**, 1619-1624 (2001).
333. Raiborg, C., Maler¯d, L., Pedersen, N.M. & Stenmark, H. Differential functions of Hrs and ESCRT proteins in endocytic membrane trafficking. *Experimental Cell Research* **314**, 801-813 (2008).
334. Westhoff, B.*, et al.* Alterations of the Notch pathway in lung cancer. *Proceedings of the National Academy of Sciences* **106**, 22293-22298 (2009).
335. Pece, S.*, et al.* Loss of negative regulation by Numb over Notch is relevant to human breast carcinogenesis. *The Journal of Cell Biology* **167**, 215-221 (2004).
336. Rhyu, M.S., Jan, L.Y. & Jan, Y.N. Asymmetric distribution of numb protein during division of the sensory organ precursor cell confers distinct fates to daughter cells. *Cell* **76**, 477-491 (1994).
337. Guo, M., Jan, L.Y. & Jan, Y.N. Control of Daughter Cell Fates during Asymmetric Division: Interaction of Numb and Notch. *Neuron* **17**, 27-41 (1996).
338. Di Marcotullio, L.*, et al.* Numb is a suppressor of Hedgehog signalling and targets Gli1 for Itch-dependent ubiquitination. *Nat Cell Biol* **8**, 1415-1423 (2006).
339. Colaluca, I.N.*, et al.* NUMB controls p53 tumour suppressor activity. *Nature* **451**, 76-80 (2008).
340. Nishimura, T. & Kaibuchi, K. Numb Controls Integrin Endocytosis for Directional Cell Migration with aPKC and PAR-3. *Developmental Cell* **13**, 15-28 (2007).
341. Rasin, M.-R.*, et al.* Numb and Numbl are required for maintenance of cadherin-based adhesion and polarity of neural progenitors. *Nat Neurosci* **10**, 819-827 (2007).
342. Rennstam, K.*, et al.* Numb protein expression correlates with a basal-like phenotype and cancer stem cell markers in primary breast cancer. *Breast Cancer Research and Treatment* **122**, 315-324 (2010).
343. Pece, S., Confalonieri, S., R. Romano, P. & Di Fiore, P.P. NUMB-ing down cancer by more than just a NOTCH. *Biochimica et Biophysica Acta (BBA) - Reviews on Cancer* **1815**, 26-43 (2011).
344. Agarwal, R., Jurisica, I., Mills, G.B. & Cheng, K.W. The Emerging Role of the RAB25 Small GTPase in Cancer. *Traffic* **10**, 1561-1568 (2009).
345. Cheng, K.W.*, et al.* The RAB25 small GTPase determines aggressiveness of ovarian and breast cancers. *Nat Med* **10**, 1251-1256 (2004).

346. Patael-Karasik, Y.*, et al.* Comparative Genomic Hybridization in Inherited and Sporadic Ovarian Tumors in Israel. *Cancer Genetics and Cytogenetics* **121**, 26-32 (2000).
347. Kiechle, M.*, et al.* Comparative genomic hybridization detects genetic imbalances in primary ovarian carcinomas as correlated with grade of differentiation. *Cancer* **91**, 534-540 (2001).
348. Zudaire, I.*, et al.* Genomic imbalances detected by comparative genomic hybridization are prognostic markers in invasive ductal breast carcinomas. *Histopathology* **40**, 547-555 (2002).
349. Chin, K.*, et al.* Genomic and transcriptional aberrations linked to breast cancer pathophysiologies. *Cancer Cell* **10**, 529-541 (2006).
350. Yang, F., Xiao-Yan, X., Bi-Liang, C. & XiangDong, M. Knockdown of Rab25 expression by RNAi inhibits growth of human epithelial ovarian cancer cellsin vitroandin vivo. *Pathology* **38**, 561-567 510.1080/00313020601024037 (2006).
351. Garcia, M.J.*, et al.* A 1[thinsp]Mb minimal amplicon at 8p11-12 in breast cancer identifies new candidate oncogenes. *Oncogene* **24**, 5235-5245 (2005).
352. Caswell, P.T.*, et al.* Rab25 Associates with [alpha]5[beta]1 Integrin to Promote Invasive Migration in 3D Microenvironments. *Developmental Cell* **13**, 496-510 (2007).
353. Caswell, P.T.*, et al.* Rab-coupling protein coordinates recycling of alpha5/beta1 integrin and EGFR1 to promote cell migration in 3D microenvironments. *The Journal of Cell Biology* **183**, 143-155 (2008).
354. Muller, P.A.J.*, et al.* Mutant p53 Drives Invasion by Promoting Integrin Recycling. *Cell* **139**, 1327-1341 (2009).
355. He, H.*, et al.* Identification and characterization of nine novel human small GTPases showing variable expressions in liver cancer tissues. *Gene Expression* **10**, 231-242 (2002).
356. Bandyopadhyay, S.*, et al.* Role of the putative tumor metastasis suppressor gene Drg-1 in breast cancer progression. *Oncogene* **23**, 5675-5681 (2004).
357. Bandyopadhyay, S.*, et al.* The Drg-1 Gene Suppresses Tumor Metastasis in Prostate Cancer. *Cancer Research* **63**, 1731-1736 (2003).
358. Kachhap, S.K.*, et al.* The N-Myc Down Regulated Gene1 (NDRG1) Is a Rab4a Effector Involved in Vesicular Recycling of E-Cadherin. *PLoS ONE* **2**, e844 (2007).
359. Wang, Y.*, et al.* Regulation of endocytosis via the oxygen-sensing pathway. *Nat Med* **15**, 319-324 (2009).
360. Magnusson, M.K.*, et al.* Rabaptin-5 is a novel fusion partner to platelet-derived growth factor Œ≤ receptor in chronic myelomonocytic leukemia. *Blood* **98**, 2518-2525 (2001).
361. Bernard, O.A., Mauchauffe, M., Mecucci, C., Van Den Berghe, H. & Berger, R. A novel gene, AF-1p, fused to HRX in t(1;11)(p32;q23), is not related to AF-4, AF-9 nor ENL. *Oncogene* **9**, 1039-1045 (1994).
362. Ross, T.S., Bernard, O.A., Berger, R. & Gilliland, D.G. Fusion of Huntingtin interacting protein 1 to platelet-derived growth factor

Œ≤receptor (PDGFŒ≤R) in chronic myelomonocytic leukemia with t(5;7)(q33;q11.2). *Blood* **91**, 4419-4426 (1998).
363. Dreyling, M.H.*, et al.* MLL and CALM are fused to AF10 in morphologically distinct subsets of acute leukemia with translocation t(10;11): Both rearrangements are associated with a poor prognosis. *Blood* **91**, 4662-4667 (1998).
364. Dreyling, M.H.*, et al.* The t(10;11)(p13;q14) in the U937 cell line results in the fusion of the AF10 gene and CALM, encoding a new member of the AP-3 clathrin assembly protein family. *Proceedings of the National Academy of Sciences* **93**, 4804-4809 (1996).
365. So, C.W.*, et al.* EEN encodes for a member of a new family of proteins containing an Src homology 3 domain and is the third gene located on chromosome 19p13 that fuses to MLL in‚Äâhuman‚Äâleukemia. *Proceedings of the National Academy of Sciences* **94**, 2563-2568 (1997).
366. Bridge, J.A.*, et al.* Fusion of the ALK Gene to the Clathrin Heavy Chain Gene, CLTC, in Inflammatory Myofibroblastic Tumor. *The American Journal of Pathology* **159**, 411-415 (2001).
367. Crosetto, N., Tikkanen, R. & Dikic, I. Oncogenic breakdowns in endocytic adaptor proteins. *FEBS Letters* **579**, 3231-3238 (2005).
368. Matsumura, I., Mizuki, M. & Kanakura, Y. Roles for deregulated receptor tyrosine kinases and their downstream signaling molecules in hematologic malignancies. *Cancer Science* **99**, 479-485 (2008).
369. Sorensen, P.H.B. & Triche, T.J. Gene fusions encoding chimaeric transcription factors in solid tumours. *Seminars in Cancer Biology* **7**, 3-14 (1996).
370. Mak, H.H.L.*, et al.* Oncogenic activation of the Met receptor tyrosine kinase fusion protein, Tpr-Met, involves exclusion from the endocytic degradative pathway. *Oncogene* **26**, 7213-7221 (2007).
371. Ma, P.C.*, et al.* c-MET Mutational Analysis in Small Cell Lung Cancer: Novel Juxtamembrane Domain Mutations Regulating Cytoskeletal Functions. *Cancer Res* **63**, 6272-6281 (2003).
372. Onozato, R.*, et al.* Activation of MET by Gene Amplification or by Splice Mutations Deleting the Juxtamembrane Domain in Primary Resected Lung Cancers. *Journal of Thoracic Oncology* **4**, 5-11 10.1097/JTO.1090b1013e3181913e3181910e (2009).
373. Frederick, L., Wang, X.-Y., Eley, G. & James, C.D. Diversity and Frequency of Epidermal Growth Factor Receptor Mutations in Human Glioblastomas. *Cancer Research* **60**, 1383-1387 (2000).
374. Ridge, S.A., Worwood, M., Oscier, D., Jacobs, A. & Padua, R.A. FMS mutations in myelodysplastic, leukemic, and normal subjects. *Proceedings of the National Academy of Sciences* **87**, 1377-1380 (1990).
375. Niemeyer, C.M.*, et al.* Germline CBL mutations cause developmental abnormalities and predispose to juvenile myelomonocytic leukemia. *Nat Genet* **42**, 794-800 (2010).
376. Caligiuri, M.A.*, et al.* Novel c-CBL and CBL-b ubiquitin ligase mutations in human acute myeloid leukemia. *Blood* **110**, 1022-1024 (2007).

377. Sargin, B.l*., et al.* Flt3-dependent transformation by inactivating c-Cbl mutations in AML. *Blood* **110**, 1004-1012 (2007).
378. Slape, C., Liu, L.Y., Beachy, S. & Aplan, P.D. Leukemic transformation in mice expressing a NUP98-HOXD13 transgene is accompanied by spontaneous mutations in Nras, Kras, and Cbl. *Blood* **112**, 2017-2019 (2008).
379. Abella, J.V. & Park, M. Breakdown of endocytosis in the oncogenic activation of receptor tyrosine kinases. *American Journal of Physiology - Endocrinology And Metabolism* **296**, E973-E984 (2009).
380. Lauffenburger, D.A. & Horwitz, A.F. Cell Migration: A Physically Integrated Molecular Process. *Cell* **84**, 359-369 (1996).
381. Small, J.V., Stradal, T., Vignal, E. & Rottner, K. The lamellipodium: where motility begins. *Trends in Cell Biology* **12**, 112-120 (2002).
382. Welch, M.D. & Mullins, R.D. CELLULAR CONTROL OF ACTIN NUCLEATION. *Annual Review of Cell and Developmental Biology* **18**, 247-288 (2002).
383. Ridley, A.J*., et al.* Cell Migration: Integrating Signals from Front to Back. *Science* **302**, 1704-1709 (2003).
384. Cory, G.O.C. & Ridley, A.J. Cell motility: Braking WAVEs. *Nature* **418**, 732-733 (2002).
385. Eden, S., Rohatgi, R., Podtelejnikov, A.V., Mann, M. & Kirschner, M.W. Mechanism of regulation of WAVE1-induced actin nucleation by Rac1 and Nck. *Nature* **418**, 790-793 (2002).
386. Katoh, H. & Negishi, M. RhoG activates Rac1 by direct interaction with the Dock180-binding protein Elmo. *Nature* **424**, 461-464 (2003).
387. Fukuoka, M*., et al.* A Novel Neural Wiskott-Aldrich Syndrome Protein (N-Wasp) Binding Protein, Wish, Induces Arp2/3 Complex Activation Independent of Cdc42. *The Journal of Cell Biology* **152**, 471-482 (2001).
388. Parsons, J.T., Horwitz, A.R. & Schwartz, M.A. Cell adhesion: integrating cytoskeletal dynamics and cellular tension. *Nat Rev Mol Cell Biol* **11**, 633-643 (2010).
389. Zimerman, B., Volberg, T. & Geiger, B. Early molecular events in the assembly of the focal adhesion-stress fiber complex during fibroblast spreading. *Cell Motility and the Cytoskeleton* **58**, 143-159 (2004).
390. Kuo, J.-C., Han, X., Hsiao, C.-T., Yates Iii, J.R. & Waterman, C.M. Analysis of the myosin-II-responsive focal adhesion proteome reveals a role for [beta]-Pix in negative regulation of focal adhesion maturation. *Nat Cell Biol* **13**, 383-393 (2011).
391. Vicente-Manzanares, M., Ma, X., Adelstein, R.S. & Horwitz, A.R. Non-muscle myosin II takes centre stage in cell adhesion and migration. *Nat Rev Mol Cell Biol* **10**, 778-790 (2009).
392. Watanabe, T., Noritake, J. & Kaibuchi, K. Regulation of microtubules in cell migration. *Trends in Cell Biology* **15**, 76-83 (2005).
393. Galjart, N. CLIPs and CLASPs and cellular dynamics. *Nat Rev Mol Cell Biol* **6**, 487-498 (2005).
394. Cheeseman, I.M. & Desai, A. Molecular architecture of the kinetochore-

microtubule interface. *Nat Rev Mol Cell Biol* **9**, 33-46 (2008).
395. Wloga, D. & Gaertig, J. Post-translational modifications of microtubules. *Journal of Cell Science* **123**, 3447-3455 (2010).
396. Mandelkow, E.M., Mandelkow, E. & Milligan, R.A. Microtubule dynamics and microtubule caps: a time-resolved cryo-electron microscopy study. *The Journal of Cell Biology* **114**, 977-991 (1991).
397. Gundersen, G.G. Evolutionary conservation of microtubule-capture mechanisms. *Nat Rev Mol Cell Biol* **3**, 296-304 (2002).
398. Akhmanova, A. & Steinmetz, M.O. Microtubule +TIPs at a glance. *Journal of Cell Science* **123**, 3415-3419 (2010).
399. Soldati, T. & Schliwa, M. Powering membrane traffic in endocytosis and recycling. *Nat Rev Mol Cell Biol* **7**, 897-908 (2006).
400. Hoepfner, S.*, et al.* Modulation of Receptor Recycling and Degradation by the Endosomal Kinesin KIF16B. *Cell* **121**, 437-450 (2005).
401. Nielsen, E., Severin, F., Backer, J.M., Hyman, A.A. & Zerial, M. Rab5 regulates motility of early endosomes on microtubules. *Nat Cell Biol* **1**, 376-382 (1999).
402. Ueno, H., Huang, X., Tanaka, Y. & Hirokawa, N. KIF16B/Rab14 Molecular Motor Complex Is Critical for Early Embryonic Development by Transporting FGF Receptor. *Developmental Cell* **20**, 60-71 (2011).
403. Goldstein, L.S.B. Molecular motors: from one motor many tails to one motor many tales. *Trends in Cell Biology* **11**, 477-482 (2001).
404. Scheel, J. & Kreis, T.E. Motor protein independent binding of endocytic carrier vesicles to microtubules in vitro. *Journal of Biological Chemistry* **266**, 18141-18148 (1991).
405. Rickard, J.E. & Kreis, T.E. Identification of a novel nucleotide-sensitive microtubule-binding protein in HeLa cells. *The Journal of Cell Biology* **110**, 1623-1633 (1990).
406. Pierre, P., Scheel, J., Rickard, J.E. & Kreis, T.E. CLIP-170 links endocytic vesicles to microtubules. *Cell* **70**, 887-900 (1992).
407. Fukata, M.*, et al.* Rac1 and Cdc42 Capture Microtubules through IQGAP1 and CLIP-170. *Cell* **109**, 873-885 (2002).
408. Akhmanova, A.*, et al.* CLASPs Are CLIP-115 and -170 Associating Proteins Involved in the Regional Regulation of Microtubule Dynamics in Motile Fibroblasts. *Cell* **104**, 923-935 (2001).
409. Scheel, J.*, et al.* Purification and Analysis of Authentic CLIP-170 and Recombinant Fragments. *Journal of Biological Chemistry* **274**, 25883-25891 (1999).
410. Lansbergen, G.*, et al.* Conformational changes in CLIP-170 regulate its binding to microtubules and dynactin localization. *The Journal of Cell Biology* **166**, 1003-1014 (2004).
411. Coquelle, F.M.*, et al.* LIS1, CLIP-170's Key to the Dynein/Dynactin Pathway. *Mol. Cell. Biol.* **22**, 3089-3102 (2002).
412. Gill, S.R.*, et al.* Dynactin, a conserved, ubiquitously expressed component of an activator of vesicle motility mediated by cytoplasmic dynein. *The Journal of Cell Biology* **115**, 1639-1650 (1991).

413. Schroer, T.A. & Sheetz, M.P. Two activators of microtubule-based vesicle transport. *The Journal of Cell Biology* **115**, 1309-1318 (1991).
414. Kardon, J.R. & Vale, R.D. Regulators of the cytoplasmic dynein motor. *Nat Rev Mol Cell Biol* **10**, 854-865 (2009).
415. Tai, C.-Y., Dujardin, D.L., Faulkner, N.E. & Vallee, R.B. Role of dynein, dynactin, and CLIP-170 interactions in LIS1 kinetochore function. *The Journal of Cell Biology* **156**, 959-968 (2002).
416. Rickard, J.E. & Kreis, T.E. Binding of pp170 to microtubules is regulated by phosphorylation. *Journal of Biological Chemistry* **266**, 17597-17605 (1991).
417. Nakano, A.*, et al.* AMPK controls the speed of microtubule polymerization and directional cell migration through CLIP-170 phosphorylation. *Nat Cell Biol* **12**, 583-590 (2010).
418. Perez, F., Diamantopoulos, G.S., Stalder, R. & Kreis, T.E. CLIP-170 Highlights Growing Microtubule Ends In Vivo. *Cell* **96**, 517-527 (1999).
419. Dujardin, D.*, et al.* Evidence for a Role of CLIP-170 in the Establishment of Metaphase Chromosome Alignment. *The Journal of Cell Biology* **141**, 849-862 (1998).
420. Komarova, Y.A., Akhmanova, A.S., Kojima, S.-i., Galjart, N. & Borisy, G.G. Cytoplasmic linker proteins promote microtubule rescue in vivo. *The Journal of Cell Biology* **159**, 589-599 (2002).
421. Lomakin, A.J.*, et al.* CLIP-170-Dependent Capture of Membrane Organelles by Microtubules Initiates Minus-End Directed Transport. *Developmental cell* **17**, 323-333 (2009).
422. Watson, P. & Stephens, D.J. Microtubule plus-end loading of p150Glued is mediated by EB1 and CLIP-170 but is not required for intracellular membrane traffic in mammalian cells. *Journal of Cell Science* **119**, 2758-2767 (2006).
423. Marmor, M.D. & Yarden, Y. Role of protein ubiquitylation in regulating endocytosis of receptor tyrosine kinases. *Oncogene* **23**, 2057-2070 (2004).
424. Hicke, L. & Dunn, R. REGULATION OF MEMBRANE PROTEIN TRANSPORT BY UBIQUITIN AND UBIQUITIN-BINDING PROTEINS. *Annual Review of Cell and Developmental Biology* **19**, 141 (2003).
425. Raiborg, C., Rusten, T.E. & Stenmark, H. Protein sorting into multivesicular endosomes. *Current Opinion in Cell Biology* **15**, 446-455 (2003).
426. Sorkin, A. & von Zastrow, M. SIGNAL TRANSDUCTION AND ENDOCYTOSIS: CLOSE ENCOUNTERS OF MANY KINDS. *Nat Rev Mol Cell Biol* **3**, 600-614 (2002).
427. Hicke, L. A New Ticket for Entry into Budding Vesicles--Ubiquitin. *Cell* **106**, 527-530 (2001).
428. Le Roy, C. & Wrana, J.L. CLATHRIN- AND NON-CLATHRIN-MEDIATED ENDOCYTIC REGULATION OF CELL SIGNALLING. *Nat Rev Mol Cell Biol* **6**, 112-126 (2005).
429. Jeffers, M., Rong, S. & Woude, G.F. Hepatocyte growth factor/scatter

factor-Met signaling in tumorigenicity and invasion/metastasis. *J Mol. Med.* **74**, 505-513 (1996).
430. Hammond, D.E., Urbe, S., Woude, G.F.V. & Clague, M.J. Down-regulation of MET, the receptor for hepatocyte growth factor. *Oncogene* **20**, 2761-2770 (2001).
431. Jeffers, M., Taylor, G.A., Weidner, K.M., Omura, S. & Vande Woude, G.F. Degradation of the Met tyrosine kinase receptor by the ubiquitin-proteasome pathway. *Mol. Cell. Biol.* **17**, 799-808 (1997).
432. Li, N., Xiang, G.-S., Dokainish, H., Ireton, K. & Elferink, L.A. The Listeria Protein Internalin B Mimics Hepatocyte Growth Factor-Induced Receptor Trafficking
doi:10.1111/j.1600-0854.2005.00290.x. *Traffic* **6**, 459-473 (2005).
433. Riezman, H. Cell biology: The ubiquitin connection. *Nature* **416**, 381-383 (2002).
434. Gorden, P., Carpentier, J.L., Cohen, S. & Orci, L. Epidermal growth factor: morphological demonstration of binding, internalization, and lysosomal association in human fibroblasts. *Proc. Natl Acad. Sci. USA* **75**, 5025-5029 (1978).
435. Sorkina, T., Huang, F., Beguinot, L. & Sorkin, A. Effect of Tyrosine Kinase Inhibitors on Clathrin-coated Pit Recruitment and Internalization of Epidermal Growth Factor Receptor
10.1074/jbc.M201595200. *J. Biol. Chem.* **277**, 27433-27441 (2002).
436. Hillman, G.M. & Schlessinger, J. Lateral diffusion of epidermal growth factor complexed to its surface receptors does not account for the thermal sensitivity of patch formation and endocytosis. *Biochemistry* **21**, 1667-1672 (1982).
437. Confalonieri, S., Salcini, A.E., Puri, C., Tacchetti, C. & Di Fiore, P.P. Tyrosine Phosphorylation of Eps15 Is Required for Ligand-regulated, but Not Constitutive, Endocytosis
10.1083/jcb.150.4.905. *J. Cell Biol.* **150**, 905-912 (2000).
438. Hoeller, D*., et al.* Regulation of ubiquitin-binding proteins by monoubiquitination. *Nat Cell Biol* **8**, 163-169 (2006).
439. Klapisz, E*., et al.* A Ubiquitin-interacting Motif (UIM) Is Essential for Eps15 and Eps15R Ubiquitination
10.1074/jbc.M203004200. *J. Biol. Chem.* **277**, 30746-30753 (2002).
440. Fallon, L*., et al.* A regulated interaction with the UIM protein Eps15 implicates parkin in EGF receptor trafficking and PI(3)K-Akt signalling. *Nat Cell Biol* **8**, 834-842 (2006).
441. Torrisi, M.R*., et al.* Eps15 Is Recruited to the Plasma Membrane upon Epidermal Growth Factor Receptor Activation and Localizes to Components of the Endocytic Pathway during Receptor Internalization. *Mol. Biol. Cell* **10**, 417-434 (1999).
442. de Melker, A.A., van der Horst, G. & Borst, J. Ubiquitin Ligase Activity of c-Cbl Guides the Epidermal Growth Factor Receptor into Clathrin-coated Pits by Two Distinct Modes of Eps15 Recruitment
10.1074/jbc.M409765200. *J. Biol. Chem.* **279**, 55465-55473 (2004).

443. Stang, E.*, et al.* Cbl-dependent Ubiquitination Is Required for Progression of EGF Receptors into Clathrin-coated Pits. *Mol. Biol. Cell* **15**, 3591-3604 (2004).
444. Barriere, H.*, et al.* Molecular Basis of Oligoubiquitin-Dependent Internalization of Membrane Proteins in Mammalian Cells. *Traffic* **7**, 282-297 (2006).
445. Obenauer, J.C., Cantley, L.C. & Yaffe, M.B. Scansite 2.0: proteome-wide prediction of cell signaling interactions using short sequence motifs. *Nucl. Acids Res.* **31**, 3635-3641 (2003).
446. Fournier, T.M., Kamikura, D., Teng, K. & Park, M. Branching Tubulogenesis but Not Scatter of Madin-Darby Canine Kidney Cells Requires a Functional Grb2 Binding Site in the Met Receptor Tyrosine Kinase. *Journal of Biological Chemistry* **271**, 22211-22217 (1996).
447. Jiang, X., Huang, F., Marusyk, A. & Sorkin, A. Grb2 Regulates Internalization of EGF Receptors through Clathrin-coated Pits. *Mol. Biol. Cell* **14**, 858-870 (2003).
448. Li, N., Lorinczi, M., Ireton, K. & Elferink, L.A. Specific Grb2-mediated Interactions Regulate Clathrin-dependent Endocytosis of the cMet-tyrosine Kinase. *J. Biol. Chem.* **282**, 16764-16775 (2007).
449. Pawson, T. & Scott, J.D. Signaling Through Scaffold, Anchoring, and Adaptor Proteins. *Science* **278**, 2075-2080 (1997).
450. Huang, F., Khvorova, A., Marshall, W. & Sorkin, A. Analysis of Clathrin-mediated Endocytosis of Epidermal Growth Factor Receptor by RNA Interference
10.1074/jbc.C400046200. *J. Biol. Chem.* **279**, 16657-16661 (2004).
451. Veiga, E. & Cossart, P. Listeria hijacks the clathrin-dependent endocytic machinery to invade mammalian cells. *Nat Cell Biol* **7**, 894-900 (2005).
452. Aguilar, R.C. & Wendland, B. Endocytosis of membrane receptors: Two pathways are better than one. *Proceedings of the National Academy of Sciences* **102**, 2679-2680 (2005).
453. Schumacher, C.*, et al.* The SH3 Domain of Crk Binds Specifically to a Conserved Proline-rich Motif in Eps15 and Eps15R
10.1074/jbc.270.25.15341. *J. Biol. Chem.* **270**, 15341-15347 (1995).
454. Rodrigues, G.A., Naujokas, M.A. & Park, M. Alternative splicing generates isoforms of the met receptor tyrosine kinase which undergo differential processing. *Mol. Cell. Biol.* **11**, 2962-2970 (1991).
455. Sorkin, A. & von Zastrow, M. Endocytosis and signalling: intertwining molecular networks. *Nat Rev Mol Cell Biol* **10**, 609-622 (2009).
456. Schmidt, C.*, et al.* Scatter factor/hepatocyte growth factor is essential for liver development. *Nature* **373**, 699-702 (1995).
457. Bladt, F., Riethmacher, D., Isenmann, S., Aguzzi, A. & Birchmeier, C. Essential role for the c-met receptor in the migration of myogenic precursor cells into the limb bud. *Nature* **376**, 768-771 (1995).
458. Huh, C.-G.*, et al.* Hepatocyte growth factor/c-met signaling pathway is required for efficient liver regeneration and repair. *PNAS* **101**, 4477-4482 (2004).

459. Borowiak, M.*, et al.* Met provides essential signals for liver regeneration. *PNAS* **101**, 10608-10613 (2004).
460. Nakamura, T.*, et al.* Myocardial protection from ischemia/reperfusion injury by endogenous and exogenous HGF. *The Journal of Clinical Investigation* **106**, 1511-1519 (2000).
461. Kawaida, K., Matsumoto, K., Shimazu, H. & Nakamura, T. Hepatocyte Growth Factor Prevents Acute Renal Failure of Accelerates Renal Regeneration in mice. *PNAS* **91**, 4357-4361 (1994).
462. Birchmeier, C., Birchmeier, W., Gherardi, E. & Vande Woude, G.F. Met, metastasis, motility and more. *Nat Rev Mol Cell Biol* **4**, 915-925 (2003).
463. Lee, J.-H.*, et al.* A novel germ line juxtamembrane Met mutation in human gastric cancer. *Oncogene* **19**, 4947-4953 (2000).
464. Sigismund, S.*, et al.* Clathrin-independent endocytosis of ubiquitinated cargos. *PNAS* **102**, 2760-2765 (2005).
465. Hammond, D.E., Urbé, S., Woude, G.F.V. & Clague, M.J. Down-regulation of MET, the receptor for hepatocyte growth factor. *Oncogene* **20**, 2761-2770 (2001).
466. Orth, J.D., Krueger, E.W., Weller, S.G. & McNiven, M.A. A Novel Endocytic Mechanism of Epidermal Growth Factor Receptor Sequestration and Internalization. *Cancer Research* **66**, 3603-3610 (2006).
467. D'Souza-Schorey, C. & Chavrier, P. ARF proteins: roles in membrane traffic and beyond. *Nat Rev Mol Cell Biol* **7**, 347-358 (2006).
468. Palacios, F., Price, L., Schweitzer, J., Collard, J.G. & D'Souza-Schorey, C. An essential role for ARF6-regulated membrane traffic in adherens junction turnover and epithelial cell migration. *EMBO J* **20**, 4973-4986 (2001).
469. Kimura, T., Sakisaka, T., Baba, T., Yamada, T. & Takai, Y. Involvement of the Ras-Ras-activated Rab5 Guanine Nucleotide Exchange Factor RIN2-Rab5 Pathway in the Hepatocyte Growth Factor-induced Endocytosis of E-cadherin. *Journal of Biological Chemistry* **281**, 10598-10609 (2006).
470. Zhao, Y. & Keen, J.H. Gyrating Clathrin: Highly Dynamic Clathrin Structures Involved in Rapid Receptor Recycling. *Traffic* **9**, 2253-2264 (2008).
471. Stenmark, H. Rab GTPases as coordinators of vesicle traffic. *Nat Rev Mol Cell Biol* **10**, 513-525 (2009).
472. Driskell, O.J., Mironov, A., Allan, V.J. & Woodman, P.G. Dynein is required for receptor sorting and the morphogenesis of early endosomes. *Nat Cell Biol* **9**, 113-120 (2007).
473. Puertollano, R., Randazzo, P.A., Presley, J.F., Hartnell, L.M. & Bonifacino, J.S. The GGAs Promote ARF-Dependent Recruitment of Clathrin to the TGN. *Cell* **105**, 93-102 (2001).
474. Volpicelli-Daley, L.A., Li, Y., Zhang, C.-J. & Kahn, R.A. Isoform-selective Effects of the Depletion of ADP-Ribosylation Factors 1-5 on Membrane Traffic. *Mol. Biol. Cell* **16**, 4495-4508 (2005).
475. Wang, J.*, et al.* PI4P Promotes the Recruitment of the GGA Adaptor Proteins to the Trans-Golgi Network and Regulates Their Recognition of

the Ubiquitin Sorting Signal. *Mol. Biol. Cell* **18**, 2646-2655 (2007).
476. Wakasugi, M.*, et al.* Predominant expression of the short form of GGA3 in human cell lines and tissues. *Biochemical and Biophysical Research Communications* **306**, 687-692 (2003).
477. Sonnichsen, B., De Renzis, S., Nielsen, E., Rietdorf, J. & Zerial, M. Distinct Membrane Domains on Endosomes in the Recycling Pathway Visualized by Multicolor Imaging of Rab4, Rab5, and Rab11. *J. Cell Biol.* **149**, 901-914 (2000).
478. van der Sluijs, P.*, et al.* The small GTP-binding protein rab4 controls an early sorting event on the endocytic pathway. *Cell* **70**, 729-740 (1992).
479. Mattera, R., Arighi, C.N., Lodge, R., Zerial, M. & Bonifacino, J.S. Divalent interaction of the GGAs with the Rabaptin-5-Rabex-5 complex. *EMBO J* **22**, 78-88 (2003).
480. Vitale, G.*, et al.* Distinct Rab-binding domains mediate the interaction of Rabaptin-5 with GTP-bound rab4 and rab5. *EMBO J* **17**, 1941-1951 (1998).
481. Horiuchi, H.*, et al.* A Novel Rab5 GDP/GTP Exchange Factor Complexed to Rabaptin-5 Links Nucleotide Exchange to Effector Recruitment and Function. **90**, 1149-1159 (1997).
482. Lamorte, L., Royal, I., Naujokas, M. & Park, M. Crk Adapter Proteins Promote an Epithelial-Mesenchymal-like Transition and Are Required for HGF-mediated Cell Spreading and Breakdown of Epithelial Adherens Junctions. *Mol. Biol. Cell* **13**, 1449-1461 (2002).
483. Palamidessi, A.*, et al.* Endocytic Trafficking of Rac Is Required for the Spatial Restriction of Signaling in Cell Migration. *Cell* **134**, 135-147 (2008).
484. Hamon, M.l., Bierne, H.l.n. & Cossart, P. Listeria monocytogenes: a multifaceted model. *Nat Rev Micro* **4**, 423-434 (2006).
485. Lock, L.S., Maroun, C.R., Naujokas, M.A. & Park, M. Distinct Recruitment and Function of Gab1 and Gab2 in Met Receptor-mediated Epithelial Morphogenesis. *Mol. Biol. Cell* **13**, 2132-2146 (2002).
486. Joshi, A., Garg, H., Nagashima, K., Bonifacino, J.S. & Freed, E.O. GGA and Arf Proteins Modulate Retrovirus Assembly and Release. *Molecular Cell* **30**, 227-238 (2008).
487. Jekely, G., Sung, H.-H., Luque, C.M. & Rorth, P. Regulators of Endocytosis Maintain Localized Receptor Tyrosine Kinase Signaling in Guided Migration. *Developmental cell* **9**, 197-207 (2005).
488. Wang, X.*, et al.* Analysis of Cell Migration Using Whole-Genome Expression Profiling of Migratory Cells in the Drosophila Ovary. *Developmental cell* **10**, 483-495 (2006).
489. Parachoniak, C. & Park, M. Distinct Recruitment of Eps15 via Its Coiled-coil Domain Is Required For Efficient Down-regulation of the Met Receptor Tyrosine Kinase. *J. Biol. Chem.* **284**, 8382-8394 (2009).
490. Anton, S., Markus, H. & Michael, F. Quantification of ARF-GTP in HepG2 by pulldown with GST-GGA3(1-316). (2006).
491. Paliouras, G.N., Naujokas, M.A. & Park, M. Pak4, a Novel Gab1 Binding

Partner, Modulates Cell Migration and Invasion by the Met Receptor. *Mol. Cell. Biol.* **29**, 3018-3032 (2009).
492. Parachoniak, C.A., Luo, Y., Abella, J.V., Keen, J.H. & Park, M. GGA3 Functions as a Switch to Promote Met Receptor Recycling, Essential for Sustained ERK and Cell Migration. *Developmental Cell* **20**, 751-763 (2011).
493. Joffre, C.*, et al.* A direct role for Met endocytosis in tumorigenesis. *Nat Cell Biol* **13**, 827-837 (2011).
494. Schuyler, S.C. & Pellman, D. Microtubule "Plus-End-Tracking Proteins": The End Is Just the Beginning. *Cell* **105**, 421-424 (2001).
495. Arnal, I., Heichette, C., Diamantopoulos, G.S. & ChrÈtien, D. CLIP-170/Tubulin-Curved Oligomers Coassemble at Microtubule Ends and Promote Rescues. *Current Biology* **14**, 2086-2095 (2004).
496. Insall, R.H. & Machesky, L.M. Actin Dynamics at the Leading Edge: From Simple Machinery to Complex Networks. *Developmental cell* **17**, 310-322 (2009).
497. Pollard, T.D. & Cooper, J.A. Actin, a Central Player in Cell Shape and Movement. *Science* **326**, 1208-1212 (2009).
498. Choi, C.K.*, et al.* Actin and [alpha]-actinin orchestrate the assembly and maturation of nascent adhesions in a myosin II motor-independent manner. *Nat Cell Biol* **10**, 1039-1050 (2008).
499. Pierre, P., Pepperkok, R. & Kreis, T.E. Molecular characterization of two functional domains of CLIP-170 in vivo. *Journal of Cell Science* **107**, 1909-1920 (1994).
500. Pollard, T.D. Regulation of Actin Filament Assembly by Arp2/3 Complex and Formins. *Annual Review of Biophysics and Biomolecular Structure* **36**, 451-477 (2007).
501. Krause, M., Dent, E.W., Bear, J.E., Loureiro, J.J. & Gertler, F.B. Ena/VASP Proteins: Regulators of the Actin Cytoskeleton and Cell Migration. Vol. 19 541-564 (2003).
502. Zaoui, K., Honore, S., Isnardon, D., Braguer, D. & Badache, A. Memo-RhoA-mDia1 signaling controls microtubules, the actin network, and adhesion site formation in migrating cells. *The Journal of Cell Biology* **183**, 401-408 (2008).
503. Lakadamyali, M., Rust, M.J. & Zhuang, X. Ligands for Clathrin-Mediated Endocytosis Are Differentially Sorted into Distinct Populations of Early Endosomes. *Cell* **124**, 997-1009 (2006).
504. Montagnac, G.*, et al.* Decoupling of Activation and Effector Binding Underlies ARF6 Priming of Fast Endocytic Recycling. *Current Biology* **21**, 574-579 (2011).
505. Kermorgant, S., Zicha, D. & Parker, P.J. Protein Kinase C Controls Microtubule-based Traffic but Not Proteasomal Degradation of c-Met. *Journal of Biological Chemistry* **278**, 28921-28929 (2003).
506. Kermorgant, S., Zicha, D. & Parker, P.J. PKC controls HGF-dependent c-Met traffic, signalling and cell migration. *EMBO J* **23**, 3721-3734 (2004).
507. Meunier, B., Quaranta, M., Daviet, L., Hatzoglou, A. & Leprince, C. The

membrane-tubulating potential of amphiphysin 2/BIN1 is dependent on the microtubule-binding cytoplasmic linker protein 170 (CLIP-170). *European Journal of Cell Biology* **88**, 91-102 (2009).
508. Peter, B.J.*, et al.* BAR Domains as Sensors of Membrane Curvature: The Amphiphysin BAR Structure. *Science* **303**, 495-499 (2004).
509. Zimmerberg, J. & McLaughlin, S. Membrane Curvature: How BAR Domains Bend Bilayers. *Current Biology* **14**, R250-R252 (2004).
510. Lee, H.-S.*, et al.* Phosphorylation Controls Autoinhibition of Cytoplasmic Linker Protein-170. *Mol. Biol. Cell* **21**, 2661-2673 (2010).
511. Parachoniak, C.A. & Park, M. Distinct Recruitment of Eps15 via Its Coiled-coil Domain Is Required For Efficient Down-regulation of the Met Receptor Tyrosine Kinase. *Journal of Biological Chemistry* **284**, 8382-8394 (2009).
512. Potempa, S. & Ridley, A.J. Activation of Both MAP Kinase and Phosphatidylinositide 3-Kinase by Ras Is Required for Hepatocyte Growth Factor/Scatter Factor-induced Adherens Junction Disassembly. *Mol. Biol. Cell* **9**, 2185-2200 (1998).
513. Liang, C.-C. & Chen, H.-C. Sustained Activation of Extracellular Signal-regulated Kinase Stimulated by Hepatocyte Growth Factor Leads to Integrin Œ±2 Expression That Is Involved in Cell Scattering. *Journal of Biological Chemistry* **276**, 21146-21152 (2001).
514. Futter, C.E., Pearse, A., Hewlett, L.J. & Hopkins, C.R. Multivesicular endosomes containing internalized EGF-EGF receptor complexes mature and then fuse directly with lysosomes. *The Journal of Cell Biology* **132**, 1011-1023 (1996).
515. Van Etten, R.A. Cycling, stressed-out and nervous: cellular functions of c-Abl. *Trends in Cell Biology* **9**, 179-186 (1999).
516. Miyoshi-Akiyama, T., Aleman, L.M., Smith, J.M., Adler, C.E. & Mayer, B.J. Regulation of Cbl phosphorylation by the Abl tyrosine kinase and the Nck SH2/SH3 adaptor. *Oncogene* **29**, 4058-4069 (2001).
517. Ren, R., Ye, Z.S. & Baltimore, D. Abl protein-tyrosine kinase selects the Crk adapter as a substrate using SH3-binding sites. *Genes & Development* **8**, 783-795 (1994).
518. Babst, M. GGAing ubiquitin to the endosome. *Nat Cell Biol* **6**, 175-177 (2004).
519. Scott, P.M.*, et al.* GGA proteins bind ubiquitin to facilitate sorting at the trans-Golgi network. *Nat Cell Biol* **6**, 252-259 (2004).
520. Boman, A.L.*, et al.* ADP-Ribosylation Factor (ARF) Interaction Is Not Sufficient for Yeast GGA Protein Function or Localization. *Mol. Biol. Cell* **13**, 3078-3095 (2002).
521. Hirst, J.*, et al.* A Family of Proteins with {gamma}-Adaptin and VHS Domains that Facilitate Trafficking between the Trans-Golgi Network and the Vacuole/Lysosome. *J. Cell Biol.* **149**, 67-80 (2000).
522. Nogi, T.*, et al.* Structural basis for the accessory protein recruitment by the [gamma]-adaptin ear domain. *Nat Struct Mol Biol* **9**, 527-531 (2002).
523. Horiuchi, H.*, et al.* A Novel Rab5 GDP/GTP Exchange Factor Complexed

to Rabaptin-5 Links Nucleotide Exchange to Effector Recruitment and Function. *Cell* **90**, 1149-1159 (1997).
524. Walseng, E., Bakke, O. & Roche, P.A. Major Histocompatibility Complex Class II-Peptide Complexes Internalize Using a Clathrin- and Dynamin-independent Endocytosis Pathway. *Journal of Biological Chemistry* **283**, 14717-14727 (2008).
525. Allaire, P.D.*, et al.* The Connecdenn DENN Domain: A GEF for Rab35 Mediating Cargo-Specific Exit from Early Endosomes. *Molecular Cell* **37**, 370-382 (2010).
526. Kay, B.K., Williamson, M.P. & Sudol, M. The importance of being proline: the interaction of proline-rich motifs in signaling proteins with their cognate domains. *The FASEB Journal* **14**, 231-241 (2000).
527. Pawson, T. & Nash, P. Assembly of Cell Regulatory Systems through Protein Interaction Domains. *Science* **300**, 445-452 (2003).
528. Ren, X. & Hurley, J.H. Proline-Rich Regions and Motifs in Trafficking: From ESCRT Interaction to Viral Exploitation. *Traffic*, no-no (2011).
529. Mongiovi, A.M.*, et al.* A novel peptide-SH3 interaction. *EMBO J* **18**, 5300-5309 (1999).
530. Lim, W.A., Richards, F.M. & Fox, R.O. Structural determinants of peptide-binding orientation and of sequence specificity in SH3 domains. *Nature* **372**, 375-379 (1994).
531. Feng, S., Chen, J., Yu, H., Simon, J. & Schreiber, S. Two binding orientations for peptides to the Src SH3 domain: development of a general model for SH3-ligand interactions. *Science* **266**, 1241-1247 (1994).
532. Kuriyan, J. & Cowburn, D. MODULAR PEPTIDE RECOGNITION DOMAINS IN EUKARYOTIC SIGNALING. *Annual Review of Biophysics and Biomolecular Structure* **26**, 259-288 (1997).
533. Matsumoto, T.*, et al.* Differential Interaction of CrkII Adaptor Protein with Platelet-Derived Growth Factor [alpha]- and [beta]-Receptors Is Determined by Its Internal Tyrosine Phosphorylation. *Biochemical and Biophysical Research Communications* **270**, 28-33 (2000).
534. Sorokin, A., Reed, E., Nnkemere, N., Dulin, N.O. & Schlessinger, J. Crk protein binds to PDGF receptor and insulin receptor substrate-1 with different modulating effects on PDGF- and insulin-dependent signaling pathways. *Oncogene* **16**, 2425-2434 (1998).
535. De Falco, V.*, et al.* RET/Papillary Thyroid Carcinoma Oncogenic Signaling through the Rap1 Small GTPase. *Cancer Research* **67**, 381-390 (2007).
536. Noren, N.K., Foos, G., Hauser, C.A. & Pasquale, E.B. The EphB4 receptor suppresses breast cancer cell tumorigenicity through an Abl-Crk pathway. *Nat Cell Biol* **8**, 815-825 (2006).
537. Chavrier, P. & MÈnÈtrey, J. Toward a Structural Understanding of Arf Family:Effector Specificity. *Structure* **18**, 1552-1558 (2010).
538. Peters, P.J.*, et al.* Overexpression of wild-type and mutant ARF1 and ARF6: distinct perturbations of nonoverlapping membrane compartments. *The Journal of Cell Biology* **128**, 1003-1017 (1995).

539. Manolea, F.*, et al.* Arf3 Is Activated Uniquely at the trans-Golgi Network by Brefeldin A-inhibited Guanine Nucleotide Exchange Factors. *Mol. Biol. Cell* **21**, 1836-1849 (2010).
540. Jackson, C.L. & Casanova, J.E. Turning on ARF: the Sec7 family of guanine-nucleotide-exchange factors. *Trends in Cell Biology* **10**, 60-67 (2000).
541. Randazzo, P.A. & Hirsch, D.S. Arf GAPs: multifunctional proteins that regulate membrane traffic and actin remodelling. *Cellular Signalling* **16**, 401-413 (2004).
542. Morishige, M.*, et al.* GEP100 links epidermal growth factor receptor signalling to Arf6 activation to induce breast cancer invasion. *Nat Cell Biol* **10**, 85-92 (2008).
543. Batzer, A.G., Rotin, D., Urena, J.M., Skolnik, E.Y. & Schlessinger, J. Hierarchy of binding sites for Grb2 and Shc on the epidermal growth factor receptor. *Mol. Cell. Biol.* **14**, 5192-5201 (1994).
544. Sabe, H. Requirement for Arf6 in Cell Adhesion, Migration, and Cancer Cell Invasion. *Journal of Biochemistry* **134**, 485-489 (2003).
545. Yang, C.Z., Heimberg, H., D‚ÄôSouza-Schorey, C., Mueckler, M.M. & Stahl, P.D. Subcellular Distribution and Differential Expression of Endogenous ADP-ribosylation Factor 6 in Mammalian Cells. *Journal of Biological Chemistry* **273**, 4006-4011 (1998).
546. Palacios, F. & D'Souza-Schorey, C. Modulation of Rac1 and ARF6 Activation during Epithelial Cell Scattering. *J. Biol. Chem.* **278**, 17395-17400 (2003).
547. Tushir, J.S. & D'Souza-Schorey, C. ARF6-dependent activation of ERK and Rac1 modulates epithelial tubule development. *EMBO J* **26**, 1806-1819 (2007).
548. Claing, A.*, et al.* Œ≤-Arrestin-mediated ADP-ribosylation Factor 6 Activation and Œ≤2-Adrenergic Receptor Endocytosis. *Journal of Biological Chemistry* **276**, 42509-42513 (2001).
549. Mukherjee, S.*, et al.* The ADP ribosylation factor nucleotide exchange factor ARNO promotes Œ≤-arrestin release necessary for luteinizing hormone/choriogonadotropin receptor desensitization. *Proceedings of the National Academy of Sciences* **97**, 5901-5906 (2000).
550. D'Souza-Schorey, C., Li, G., Colombo, M. & Stahl, P. A regulatory role for ARF6 in receptor-mediated endocytosis. *Science* **267**, 1175-1178 (1995).
551. Powelka, A.M.*, et al.* Stimulation-Dependent Recycling of Integrin β1 Regulated by ARF6 and Rab11. *Traffic* **5**, 20-36 (2004).
552. Li, J.*, et al.* Phosphorylation of ACAP1 by Akt Regulates the Stimulation-Dependent Recycling of Integrin [beta]1 to Control Cell Migration. *Developmental Cell* **9**, 663-673 (2005).
553. Hashimoto, S.*, et al.* Requirement for Arf6 in breast cancer invasive activities. *Proceedings of the National Academy of Sciences of the United States of America* **101**, 6647-6652 (2004).
554. Caswell, P.T., Vadrevu, S. & Norman, J.C. Integrins: masters and slaves of

endocytic transport. *Nat Rev Mol Cell Biol* **10**, 843-853 (2009).
555. Caswell, P. & Norman, J. Endocytic transport of integrins during cell migration and invasion. *Trends in Cell Biology* **18**, 257-263 (2008).
556. Caswell, P.T. & Norman, J.C. Integrin Trafficking and the Control of Cell Migration. *Traffic* **7**, 14-21 (2006).
557. Pellinen, T. & Ivaska, J. Integrin traffic. *Journal of Cell Science* **119**, 3723-3731 (2006).
558. McCall-Culbreath, K.D., Li, Z. & Zutter, M.M. Crosstalk between the alpha2/beta1 integrin and c-met/HGF-R regulates innate immunity. *Blood* **111**, 3562-3570 (2008).
559. Wang, R., Kobayashi, R. & Bishop, J.M. Cellular adherence elicits ligand-independent activation of the Met cell-surface receptor. *Proceedings of the National Academy of Sciences* **93**, 8425-8430 (1996).
560. Hui, A.Y.*, et al.* Src and FAK mediate cell–matrix adhesion-dependent activation of met during transformation of breast epithelial cells. *Journal of Cellular Biochemistry* **107**, 1168-1181 (2009).
561. Liu, Y.*, et al.* Coordinate integrin and c-Met signaling regulate Wnt gene expression during epithelial morphogenesis. *Development* **136**, 843-853 (2009).
562. Mitra, A.K.*, et al.* Ligand-independent activation of c-Met by fibronectin and [alpha]5[beta]1-integrin regulates ovarian cancer invasion and metastasis. *Oncogene* **30**, 1566-1576 (2011).
563. Trusolino, L., Bertotti, A. & Comoglio, P.M. A Signaling Adapter Function for ±6≤4 Integrin in the Control of HGF-Dependent Invasive Growth. *Cell* **107**, 643-654 (2001).
564. Temkin, P.*, et al.* SNX27 mediates retromer tubule entry and endosome-to-plasma membrane trafficking of signalling receptors. *Nat Cell Biol* **13**, 715-721 (2011).
565. Seachrist, J.L., Anborgh, P.H. & Ferguson, S.S.G. Œ≤2-Adrenergic Receptor Internalization, Endosomal Sorting, and Plasma Membrane Recycling Are Regulated by Rab GTPases. *Journal of Biological Chemistry* **275**, 27221-27228 (2000).
566. McCaffrey, M.W.*, et al.* Rab4 affects both recycling and degradative endosomal trafficking. *FEBS Letters* **495**, 21-30 (2001).
567. Gasman, S., Kalaidzidis, Y. & Zerial, M. RhoD regulates endosome dynamics through Diaphanous-related Formin and Src tyrosine kinase. *Nat Cell Biol* **5**, 195-204 (2003).
568. Valetti, C.*, et al.* Role of dynactin in endocytic traffic: Effects of dynamitin overexpression and colocalization with CLIP-170. *Molecular Biology of the Cell* **10**, 4107-4120 (1999).
569. Aschenbrenner, L., Naccache, S.N. & Hasson, T. Uncoated Endocytic Vesicles Require the Unconventional Myosin, Myo6, for Rapid Transport through Actin Barriers. *Mol. Biol. Cell* **15**, 2253-2263 (2004).
570. Montagnac, G.*, et al.* Decoupling of Activation and Effector Binding Underlies ARF6 Priming of Fast Endocytic Recycling. *Current biology : CB* **21**, 574-579 (2011).

571. Zhao, Y., Gaidarov, I. & Keen, J.H. Phosphoinositide 3-Kinase C2Œ± Links Clathrin to Microtubule-dependent Movement. *Journal of Biological Chemistry* **282**, 1249-1256 (2007).
572. Yano, H.*, et al.* Association of Trk neurotrophin receptors with components of the cytoplasmic dynein motor. *Journal of Neuroscience* **21**, 1-7 (2001).
573. Verhey, K.J.*, et al.* Cargo of Kinesin Identified as Jip Scaffolding Proteins and Associated Signaling Molecules. *The Journal of Cell Biology* **152**, 959-970 (2001).
574. Bowman, A.B.*, et al.* Kinesin-Dependent Axonal Transport Is Mediated by the Sunday Driver (SYD) Protein. *Cell* **103**, 583-594 (2000).
575. Chibalina, M.V., Poliakov, A., Kendrick-Jones, J. & Buss, F. Myosin VI and Optineurin Are Required for Polarized EGFR Delivery and Directed Migration. *Traffic* **11**, 1290-1303 (2010).
576. Guglielmo, G.M.D., Baass, P.C., Ou, W.J., Posner, B.I. & Bergeron, J.J. Compartmentalization of SHC, GRB2 and mSOS, and hyperphosphorylation of Raf-1 by EGF but not insulin in liver parenchyma. *EMBO J* **13**, 4269-4277 (1994).
577. Vieira, A.V., Lamaze, C. & Schmid, S.L. Control of EGF Receptor Signaling by Clathrin-Mediated Endocytosis. *Science* **274**, 2086-2089 (1996).
578. Liu, F.*, et al.* α(1A)-Adrenergic Receptor Induces Activation of Extracellular Signal-Regulated Kinase 1/2 through Endocytic Pathway. *PLoS One* **6**, e21520 (2011).
579. Grimes, M.L.*, et al.* Endocytosis of Activated TrkA: Evidence that Nerve Growth Factor Induces Formation of Signaling Endosomes. *The Journal of Neuroscience* **16**, 7950-7964 (1996).
580. Wang, Y., Pennock, S.D., Chen, X., Kazlauskas, A. & Wang, Z. Platelet-derived Growth Factor Receptor-mediated Signal Transduction from Endosomes. *Journal of Biological Chemistry* **279**, 8038-8046 (2004).
581. Wang, Y., Pennock, S., Chen, X. & Wang, Z. Endosomal Signaling of Epidermal Growth Factor Receptor Stimulates Signal Transduction Pathways Leading to Cell Survival. *Mol. Cell. Biol.* **22**, 7279-7290 (2002).
582. Teis, D., Wunderlich, W. & Huber, L.A. Localization of the MP1-MAPK Scaffold Complex to Endosomes Is Mediated by p14 and Required for Signal Transduction. *Developmental Cell* **3**, 803-814 (2002).
583. Sigismund, S.*, et al.* Clathrin-Mediated Internalization Is Essential for Sustained EGFR Signaling but Dispensable for Degradation. *Developmental Cell* **15**, 209-219 (2008).
584. Woods, A.J., White, D.P., Caswell, P.T. & Norman, J.C. PKD1/PKC[mu] promotes [alpha]v[beta]3 integrin recycling and delivery to nascent focal adhesions. *EMBO J* **23**, 2531-2543 (2004).
585. Roberts, M., Barry, S., Woods, A., van der Sluijs, P. & Norman, J. PDGF-regulated rab4-dependent recycling of [alpha]v[beta]3 integrin from early endosomes is necessary for cell adhesion and spreading. *Current Biology* **11**, 1392-1402 (2001).

586. Dowrick, P., Kenworthy, P., McCann, B. & Warn, R. Circular ruffle formation and closure lead to macropinocytosis in hepatocyte growth factor/scatter factor-treated cells. *Eur J Cell Biol.* **61**, 44-53 (1993).
587. Buccione, R., Orth, J.D. & McNiven, M.A. Foot and mouth: podosomes, invadopodia and circular dorsal ruffles. *Nat Rev Mol Cell Biol* **5**, 647-657 (2004).
588. Krueger, E.W., Orth, J.D., Cao, H. & McNiven, M.A. A Dynamin-Cortactin-Arp2/3 Complex Mediates Actin Reorganization in Growth Factor-stimulated Cells. *Mol. Biol. Cell* **14**, 1085-1096 (2003).
589. Conner, S.D. & Schmid, S.L. Regulated portals of entry into the cell. *Nature* **422**, 37-44 (2003).
590. Harris, R.C., Chung, E. & Coffey, R.J. EGF receptor ligands. *Experimental Cell Research* **284**, 2-13 (2003).
591. Roepstorff, K.*, et al.* Differential Effects of EGFR Ligands on Endocytic Sorting of the Receptor. *Traffic* **10**, 1115-1127 (2009).
592. Alwan, H.A.J., van Zoelen, E.J.J. & van Leeuwen, J.E.M. Ligand-induced Lysosomal Epidermal Growth Factor Receptor (EGFR) Degradation Is Preceded by Proteasome-dependent EGFR De-ubiquitination. *Journal of Biological Chemistry* **278**, 35781-35790 (2003).
593. Lenferink, A.E.*, et al.* Superagonistic behaviour of epidermal growth factor/transforming growth factor-alpha chimaeras: correlation with receptor routing after ligand-induced internalization. *Biochem. J.* **327**, 859-865 (1997).
594. Lenferink, A.E.G.*, et al.* Differential endocytic routing of homo- and hetero-dimeric ErbB tyrosine kinases confers signaling superiority to receptor heterodimers. *EMBO J* **17**, 3385-3397 (1998).
595. Schreiber, A., Winkler, M. & Derynck, R. Transforming growth factor-alpha: a more potent angiogenic mediator than epidermal growth factor. *Science* **232**, 1250-1253 (1986).
596. Barrandon, Y. & Green, H. Cell migration is essential for sustained growth of keratinocyte colonies: The roles of transforming growth factor-[alpha] and epidermal growth factor. *Cell* **50**, 1131-1137 (1987).
597. Ebner, R. & Derynck, R. Epidermal growth factor and transforming growth factor-alpha: differential intracellular routing and processing of ligand-receptor complexes. *Cell Regulation* **2**, 599-612 (1991).
598. R√©villion, F., Lhotellier, V., Hornez, L., Bonneterre, J. & Peyrat, J.-P. ErbB/HER ligands in human breast cancer, and relationships with their receptors, the bio-pathological features and prognosis. *Annals of Oncology* **19**, 73-80 (2008).
599. Th√∏gersen, V.B.*, et al.* A Subclass of HER1 Ligands Are Prognostic Markers for Survival in Bladder Cancer Patients. *Cancer Research* **61**, 6227-6233 (2001).
600. Lafky, J.M., Wilken, J.A., Baron, A.T. & Maihle, N.J. Clinical implications of the ErbB/epidermal growth factor (EGF) receptor family and its ligands in ovarian cancer. *Biochimica et Biophysica Acta (BBA) - Reviews on Cancer* **1785**, 232-265 (2008).

601. Tørring, N., Jørgensen, P., Sørensen, B. & Nexø, E. Increased expression of heparin binding EGF (HB-EGF), amphiregulin, TGF alpha and epiregulin in androgen-independent prostate cancer cell lines. *Anticancer Research* **20**, 91-95 (2000).
602. Khambata-Ford, S.*, et al.* Expression of Epiregulin and Amphiregulin and K-ras Mutation Status Predict Disease Control in Metastatic Colorectal Cancer Patients Treated With Cetuximab. *Journal of Clinical Oncology* **25**, 3230-3237 (2007).
603. Yonesaka, K.*, et al.* Autocrine Production of Amphiregulin Predicts Sensitivity to Both Gefitinib and Cetuximab in EGFR Wild-type Cancers. *Clinical Cancer Research* **14**, 6963-6973 (2008).

# 7. APPENDIX

## 7.1. SUPPLEMENTAL EXPERIMENTAL PROCEDURES

### 7.1.1. Related to Chapter 3

**Antibodies and Reagents**

Antibody 147 was raised in rabbit against a carboxyl-terminal peptide of human Met as described previously (Rodrigues et al., 1991). Antibodies to GGA1, ubiquitin (P4D1) and Arf6 were obtained from Santa Cruz Biotechnology Inc. (Santa Cruz, CA); GGA2 was a kind gift from Dr. Juan Bonifacino; Met antibody AF276 from R&D Systems (Minneapolis, MN); actin from Sigma-Aldrich; GFP, Alexa-Fluor 488, 555, 647 and phalloidin-488 conjugated secondary antibodies were purchased from Molecular Probes (Eugene, OR); pMet(Y1234/Y1235), pERK1/2(T202/Y204), pAkt(S473), ERK1/2 and Akt were purchased from Cell Signaling Technology (Mississauga, ON, Canada); GGA3, Crk, Arf3 and EEA1 antibodies were obtained from BD Biosciences (Mississauga, ON, Canada); HA.11 and Giantin were obtained from Covance (Berkeley, CA); Myc 9E10 was obtained from Babco (Richmond, CA); Rab4 was purchased from Abcam (Cambridge, MA), Tsg101 from Genetex (Irvine, CA). ARF1 as described previously (Lamorte and Park, 2003), Mannose 6-phosphate receptor, cation-dependent antibody (22d4) was obtained from the developmental studies hybridoma bank (Iowa City, IA); IRDyes 680 and 800-conjugated secondary antibodies were from Rockland Immunochemicals (Gilbertsville, PA). HGF was a kind gift from Genentech (San Francisco, USA). Alexa-555 conjugated HGF was obtained using the Alexa Fluor 555 protein labeling kit Molecular Probes (Eugene, OR), cycloheximide, sodium 2-mercaptoethanesulfonic acid, myc peptide and iodoacetamide were purchased from Sigma. EZ-Link Sulfo-NHS-SS-Biotin and NeutrAvidin were obtained from Pierce Chemicals. Lactacystin and concanamycin were from Calbiochem (La Jolla, CA).

**DNA Constructs and Cell Lines**

GFP-Rab constructs were kindly provided by Dr. Stephen Ferguson and Dr. Robert Lodge. Arf6 constructs are as described in (Lamorte and Park, 2003) . GFP-GGA3 was kindly provided by Dr. Juan Bonifacino. siRNA-resistant GFP-GGA3 was made by performing site-directed mutagenesis to introduce three silent mutations against GGA3 duplex#1 (forward primer: 5'-GCGTCTGCAC ACC TTA GAA GAA GTC AAC AAC AAC GTG AGACTGC-3'; reverse primer: 5'-GCAG TCT CAC GTT GTT GTT GAC TTC TTC TAA GGT GTG CAG ACGC) according to manufacturer's instructions (Stratagene, La Jolla, CA). Further mutations were introduced to obtain GGA3 N194A, P404A and P463A mutants. (primers: N194A forward 5'-GACCTGCAGGAGGCCGCCAAGCTCATCAAGTC-3', N194A reverse 5'-GACTTGATGAGCTTGGCGGCCTCCTGCAGGTC-3', P463A forward: 5'-CCCAAGCTCCACTGCCGGCTCCCTTCCCAGCTCCTG-3'; P463A reverse 5'-CAGGAGCTGGGAAGGGAGCCGGCAGTGGAGCTTGGG-3', P404A forward 5'- CTCGCCGACCCAGCCGCTAATGTTCCTCCCAAAGAG-3', P404A reverse 5'-CTC TTTGGGAGGAACATTAGCGGCTGGGTCGGCGAG-3'). Stable cell lines were established by transfecting HeLa cells using superfect with siRNA-resistant constructs followed by G418 selection. Selected cell population were then sorted using a FACSAria sorter (Becton Dickinson). Green positive cells were sorted under sterile conditions using plots of size versus granularity and green fluorescence to determine baseline fluorescence versus cells with positive green emission using appropriate negative and positive control samples. Final populations expressed GFP-GGA3 levels similar to those of endogenous GGA3 protein levels as assessed by IB and were maintained in the presence of 12μg/ml G418.

**Biosythetic Pathway Export Assay**

To look at TGN vesicular transport to the plasma membrane, TGN export was blocked by incubating cells at 20°C for 1 h in serum-free media the presence of cycloheximide (to prevent protein new sythesis) followed by releasing cells into

serum-free media plus cycloheximide at 37°C to follow subsequent TGN export to the plasma membrane.

**GST-Pulldown Assay**

GST-fusion proteins have been described previously (Maroun et al., 2003). For pulldown assays, cell lysates were pre-cleared with glutathione-sepharose beads for 1 h at 4°C, while 10µg of fusion proteins were immobilized to 25ul of glutathione sepharose beads at room temperature. For Myc-GGA3 assay, Myc-GGA3 recombinant protein from HEK293 cell lysates was purified by binding to anti-myc antibody bound to beads, followed by elution by adding excess soluble myc peptide. Beads were washed three times with TGH lysis buffer containing inhibitors, then pre-ceared lysates were added to the beads. Samples were nutated at 4°C for 1 h, washed three times with TGH plus inhibitors, eluted with SDS sample buffer and processed for western blotting.

**Flow Cytometry Cell Surface Assay**

For flow cytometry, after HGF pulse/chase, cells were trypsinized, spun down (700xg, 5 min), incubated with Met receptor antibodies for 30 min at 4°C, washed twice with FACS buffer (DMEM, 1mM NaCl, 1mM MgCl, 1% FBS) then incubated with Alexa-conjuaged 488 secondary antibodies for 30 min at 4°C. Cell were then washed three times with FACS buffer and analyzed on a FACScan (1 laser) analyzer (Becton Dickson). In each assay 10,000 cells were analyzed for each sample.

**Live-cell imaging**

Imaging was performed as described previously (Zhao and Keen, 2008) using a Zeiss Axiovert 200 microscope and Olympus 150X/1.45 NA objective. COS1 cells transiently expressing GFP-GGA3 and mCherry-clathrin (Zhao et al., 2007), or expressing GFP-GGA3 and then incubated with 0.625 nM Alexa555-HGF for 20 min at 23°, were imaged using continuous streaming 30 msec exposures. Simulanteous acquisition of two colors was performed using a Dual-View system

equipped with appropriate filters and interfaced to an Evolve 512 EM-CCD camera operated in quantitative mode (Photometrics, Inc.). Image acquisition and analysis were performed using Metamorph (Molecular Devices, Inc.). For quantitation of Alexa555-HGF intensities, ten sets of 30 continuous images, each of 30 msec exposure, were collected at 2 sec intervals. For each field the ten image stacks were then combined into a single stack, and each Alexa555-HGF spot was tracked using a 6x6 pixel box to obtain intensity (Metamorph 'Track' function). Two other regions of identical size but lacking Alexa555-HGF throughout the stack were averaged to determine local background, which was then subtracted frame by frame to give a background corrected stack. The 30 frames for each ≈1 sec timepoint were then averaged, normalized to the initial timepoint, and intensities ± SEM were calculated for 16 spots from four different experiments.

**siRNA duplexes**

Allstars negative control siRNA (Qiagen)

GGA3 siRNA duplexes D#1 (CACGTTAGAGGAAGTTAACAA);Qiagen

D#2: (GUGAGAUGCUGCUUCAUUA); Dharmacon

D#3: (GAACACGGCUCCCUUACCU); Dharmacon

Tsg101: (ATGGTTACCCGTTTAGATCAA);Qiagen

Crk: (CTGAGTATAGTTCAACAGTTT); Dharmacon

Arf1: (CGGCCGAGAUCACAGACAA); Dharmacon

Arf3: (UAUGAACGCUGCUGAGAUC); Dharmacon

ARF6: (GGAUACAACUAAAGUACGA); Dharmacon

Rab4A: (UUAGAAGCCUCCAGAUUUG); Dharmacon

**Supplemental References**

Lamorte, L., and Park, M. (2003). ARF1 and ARF6 are dispensable for Crk-dependent epithelial-mesenchymal-like transitions. Anticancer Res 23, 2085-2092.

Maroun, C.R., Naujokas, M.A., and Park, M. (2003). Membrane Targeting of Grb2-associated Binder-1 (Gab1) Scaffolding Protein through Src Myristoylation

Sequence Substitutes for Gab1 Pleckstrin Homology Domain and Switches an Epidermal Growth Factor Response to an Invasive Morphogenic Program. Mol Biol Cell 14, 1691-1708.

Matlin, K.S., and Simons, K. (1983). Reduced temperature prevents transfer of a membrane glycoprotein to the cell surface but does not prevent terminal glycosylation. Cell 34, 233-243.

Puertollano, R., and Bonifacino, J.S. (2004). Interactions of GGA3 with the ubiquitin sorting machinery. Nat Cell Biol 6, 244-251.

Rodrigues, G.A., Naujokas, M.A., and Park, M. (1991). Alternative splicing generates isoforms of the met receptor tyrosine kinase which undergo differential processing. Mol Cell Biol 11, 2962-2970.

Zhao, Y., Gaidarov, I., and Keen, J.H. (2007). Phosphoinositide 3-Kinase C2Œ± Links Clathrin to Microtubule-dependent Movement. Journal of Biological Chemistry 282, 1249-1256.

Zhao, Y., and Keen, J.H. (2008). Gyrating Clathrin: Highly Dynamic Clathrin Structures Involved in Rapid Receptor Recycling. Traffic 9, 2253-2264.

### 7.1.2. Related To Chapter 4

**Constructs**

GFP–Rab4A was a gift from S. Ferguson (Robarts Institute, London, Ontario, Canada). mCherry-Rab4 was created by PCR-mediated amplification of GFP-Rab4 into a pEGFP-C2 vector backbone with the mCherry inserted in place of GFP[149]. RFP-CLIP170 WT, EGFP-CLIP-170-ΔH and HA-CLIP-170-ΔH (provided by Yulia Komarova, University of Illinois Chicago). pEGFP-C1-CLIP-170-NT, pEGFP-C1-CLIP-170-CC, pEGFP-C1-CLIP-170-ΔC, pEGFP-C1-CLIP-170-CT, pGEX-4T-1-CLIP-170-CC, (provided by Kozo Kaibuchi, Nagoya University Japan). EGFP–tubulin (Clontech Laboratories, Inc.), EB3-EGFP (provided by Niels Galjart, Erasmus MC Netherland), EGFP-Arp3 (Addgene; provided by L Welch, University of California). mCherry-actin (provided by Victor Small, IMBA Austria). Paxillin-EGFP (provided by A.R. Horwitz, University of Virginia, Charlottesville, VA). EGFP–VASP (Addgene; provided by J Wehland, Helmholtz Centre for Infection Germany).

**Antibodies**

Met antibody was raised against a carboxy-terminal peptide of the human Met protein[454], CLIP-170, (Santa Cruz Biotechnology, Inc.), Paxillin and GFP (BD Bioscience), actin (Sigma), Tubulin (Boehringer, Ingelheim), vinculin (Cell Signaling Technology). Secondary antibodies and Alexa Fluor 488, 546 and 633, phalloidin were obtained from Molecular Probes (Eugene, OR).